CHEMISTRY OF SUBMARINE HYDROTHERMAL SOLUTIONS

AT

21° NORTH, EAST PACIFIC RISE

AND

GUAYMAS BASIN, GULF OF CALIFORNIA

by

Karen Louise Von Damm

B.S., Yale University
(1977)

SUBMITTED IN PARTIAL FULFILLMENT OF THE
REQUIREMENTS FOR THE DEGREE OF
DOCTOR OF PHILOSOPHY

at the

MASSACHUSETTS INSTITUTE OF TECHNOLOGY

and the

WOODS HOLE OCEANOGRAPHIC INSTITUTION

August 1983

© Massachusetts Institute of Technology 1983

Signature of Author_____
Joint Program in Oceanography, Massachusetts Institute of Technology - Woods Hole Oceanographic Institution, and the Department of Earth, Atmospheric and Planetary Sciences, Massachusetts Institute of Technology, August 1983

Certified by_____
John M. Edmond
Thesis Supervisor

Accepted by_____
Chairman, Joint Committee for Chemical Oceanography, Massachusetts Institute of Technology - Woods Hole Oceanographic Institution

Archives
MASSACHUSETTS INSTITUTE OF TECHNOLOGY
NOV 15 1983
LIBRARIES

CHEMISTRY OF SUBMARINE HYDROTHERMAL SOLUTIONS at 21° NORTH, EAST PACIFIC RISE and GUAYMAS BASIN, GULF OF CALIFORNIA

by

Karen Louise Von Damm

Submitted to the Joint Oceanographic Committee of the Department of Earth, Atmospheric and Planetary Sciences, Massachusetts Institute of Technology, and the Woods Hole Oceanographic Institution on August 5, 1983, in partial fulfillment of the requirements for the degree of Doctor of Philosophy.

ABSTRACT

Submarine hydrothermal solutions at 21° north latitude on the East Pacific Rise were sampled for the first time in November 1979 and again in November 1981. In the 1981 program, four vent fields were sampled and a maximum temperature of 350-355° C was measured for three of the areas (OBS, SW, and HG) and only 273° C for the fourth area (NGS). The temperatures were stable over the twelve days of the diving program. The hot springs are "black smokers" which are forming constructional features of Fe, Zn and Cu sulfides and Ca and Ba sulfates. The solutions are seawater which has been heated during convection through the oceanic crust and has reacted with basalt. The hydrothermal solutions are acid (pH = 3.3-3.8, 25° C, 1 atm), reducing (H_2S = 6.6-8.4 mmoles/kg, SO_4 <1 mmoles/kg), and metal rich (Fe = 0.8-2.4 mmoles/kg, Mn = 0.7-1.0 mmoles/kg, Zn = 40-106 µmoles/kg, Cu = 0-44 µmoles/kg, Pb = 183-359 nmoles/kg, Co = 22-227 nmoles/kg, Cd = 17-180 nmoles/kg and Ag = <1-38 nmoles/kg). Mg and SO_4 are quantitatively removed from these solutions while other elements are highly enriched. Li increases to 0.9-1.3 µmoles/kg, K to 23.2-25.8 mmoles/kg, Rb to 27-33 µmoles/kg and Ca to 11.7-20.8 mmoles/kg. Sr both increases and decreases from the seawater concentration to 65-97 µmoles/kg. Na and Cl also increase and decrease; the gain can be attributed to a ~7% loss of water due to rock hydration. Silica increases to 15.6-19.5 mmoles/kg. Silica increases along strike from the southwest to the northeast; variations in the other chemical components are not geographically consistent. Quartz geobarometry indicates a pressure of reaction between 300-600 bars, implying a depth of reaction within the oceanic crust of 0.5-3.5 kms; in agreement with the geophysical estimates. The silica data imply that the NGS vent is conductively cooling.

The Guaymas Basin, Gulf of California hydrothermal system was first sampled in January 1982. A total of ten vent areas were sampled with a maximum temperature of 315° C. In contrast to the 21° N systems where the solutions exit directly from basalt, the hydrothermal systems at Guaymas pass through and react with approximately 500 meters of sediment cover

before they exit on the seafloor. This difference is reflected in the chemistry of these solutions. The sediment also provides a trapping mechanism for the metals in solution and a sediment-hosted type ore deposit may be forming at depth. These solutions differ from those at 21° N as they are less acid (pH = 5.9, 25° C, 1 atm), sulfur rich (H_2S = 3.8-6.0 mmoles/kg, SO_4 <1 mmole/kg) and metal rich (Fe = 0.02-0.18 mmoles/kg, Mn = 0.13-0.24 mmoles/kg, Zn = 0-40 µmoles/kg, Cu <6 µmoles/kg, Pb = 230-652 nmoles/kg, Ag $\leq$230 nmoles/kg, Cd $\leq$46 nmoles/kg and Co <5 nmoles/kg). The higher pH and extremely high alkalinity (2.8-10.6 meq/kg) can be attributed to dissolution of $CaCO_3$ and thermal degradation of organic matter which occur in the sediment column. The organic matter degradation is also responsible for the very high levels of ammonium (10.3-15.6 mmoles/kg) found in the solutions. The high pH and alkalinity are responsible for the lower concentrations of the metals which form insoluble sulfides. The ammonium exchanges for K and Rb in the sediments raising their levels in solution to a maximum of 49.2 mmoles/kg and 86 µmoles/kg, respectively; significantly higher than the values observed at 21° N. Li increases to 0.6-1.1 mmoles/kg, Ca to 41.5 mmoles/kg and Sr to 253 µmoles/kg. Na and Cl increase between 8-18%; this is attributed to hydration. Na is lost preferentially to Cl. Quartz geobarometry indicates a depth of reaction of ~0.5 kms into the oceanic crust.

These two sites demonstrate the importance of seawater reactions with basalt in altering the composition of seawater. The 21° N system is dependent only on reactions between seawater and basalt at elevated temperatures for its chemistry. The Guaymas system is a more complicated case in which reactions between the hydrothermal solutions and sediment overprint the basalt signature. The presence of large amounts of $CaCO_3$ and organic matter in the sediments at Guaymas is probably very important in determining the solution chemistry.

Thesis Supervisor: Professor John M. Edmond, M.I.T.

To my parents

ACKNOWLEDGEMENTS

Without the enthusiasm of my advisor John Edmond this thesis would not have succeeded. I would like to thank him for the opportunity to work with him on this project.

Barry Grant and Chris Measures provided tireless help at sea and back in the lab, as well as good company through it all. Without their help this thesis would not have been finished. Ed Boyle, Russ McDuff, Alan Shiller, Bob Stallard, Bob Collier, Peggy Delaney, Art Spivack and Glen Shen were always ready to have a perceptive discussion.

Special thanks to Karl Turekian who provided me with my first exposure to this field as a college freshman. As my undergraduate thesis supervisor, and as a member of my thesis committee he has enriched my understanding of global processes and has provided immeasurable help. Bill Jenkins explained the mysteries of ^{3}He to me and as a member of my thesis committee was always ready to listen and to help. As a member of the committee, Mike Mottl's discussions aided the interpretation of the data set.

This thesis is based on several field sampling programs of hydrothermal solutions. Without the help of the captain and crew of the Alvin/Lulu these programs would not have succeeded. Special thanks to the Alvin pilots Ralph Hollis, George Ellis and Bob Brown whose virtuousity in handling the submarine and samplers obtained the most pristine hydrothermal samples yet. Barrie Walden's sampler design has worked flawlessly on three diving cruises to date. The captains and crews of the Gilliss, Melville and E.B. Scripps provided the support facilities which made these cruises a success. Bob Ballard and the ANGUS group and many co-workers from Scripps helped to make these cruises a success as well as enjoyable.

My parents and friends have stood by me the last five years. I cannot thank them enough for their support.

The National Science Foundation through grants OCE-8020203, OCE-8118481, and 7919843-OCE provided financial support for this research.

TABLE OF CONTENTS

Page Number

LIST OF FIGURES

Page Number

LIST OF TABLES

CHAPTER 1

Introduction

The existence of oceanic hot springs had been postulated for several years on a geophysical (Elder, 1965) and a geochemical basis (Corliss, 1971) before their discovery in 1977. On a geophysical basis they were postulated to explain the anomalously low conductive heat flow observed on young ocean crust as being due to convective cooling (Wolery and Sleep, 1976). On a geochemical basis they were invoked as being a possible control on the composition of seawater and sediments, as well as providing the missing source/sink in several elemental mass balance calculations. The metalliferous sediments found on the ocean ridges and as the basal section of the sediment column (Bonatti, 1975) implied that these waters might be an effective medium of metal transfer from basalt to the seafloor (Corliss, 1971). The ophiolite sections observed on land provided evidence for the hydrothermal alteration of oceanic crust as well as the deposition of massive metal sulfides by these fluids (Coleman, 1977). Further evidence for pervasive high and low temperature hydrothermal alteration of the oceanic crust came from rocks dredged from the seafloor (Humphris and Thompson, 1978a,b; Delaney et al., 1983). Water column anomalies of helium-3 (Craig and Lupton, 1981) and manganese (Weiss, 1977; Klinkhammer et al., 1977) over the ridge crest implied that an injection process must be active at the present time.

Submarine hot springs were first observed and sampled at the Galapagos Spreading Center (GSC) (0°47'N, 86°08'W) (Corliss et al., 1979) . The hot water reached a maximum temperature of ~30° C. Various chemical parameters indicated that the water was seawater which had reacted with basalt at

temperatures of ~350° C and then mixed subsurface with ambient seawater resulting in the deposition of metal sulfides and alkaline earth sulfates at depth (Edmond et al., 1979a,b). The chemistry of the hydrothermal water was greatly altered from that of normal seawater. The helium/heat relationship found in these samples (Jenkins et al., 1978), when combined with the global helium budget implied that these hydrothermal waters have a great influence on the chemistry of seawater. The 350° C endmember had, however, not been observed. The mixing with ambient seawater at depth in the system and resulting oxidation and precipitation reactions precluded "seeing back" to the original endmember composition for many of the trace metals. The iron, copper, zinc, silver, sulfur, etc. concentrations in the endmember, which are important for the interpretation of massive sulfide deposits in ophiolite and other terrains could not be determined. Experimental work on seawater-basalt reactions at temperatures in the 300-400° C range suggested that these solutions carried significant amounts of these "ore-forming" species (Bischoff and Dickson, 1975; Hajash, 1975; Seyfried and Bischoff, 1977; Seyfried and Mottl, 1977; Mottl and Holland, 1978; Mottl, Holland and Corr, 1979; Seyfried and Dibble, 1980).

In early 1979 hot springs were found at 21° N on the East Pacific Rise (EPR) with exit temperatures of 380±30° C (RISE Project Group, 1980). In November 1979 in a series of five Alvin dives we sampled these "black smokers" and measured temperatures of 350±5° C. This was a reconnaissance cruise to test sampling schemes and based on this experience we returned to 21° N in 1981 with new sampling equipment. Most of this thesis is based on the 1981 sampling of the hot springs, although occasional reference is made to the 1979 samples. Four vent areas were sampled in 1981: the same three as were sampled in 1979 as well as one newly discovered one. A fuller

description of the sample collection is given in Appendix 1.

The solutions sampled at 21° N do not mix with ambient seawater until they exit on the seafloor. There, as the hot, acid, metal and sulfide rich hydrothermal solution mixes with the cold, alkaline sulfate rich seawater, sulfides and sulfates are precipitated building large (up to 20 meter) constructional features on the pillow terrain. The buoyant solutions form plumes of "black smoke" (predominately pyrrhotite (FeS) with other metal sulfides present) as they mix with seawater and these particles are dispersed through the water column. The hydrothermal solutions are clear until they mix with seawater and with the samplers used in 1981, which could reach into the "throat" of the vents, the "pure" hydrothermal solution was sampled. This allowed the concentrations of iron, copper, zinc, sulfur, etc. to be measured directly in these solutions.

North of the vent fields at 21° N the East Pacific Rise enters the Gulf of California. The Gulf is the closest western hemisphere analog to the Red Sea and the spreading center is covered by several hundred meters of sediment. Guaymas Basin, located approximately halfway up the Gulf, is divided into a northern and southern trough by a transform fault. This basin was thought to be a present site of hydrothermal activity based on heat flow (Lawver et al., 1975), helium-3 in the water column (Lupton, 1979), deposits sampled by submersible (Lonsdale et al., 1980) and the results of DSDP drilling in the basin (Curray, Moore, et al., 1982).

In January 1982 we sampled the hydrothermal solutions in the Guaymas Basin for the first time. The temperatures were not as high as at 21° N (315° C was the maximum measured temperature) but the main difference between the two areas is that the solutions at Guaymas must pass through ~500 meters of sediment before they exit (some also as "black smokers") on

the seafloor.

In the spring of 1982 the French found many smokers at 13° N on the East Pacific Rise and sampled several of them (Michard et al., 1983). Based on water column anomalies of helium-3, manganese and methane there is good evidence that hot springs also exist on the East Pacific Rise at 15-20° S (Lupton and Craig, 1981), although they have not been sampled directly. Similar water column and pictorial evidence exists for hot springs on the Juan de Fuca/Gorda Ridge (Normark et al., 1982) but they have not as yet been sampled directly. The discovery of these other areas suggests that hot springs are a common phenomenon on the intermediate to fast spreading sections of the world ridge crest (Figure 1-1). Additional evidence that this is so comes from the same specialized fauna ($\pm$ a few species) found at all these sites, although they are separated by thousands of kilometers.

The main objective of this thesis is to define the chemistry of the hydrothermal solutions at two of these sites: 21° N EPR and Guaymas Basin, Gulf of California, and to evaluate their importance to ocean chemistry and other phenomena such as massive sulfide deposits. These two areas will be compared to the solutions sampled at the GSC. These areas provide examples of three kinds of seafloor hydrothermal activity, although the basic process occurring at all three is the same. In all cases seawater reacts with basalt at temperatures of >300° C. At GSC the system is "leaky" and the hydrothermal solutions mix with ambient seawater and precipitate below the seafloor. As a result the solutions are relatively cool and depleted in metals and sulfur when they reach the seafloor. At 21° N the system is "tight" and it is at the seafloor that the hydrothermal solutions mix with ambient seawater and precipitate metal sulfides and sulfates as the

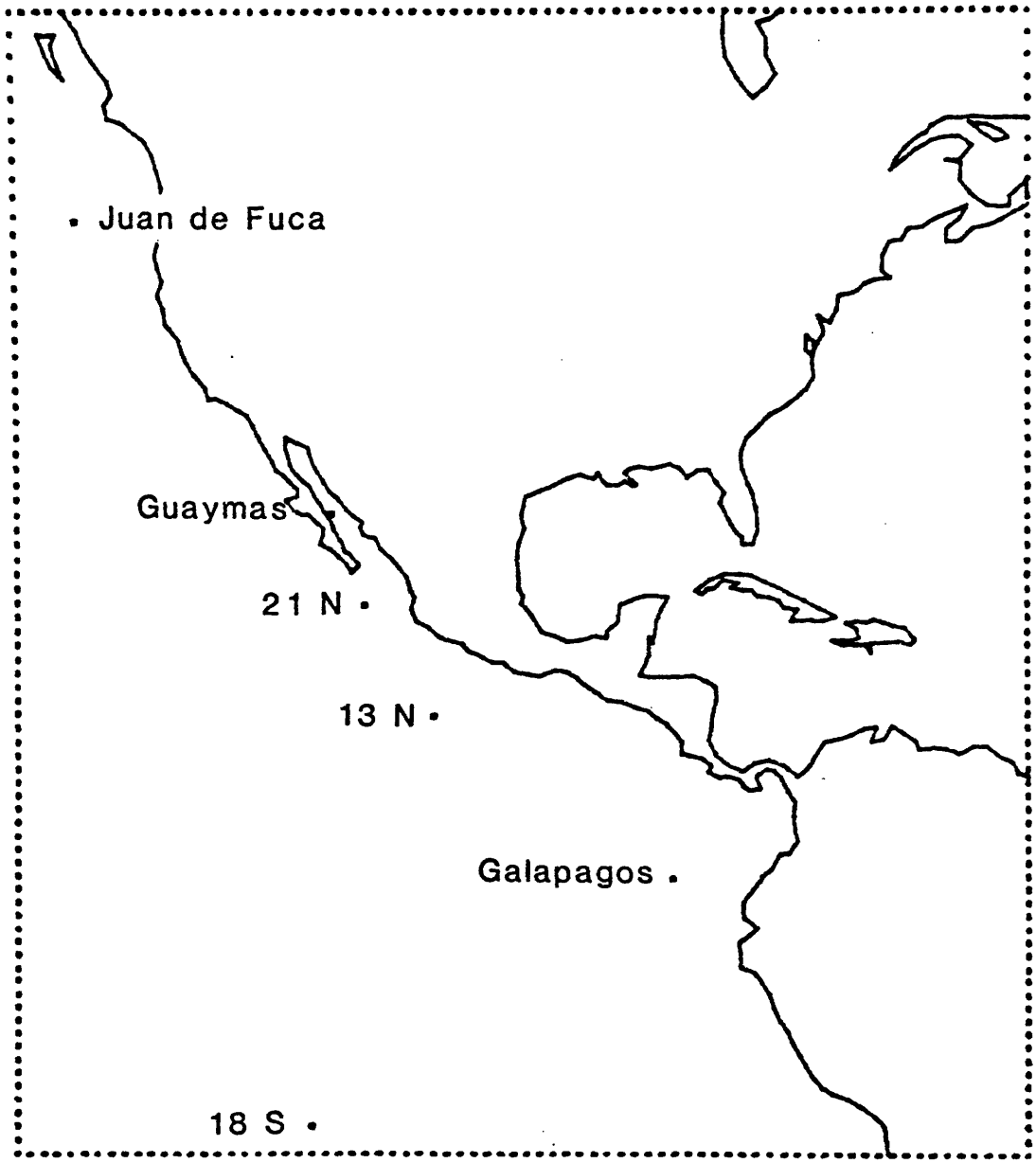

Figure 1-1: Map of discovered submarine hydrothermal systems.

constructional "chimneys" and plumes of "black smoke". At Guaymas the hydrothermal solutions react with the sediments through which they pass on their way to the seafloor, depositing some of their metal sulfides in the sediment column as well as increasing their concentration of other species. These solutions retain enough metals and sulfide to still build chimneys and be black smokers when they exit on the seafloor. Figure 1-2 is a schematic comparison of these three systems.

It is important to understand what causes the differences in chemistry between these systems, as whether they are low temperature and "leaky" (like GSC), high temperature and "tight" (like 21° N), or sediment covered (like Guaymas) will affect their net input to the ocean. Understanding their chemistry is also important for an understanding of the deposits they can form. The 21° N solutions can be called "ore-forming" based on their solution chemistry but much of this metal content is dispersed in the water column. At Guaymas, the sediment cover provides a trapping mechanism and it may be an example of a sediment-hosted or Besshi-type ore deposit (Franklin et al., 1981) in formation.

Chapter 2 of this thesis contains the results of the major and trace element analyses of the 21° N hydrothermal solutions as well as a discussion of the data. It addresses the question of what is controlling the solution chemistry. The solution chemistry is also compared to what is known about the alteration assemblages found in oceanic rocks, the composition of the chimneys at the 21° N site, the composition of massive sulfide deposits in ophiolites, metalliferous sediments, and to the experimental work on seawater-basalt interaction. Chapter 3 contains the results and discussion of the Guaymas data. It addresses the same questions as were posed in Chapter 2. In addition the solution composition

Figure 1-2: Schematic showing a comparison of three hydrothermal systems.

Galapagos Spreading Center where seawater mixes with the hydrothermal solutions subsurface leading to the subsurface precipitation of metal sulfides (shown by the ##).

21° North, East Pacific Rise where seawater mixes with the hydrothermal solutions on the seafloor leading to the precipitation of metal sulfides as chimneys and black smoke.

Guaymas Basin, Gulf of California where the hydrothermal solutions also react with sediments leading to the precipitation of metal sulfides in the sediments and on the seafloor. Secondary hydrothermal systems driven by dike intrusions also occur in the basin.

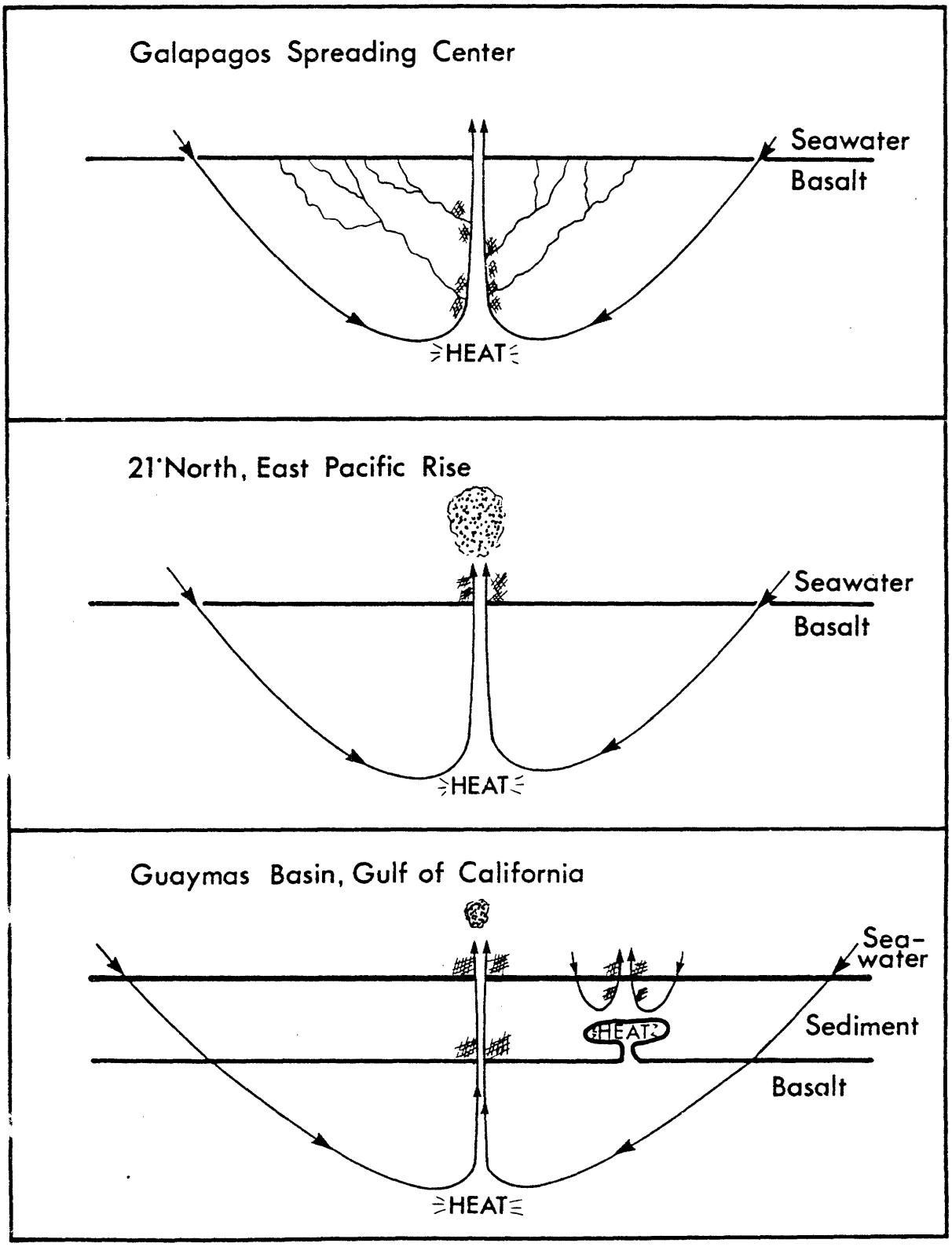
Galapagos Spreading Center
Seawater
Basalt
HEAT
21°North, East Pacific Rise
Seawater
Basalt
HEAT
Guaymas Basin, Gulf of California
Sea-
water
Sediment
Basalt
HEAT?
HEAT

is compared to the results of pore water and sediment analyses in DSDP sites 477 and 477A, which were in the Guaymas Basin. Chapter 4 is a comparison of the two systems and in conclusion attempts to access the general importance of seafloor hydrothermal activity to ocean chemistry.

CHAPTER 2

21° N - Results and Discussion

Two major questions need to be addressed with respect to the 21° N solution chemistry. As these were the first high temperature submarine hot springs sampled and as they comprise the most complete data set it is important to define their composition and the magnitude of variability which exists between vents. To be able to generalize the hot spring composition in an attempt to define their total input to the oceans it is necessary to understand what is controlling their chemistry. This chapter is a presentation of the results from 21° N, followed by a discussion of the data. The discussion addresses the question of what is controlling the solution chemistry.

Submarine hydrothermal solutions were postulated to be the source of massive sulfide deposits and metalliferous sediments and to be responsible for the alteration of seafloor rocks. The final part of this chapter is a comparison of the hot spring chemistry to the chemistry of these other observed phenomenon, in order to set some constraints on whether the hot springs could be responsible and what major disparities exist.

2.1 Sample Setting

At the 21° N site three active vent areas were sampled in 1979 and a fourth area was found and sampled in the 1981 series of ANGUS tows and Alvin dives. The ridge axis here trends N38°E (Ballard et al., 1981) and the vents occur over a distance of 8.4 km (Figure 2-1). Starting from the north the vent areas are: National Geographic Society (NGS), Ocean Bottom Seismograph (OBS), Southwest (SW) and Hanging Gardens (HG). Their x,y

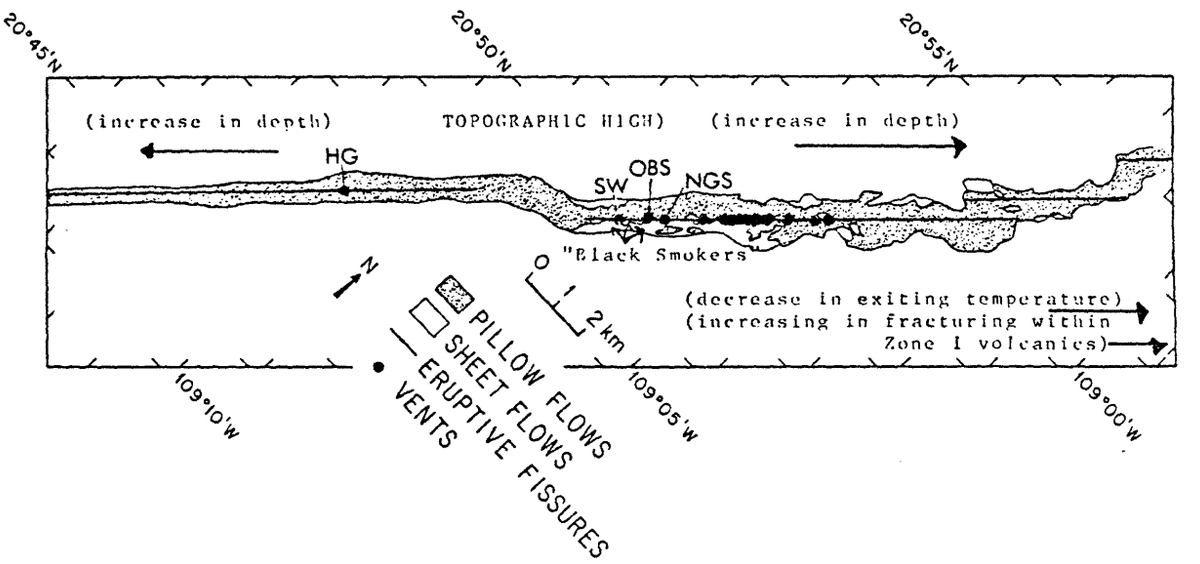

Figure 2-1: Simplified geology and vent locations at 21°N. From Ballard and Francheteau (1982). The four 21° N vent areas sampled are noted.

locations in the 1981 transponder net as well as their absolute latitude and longitude and distance from each other are given in Table 2-1.

The East Pacific Rise at 21° N has a moderate spreading rate of 6.2 cm/yr (Larson, 1971) and the axial valley averages 5 km in width (Ballard et al., 1981). Ballard et al. (1981) describe in detail the ridge axis at 21° N based on 1979 ANGUS tows and submersible work, as well as earlier results. The HG vent area (the one furthest to the southwest) was not found at the time of that survey but is included in a discussion by Ballard and Francheteau (1982) which includes some of the results of the 1981 cruise. From the 1981 survey Ballard et al. (1981) assigned relative ages to the lava flows on which the vents occur, based on the relative sediment cover. NGS and SW are on the youngest flows while OBS is on a slightly older one (HG was not included in this survey). All four of the vent areas appear to be above eruptive fissures which are presumed to be the source of the lava flows. Ballard and Francheteau (1982) point out that all of the axial springs found to date occur on the topographic high between two fracture zones. At 21° N, NGS, OBS and SW are north of this high while HG is south of it (and separated from SW by 7.2 km) (Figure 2-1). HG is on very young sheet flows, as are the other three vent areas, although the flows at HG appear to be fed by a different fissure. At both GSC and 21° N as the distance from this high increases, the temperature of the vents decreases. NGS is the most northerly vent sampled and is cooler. Cooler vents (not black smokers) exist further to the north. The survey with the French submersible Cyana was still further to the north at 21° N and found extinct vents but not active ones (Cyamex Scientific Team, 1981).

At the NGS area two vents exist; both were sampled in 1979 while only one was sampled in 1981. The vent sampled in 1981 is the more southerly of

Table 2-1: 21° N Vent Locations

Vent	x m[1]	y m	Latitude[2]	Longitude	Distance m[3]
NGS	7320	5452	20°50.26 N	109°5.65 W	
OBS	6973	5240	20°50.47 N	109°5.83 W	
SW 1[4,5]	6626	4540	20°49.05 N	109°6.85 W	
2	6618	4531	20°49.05 N	109°6.85 W	
3	6562	4510			
4	6616	4626	20°49.82 N	109°6.40 W	
5	6606	4628	20°49.82 N	109°6.40 W	
HG	1720	-769	20°47.26 N	109°8.79 W	
NGS → OBS					406
OBS → SW 1					781
→ SW 2					793
→ SW 3					838
→ SW 4					710
→ SW 5					714
SW 1 → HG					7229
SW 2 → HG					7217
SW 3 → HG					7163
SW 4 → HG					7287
SW 5 → HG					7280
NGS → HG					8370

[1]x and y are in meters within the 1981 transponder net. They are the average values based on the coordinates at the times of water sampling.

[2]Latitude and longitude are from R. Ballard and C. Sheer (personal communication).

[3]Distance is in meters.

[4]Vents SW 1 and SW 2 are so close to each other that except on dive 1149 when they were both sampled, it is difficult to distinguish which vent was sampled based on the x,y coordinates.

[5]For a more complete description of the vent sites at SW see Table 2-2.

the two sampled in 1979. No water was exiting from this vent when the submarine first approached it but after excavating it, the chimney began to flow freely and the measured temperature of 273° C was stable over the five days during which this vent was visited three times. In 1979 its measured temperature was 350° C.

Only one active vent was found at the OBS site although the several large extinct chimneys at this site have sometimes caused it to be called the "Black Forest". This vent was a triptych of three approximately three meter high chimneys on top of a large basal mound. The biology at this site is extremely sparse and only a few crabs were observed. Of the four vent areas visited at 21° N it has the largest visible sulfide deposit. The maximum measured temperature was 350° C.

The SW vent has four active black smokers along with several extinct ones and numerous warm vents or seeps between the pillows. At least one of the vents at SW was extinct and began flowing after the submersible excavated it. At another extinct chimney, overgrown by tube worms, water of 274° C was found under the worms. The maximum temperature of 355° C was measured in this area. A fuller description of the vent sites is given in Table 2-2. The vents at SW lie close to the edge of a collapse pit believed to have been formed by the draining of a lava lake. There is a greater profusion of biological activity at SW than at either NGS or OBS and there are large areas with clams nestled between pillows.

The HG area consists of one mound with several chimneys on it. It also contains a very profuse biological community. The maximum measured temperature was 351° C.

An additional vent was observed north of NGS on dive 915 during the RISE expedition in the spring of 1979. However only extinct chimneys were found on the 1981 dives.

Table 2-2: SW Vent Descriptions

Vent	Description
SW 1	(x=6626, y=4540) A single vent with three orifices, it was first sampled on dive 1149 (all three orifices). It was also sampled on dive 1153 and may have been sampled on dives 1150 and 1157. (Samples 1149-3,4,7,8,9,10,11,12, all 1150?, 1153-5,9,13,14, 1157-2?,4?,7?,8?,9?,13?) Maximum temperature = 355° C.
SW 2	(x=6618, y=4531) A single vent on a large mound, it was first sampled on dive 1149. It is very close to SW 1 and it is difficult to discern if SW 1 or SW 2 were sampled on dives 1150 (probably SW 2) and 1157. (Samples 1149-1,2,6,13, all 1150?, 1157-2?,4?,7?,8?,9?,9?,13?) Maximum temperature = 346° (350°?) C.
SW 3	(x=6562, y=4510) This vent was sampled on dive 1153 and was extinct until it was excavated by the submarine. It is approximately 8.9 m high. (Samples 1153-6,12,13,18) Maximum temperature = 270° C.
SW 4	(x=6616, y=4626) This vent was sampled on dive 1157. (Samples 1157-6,10,14,15,17,18) Maximum temperature = 275° C.
SW 5	(x=6606, y=4628) This was an extinct vent buried under tube worms. (Samples 1153-10,11) Maximum temperature = 274° C.

2.2 Solution Chemistry

In very general terms the final hydrothermal solution chemistry is determined by that of the reactants: seawater and basalt. This is complicated by the relative proportions of seawater and basalt reacting (either the composition of the rock or of the seawater may be limiting) as well as by the mineral alteration assemblage formed. A major question in these systems is whether equilibrium (with potential solubility controls) is achieved or whether the kinetics of the various reactions are most important. The chimneys are disequilibrium assemblages and this may also be true of the alteration assemblages at depth. If kinetics are important the length of time the solutions spend in contact with the rock must be addressed. Time is the parameter for which we have the least information (section 2.5). Laboratory experiments reacting seawater and basalt at elevated temperatures and pressures have shown that a finite amount of time, which varies with the crystallinity of the rock (diabase reacts slower than glass), is required for the reactions to occur. A second important parameter is temperature. From observation we can place some constaints on the temperature of the hydrothermal solutions but little is known about how the inferred reactions will proceed with variations in temperature. A generalized equation summarizing the above can be written as:

$$x\ \text{seawater} + y\ \text{rock} \rightleftarrows [\text{alteration products}]_i + [\text{hydrothermal solution}]_i \rightleftarrows \ldots$$

$$\rightleftarrows [\text{alteration products}]_f + [\text{hydrothermal solution}]_f$$

where i represents some unknown intermediate assemblage(s) for a given set of conditions

and f represents the final equilibrium assemblage for the same set of conditions.

These assemblages will be influenced by x/y, the water/rock ratio as well as by the differences between the various reaction rate constants. Changes in temperature will affect the reaction rates and products. In a closed system with increasing time this series of reactions and assemblages will proceed to the right (i.e. the reactions should have gone further towards the equilibrium assemblage). The reaction sequence is more complicated in an open system (more representative of the actual case), because new rock surfaces and/or new solutions are continuously available.

The concentration of an individual species can be expressed as:

$$C = (C_o + f(C_r) - w)h$$

where C = concentration in the hydrothermal solution
C_o = starting concentration in seawater
$f(C_r)$ = some function of the concentration in the rock
w = a removal term which may be related to solubility or the production of alteration phases.
h = hydration factor.

In this expression the water/rock ratio (x/y), time and temperature parameters are included in the $f(C_r)$ term. It is not known how each of these factors will affect the concentration and since they cannot be separated, they are combined in one term. Most of the major elements, excepting magnesium and sulfur, show a net gain as the solutions traverse the hydrothermal system; therefore $f(C_r)-w>0$.

ENDMEMBER CONCENTRATIONS

As mentioned above, magnesium is lost from seawater during reaction at elevated temperatures with basalt. Experimental work on these systems has shown that the magnesium is essentially quantitatively removed from the seawater at low water/rock ratios as are found at 21° N. (Water/rock ratios will be discussed below.) Bischoff and Dickson (1975) have shown that the magnesium reacts with a silicate species and water to form a

Mg-hydroxy-silicate with a resultant release of protons. These protons then undergo further reaction with silicates, exchanging for cations such as K^+ and Ca^{2+} and releasing them to solution.

At 21° N, Guaymas and the GSC magnesium decreases in all the vent fields and is assumed to reach zero in the pristine hydrothermal solution. Surface seawater is used to fill the dead volume in the samplers (3.8 out of 755 milliliters - Appendix 1), therefore seawater (and some magnesium) is present in all the samples. Some ambient seawater may also be entrained during sampling and based on mineralogical evidence the chimneys themselves are somewhat "leaky" to seawater (Haymon and Kastner, 1981; Goldfarb, 1982). The assumption that magnesium is zero in the pure hydrothermal solution can therefore not be proven directly. The magnesium content of a solution is used as a mixing indicator. At 21° N samples with Mg <2.1 mmoles/kg (>96% hydrothermal water) were obtained in all the vent fields. A check that the magnesium is actually a sampling artifact comes from the Mg/SO_4 ratio. If this (molar) ratio is equal to the seawater value, both of these species can be assumed to be from seawater entrainment. The observed Mg/SO_4 ratio is close to the seawater value in all of the samples and within a small error they extrapolate to zero together (see sulfur discussion and Table 2-8).

The concentration of the "pure" hydrothermal endmember for a given element is obtained by fitting a least squares line to the data, forcing it through the composition of ambient seawater at the appropriate depth and extrapolating to zero magnesium. These calculated endmember concentrations are the ones given in the tables throughout this chapter. The complete data set is given in Appendix 3.

Once the endmember concentration has been determined several other

parameters can be calculated. A simple but important calculation is to find the net addition (δ) of an element to the solution and to then determine what fraction of the original rock composition this represents. The net addition (δ) is arrived at by correcting for the water loss due to rock hydration and the amount of the element originally present in the seawater:

$$\delta = \frac{C}{h} - C_o = f(C_r) - w.$$

The correction for hydration can be made based on either of two parameters. From the $\delta^{18}O$-δD results (Craig and Welhan, personal communication) it appears that the solutions from all of the 21° N vent areas have lost approximately 10% of their water; presumably due to rock hydration. From the chloride data, which only show an increase in the NGS vent, the water loss appears to be 7%. (In the other vents there is a net Cl loss.) To calculate the net additions (δ) to the solution given in Table 2-3, all of the solutions are corrected for a 7% loss of water (as the isotopes show the same loss for all the areas) and then corrected for the original composition of the seawater (i.e. assuming w is zero and solving for $f(C_r)$). The water loss due to Cl is used rather than that from the isotopes because the isotopic value is dependent on assumptions about the temperature of reaction and the isotopic fractionation factors which are not well known. If the 7% water loss from Cl is an underestimate (i.e. a Cl sink is also active at NGS) the δ values will be too large. The tabulated δ values can be viewed as an upper limit.

A calculation based on the net addition (δ) of an element to seawater can be made to derive the approximate water/rock ratio. If it is assumed that the element of interest is quantitatively leached from the rock (extraction efficiency = 1), the amount originally present in the rock

Table 2-3: Calculated Water/Rock Ratios and Extraction Efficiencies for 21° N

Element		Rock	δ	Water/ Rock	Extraction Efficiency[3]	Alkali Extraction Efficiency[4]
Li	NGS	$1.45^{W}m^{1,2}$	937μ	1.6	0.45	1.1
	OBS		805	1.8	0.39	1.1
	SW		812	1.8	0.39	1.1
	HG		1296	1.1	0.45	1.7
Na	NGS	$0.78^{J}M$	13m	60	0.012	0.028
	OBS		-60			
	SW		-54			
	HG		-50			
K	NGS	$24^{J}m$	14.3m	1.7	0.42	≡ 1
	OBS		11.8	2.0	0.34	≡ 1
	SW		11.8	2.0	0.34	≡ 1
	HG		12.5	1.9	0.26	≡ 1
Rb	NGS	$8\text{-}46^{KH}\mu$	28μ	0.29-1.6	0.43-2.5	1.0-6.0
	OBS		25	0.32-1.8	0.38-2.2	1.1-6.3
	SW		24	0.33-1.9	0.37-2.1	1.0-6.0
	HG		30	0.27-1.5	0.33-1.9	1.2-7.1
Be	NGS	$50^{W}\mu$	25n	2000	3.5×10^{-4}	8.5×10^{-4}
	OBS		14	3600	2.0×10^{-4}	5.6×10^{-4}
	SW		9.3	5400	1.3×10^{-4}	3.7×10^{-4}
	HG		12	4200	1.2×10^{-4}	4.6×10^{-4}
Ca	NGS	$2.15^{J}M$	9.2m	230	0.003	7.2×10^{-3}
	OBS		4.3	500	0.001	4.0×10^{-3}
	SW		5.3	410	0.002	4.9×10^{-3}
	HG		0.7	3100	1.6×10^{-4}	6.2×10^{-4}
Mg	NGS		-52.7m			
	OBS		-52.7			
	SW		-52.7			
	HG		-52.7			
Sr	NGS	$0.7\text{-}1.8^{KH}m$	3μ	230-600	0.001-0.003	0.007-0.003
	OBS		-11			
	SW		-10			
	HG		-26			
Ba	NGS	$150\text{-}210^{R}\mu$	15μ	10-14	0.05-0.07	0.12-0.17
	OBS		7	21-30	0.02-0.03	0.07-0.09
	SW		9	17-23	0.03-0.04	0.09-0.12
	HG		10	15-21	0.02-0.03	0.09-0.13

Element		Rock	δ	Water/ Rock	Extraction Efficiency[3]	Alkali Extraction Efficiency[4]
Cl	NGS		≡ 0m			
	OBS		-84			
	SW		-77			
	HG		-77			
SiO_2	NGS	$8.25^{J}M$	18.0m	460	0.0015	0.0037
	OBS		16.2	510	0.0014	0.0039
	SW		15.9	520	0.0013	0.0039
	HG		14.3	580	0.0009	0.0033
Al	NGS	$3.02^{J}M$	3.7μ	8.2×10^{5}	8.6×10^{-7}	2.1×10^{-6}
	OBS		4.8	6.3×10^{5}	1.1×10^{-6}	3.2×10^{-6}
	SW		4.4	6.9×10^{5}	1.0×10^{-6}	2.9×10^{-6}
	HG		4.2	7.2×10^{5}	7.0×10^{-7}	2.6×10^{-6}
SO_4	NGS	0	-27.9m			
	OBS		-27.4			
	SW		-27.3			
	HG		-27.5			
H_2S	NGS	$13^{R}m$	6.13m	2.1	0.33	0.80
	OBS		6.81	1.9	0.37	1.1
	SW		6.95	1.9	0.37	1.7
	HG		7.81	1.7	0.30	1.1
As	NGS	$13\text{-}27^{W}\mu$	<30n	-	-	-
	OBS		203	64-130	0.005-0.011	0.015-0.031
	SW		172	76-160	0.004-0.009	0.013-0.026
	HG		393	33-69	0.007-0.015	0.028-0.057
Se	NGS	$1.9\text{-}2.3^{KH}\mu$	<1n	-	-	-
	OBS		63	30-37	0.019-0.023	0.055-0.066
	SW		63	30-37	0.019-0.023	0.055-0.066
	HG		63	30-37	0.014-0.017	0.052-0.063
Mn	NGS	$26^{J}m$	935μ	28	0.025	0.061
	OBS		895	29	0.024	0.069
	SW		652	40	0.018	0.050
	HG		819	32	0.016	0.060
Fe	NGS	$1.33^{J}M$	812μ	1600	4.3×10^{-4}	1.0×10^{-3}
	OBS		1552	860	8.2×10^{-5}	2.3×10^{-3}
	SW		699	1900	3.7×10^{-4}	1.1×10^{-3}
	HG		2265	590	8.5×10^{-4}	3.2×10^{-3}
Co	NGS	$0.75^{KH}m$	21n	36000	2.0×10^{-5}	4.8×10^{-5}
	OBS		199	3800	1.9×10^{-4}	5.3×10^{-4}
	SW		62	12000	5.8×10^{-5}	1.7×10^{-4}
	HG		212	3500	1.4×10^{-4}	5.4×10^{-4}

Element		Rock	δ	Water/ Rock	Extraction Efficiency[3]	Alkali Extraction Efficiency[4]
Ni	NGS	1-5^{KH}m	<130n	>7600-	$<9.1\times10^{-8}$	$<2.2\times10^{-7}$
	OBS			>38000	$<9.1\times10^{-8}$	$<2.6\times10^{-7}$
	SW				$<9.1\times10^{-8}$	$<2.6\times10^{-7}$
	HG				$<6.5\times10^{-8}$	$<2.5\times10^{-7}$
Cu	NGS	1.4^{KH}m	<0.02μ	-	-	-
	OBS		33	42	0.017	0.047
	SW		9.0	160	0.005	0.013
	HG		41	34	0.015	0.056
Zn	NGS	1.1^{KH}m	37μ	30	0.024	0.057
	OBS		99	11	0.063	0.18
	SW		83	13	0.053	0.15
	HG		97	11	0.044	0.17
Ag	NGS	222-417^{KH}n	<1n	-	-	-
	OBS		35	6.3-12	0.059-0.11	0.17-0.32
	SW		24	9.3-17	0.040-0.076	0.12-0.22
	HG		35	6.3-12	0.079-0.042	0.16-0.30
Cd	NGS	1.1^{KH}μ	15n	73	0.010	0.023
	OBS		155	7.1	0.099	0.28
	SW		133	8.3	0.085	0.24
	HG		167	6.6	0.076	0.29
Pb	NGS	~10^{KH}μ	170n	59	0.012	0.029
	OBS		287	35	0.020	0.057
	SW		181	55	0.013	0.036
	HG		335	30	0.017	0.064

[1]Units: M = moles/kg
m = millimoles/kg
μ = micromoles/kg
n = nanomoles/kg.

[2]The superscript denotes the source of the rock data:
J = Juteau et al. (1980)
KH = Kay and Hubbard (1978)
R = RISE Project Group (1980)
W = Wedepohl (1969)

[3]The water/rock ratio is assumed to be 0.5 for HG and 0.7 for NGS, OBS and SW.

[4]The water/rock ratio is assumed to be 1.7 for NGS, 1.9 for HG and 2.0 for OBS and SW.

divided by the net addition to the solution is the water/rock ratio:

$$\text{water/rock ratio} \equiv \text{concentration in the rock}/\delta .$$

These values are given in Table 2-3. This definition assumes a closed system. A difficulty is knowing the concentration in the rock accurately. The rock values have been taken from a variety of sources. Where possible the rock concentration data were taken from the RISE Study Group (1980); Juteau et al. (1980); or Moore et al. (1977); all of whom analyzed rocks collected from 21° N on the EPR. Otherwise the values of Kay and Hubbard (1978) were used. If no other data were available the values given in the Handbook of Geochemistry (Wedepohl, 1969) were used. As the alkalis have been shown to be almost quantitatively leached from the rocks in experiments (Mottl and Holland, 1978) and to undergo only minor secondary reactions, they are the elements best used to determine the water/rock ratio. Many of the other elements appear to undergo secondary precipitation reactions and this is apparent from their high calculated water/rock ratios (e.g. Ca and Mn). From the alkali results (Table 2-3) it can be seen that the 21° N system has a low water/rock ratio of close to 1. This has important implications for the final solution and rock composition.

A second parameter that can be determined if the water/rock ratio is known is the extraction efficiency:

$$\text{Extraction Efficiency} \equiv \frac{(\text{water/rock ratio}) \times (\text{net addition } \delta \text{ to solution})}{\text{initial rock concentration}}$$

Based on the water isotopes, Craig and Welhan (personal communication) have calculated that the water/rock ratio is 0.5 at HG and 0.7 at SW, OBS and NGS. As mentioned above their are some difficulties in using the isotopic values. The uncertainities in this case would be much greater if composition data were used because the rock composition is not good and the

assumption of total extraction from the rock is an oversimplification. The water/rock ratios of Craig and Welhan have been used to calculate the extraction efficiency in the fifth column of Table 2-3. The final column, alkali extraction efficiency, is calculated on the basis of potassium, the only alkali for which determinations in 21° N rocks are available. Potassium is assumed to be quantitatively removed from the rock (extraction efficiency = 1) and the water/rock ratio obtained for each vent area from this calculation is used to calculate the extraction efficiency for the other elements. Values greater than one are physically impossible and are a result of the uncertainities in the calculation.

As the concepts of water/rock ratio and extraction efficiency are important in the following they will be discussed more fully. The water/rock ratio is a measure of the total transfer of a species from rock to solution. It is often called an effective water/rock ratio (Ohmoto and Rye, 1974) because it is dependent on many factors. Seyfried and Mottl (1982) have defined it as the total mass of water which has passed through a hydrothermal system during its lifetime divided by the mass of altered rock within the system. In the case of 21° N this ratio is dependent on the "freshness" of the rock (i.e. if the rock has been previously altered), the pathlength (i.e. the amount of rock the solution comes in contact with, which may vary between vent areas), the time the solution spends in contact with the rock (presumably longer contact time will result in more being leached into the solution), whether the solution sees a different temperature history at depth (precipitation or retrograde reactions may occur if the temperature drops or the leaching may be more efficient at a higher temperature). 21° N is also an open system rather than a closed flow system. As all of these complexities are incorporated into the term water/rock ratio it should be kept in mind that it is not truly a physical

"water/rock" ratio, but more a measure of the extent of reaction. The importance of the low water/rock ratios calculated for 21° N are that they imply that the rock is very "fresh" and has undergone minimal previous alteration and that a small volume of water relative to rock is reacting. (It also means the degree of reaction is very complete for the alkalis.) A large water/rock ratio may imply that relatively large volumes of water have previously reacted with a given amount of rock (i.e. it is already highly altered and the easily leachable species are gone) and the actual physical water/rock ratio could still be small. Alternatively it may mean that the pathlength is short and the circulation is fast so that the degree of reaction between the solution and solid is very small. A third possibility is that the element has undergone secondary precipitation. The concept of water/rock ratio is a useful one as long as it is not taken to imply a literal physical parameter.

Extraction efficiency is a better term because it does not imply the physical parameter that water/rock ratio does. Unfortunately to calculate an extraction efficiency it is necessary to use a water/rock ratio. As much of the information to be gained from this parameter is on a comparative element-to-element basis this is not a great disadvantage. With the attendant uncertainities of the basalt composition this calculation can at best provide a semi-quantitative understanding of whether an element is being quantitatively leached from the rock into solution (i.e. the elemental composition of the solution is "rock-limited").

MAJOR ELEMENTS

The data are organized into the following groupings: Alkalis (Li, Na, K and Rb); Alkaline Earths (Be, Mg, Ca, Sr and Ba); Aluminum; Silica; Carbon (pH and Alkalinity); Halogens (F and Cl); and Sulfur (SO_4 and H_2S). The data are presented in both figures and tabular form. Data from the

Galapagos Spreading Center (GSC) hydrothermal solutions (Edmond et al., 1979a,b) are included in the tables of the 21° N and Guaymas data for comparison. All of the tabulated data are of the extrapolated endmember concentrations (Mg = 0, as discussed above). At Guaymas samples with low magnesium were sampled in some but not all of the vent fields and almost every vent sampled has a different composition. The GSC data are the result of much greater extrapolations as no samples with Mg <50 mmoles/kg (seawater = 53 mmoles/kg) were obtained in this area. Consequently these values have a greater uncertainty.

The data for each element are also presented in a figure. The figures are all of the same form with the element of interest (y-axis) versus Mg (x-axis) and they are mixing lines between the hydrothermal endmember and seawater. These mixing lines are artifacts of the sampling procedure and are only useful for the soluble elements where they can aid in determining endmember composition with more confidence than by analyzing a few endmember samples alone. A discussion on an element by element basis follows.

THE ALKALIS

Lithium, sodium, potassium and rubidium were determined in the hydrothermal solutions.

Lithium: Lithium increases in all four vent areas sampled at 21° N (Figure 2-2). The HG vent area has the highest concentration, 1322 μmoles/kg, NGS is next at 1033 and the SW site at 899 and OBS site at 891 are indistinguishable. These values are comparable to the GSC values (Table 2-4) of 689-1142 μmoles/l, although the HG vent is higher. The lithium concentration in seawater is 26 μmoles/kg; the vent concentrations represent enrichment factors of up to 50 times the ambient values.

Approximately half of the lithium is removed from the rock (Table 2-3). The water/rock ratio calculated from Li is approximately twice that

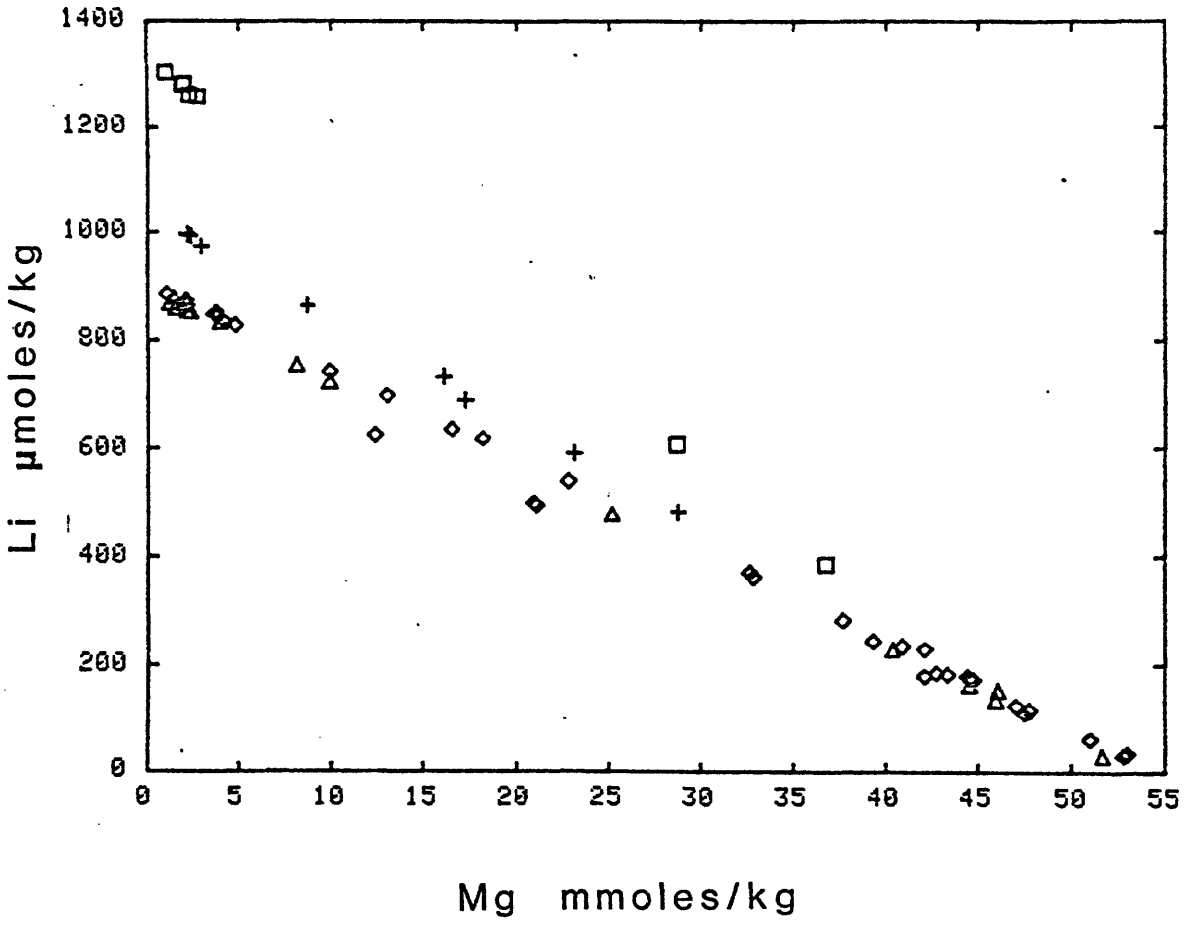

Figure 2-2: Lithium versus magnesium at 21° N. The plot symbols distinguish the four vent areas sampled and are as follows for this and all subsequent 21° N data plots:

+ = National Geographic Society (NGS)
△ = Ocean Bottom Seismograph (OBS)
◇ = Southwest (SW)
□ = Hanging Gardens (HG).

Table 2-4: Endmember Concentrations - The Alkalis

	Li μ[1]	Na (calc)[3] m	K m	Rb μ
21° NORTH				
NGS (+)	1033	510	25.8	31
OBS (△)	891	432	23.2	28
SW (◇)	899	439	23.2	27
HG (□)	1322	443	23.9	33
GUAYMAS				
Area: 1 (◇)	1054	489	48.5	85
2 (△)	954	478	46.3	77
3 (+)	720	513	37.1	57
4 (□)	873	485	40.1	66
5 (•)	933	488	43.1	74
6 (×)	896	475	45.1	74
7 (◇△)	1076	490	49.2	86
8 (△)				
9 (□□)	630	480	32.5	57
10 (*)				
GSC[2]	689-1142	+,-	18.7-18.8	13.4-21.2
SEAWATER	26	464(21°) 463(GY)	9.79	1.3

[1]Units: μ = micromoles/kg
m = millimoles/kg

[2]All GSC data is /liter.

[3]Sodium calculated from the charge balance.

determined from the water isotopes (Craig and Welhan, pers. communication).

Sodium: Sodium increases at NGS and decreases in the other three vent areas (Figure 2-3a). Sodium was measured by flame atomic absorption spectrophotometry but the 2% error precludes separating endmembers in the other three sites. Once all the major species were measured, the charge balance was calculated for all the samples. In almost all cases it was <20 meq/kg (<2% of the total charge) and was randomly distributed between excess positive and negative charge. It was therefore assumed that no major charged species was missing nor was there a systematic offset in one or other of the measurements, and sodium was calculated from the charge balance (Figure 2-3b). The charge balance sodiums have greatly reduced scatter and different endmembers can be distinguished. From the ambient value of 464 mmoles/kg sodium increases at the NGS site to 510, while it decreases to 432 at OBS, 439 at SW and 443 at HG. A more complete discussion of the sodium will be deferred until after the chloride data (which are more precise) are presented. Both positive and negative trends were also observed at the GSC (Table 2-4). Since sodium and chloride dominate over all the other charged species by at least an order of magnitude in concentration, and given the magnitude of the sodium variation they must be tied together to maintain electroneutrality.

The behavior of Na is a result of its high starting concentration in the solution (which is almost the same as that in the rock). This is one of only a few elements which has a sink in the rock (in three vent areas). Na is not conservative with respect to Cl and a small amount may be added from the rock to the solution in the NGS area. Na is probably lost due to the formation of albite from anorthite (albitization):

$$CaAl_2Si_2O_8 + Na^+ + H_4SiO_4 \rightarrow NaAlSi_3O_8 + Ca^{2+} + Al(OH)_4^-$$

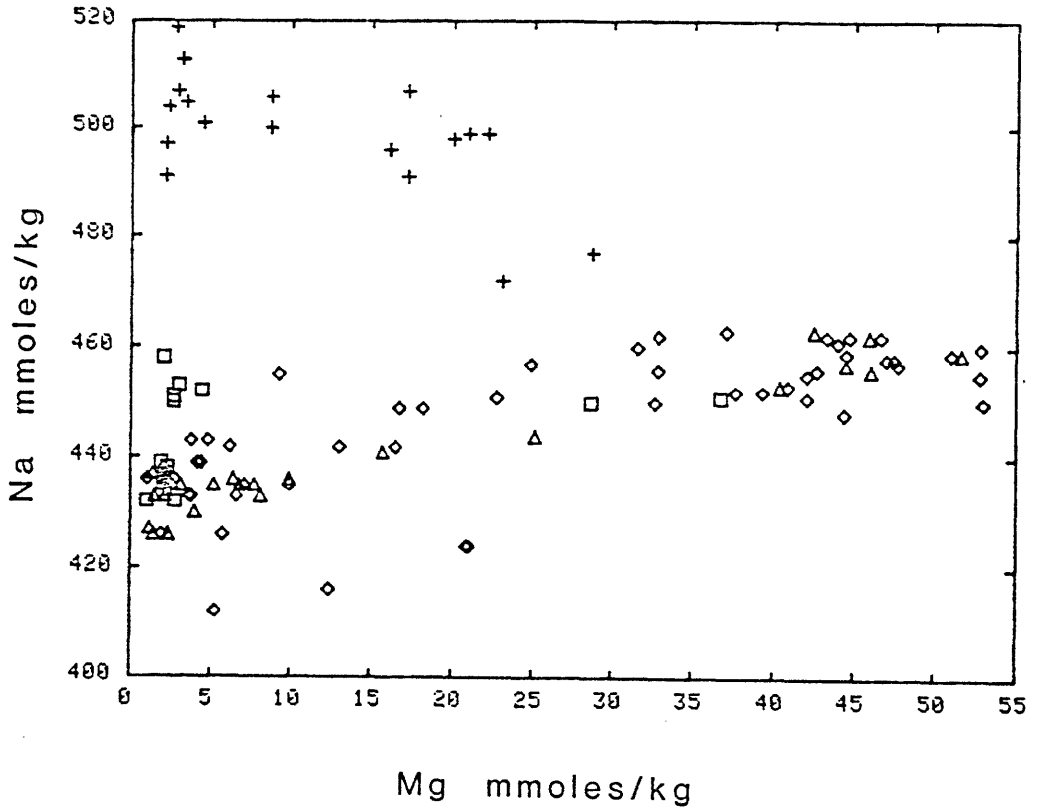

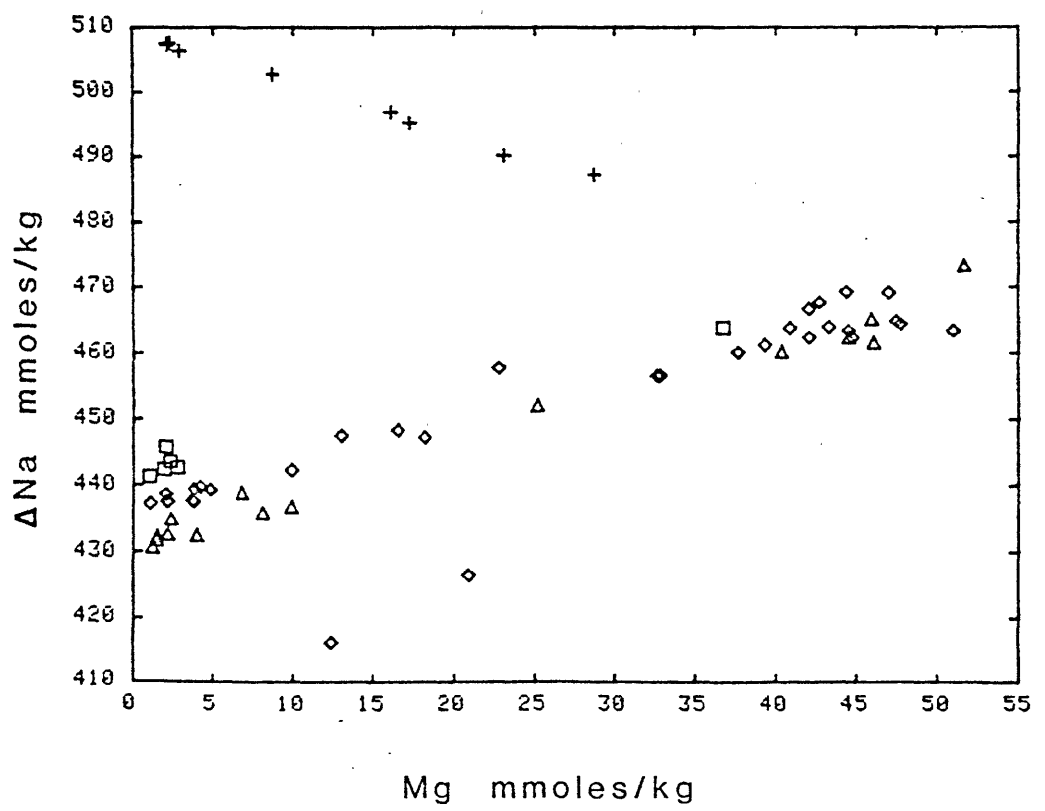

Figure 2-3: Sodium versus magnesium at 21° N.
a. measured sodium.
b. sodium calculated from the charge balance.

at depth in the system. This is a typical reaction of greenschist facies metamorphism. (Greenschist facies metamorphism occurs at temperatures of ~250-450° C and moderate to low pressures. The assemblage typically contains chlorite + albite + epidote + quartz.) The gain of sodium may be due to the conversion of albite to chlorite, which is another mineral typical of the greenschist facies.

$$NaAlSi_3O_8 + 3Mg^{2+} + 2Fe^{2+} + Al(OH)_4^- + 6H_2O$$
$$\rightarrow Mg_3Fe_2Al_2Si_3O_{10}(OH)_8 + Na^+ + 8H^+.$$

The reactions in this section are written for simplicity for the pure endmembers of the albite and anorthite solid solution series. The composition used for chlorite (which also has a range in composition) is that found by Humphris (1977). Al is written as the $Al(OH)_4^-$ species which is its dominant form in seawater. Based on thermodynamic modelling Al is probably present as $Al(OH)_3^\circ$ at the pH of the hydrothermal solutions. As its speciation at the high temperature and pressure is unknown, although probably still a hydroxy species, the equations are written with $Al(OH)_4^-$. A different speciation will change the proton balance but will not affect any of the other conclusions.

Potassium: Potassium exhibits a very limited variability between vent fields (Figure 2-4). NGS, at 25.8 mmoles/kg, has the highest potassium concentration while HG has 23.9 and is just barely resolvable from the OBS and SW sites at 23.2. These values are significantly higher than the 18.7-18.8 mmoles/l observed at the Galapagos (Table 2-4). The K values are approximately 2.5 times the seawater value of 9.79 mmoles/kg. Potassium, like Li, has a high extraction efficiency from the rock and its calculated water/rock ratio (Table 2-3) is slightly higher than that of Craig and Welhan. K is assumed to be leached from the rocks by a H^+ for K^+ exchange.

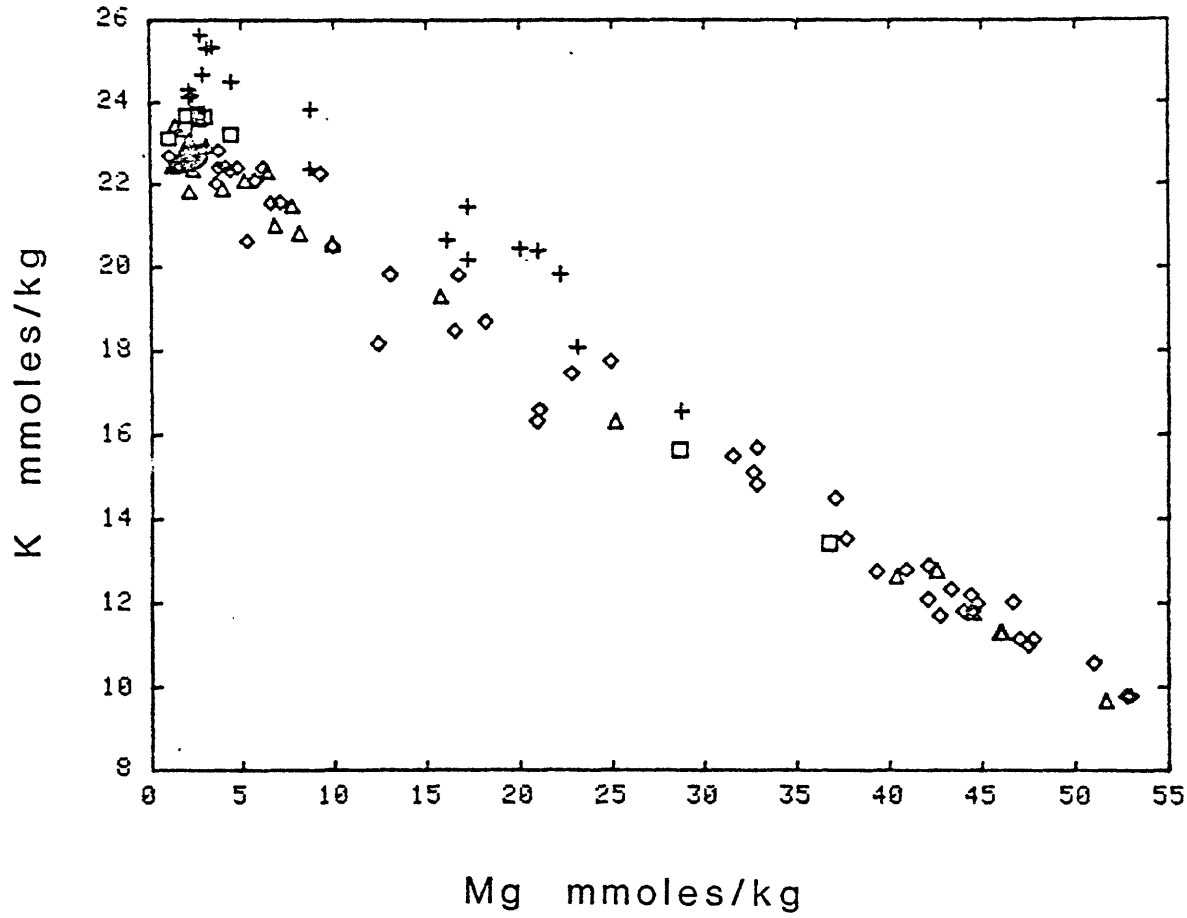

Figure 2-4: Potassium versus magnesium at 21° N.

Rubidium: As for potassium, there is very little variability in rubidium concentration in the 21° N vent fields (Figure 2-4). HG contains the most rubidium, 33 μmoles/kg, followed by NGS at 31, OBS at 28 and 27 at SW. These values are consistently higher than the GSC values of 13.4-21.2 μmoles/l (Table 2-4). Rubidium and potassium both undergo retrograde reactions and are taken up by basalt during low temperature (<200° C.) alteration (Hart, 1969). The lower values for both these elements at GSC may indicate that uptake reactions are occurring in that system. Alternatively the GSC rocks may contain less of these elements due to either their original composition, or they may be more altered and have already had substantial amounts of these elements leached out. The 21° N values for rubidium are approximately 25 times the seawater concentrations of 1.3 μmoles/kg. Rubidium, like Li and K has a very high extraction efficiency. Its implied extraction efficiency may be >1, but this is probably a result of the uncertainty in the rock values.

Li/K is greatest at HG (0.06) and is approximately the same at the other three areas (NGS, OBS, SW = 0.04) (Figure 2-6). This is due to the higher concentration of Li at HG rather than a lower concentration of K. The basalt Li/K ≃ 0.05 implying that the HG solutions may Li-rich and the other three vents Li-poor with respect to basalt. Li is an incompatible element and may be leached more quickly. The higher ratio may imply that HG is "fresher" rock that has undergone less leaching. Alternatively it could imply a different substrate composition at HG or a higher glass/crystallinity ratio.

The above suggests that the alkalis (except for Na) are almost quantitatively leached from the rock into the hydrothermal solutions at 21° N. Na is the only alkali which appears to undergo quantitatively important secondary reactions, such as incorporation into an albite phase.

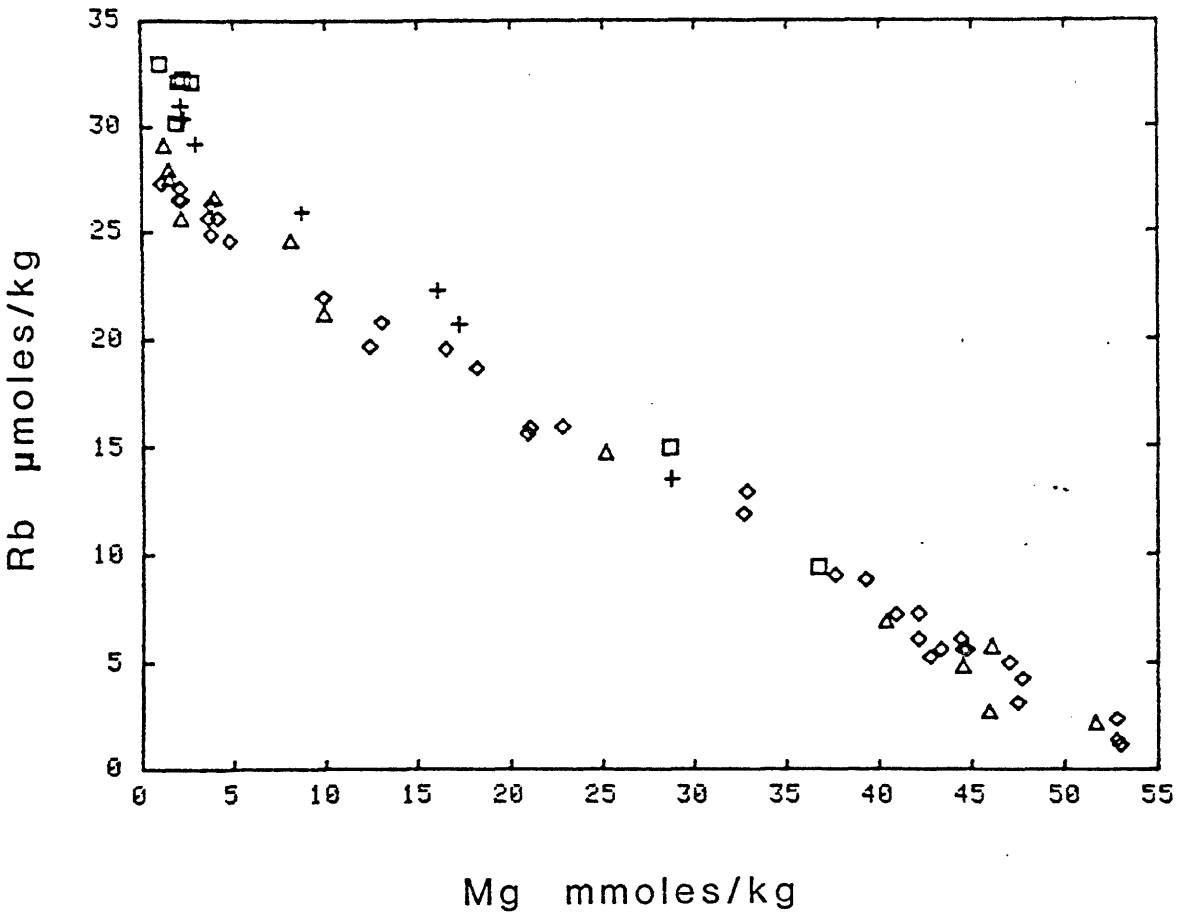

Figure 2-5: Rubidium versus magnesium at 21° N.

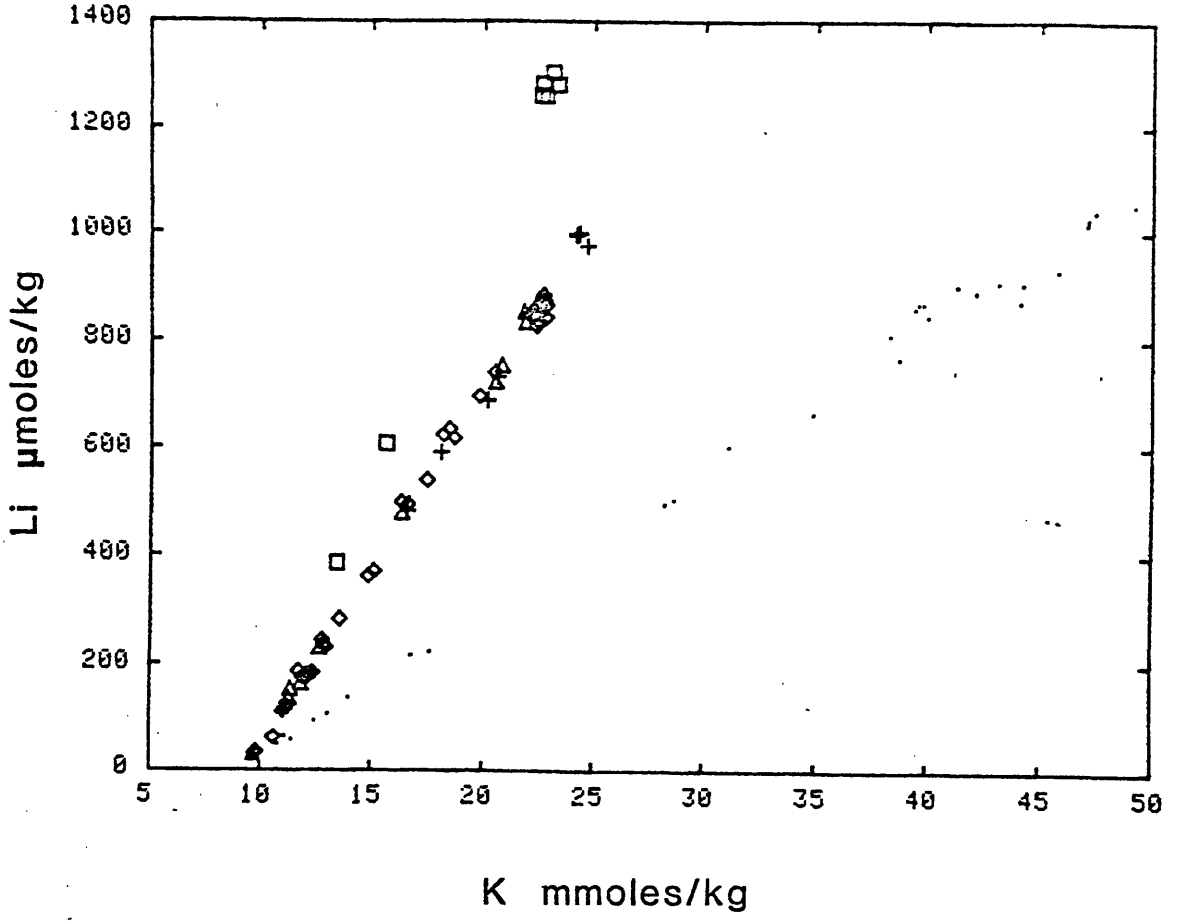

Figure 2-6: Lithium versus potassium at 21° N and Guaymas. All Guaymas vent areas are represented by •.Li/K in tholeiitic basalt is ~0.05 and in marine sediments is ~0.01. The 21° N vent areas range from 0.06 (HG) to 0.04 (NGS, OBS, SW). The Guaymas areas are ~0.02.

THE ALKALINE EARTHS

This group of elements (Be, Mg, Ca, Sr and Ba were measured) shows the largest diversity of behavior. Beryllium, calcium and barium all increase in the solutions while Mg decreases and strontium both increases and decreases.

Beryllium: Beryllium in the 21° N vents is enriched more than a thousandfold over the ambient seawater concentration of 20 pmoles/kg (Table 2-5). Although Be has a large enrichment in the hydrothermal solutions, it is second only to Al in its low extraction efficiency from the rock (Table 2-3). NGS shows the largest increase to 37 nmoles/kg followed by OBS 15, HG 13 and SW at 10 (Figure 2-7). The same range in concentration is observed at the GSC. Several of the vents at SW were sealed (inactive) until excavated by the submarine. These vents have higher beryllium contents (up to 17 nmoles/kg); second only to NGS. These higher concentrations may be due to the hot water sitting inside the chimney or rock conduits and "cooking", causing additional leaching of Be into the solutions. This hypothesis cannot at present be proven as too little is known about the geochemistry of this element to postulate possible controls on its solution chemistry.

Magnesium: Magnesium decreases in all the vent fields and is assumed to reach zero in the hydrothermal endmember (Table 2-5) although this cannot be directly proven. As discussed above, magnesium is used as an indicator of mixing between the hydrothermal solutions and seawater. Magnesium decreases to approximately 1 mmole/kg in all the fields except for NGS where 2.1 mmoles/kg is the minimum value measured. The zero magnesium endmember agrees with the Galapagos extrapolation of zero magnesium at 344° C. (Edmond et al., 1979a).

Table 2-5: Endmember Concentrations - The Alkaline Earths

	Be	Mg	Ca	Sr	Ba (ΣBa)
	n[1]	m	m	μ	μ
21° NORTH					
NGS (+)	37	0	20.8	97	>15 (16)
OBS (△)	15	0	15.6	81	> 7 (8)
SW (◇)	10	0	16.6	83	> 9 (10)
HG (□)	13	0	11.7	65	>10 (11)
GUAYMAS					
Area: 1 (◇)	12	0	29.0	202	>12
2 (△)	18	0	28.7	184	>15 (20)
3 (+)	42	0	41.5	253	> 7 (15)
4 (□)	29	0	34.0	226	>42 (54)
5 (•)	29	0	30.9	211	>13
6 (×)	60	0	26.6	172	>16
7 (◈)	17	0	29.5	212	>24
8 (⧋)					
9 (⊞)	91	0	30.2	160	
10 (✳)					
GSC[2]	11-37	0	24.6-40.2	87	17.2-42.6
SEAWATER	0.02	52.7(21°) 52.6(GY)	10.2	87	0.14

[1]Units: n = nanomoles/kg
μ = micromoles/kg
m = millimoles/kg

[2]All GSC data is /liter.

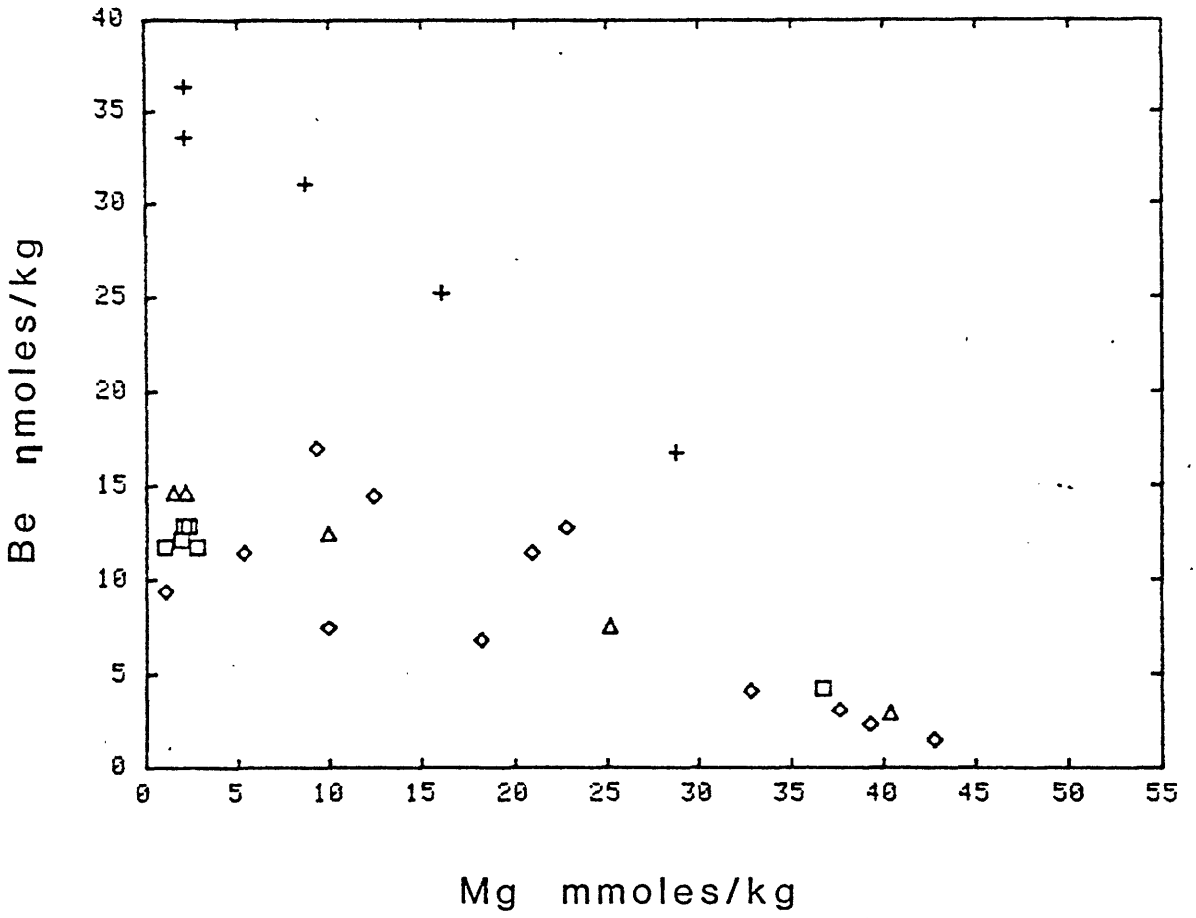

Figure 2-7: Beryllium versus magnesium at 21° N.

Calcium: Calcium increases by varying amounts in all the vent areas (Figure 2-8). The HG area has the smallest increase to only 11.7 mmoles/kg (seawater contains 10.2 mmoles/kg), while OBS reaches 15.6, SW 16.6 and NGS 20.8. Once a correction is made for water loss due to hydration, HG has only a 0.7 mmole/kg increase (see Cl discussion). These calcium increases are considerably less than the 24.6-40.2 mmoles/l observed in the GSC vents (Table 2-5). The scatter in the 21° N calcium is greatly reduced when it is examined relative to the sulfate data (Figure 2-9). Apparently anhydrite ($CaSO_4$) particles from the chimneys were entrained in several of the samples, especially those from the SW vent area, and its dissolution caused anomalously high calcium and sulfate values.

The 21° N calcium concentrations are the lowest observed in any submarine hydrothermal system and this low extraction efficiency (Table 2-5) is probably due to the secondary precipitation of Ca-silicates at depth. Epidote is the most common Ca-silicate mineral found in greenschist facies altered submarine rocks. Epidote was not formed in the experiments (the reason for this is not clear but may be a nucleation problem) but other Ca phases were. For the purpose of simplicity Ca will be assumed to enter an epidote phase. Ca may be leached into solution by a H^+ exchange or by albitization of anorthite:

$$Na^+ + CaAl_2Si_2O_8 + H_4SiO_4 \rightarrow NaAlSi_3O_8 + Ca^{2+} + Al(OH)_4^-.$$

It may be lost by the formation of epidote:

$$Ca^{2+} + CaAl_2Si_2O_8 + Al(OH)_4^- + H_4SiO_4 \rightarrow Ca_2Al_3Si_3O_{12}(OH) + 3H_2O + H^+.$$

If alteration under the temperature and pressure conditions of greenschist facies metamorphism continues epidote may be converted to chlorite with a resultant release of Ca:

$$Ca_2Al_3Si_3O_{12}(OH) + 3Mg^{2+} + 2Fe^{2+} + 9H_2O$$
$$\rightarrow Mg_3Fe_2Al_2Si_3O_{10}(OH)_8 + 2Ca^{2+} + Al(OH)_4^- + 7H^+.$$

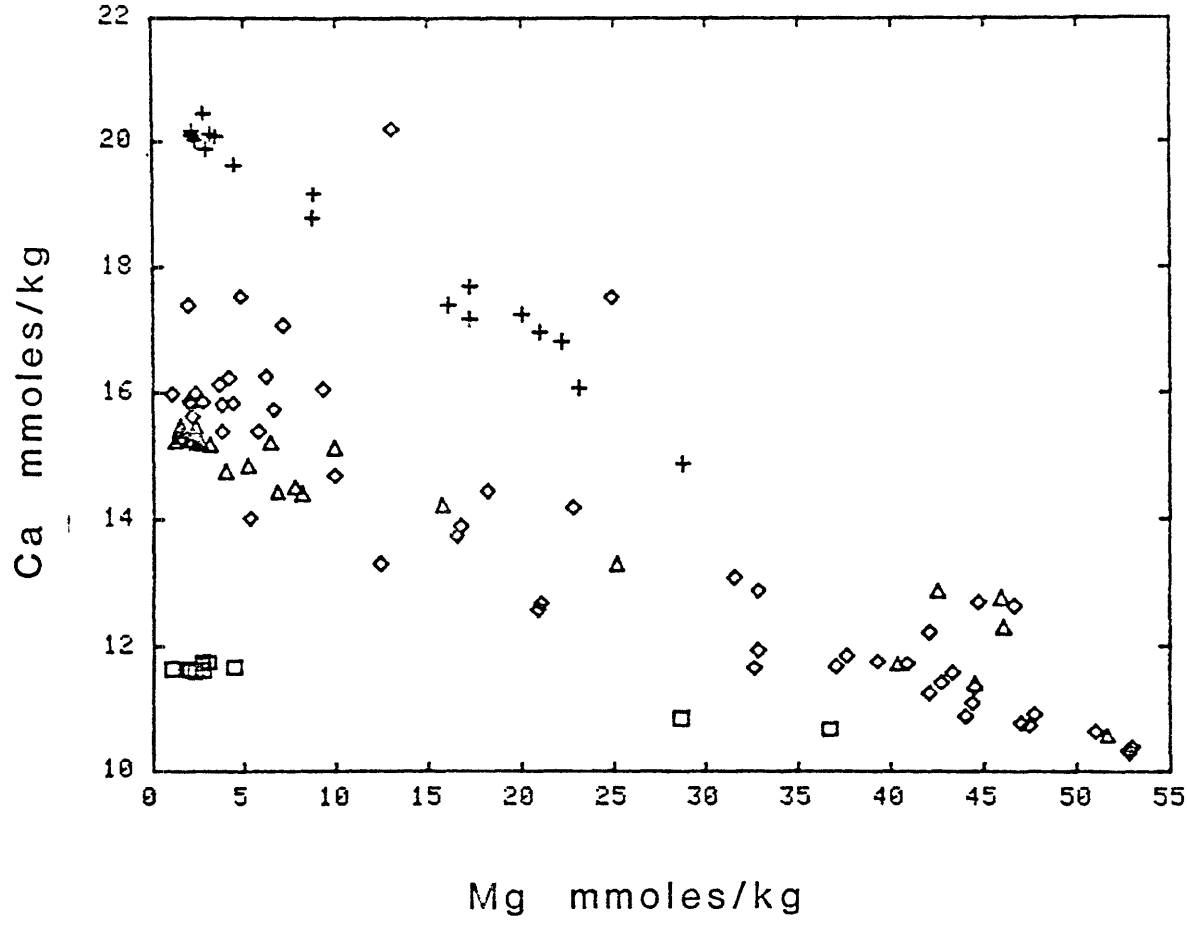

Figure 2-8: Calcium versus magnesium at 21° N.

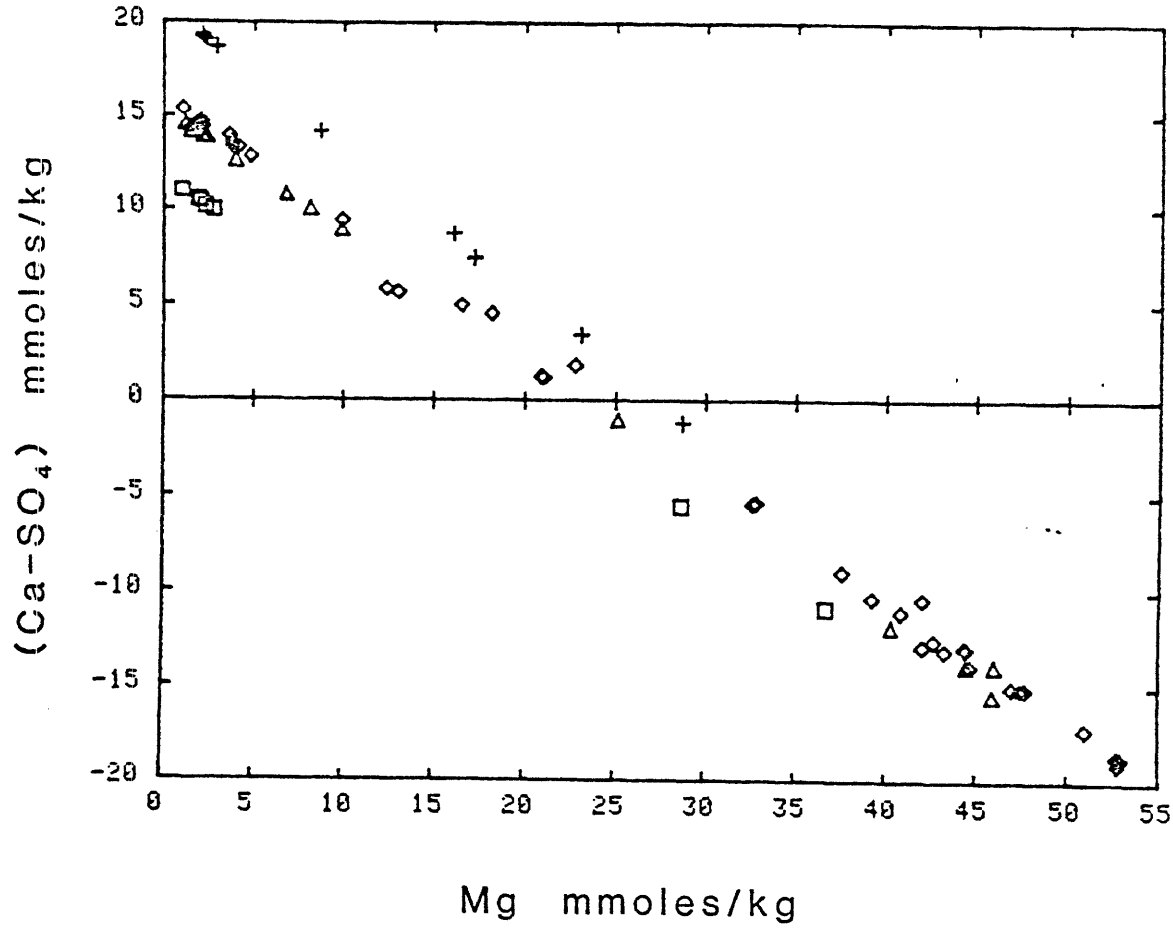

Figure 2-9: (Calcium - sulfate) versus magnesium at 21° N.

The cycle of Ca is therefore complex with numerous source and sink reactions available. Note that the precipitation of calcium, as in an epidote phase causes the release of protons. These reactions may aid in maintaining the acidity of the solutions once the Mg is consumed.

Strontium: Strontium is the only element besides sodium (and chloride) to have both increasing and decreasing trends (Figure 2-10). Like sodium (and chloride), it increases at NGS to 95 μmoles/kg while decreasing at HG to 65 μmoles/kg. It decreases slightly from the seawater concentration of 87 μmoles/kg to 83 μmoles/kg at SW and to 81 μmoles/kg at OBS. The endmember concentration was calculated using only those samples with Mg <5 mmoles/kg as entrainment of anhydrite containing strontium in the middle (mixed) samples gives artificially high values. Within the resolution of the GSC data, strontium appeared to remain unchanged from the seawater value (Table 2-5), which is consistent with the small concentration anomalies seen at GSC.

The Sr isotopes vary very slightly between the vents, but with values of ~0.703 (T. Trull, unpublished data) they are almost completely exchanged with the basalt.

Strontium has a very low extraction efficiency (Table 2-3) yet the isotopic data show that it is almost completely exchanged with the basalt. The most likely explanation is either that the small total change in concentration is just fortuitous or solubility controlled by an unspecified phase, and that it undergoes the same release/precipitation reactions as Ca at depth which allow the isotopes to become completely exchanged. Humphris and Thompson (1978a) found enrichments of Sr in epidotes, in support of this hypothesis.

Barium: Barium increases in all the vent fields (Figure 2-11). The

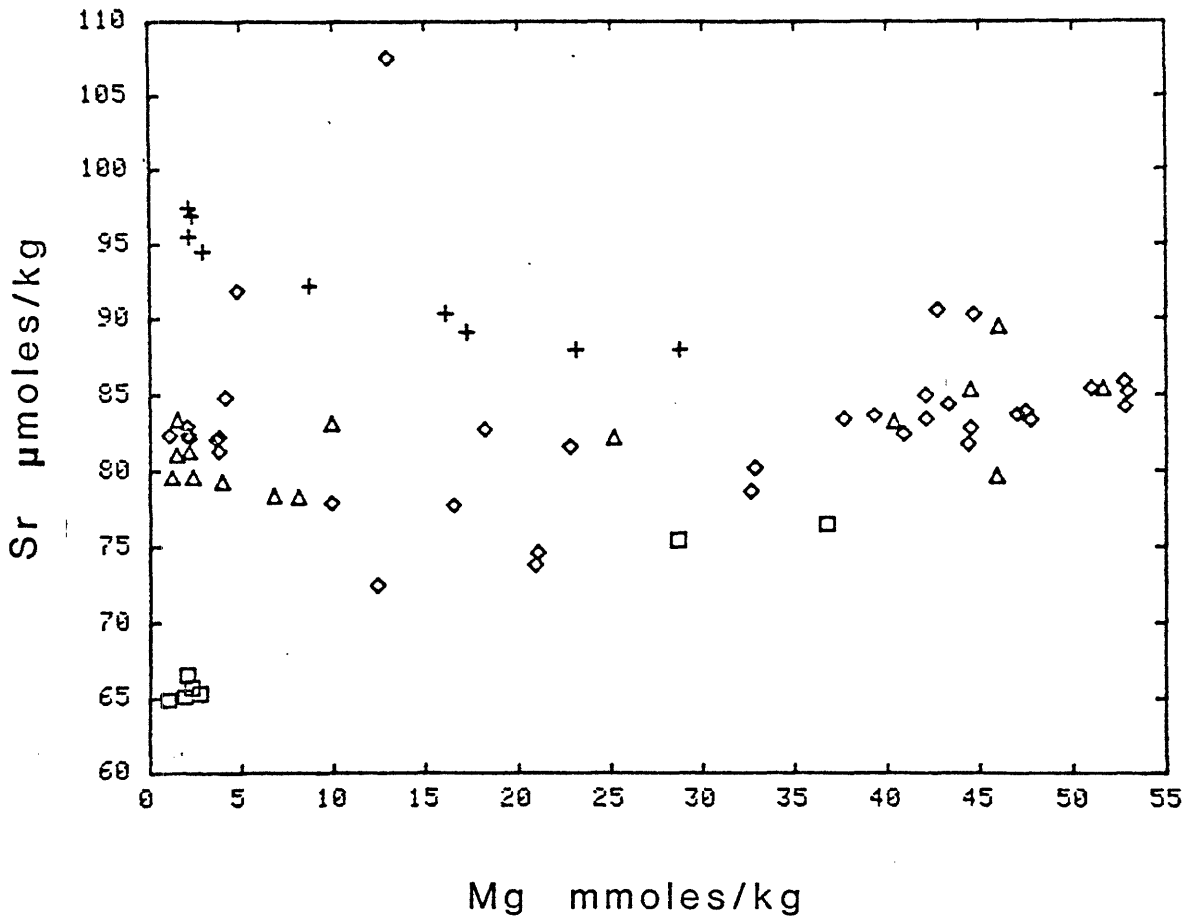

Figure 2-10: Strontium versus magnesium at 21° N.

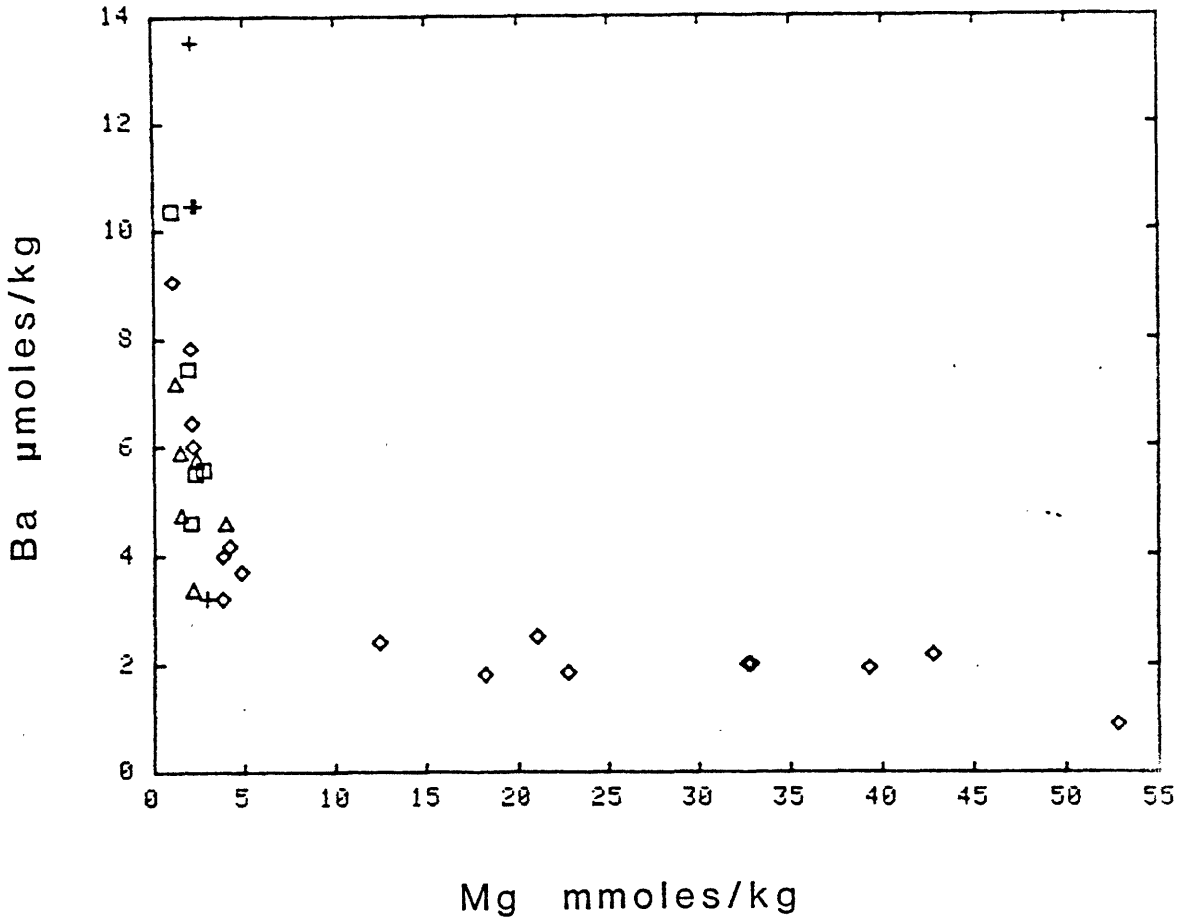

Figure 2-11: Barium versus magnesium at 21° N.

endmember concentration cannot be precisely determined because some sulfate is always present in the samples and barite solubility is exceeded. Approximately 4.4 µmoles/kg barite are soluble in water at 300° C and 500 bars (Blount, 1977) therefore the smallest amount of sulfate will cause precipitation. From the solution data the lower limits of 10 µmoles/kg at HG, 9 at SW, 7 at OBS and 15 at NGS can be set (Table 2-5). The upper limit can be set by the barium concentration in rocks, 150-210 µmoles/kg (RISE Project Group, 1980). Particles filtered from the solutions contained up to another 2 µmoles/kg barium, raising the endmember concentration to 16 µmoles/kg at NGS, 11 at HG, 10 at SW and 8 at OBS. Since the chimneys are "leaky" to seawater (Goldfarb, 1982; Haymon, 1983) which has caused barite deposition in their walls, these values may still be an underestimate of the total barium in the solutions. The GSC extrapolations for barium in the endmember are probably incorrect due to the precipitation of barium sulfate at depth (McDuff and Edmond, 1982).

From the reconstruction of the solution composition (Table 2-5) an extraction efficiency was calculated. Up to ~20% of the Ba may be leached from the rocks, making it second only to most of the alkalis for extraction efficiency from the rock.

ALUMINUM

Aluminum: Aluminum increases in all the vent fields, ranging from 4.0 µmoles/kg in the NGS area to 5.2 µmoles/kg in the HG area (Table 2-6). No figure is presented as only those samples with Mg <5 mmoles/kg were analyzed. The scatter may be due to the poorer analytical precision of the graphite furnace atomic absorption spectrophotometric (GFAAS) method (±10%). This is a 500 fold increase over the 20 nmoles/kg found in seawater.

Table 2-6: Endmember Concentrations

	pH	Alk	Cl	SiO_2	Al	NH_4
		meq[1]	m	m	μ	m
21° NORTH						
NGS (+)	3.8	-0.19	579	19.5	4.0	<0.01
OBS (△)	3.4	-0.40	489	17.6	5.2	<0.01
SW (◇)	3.6	-0.30	496	17.3	4.7	<0.01
HG (□)	3.3	-0.50	496	15.6	4.5	<0.01
GUAYMAS						
Area: 1 (◇)	5.9	10.6	601	12.9	0.9	15.6
2 (△)	5.9	9.6	589	12.5	1.2	15.3
3 (+)	5.9	6.5	637	13.5	6.7	10.3
4 (□)	5.9	8.1	599	13.8	3.7	12.9
5 (•)	5.9	9.7	599	12.4	3.0	14.5
6 (×)	5.9	7.3	582	10.8	3.9	14.5
7 (◇)	5.9	10.5	606	12.8	1.0	15.2
8 (△)						
9 (□)	5.9	2.8	581	9.3	7.9	10.7
10 (×)						
GSC[2]		0	+,-	21.9	n.a.	n.a.
SEAWATER	7.8	2.3	541(21°) 540(GY)	0.16(21°) 0.18(GY)	0.02	<0.01

[1]Units: meq = milliequivalents/kg
μ = micromoles/kg
m = millimoles/kg

[2]All GSC data is /liter.

[3]n.a. = not analyzed.

Aluminium has the lowest extraction efficiency of any element measured. This low number is probably indicative of secondary reactions and precipitation, rather than low extraction efficiency from the rock. Many of the reactions written in this section involve Al either as a product or as a reactant. This indicates that it is an important species in the hydrothermal reactions occurring within the system, even if its final concentration in the hydrothermal solutions is low.

SILICA

Silica: Silica varies in the 21° N vent fields from 15.6 mmoles/kg at HG to 17.3 at SW, 17.6 at OBS and 19.5 at NGS (Figure 2-12). These values are lower than the extrapolated Galapagos value of 21.9 mmoles/l (Table 2-5). Within the resolution of the data, all the GSC vent areas had the same silica concentration. The endmember concentrations for silica were calculated using only those samples with Mg <10 mmoles/kg due to the scatter (due to polymerization/precipitation and entrainment) in the more mixed samples.

Silica has a relatively low apparent extraction efficiency from the rock. The silica concentration in solution is assumed to be controlled by quartz solubility and this assumption is supported by the solubility calculations (Bowers, Von Damm and Edmond, 1983). Quartz solubility is a function of pressure and temperature and the silica content of the solution may be used as a geobarometer. This will be discussed in section 2.4.

pH

pH: The pH values are from shipboard measurements at approximately 25° C and 1 atmosphere. There is less free hydrogen ion at higher temperature and pressure therefore the *in situ* pH is 0.1 to 0.2 pH units higher than the measured values reported here. There may be a small

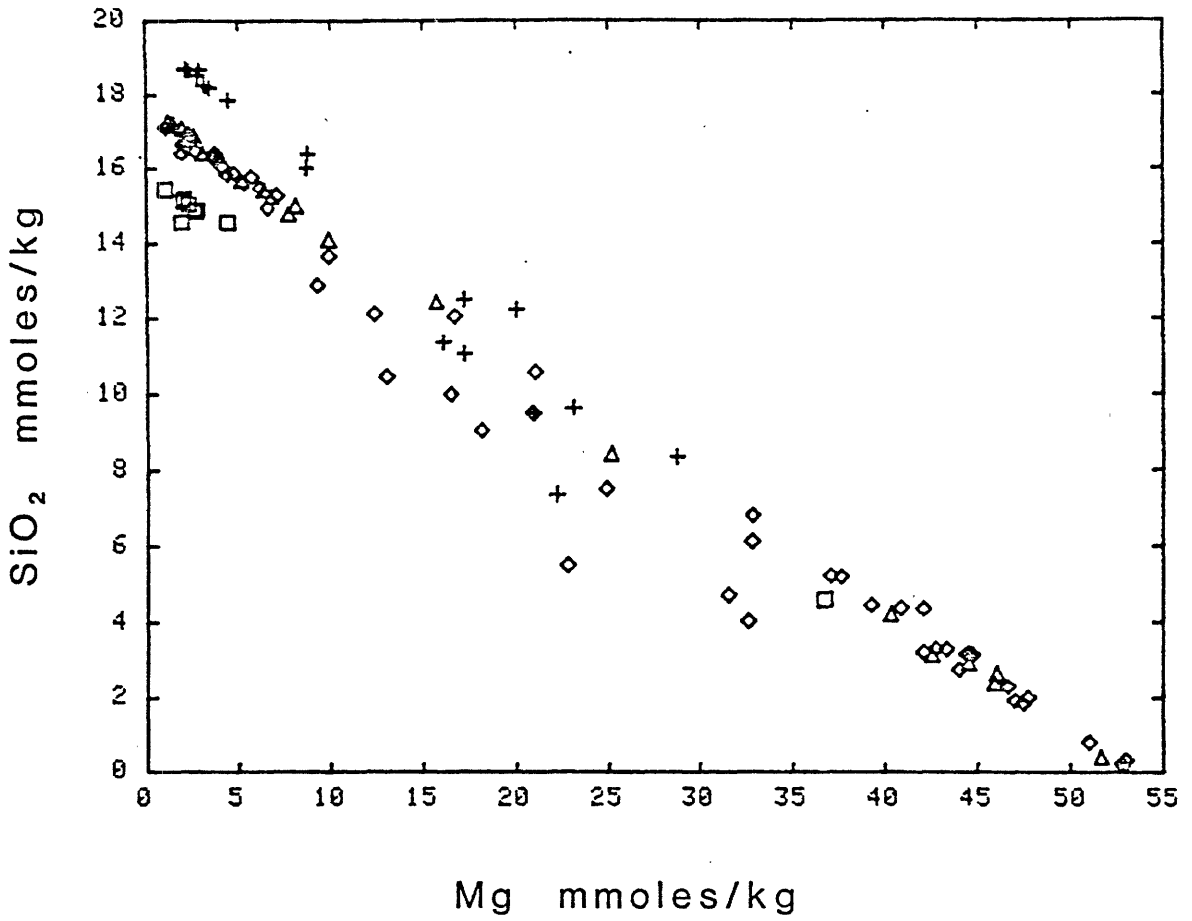

Figure 2-12: Silica versus magnesium at 21° N.

difference in pH between the vent areas with HG being the most acid at 3.3, followed by OBS at 3.4, SW at 3.6 and NGS at 3.8 (Figure 2-13, Table 2-6). These differences may not be significant because oxidation of a small amount of the hydrogen sulfide present during the analysis would cause a lowering of the pH. This oxidation would be variable and the good agreement between samples within vent areas suggests the variation may be real. HG, with the lowest pH, has the highest hydrogen sulfide concentration. Less than 0.2 mmoles/kg of the hydrogen sulfide would need to oxidize to produce the difference in observed pH between NGS and HG.

The pH is dependent upon the exchange reactions occurring in the rocks. Protons are primarily released to solution through the deposition of Mg as was discussed earlier, and are then consumed and released in various secondary reactions as discussed above. Due to the complexity of its cycle, no proton balance can be made.

CARBON

Carbon dioxide and methane were measured by Craig, Welhan and Kim at S.I.O. and will not be discussed here. Total alkalinity and pH were measured therefore a total CO_2 content could theoretically be calculated. In practice, at the very low pH and alkalinity measured in the vent solutions, the precision of the data does not permit the calculation of the total CO_2.

Alkalinity: As for the pH measurements, the alkalinity measurements can be affected by hydrogen sulfide oxidation, which would lower the total alkalinity. There appears to be a slight variability between the vent fields with HG= -0.50 meq/kg, OBS= -0.40, SW= -0.30 and NGS= -0.19 (Figure 2-14, Table 2-6). A decrease in alkalinity was also observed at the GSC.

The production of H^+ has titrated all of the alkalinity originally present in the seawater solutions, with the net result being a "negative

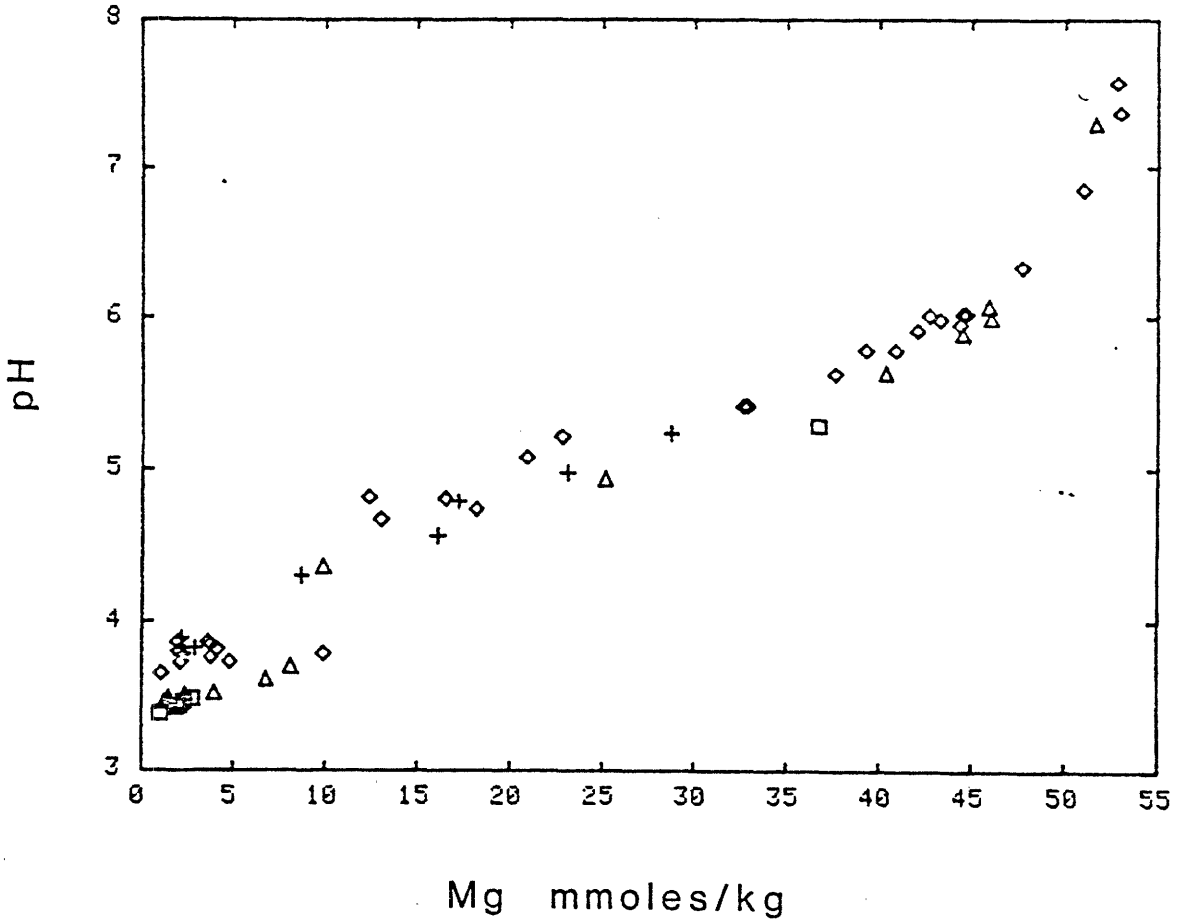

Figure 2-13: pH versus magnesium at 21° N.

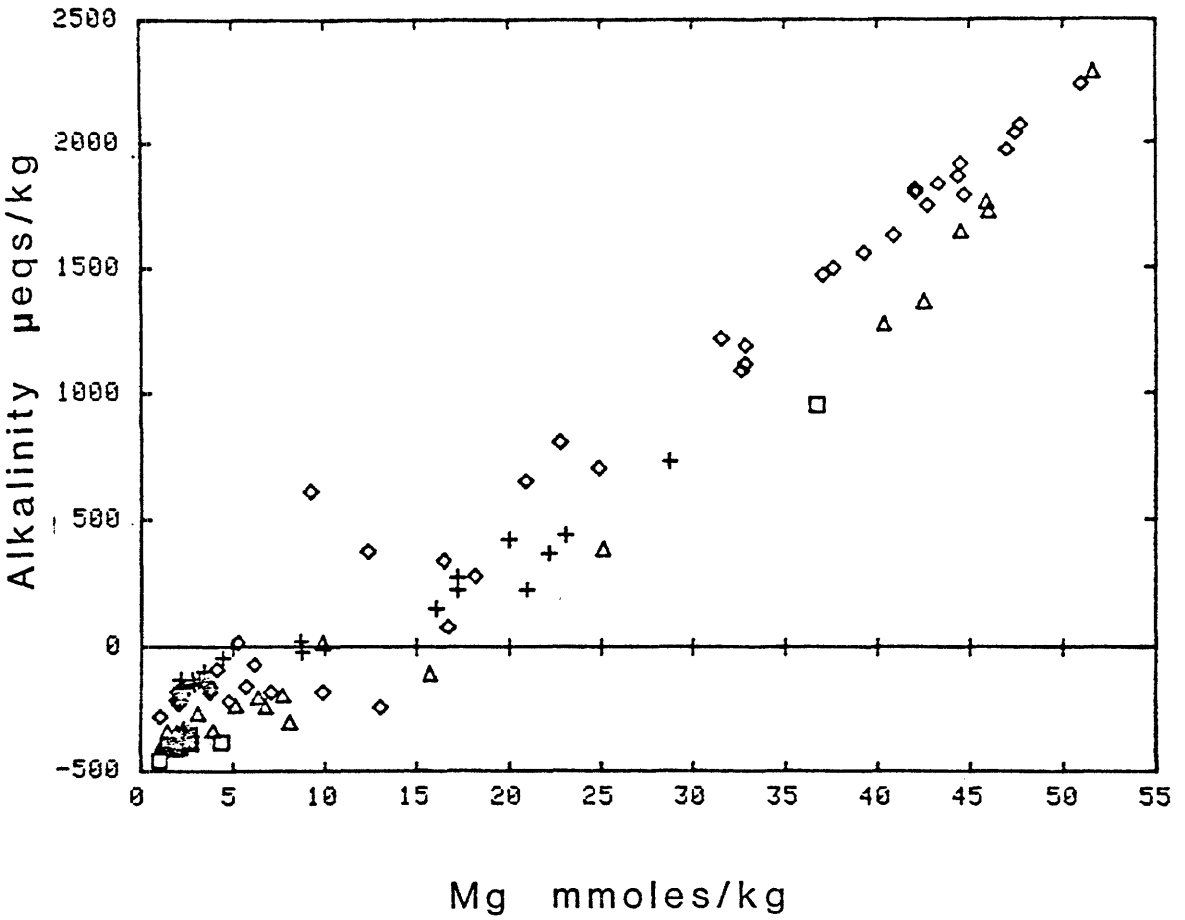

Figure 2-14: Alkalinity versus magnesium at 21° N.

alkalinity". There are no carbonate-bicarbonate species present and all of the CO_2 is present as the H_2CO_3 form.

AMMONIUM

Ammonium was determined in a few samples from all the vent areas at 21° N. It was above the detection limit in a few samples but in all cases is <0.01 mmoles/kg.

PHOSPHATE

Phosphate was measured in a few samples from all the vent areas. It decreases in concentration, but the quality of the data does not permit an exact endmember value to be calculated. It is <1 μmole/kg in all the vent areas.

NITRITE

Nitrite was analyzed only on samples from dive 1149. It is <0.1 μmoles/kg.

THE HALOGENS

Fluoride: Fluoride was not measured on the samples collected at 21° N in 1981. Measurements on the samples collected there in 1979 implied that fluoride went to zero in the hydrothermal solutions (Figure 2-15). This agrees with the fluoride depletion found in the GSC solutions.

Fluoride presumably enters one of the hydrous clay minerals formed where it can substitute for the OH^- group. It may substitute in a similar manner into amphibole phases if they are forming.

Chloride: Chloride, like sodium, increases from the ambient value of 541 mmoles/kg to 579 at NGS and decreases to 496 at HG and SW, and 489 at OBS (Figure 2-16). The increased chloride at NGS can be interpreted as a

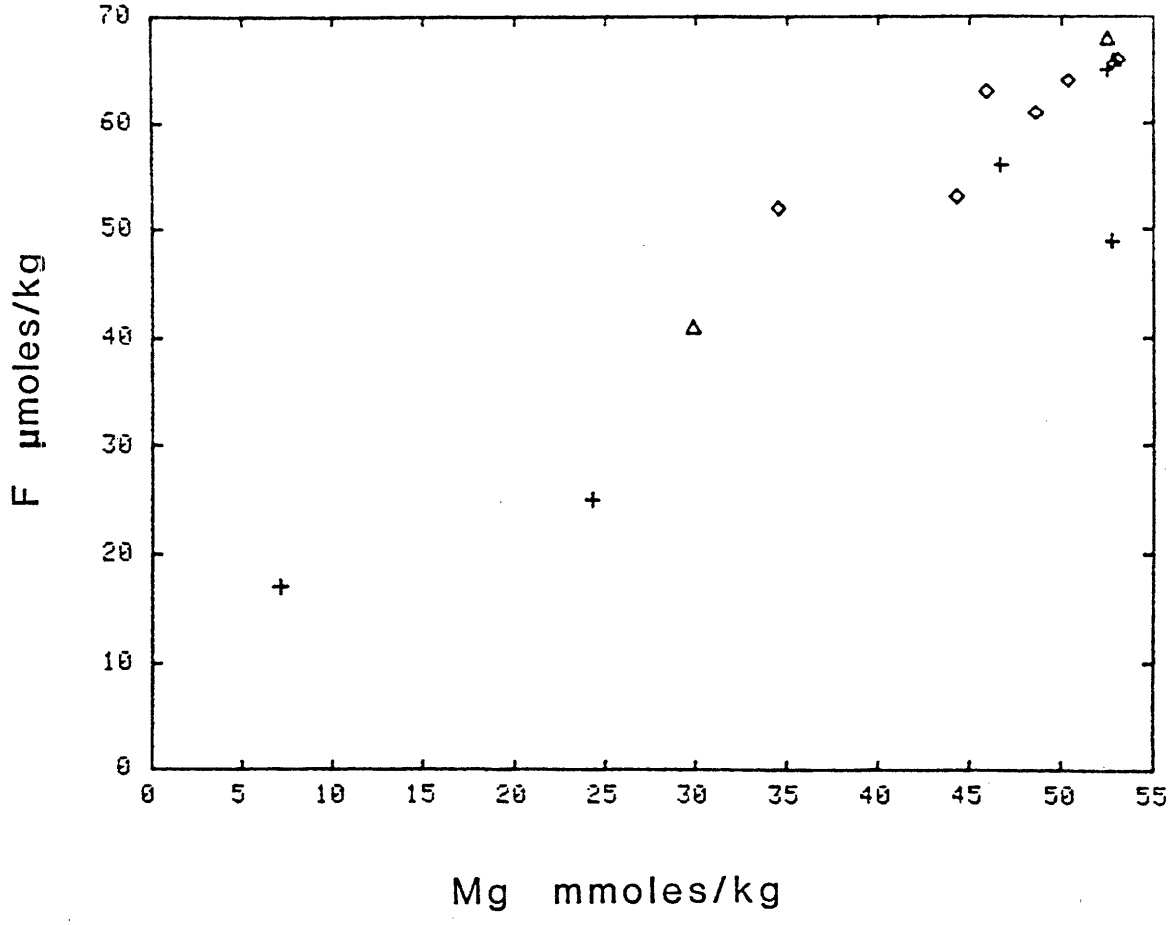

Figure 2-15: Fluoride versus magnesium at 21° N.

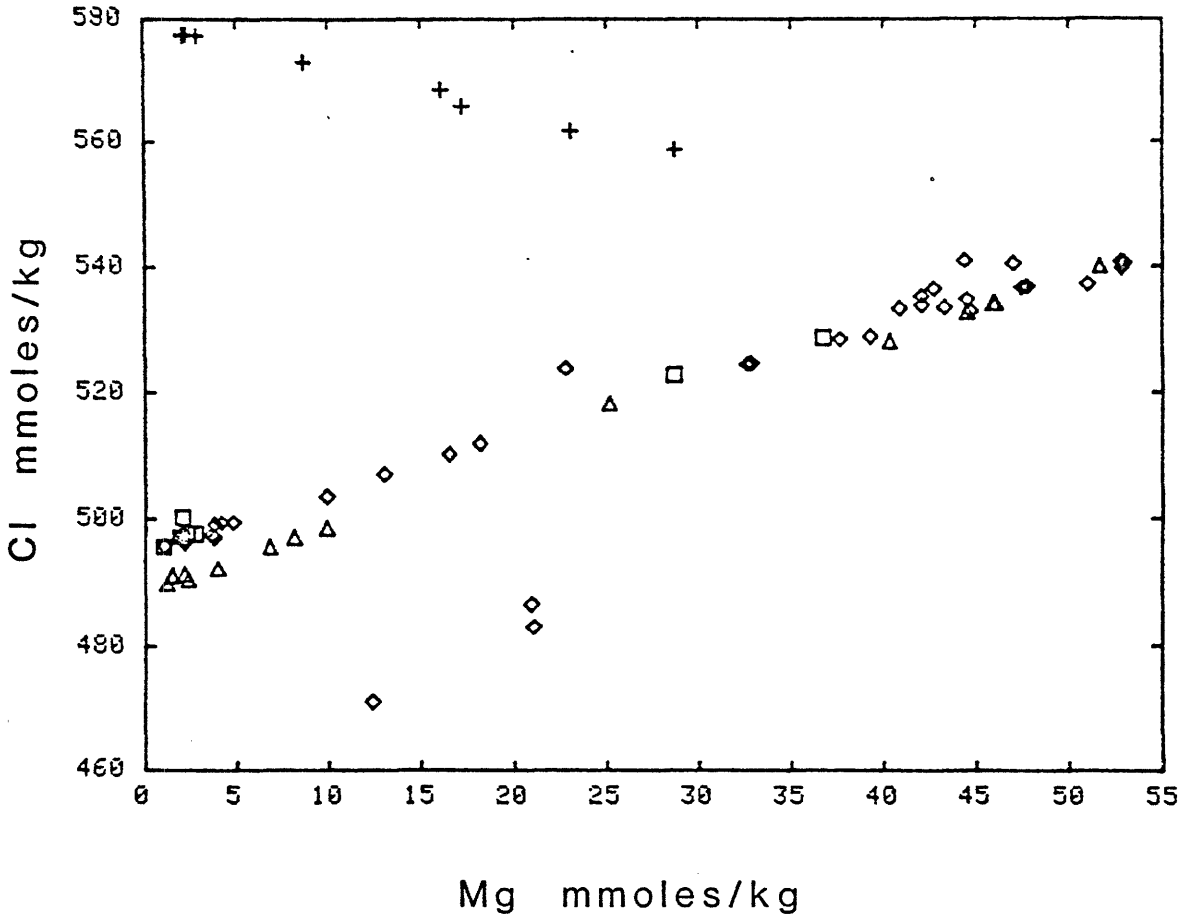

Figure 2-16: Chloride versus magnesium at 21° N.

7% loss of water to rock hydration. The other areas have lost approximately 10% of their chloride. If these areas are also hydrating, like the NGS area, then they must have lost approximately 17% of their chloride. The GSC vents also displayed this dichotomy, although the total chloride losses were inferred to be much larger (Table 2-6). The three low points (Figure 2-16) are from a chimney which was extinct until excavated by the submarine. Loss of water due to hydration is consistent with the water isotopes although the Cl indicates a smaller water loss than the isotopes. A small amount of Cl may therefore be added to this solution but this cannot be proven within the resolution of the data. The most likely sink for Cl is, as for fluoride, substituting for a hydroxyl group. Cl is present in amphiboles formed at temperatures of ~400° C, while it is excluded from the higher temperature, more crystalline forms of these minerals (Deer et al., 1963; Honnorez, personal communication).

SODIUM versus CHLORIDE

As these are the two major charged species in the solutions, additional information may be obtained based on their relative behavior. Table 2-7 gives the change in Na with respect to Cl in the four vent areas at 21° N (Figure 2-17). Cl is preferentially lost with respect to Na in the three areas which show a decrease in these species. There is a small variability between the vent areas. When looking at the net loss of Na and Cl it should be remembered that there is up to a 10% loss of water by hydration, therefore the loss of Cl is ~20% and Na ~17%, rather than the ~10% or ~7% the data itself indicates. The major Na sink is probably the formation of albite as was discussed earlier. In the NGS area, Na is gained preferentially to chloride. This indicates two possible processes may be occurring: loss of Cl with no attendant loss of Na or preferential gain of Na to the solutions. Na could be gained in a reaction shown

Table 2-7: Sodium versus Chloride - 21° N

	Na	ΔNa	Cl	ΔCl	ΔNa/ΔCl
NGS	510	+46	579	+38	1.21
OBS	432	-32	489	-52	0.62
SW	439	-25	496	-45	0.56
HG	443	-21	496	-45	0.47
SEAWATER	464		541		

All concentrations are in millimoles/kg.

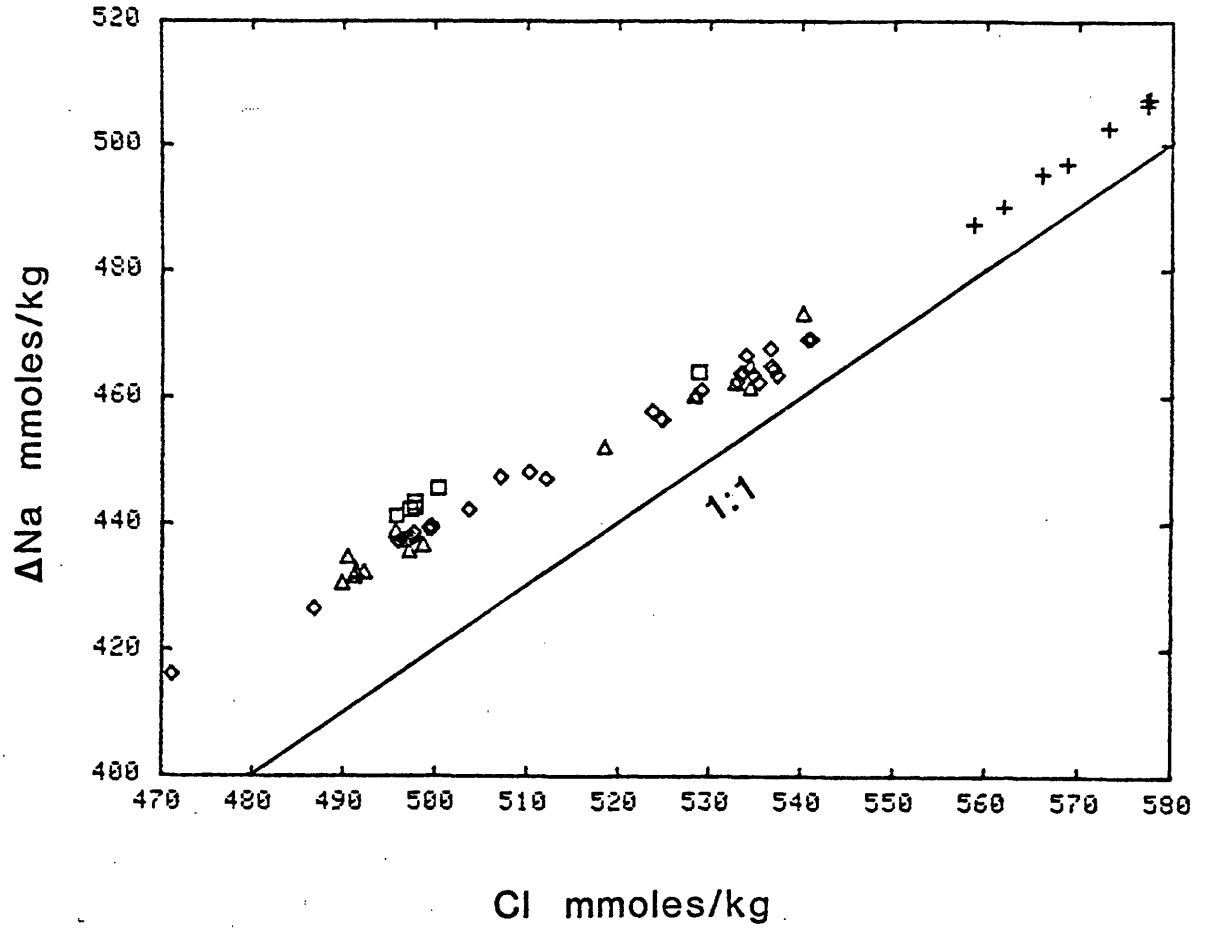

Figure 2-17: Charge balance sodium versus chloride at 21° N. Note 1:1 line.

earlier when albite is converted to chlorite with a resultant release of Na. It is not possible to choose between these two possible cases.

SULFUR

Sulfate: Sulfate decreases to a measured value of 0.61 mmoles/kg at 21° N. All the vent fields show sulfate decreasing to zero with the same slope (Figure 2-18). The residual measured sulfate is probably a sampling artifact as was discussed for magnesium. The scatter is due to the presence of anhydrite as was discussed for calcium. Sulfate was also inferred to go to zero at the GSC (Table 2-8).

Hydrogen Sulfide: Hydrogen sulfide is present in all the vent fields, and at the observed pH should be present as the H_2S form. HG has the highest hydrogen sulfide concentration at 8.7 mmoles/kg, followed by SW at 7.6, OBS at 7.5 and NGS at 6.7 (Figure 2-19). Since no sulfate is present in the endmember hydrothermal solutions, this implies a net loss of sulfur as seawater passes through the hydrothermal system. Increased levels of hydrogen sulfide were also observed at the GSC but no endmember value could be inferred due to subsurface oxidation and precipitation (Table 2-8).

Total Sulfur: As a check that no sulfur species besides sulfate and hydrogen sulfide were quantitatively important samples were taken in sealed glass ampoules with bromine present to oxidize all the sulfur species to sulfate (Appendix 2), and the sulfate measured. In three of the four vent areas at 21° N the sum of the measured sulfate and hydrogen sulfide is between 4 and 17% greater than the sulfate measured in the ampoule (Table 2-9). In the fourth area the ampoule has approximately 1% more sulfate, and is within the analytical error for the methods. The H_2S is most likely not being quantitatively trapped as the sample is introduced in to the ampoules. The sum of the measured sulfate and sulfide is always greater

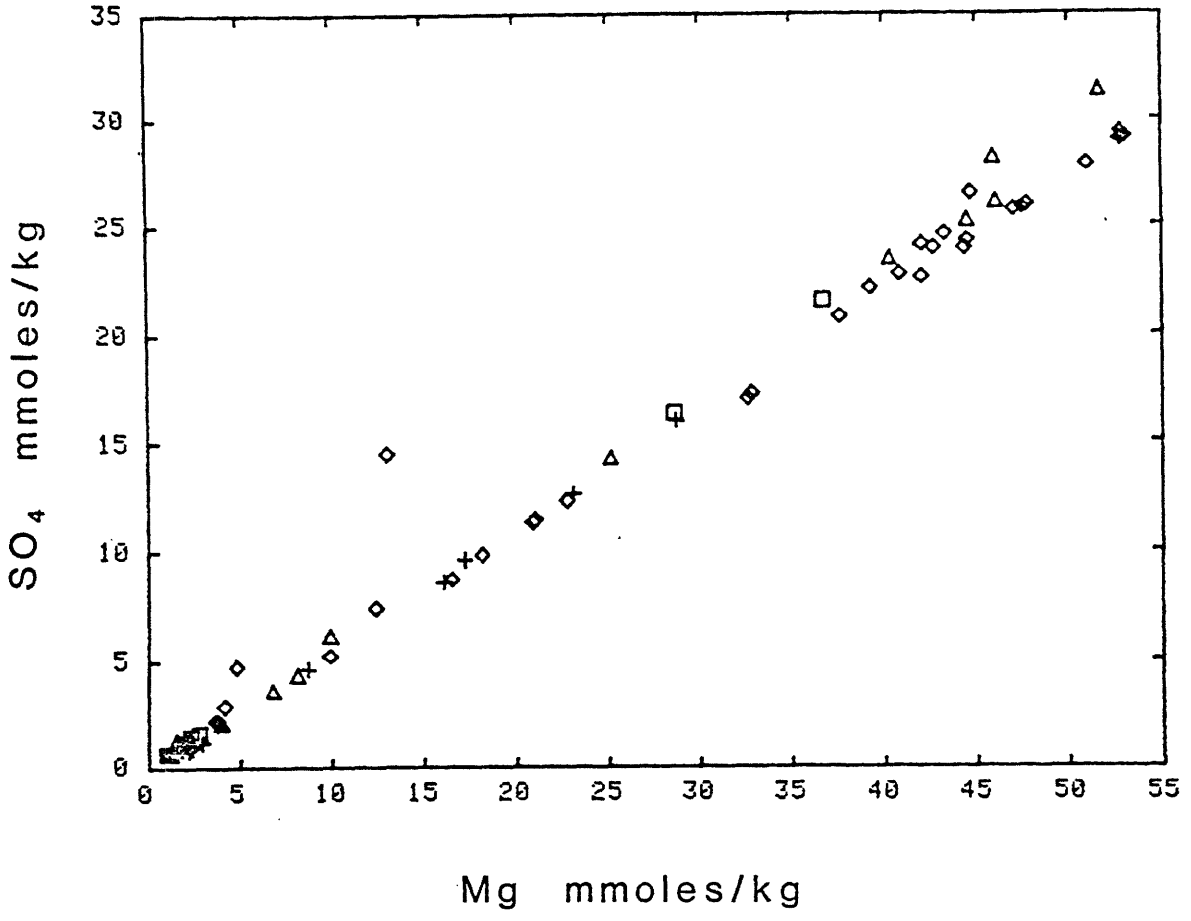

Figure 2-18: Sulfate versus magnesium at 21° N.

Table 2-8: Endmember Concentrations - Sulfur Species

	SO_4 m[1]	H_2S m
21° NORTH		
NGS (+)	0	6.57
OBS (△)	0.5	7.30
SW (◇)	0.6	7.45
HG (□)	0.4	8.37
GUAYMAS		
Area: 1 (◇)	-0.15[3]	5.82
2 (△)	-0.09	3.95
3 (+)	-0.34	5.22
4 (□)	0.06	4.79
5 (•)	-0.07	4.11
6 (×)	-0.32	3.80
7 (◇)	-0.06	5.98
8 (△)		
9 (□)	-4.2	4.56
10 (×)		
GSC[2]	0	+
SEAWATER	27.92	0

[1]Units: m = millimoles/kg.

[2]All GSC data is /liter.

[3]Negative values denote that SO_4 goes to zero before Mg = 0.

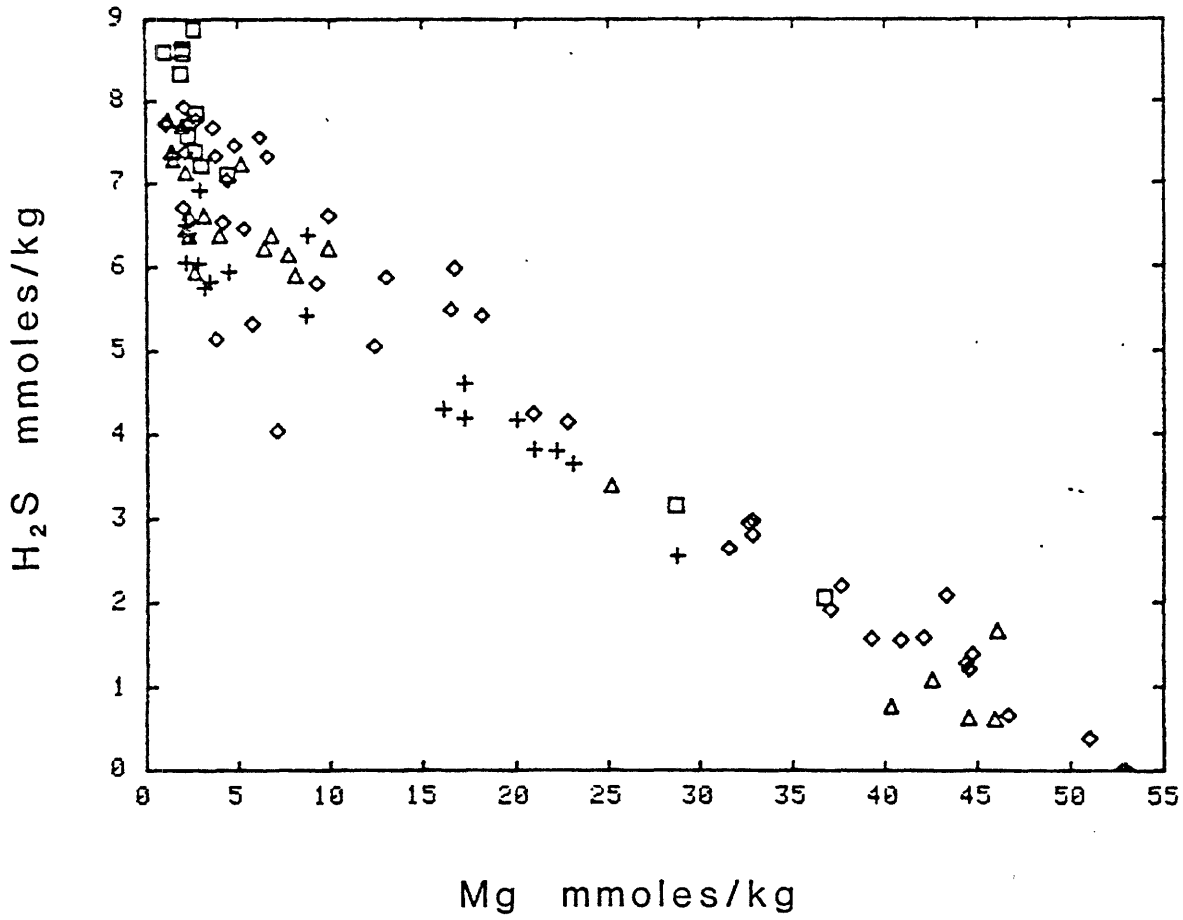

Figure 2-19: Hydrogen sulfide versus magnesium at 21° N.

Table 2-9: Total Sulfur Concentration

	Sample	Mg	SO_4	H_2S	Σ S (SO_4+H_2S)	Σ S (ampoule)
		m[1]	m	m	m	m
21° NORTH						
NGS (+)	1155-18	2.13	0.82	6.51	7.33	6.25
OBS (△)	1158-11	1.44	0.80	7.38	8.18	7.59
SW (◇)	1150-11	1.11	0.62	7.72	8.34	8.06
HG (□)	1160- 6	1.03	0.61	8.61	9.22	9.35
AMBIENT	1153- 7	52.7	28.0	0	28.0	27.5
GUAYMAS						
Area: 1 (◇)	1176- 7	1.99	0.94	5.19	6.13	5.79
2 (△)	1173- 6	1.36	0.65	4.00	4.65	5.77
3 (+)	1175-16	4.11	2.01	4.69	6.70	6.08
4 (□)	1177-11	1.05	0.53	5.11	5.64	4.39
5 (•)						
6 (X)	1173-16	1.44	0.67	4.21	4.88	6.02
7 (◇)	1176-10	1.00	0.43	5.74	6.17	5.93
8 (△)						
9 (□)						
10 (X)						

[1]Units: m = millimoles/kg

than or equal to the ampoule concentrations suggesting that at 21° N, no intermediate sulfur species are quantitatively important.

Sulfur has a very complicated and very important cycle and section 2.3 is devoted to a detailed discussion of its behavior in the vents.

TRACE METALS

This section contains the results for the transition metals Mn, Fe, Co, Ni, Cu, Zn, Ag, Cd, Pb and Hg, most of which form insoluble sulfides, as well as for the elements As and Se which can substitute for sulfur. Most of these species are present in trace amounts (nanomolar quantities) compared to those in the previous section but some, such as iron and manganese are present at millimolar levels. The chemistry of these species is more difficult to interpret as most are involved in precipitation reactions with reduced sulfur species in the plume, in building the chimney itself and probably in subsurface precipitation in the conduits. As many of these elements precipitate when they mix with ambient seawater - in the water column or in the samplers - only those samples with Mg <5 mmoles/kg were measured for most of these elements in the 21° N data set. These samples contain very little or no visible precipitate. (See Appendix 1 for a complete discussion of the particle problem.) For all of the 21° N results the endmember is calculated from the Mg <5 mmoles/kg samples (at least four samples from each vent area), forced through the seawater value and extrapolated to Mg = 0 mmoles/kg. Most of the elements in this section (excepting Mn, Fe, Zn, Cu and Se) were analyzed by graphite furnace atomic absorption spectrophotometry by the method of standard additions and hence the analytical precision is worse ($\pm$10%) than for the major elements (usually 1-2%). In many cases the differences between vent fields are not significant within the analytical uncertainty.

Manganese: Manganese is enriched by greater than 1000 times over ambient seawater at 21° N. NGS is the highest with 1002 µmoles/kg followed by OBS at 960, HG at 878 and SW at 699 (Figure 2-20, Table 2-10). This is within the range of values seen at GSC (360-1140 µmoles/1). Unlike most of the other species discussed in this chapter manganese rarely forms a sulfide and the GSC data are probably not affected by subsurface precipitation. At 21° N it has a moderate to low extraction efficiency from the rock which is most likely due to its incorporation into secondary clay phases.

Iron: Iron reaches greater than millimolar concentrations in several of the 21° N solutions and can hardly be considered a trace metal. The highest levels found at HG are 2429 µmoles/kg followed by 1664 µmoles/kg at OBS, 871 µmoles/kg at NGS and 750 µmoles/kg at SW (Figure 2-21, Table 2-10). Although iron increased at GSC no endmember concentrations could be determined due to subsurface mixing and precipitation of metal sulfides (Edmond et al., 1979b). Iron is present at high concentrations in the vents in comparison to the seawater levels (~0.5 nmoles/kg) but is present at low levels in comparison to the amount of iron which is available from the rocks. (Note low extraction efficiency in Table 2-3.) The variation in iron between vent areas cannot be explained by solubility controls. Only the NGS area at its measured 273° C temperature is saturated with respect to pyrite (Bowers, Von Damm and Edmond, 1983).

Iron/Manganese: The iron/manganese (molar) ratio varies from 0.9 in NGS to 2.9 in HG at 21° N (Figure 2-22, Table 2-10). This is much less than the basalt ratio of 50-60, but is very close to three, the value observed in metalliferous sediments (Dymond, 1981). Whether this similarity in ratios is fortuitous is unknown, but it suggests that the

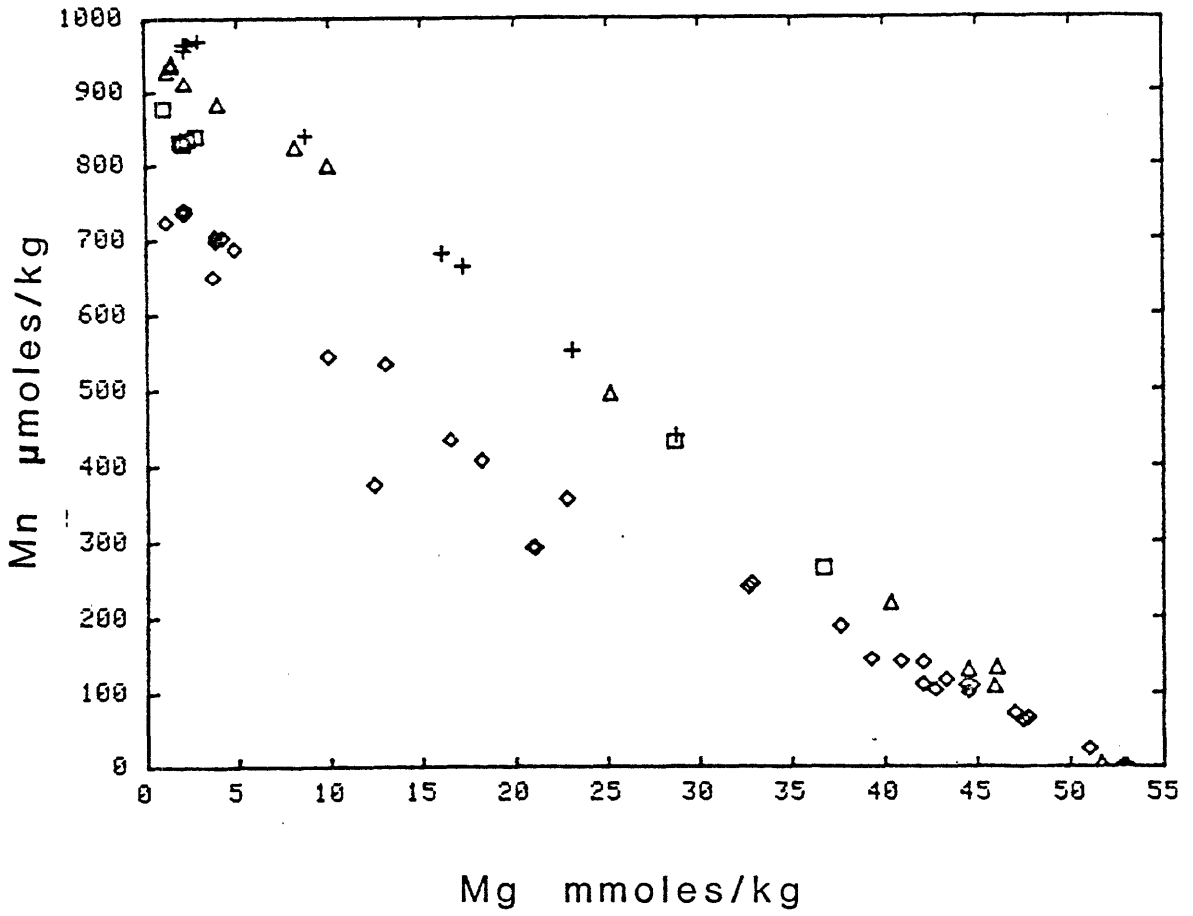

Figure 2-20: Manganese versus magnesium at 21° N.

Table 2-10: Endmember Concentrations - Trace Metals

	Mn	Fe	Fe/Mn	Co	Cu	Zn	Ag	Cd	Pb
	μ[1]	μ		n	μ	μ	n	n	n
21° NORTH									
NGS (+)	1002	871	0.9	22	<.02	40	<1	17	183
OBS (△)	960	1664	1.8	213	35	106	38	155	308
SW (◇)	699	750	1.0	66	9.7	89	26	144	194
HG (□)	878	2429	2.9	227	44	104	37	180	359
GUAYMAS									
Area: 1 (◇)	139	56	0.4	<5		4.2	230		265
2 (△)	222	49	0.2			1.8			304
3 (+)	236	180	0.8			40	24	46	652
4 (□)	139	77	0.6		1.1	19	2	27	230
5 (•)	128	33	0.3		0.1	2.2			
6 (X)	148	17	0.1			0.1			
7 (◇)	139	37	0.3			2.2			
8 (△)									
9 (□)	132	83	0.6			21			
10 (X)									
GSC[2]	360-1140	+		n.a.[3]	0	n.a.	n.a.	0	n.a.
SEAWATER	<0.001	<0.001		0.03	0.007	0.01	0.02	1	0.01

[1]Units: n = nanomoles/kg
μ = micromoles/kg
m = millimoles/kg

[2]All GSC data is /liter.

[3]n.a. = not analyzed.

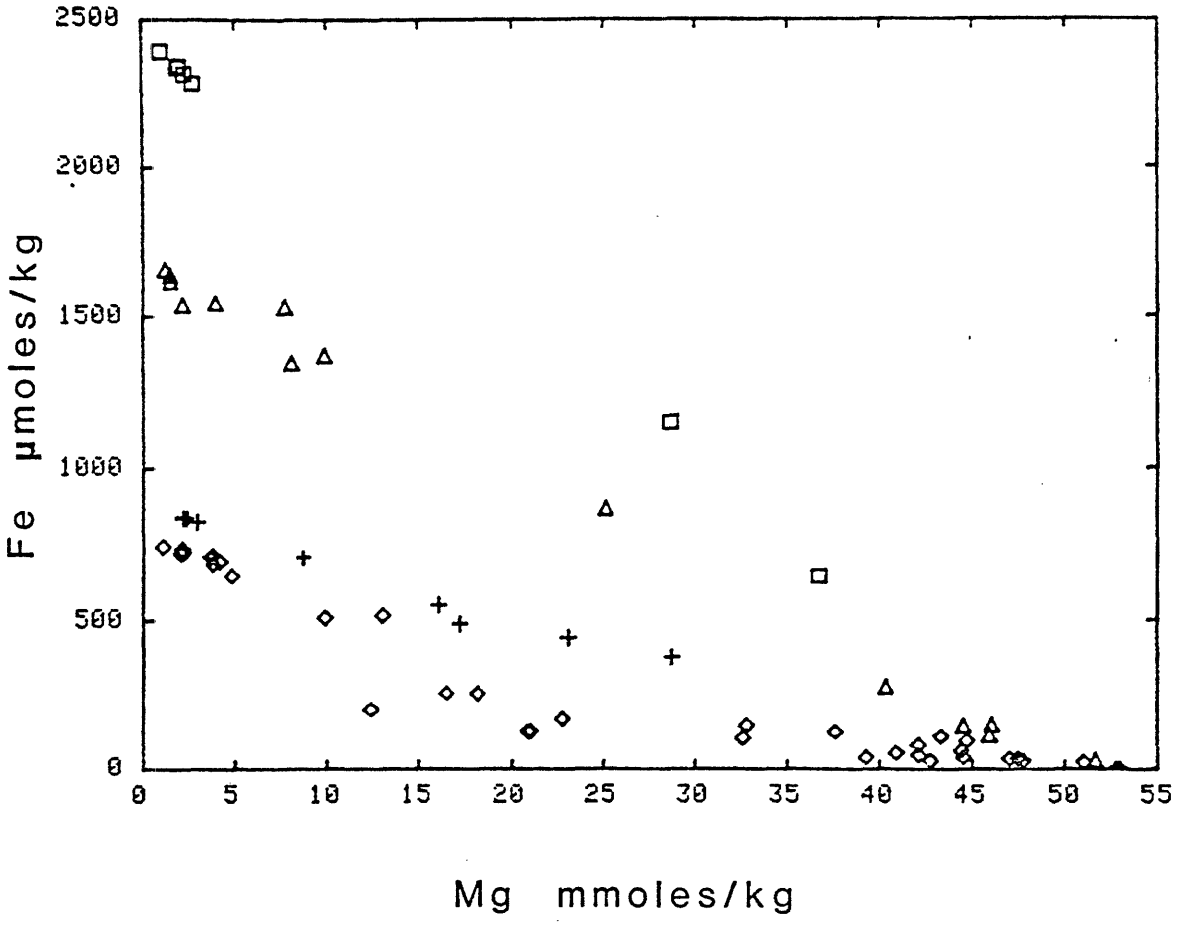

Figure 2-21: Iron versus magnesium at 21° N.

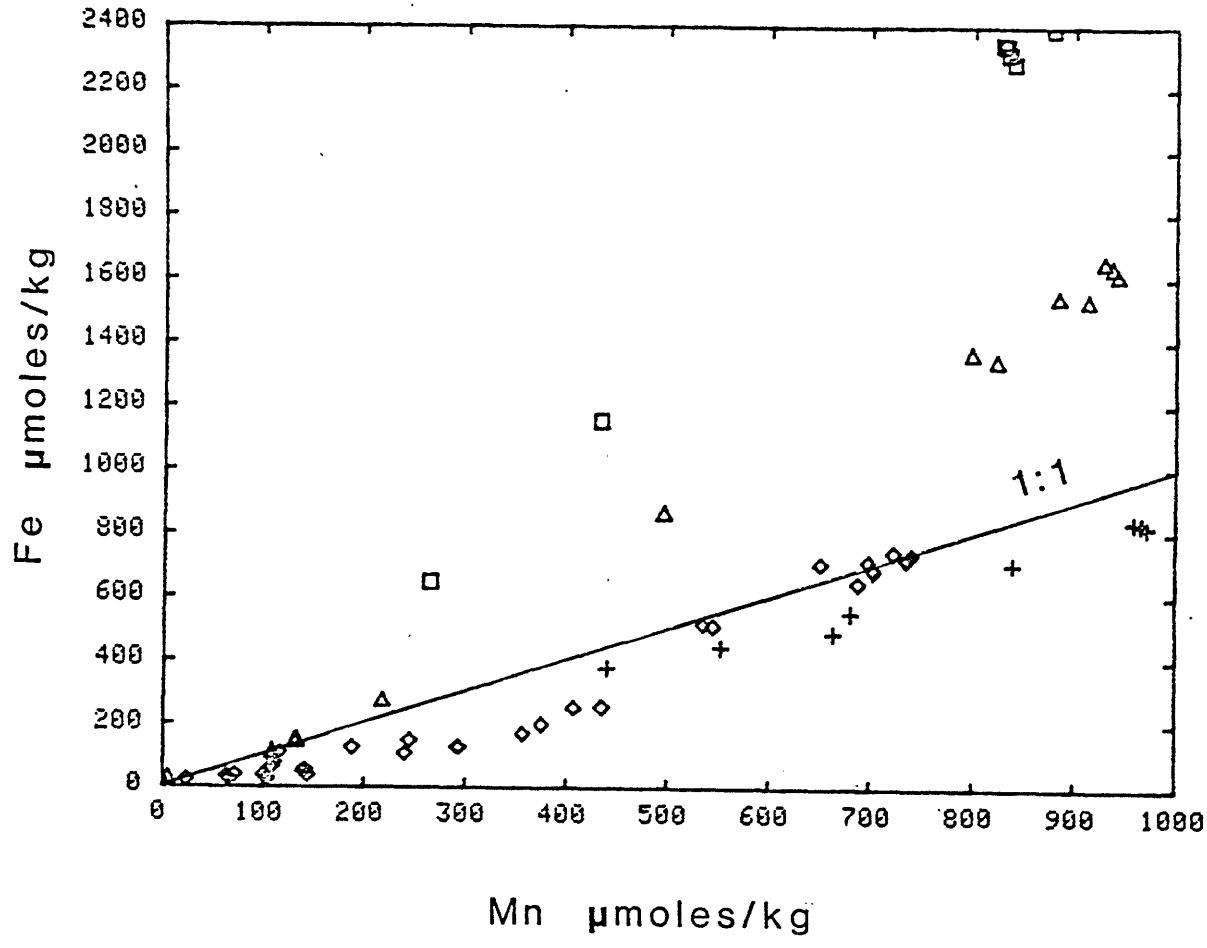

Figure 2-22: Iron versus manganese at 21° N. Note 1:1 line.

source of much of the iron and manganese in metalliferous sediments is high temperature hydrothermal activity. The low ratio is presumably due to secondary reactions of both metals, especially iron. Iron may be oxidized to Fe^{3+} by sulfate, and either valence state may be incorporated into clay minerals. The very low value at NGS is also due to the precipitation of pyrite. The observed ratio at GSC was variable, but much lower than that at 21° N.

The rest of the trace metals will be presented on an individual basis but will be discussed as a group as, for most of them very little is known about their thermodynamic properties at hydrothermal temperatures and pressures.

Cobalt: Cobalt is low in two of the areas at 21° N - 22 nmoles/kg in NGS and 66 nmoles/kg at SW - and is considerably higher in the other two areas ~213 nmoles/kg at OBS and 227 nmoles/kg at HG (Table 2-10). These values are all considerably higher than the ~30 pmoles/kg present in seawater. Cobalt was not measured in the GSC solutions.

Nickel: Nickel was below the detection limit of 140 nmoles/kg at 21° N. It was below the ambient seawater value of 10 nmoles/kg at GSC.

Copper: Copper varies widely between the different vent areas at 21° N. It reaches a maximum of 44 μmoles/kg in the HG area, 35 μmoles/kg at OBS, 9.7 μmoles/kg at SW and is below the detection limit of 0.02 μmoles/kg in the NGS solutions (Figure 2-23, Table 2-10). Several vents at SW with exit temperatures below 280° C did not contain measurable copper. The GSC solutions contained less than the ambient seawater value (7 nmoles/kg) due to subsurface mixing and precipitation of sulfides.

Zinc: Zinc is highly enriched in the 21° N solutions. The OBS and HG areas are indistinguishable at 106 and 104 μmoles/kg respectively, while SW contains 89 μmoles/kg and NGS 40 μmoles/kg (Figure 2-24, Table 2-10).

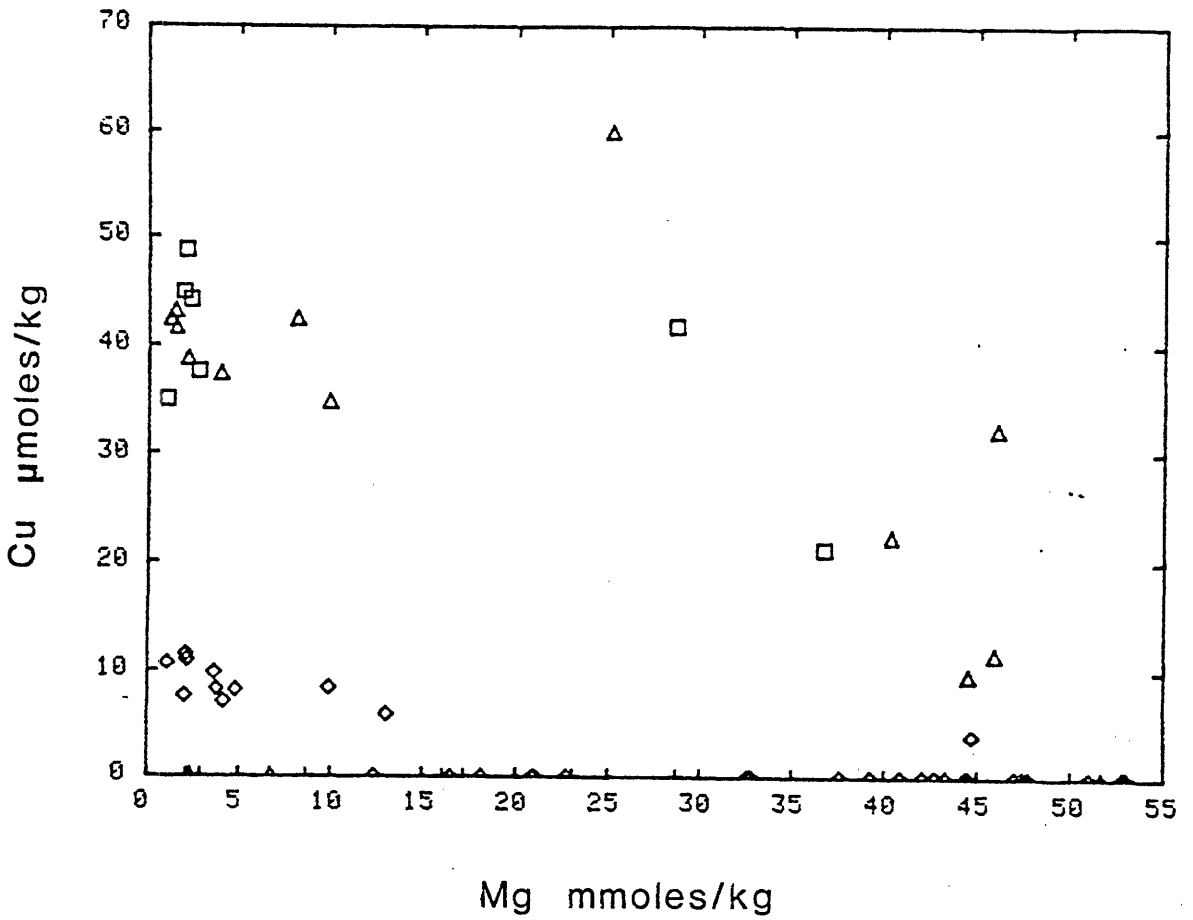

Figure 2-23: Copper versus magnesium at 21° N.

These values are all much greater than the 10 nmoles/kg present in seawater. Zinc was not determined in the GSC solutions.

Silver: Silver shows a distribution similar to zinc in the vents at 21° N. It is highest and indistinguishable at OBS and HG at 38 and 37 nmoles/kg respectively, while SW contains 26 nmoles/kg and NGS contains less than the detection limit of 1 nmole/kg (Table 2-10). There are approximately 0.02 nmoles/kg silver in seawater. Silver was not measured in the GSC solutions.

Cadmium: Cadmium increases in all the vent fields at 21° N to a maximum of 180 nmoles/kg at HG, 155 nmoles/kg at OBS, 144 nmoles/kg at SW and 17 nmoles/kg at NGS (Table 2-10). Cadmium decreased to below the seawater value of ~1 nmole/kg in the GSC solutions.

Mercury: Mercury was determined by E. Crecelius of Battelle Northwest Laboratories. The samples were found to contain several nmoles/kg mercury and appear to be contaminated, probably from storage in polyethylene bottles. Therefore at the present time no endmember mercury concentration can be determined for 21° N.

Lead: Lead shows a pattern similar to that for Co, Zn and Ag in its distribution between the vent fields at 21° N. It is highest in the HG field at 359 nmoles/kg, 308 nmoles/kg at OBS, 194 nmoles/kg at SW and 183 nmoles/kg at NGS (Table 2-10). These concentration data were confirmed by mass spectrometry at Caltech and were shown to have the same isotopic composition as MORB (Chen et al., 1983). Lead is ~0.01 nmoles/l in deep seawater. It was not measured in the GSC solutions.

Arsenic: Arsenic is enriched in the solutions at 21° N, the highest concentration of 452 nmoles/kg occurring at the HG vent area. The OBS vent contains 247 nmoles/kg, SW vent 214 nmoles/kg and NGS is below the detection limit of 30 nmoles/kg (Table 2-11). Arsenic is ~27 nmoles/kg in

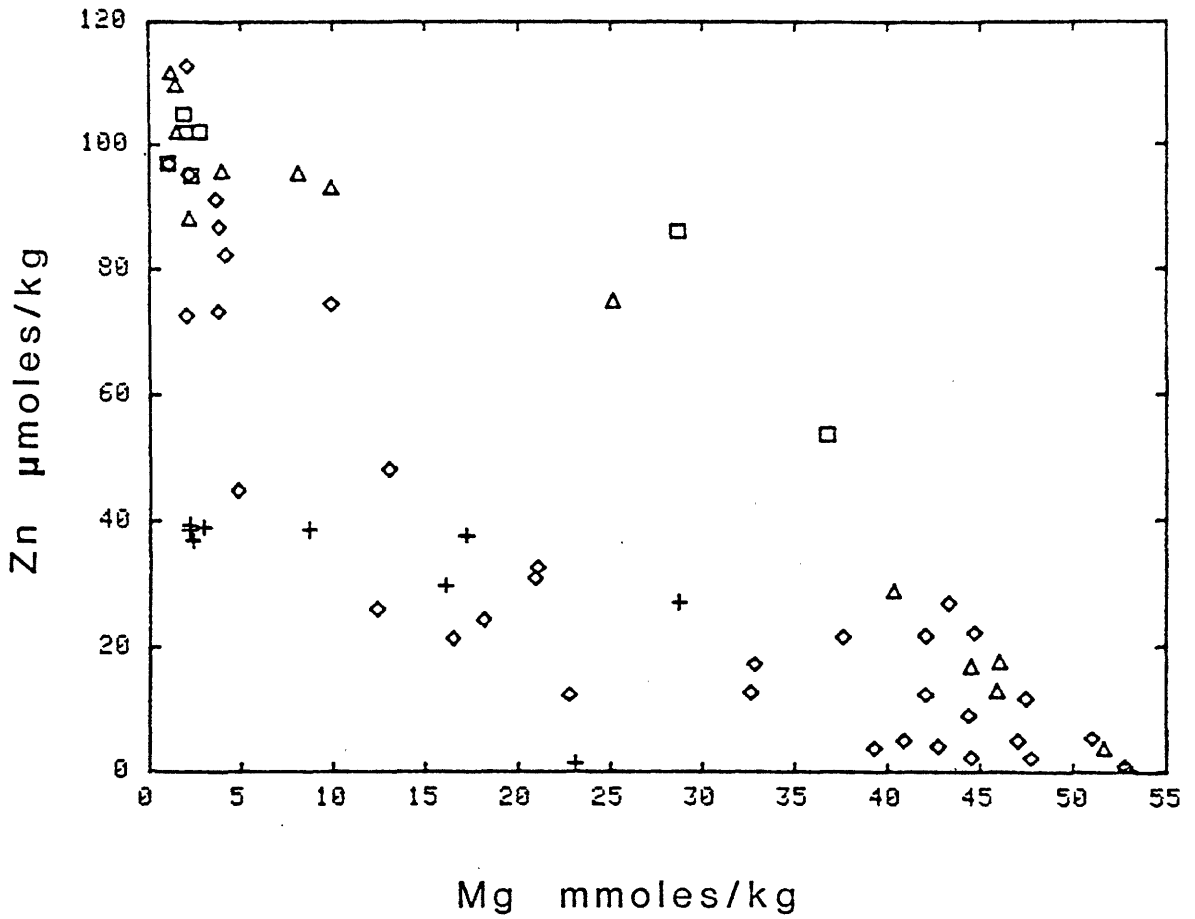

Figure 2-24: Zinc versus magnesium at 21° N.

Table 2-11: Endmember Concentrations - As and Se

	As n[1]	Sample	Se particle n	Se ampoule n
21° NORTH				
NGS (+)	<30	1155-1	0.3[3]	
		1155-18	0.4[3]	0.6[3]
OBS (△)	247	1158-6	62	
		1158-11	64	72
SW (◇)	214	1149-7	36	
		1150-11	60	70
HG (□)	452	1160-6	52	59, 61
		1160-16	58	
GUAYMAS				
Area: 1 (◇)	283	1176-7		82
2 (△)	732	1173-6	61	87
3 (+)	1071	1175-16	38	15
4 (□)	1074	1177-6	72	
		1177-11		103
		1177-13	88	
5 (•)	516			
6 (X)	669	1173-16		49
7 (◇)	711	1176-10		92
8 (△)				
9 (□)	577			
10 (*)				
GSC[2]	n.a.		0	
SEAWATER	27		2.5	

[1]Units: n = nanomoles/kg.

[2]All GSC data is /liter.

[3]These values are indistinguishable from zero.

As values are extrapolated endmember concentrations. Se data are the measured values. The particle and ampoule determinations are given for comparison.

seawater. It was not measured in the GSC solutions.

Selenium: A selenium signal was only observed in a water sample from HG, and is less than 190 pmoles/kg. Se was found in the particle fraction filtered from the water samples in all the vent areas at 21° N except NGS. Se was also determined in the sealed glass ampoules treated with Br_2 which were used for total S, as this method should also trap H_2Se. In every case the Se concentration in the ampoules is greater than or equal to the particle value (Table 2-11). A large uncertainty (>10%) must be placed on these values. At 21° N the values range from <1 nmole/kg at NGS to approximately 70 nmoles/kg at the other three vent areas. In deep water there are ~2.5 nmoles/kg. Se decreased in the GSC solutions.

All of the metals follow the same relative distribution pattern:

HG $\geq$ OBS > SW > NGS

Co:	227 > 213 > 66 > 22	nmoles/kg
Cu:	44 > 35 > 9.7 > (<0.02)	µmoles/kg
Zn:	104 ≈ 106 > 89 > 40	µmoles/kg
Ag:	37 ≈ 38 > 26 > (<1)	nmoles/kg
Cd:	180 > 155 > 144 > 17	nmoles/kg
Pb:	343 > 294 > 185 > 175	nmoles/kg
As:	452 > 247 > 214 > (<30)	nmoles/kg
Se:	~70 > 0	nmoles/kg.

The low values at NGS are presumably due to reduced solubilities of these insoluble sulfide formers at 273° C versus the 350° C of the other vents and their incorporation into pyrite. Where data exist, most of these metals are complexed as Cl species at temperatures >300° C (sulfide

species complexes only become important below this temperature). The strength of the Cl complexes and hence the solubilities of most of these metals drops rapidly from 350-250° C. Crerar and Barnes (1976) have shown this to be the case for Cu. Based on thermodynamic calculations (Bowers, Von Damm and Edmond, 1983) the NGS solutions are saturated with respect to pyrite but not chalcopyrite. Fe is present in much greater amounts than Cu and presumably the Cu is being lost into the pyrite. Selenium often occurs in pyrite, substituting for S. Ag is also found in pyrite. Oudin (1981, 1983) reports the presence of tennantite $[(CuAg)_{10}(Fe,Zn,Cu)_2As_4S_{13}]$ in the chimneys which contains Ag, As and Cu in addition to Fe. The precipitation of pyrite may account for the quantitative (within the analytical precision) loss of Cu and may account for similar losses of Ag, As and Se with these elements being incorporated into the Fe-Cu phase. Co and Cd which are still present in measurable amounts behave more like Zn, of which a large amount is still present. Pb is also still present in large amounts.

It is important to examine other arguments which could account for the observed distributions. The first of these is to examine the extraction efficiencies of these elements from the basalt (Table 2-3) . All of these elements are far from being quantitatively removed from the rock. This suggests that the rock composition is not, per se, controlling the solution chemistry of these elements but that another factor such as formation of a secondary phase is important. As all of these elements tend to form sulfides, they may be the secondary phase.

Much work has been done on the observed zoning in ore deposits. Hence even if the experimental work has not been done and the thermodynamic data do not exist a good empirical understanding of the relative ease of metal

transport exists. From a composite of ore deposits (the entire sequence does not exist in any one ore deposit) the decreasing order of metal mobility is:

$$Hg > Pb > Zn > Cu > Sn > Ni > Fe > Co$$

and the relative strength of complex stability from the available thermodynamic data is:

$$Hg > Cd > Pb > Cu \geq Zn > Sn > Ni > Fe > Co > Mn$$

(Barnes and Czamanske, 1967).

The relative extraction efficiency for the solutions at 21° N is:

$$Ag \geq Cd \geq Zn > Mn \geq Pb \geq Cu > Fe \cong Co > Ni.$$

This is in reasonable agreement with the above sequences. This suggests that these metals in the 21° N solutions are in part controlled by transport and solubility (secondary processes) rather than by leaching from the rock.

Nickel was below the detection limit of 140 nmoles/kg at 21° N. The nickel concentration in deep water is ~10 nmoles/kg while in rock it is 1-5 mmoles/kg (Kay and Hubbard, 1978). Therefore while it cannot be definitively stated that it is not enriched in the solutions a limit can be placed on its extraction efficiency. As and Se are omitted from most of the above discussion because the thermodynamic and rock data for them is virtually nonexistent.

Another possible explanation for the low values in some of the vent areas is an aging phenomenon. If the rock is old and has been altered it may be depleted in some of these elements and hence less is leached into solution. The extraction efficiencies are so low that it is unlikely that this can explain a total absence of an element in the solution. Lithium,

one of the most soluble elements, does not appear to be depleted from the rocks prior to this alteration episode, although it shows variations between the vent fields (not in exactly the same order as the sulfide formers). Based on the higher Li/K ratio, HG may be "fresher" rock or younger and this is consistent with all the trace metals being higher in this vent.

2.3 Sulfur System

Sulfur plays a critical role in hydrothermal circulation, yet its cycle is very complex, and as will be seen below, cannot be completely constrained with the available data. Reduced sulfur may be important in limiting the transport of metal species and is responsible for the formation of mineral deposits at 21° N. Besides its importance in inorganic reactions, reduced sulfur from the vents is the primary food source for the chemosynthetic biological communities living around the vents. It is difficult to balance the present day oceanic sulfur cycle and hydrothermal circulation may provide a needed sink (see discussion in McDuff and Edmond, 1982) as well as a mechanism for changing the sulfur isotopic composition of seawater through time.

Seawater is the input fluid and before undergoing any reactions in the hydrothermal system it contains ~28 mmoles/kg sulfate and no reduced sulfur. When the reacted seawater exits from the hydrothermal vent it contains <9 mmoles/kg of hydrogen sulfide and no sulfate (Table 2-8). Thus a net loss of sulfur occurs as seawater traverses the hydrothermal system. Whether this is a permanent sink will be discussed below.

The first complication in the sulfur system is that there are two possible sources: seawater sulfate and basaltic sulfur. The second

complication is that there are two possible sinks: deposition of seawater sulfate as anhydrite ($CaSO_4$) or reduction of seawater sulfate (with possible admixture of basaltic sulfur) and precipitation at depth in the system as pyrite or other metal sulfides. The sulfur content alone provides no information on the relative importance of the various sources and sinks. Other lines of evidence can provide additional constraints - although these may also not be definitive. Sulfur has 4 naturally occurring stable isotopes of which ^{32}S (95.0%) and ^{34}S (4.22%) are the most abundant. Seawater sulfate is enriched in ^{34}S ($\delta^{34}S \simeq 20^{\circ}/\circ\circ$) at the present time while basaltic sulfur ($\delta^{34}S \simeq 0^{\circ}/\circ\circ$) is more depleted. As the two possible sulfur sources have distinctly different isotopic contents, the isotopic composition of the exiting solution may provide information on the source. A major drawback to this interpretation is the approximately $-20^{\circ}/\circ\circ$ fractionation that occurs when sulfate is reduced to sulfide at 350° C (Ohmoto and Rye, 1979). Thus the first sulfide formed from the reduction of sulfate will have $\delta^{34}S \simeq 0^{\circ}/\circ\circ$; the same as the basalt value. If all the sulfate is reduced the isotopic composition must be conserved and the resulting sulfide will be $+20^{\circ}/\circ\circ$. If the sulfate is only partially reduced, the resulting isotopic composition of the sulfide will be in the range $0\text{-}20^{\circ}/\circ\circ$; the same range as would be achieved by mixing basaltic sulfur with seawater sulfate. Sulfur isotopes by themselves are therefore not completely diagnostic of source. Several models will be presented below which address this question in more detail.

Additional constraints may be derived by examining other species which may act as sulfur analogs. Arsenic and especially selenium can substitute for sulfur. Both of these elements have low concentrations in seawater and much higher concentrations in basalt. The total concentration of these

elements in the hydrothermal solution can be treated as wholly basalt derived. If they truly behave like sulfur their extraction efficiencies from basalt should be the same as for sulfur, and therefore the total input of basaltic sulfur can be determined. There are several problems with this approach. First the basalt content of Se and especially As is poorly known, making calculation of an extraction efficiency difficult. Second, As and Se and may behave differently than sulfur especially if metal sulfides (selenides, arsenides) are being precipitated at depth. An advantage of using As and Se is that if they both give the same results, although they themselves are different elements, this will provide more confidence that S behaves the same way. Se and As may therefore provide some constraint on the sulfur system.

Additional limits are placed on the sulfur system based on the chemical composition of the basalt. The basalt at 21° N contains ~13 mmoles/kg sulfur (RISE Project Group, 1980), therefore this is the maximum amount that can be leached into solution. If all the seawater sulfate is deposited as anhydrite the basalt must contain enough Ca to do this and to provide the remaining Ca to achieve the observed solution composition. The rock contains a large amount of Ca (2.2 moles/kg) and this provides no constraint. Similarly the Fe content of the rock provides a potential constraint. Eight moles of Fe^{2+} must be oxidized to Fe^{3+} to reduce each mole of sulfate (S^{6+}) to sulfide (S^{2-}) but at the low water/rock ratio observed in this system enough Fe is available for the reduction and it is not a limiting factor.

Based on the above constraints and the available data several models for the sulfur system will be examined. These models demonstrate that while the processes cannot be uniquely quantified, certain constraints can

be made.

Case I: Everything is taken at face value. An average of 7.4 mmoles/kg of H_2S (Table 2-8) with an isotopic composition of $\delta^{34}S \simeq 3.7^{\circ}/\circ\circ$ (Kerridge et al., 1983) exits from the vents. Sulfate reduction is assumed to have gone to completion with no resulting isotopic fractionation.

$$x(+20^{\circ}/\circ\circ) + (1-x)(0^{\circ}/\circ\circ) = 1(3.7^{\circ}/\circ\circ)$$
$$x = 0.185$$
$$(1-x) = 0.815$$

where x = the fraction of sulfur derived from seawater sulfate
and (1-x) = the fraction of sulfur derived from basaltic sulfur.

Approximately 20% of the H_2S is from the reduction of seawater sulfate and 80% is from the basalt.

0.2(7.4) = 1.5 mmoles/kg from seawater sulfate
0.8(7.4) = 5.9 mmoles/kg from basalt sulfur.

This implies several things:

a. no subsurface precipitation of sulfides has occurred.

b. the rest of the sulfate (~27 mmoles/kg) was deposited as anhydrite implying that >17 mmoles/kg Ca was leached from the rock.

c. the extraction efficiency of the S from basalt is 45%.

This case cannot, per se, eliminate precipitation of sulfides at depth. For precipitation to occur it requires that the ratio of basaltic S to seawater sulfate be maintained at ~4:1, and that the reduction occurs before sulfide precipitation. If precipitation is occurring, more basaltic S and less Ca are being extracted. The above discussion assumes the simplest kind of precipitation: the precipitates have the same sulfur isotopic composition as the solutions. If precipitation were occurring in equilibrium with the solutions at 350° C, the sulfides formed should be $0.3^{\circ}/\circ\circ$ lighter (Kerridge et al., 1983) than the solutions and this would have a small affect on the isotopic composition of the solutions. In

practice, the sulfides in the chimneys appear to average +1.9°/oo (Kerridge et al., 1983), 1.8°/oo lighter than the solutions. (Hekinian et al., (1980), Styrt et al., (1981) and Arnold and Sheppard (1981) found $\delta^{34}S$ values in the sulfides of +1.4 → + 4°/oo.) Continued deposition of sulfides with this isotopic content would result in the solution S becoming progressively heavier. This would imply that less than 20% of the S is seawater derived; resulting in a higher S (and Ca) extraction from basalt.

This case therefore implies a maximum of 20% seawater sulfate being in the endmember. It is not constrained by the absolute amount of sulfate reduced (and iron oxidized), the amount of anhydrite precipitated or the amount of S and Ca leached from the rock.

Case II: The seawater sulfate is quantitatively reduced.

From Case I, the seawater sulfate must comprise $\leq$20% of the total sulfur emanating from the hydrothermal vent to maintain the observed isotopic composition. Since seawater contains 28 mmoles/kg of sulfate this implies that $\geq$112 mmoles/kg must be leached from the basalt. Basalt contains ~13 mmoles/kg of sulfur therefore this case can be eliminated in a simple flow system. (This case cannot be eliminated in a more complex flow system where it could be postulated that all the seawater sulfate is reduced and 80% is deposited before the conditions are such that the basaltic sulfur is leached into solution. Although this appears unlikely, the Fe content of the basalts does not prohibit complete reduction of the sulfate.)

Case III: The basaltic sulfur is quantitatively extracted.

From Case I the basaltic S is $\geq$80% of the total sulfur. Since basalt contains ~13 mmoles/kg S this implies $\leq$3 mmoles/kg of seawater sulfate

must be reduced. This case requires:

a. deposition of 9 mmoles/kg of S as metal sulfides at depth.

b. deposition of $\geq$25 mmoles/kg anhydrite, implying that $\geq$15 mmoles/kg of Ca must be leached from the basalt.

This case does not contradict any of the arguments presented thus far. However if the arguments presented in Case V are correct they suggest that Case III is not be a likely scenario. Those arguments are not strong enough to eliminate Case III based on present data.

Case IV: No basaltic sulfur is leached from the rock, therefore all the sulfur is from the reduction of seawater sulfate.

It was noted earlier that the fractionation of sulfur reduced from sulfate to sulfide at 350° C is -20°/‰ (Ohmoto and Rye, 1979). If a Rayleigh distillation is assumed (which is not necessary but gives the lowest isotopic value) and the total amount of sulfur reduced is assumed to be the total amount observed in solution (7.4 mmoles/kg implies 26% of the seawater sulfate is reduced):

$$\alpha = \frac{\delta^{34}S_r + 1000}{\delta^{34}S_{ox} + 1000}$$

where S_r = reduced sulfur and S_{ox} = oxidized sulfur.

$$= \frac{0 + 1000}{20 + 1000}$$

$$\alpha = 0.98$$

$$\delta^{34}S_{ox} = [(\delta^{34}S)_{init} + 1000]f^{(\alpha-1)} - 1000$$

where $(\delta^{34}S)_{init}$ = the initial isotopic composition of the sulfur
and f = the fraction of the oxidized (ox) species remaining.

$$= [20 + 1000](0.74^{-0.02}) - 1000$$

$$\delta^{34}S_{ox} = 26$$

$$\delta^{34}S_r = \alpha[(\delta^{34}S_{ox}) + 1000] - 1000$$

$$\delta^{34}S_r = 5.5$$

If 26% of the seawater sulfate is reduced the sulfide formed will have a

$\delta^{34}S = +5.5°/oo$. This is higher than the observed value of $+3.7°/oo$. The reduced sulfur exiting from the hot springs must therefore contain at least some basaltic sulfur. However based on this calculation about two-thirds of the sulfur could be derived from the reduction of seawater sulfate, if the reduction process has not gone to completion.

Case V: Initially ignore the constraints from the isotopic composition. Assume that As and Se are good sulfur analogs and that As, Se and S have the same extraction efficiency from basalt.

Se has a maximum 2.3% and As a maximum 1.5% extraction efficiency from the basalt (in three of the vent areas). If S is also assumed to have a maximum 2.3% extraction efficiency this implies that 0.3 mmoles/kg S is from the basalt and the rest (7.1 mmoles/kg) is from the reduction of seawater sulfate. This implies that 25% of the seawater sulfate is reduced. This reduces to essentially Case IV when the isotopes are considered, as the seawater contribution has $\delta^{34}S = 5.3°/oo$ (if Rayleigh distillation is assumed which is not necessary but it gives the lower isotopic value).

$$\frac{7.1}{7.4}(5.3) + \frac{0.3}{7.4}(0) = 3.7$$

$$5.1 > 3.7$$

The sulfur extraction efficiency cannot be as low as that implied by the As and Se data, or the sulfur isotopes would be higher. The apparently too low extraction efficiencies may be due to unrealistically high concentration values for the basalt, as these values are poorly known. Case V provides no additional constraints beyond Case IV. The Se and As however do imply that some basaltic S must be present.

From the above discussion it can be concluded that the sulfur in the exiting hydrothermal solutions must be a mix of both basaltic S and seawater sulfate. The relative proportions of each cannot be defined with

the present data. Unless a two stage model is invoked all the seawater sulfate cannot be reduced and agreement maintained with the isotopic data. This implies that some anhydrite must form and that some seawater sulfate must be reduced. The relative proportion of each may be dependent on the flow system (section 2-5). The experiments have shown that the reduction of sulfate to sulfide is rapid (on the scale of days) if the fluid is at >300° C (Shanks et al., 1981). The complication is that if seawater is heated to >150° C it becomes supersaturated with anhydrite. If the flow system is such that the water traverses the isotherms from 100-300° C rapidly, minor sulfate will be lost as anhydrite and the rest can be reduced. If the solution spends a long time at 100-200° C it will lose much of its sulfate as anhydrite. The experimental work has shown that Ca can be leached out of the rock at low (150° C) temperatures (Seyfried and Bischoff, 1979) so the amount of anhydrite which can form is not limited by this. Additional experiments have shown that it takes 175 hours with glass and 600 hours with diabase (water/rock = 10) to remove half the sulfate at 150° C (Seyfried and Bischoff, 1979); and less than 24 hours with glass and less than 86 hours with diabase (water/rock = 10) to remove all the sulfate at 300° C (Seyfried and Bischoff, 1981). These experiments provide some constraint on how fast the flow across the isotherms must be if sulfate is to be deposited as anhydrite or reduced to sulfide. If major amounts of anhydrite form, it must later be redissolved as it has only been observed as veins in DSDP Hole 504B where it is interpreted as a late alteration product in the oceanic crust (Anderson et al., 1982). Anhydrite would provide therefore only a temporary sink for any sulfur deposited. If on the other hand the sulfate is reduced and precipitated as a metal sulfide hydrothermal circulation is a permanent sink for sulfur. Subsurface

precipitation of sulfides should be occurring at NGS based on the calculated saturation of pyrite (Bowers, Von Damm and Edmond, 1983) and the stockwork zone observed in ophiolites. Therefore hydrothermal circulation is most likely an active S sink but its magnitude is less than the total 28 mmoles/kg which entered the system.

2.4 Silica Concentration and the Depth of Reaction

Extensive work on continental hydrothermal systems has shown that the dissolved SiO_2 concentration is often in equilibrium with quartz, present in the solid phase. As quartz solubility is a function of both temperature and pressure, if the SiO_2 content of the solution and either temperature or pressure is measured, the other parameter can be determined. A large amount of experimental work has been done on the system SiO_2-H_2O over a wide range of pressure and temperature conditions in order to apply it accurately to continental hydrothermal systems (Fournier et al., 1982 and references therein). An obvious extension is to apply it to submarine hydrothermal systems where similar pressure and temperature conditions of reaction occur.

At 21° N the SiO_2 content and temperature of the exit solutions were measured (Table 2-12). The pressure at which the solutions were last in equilibrium with quartz can then be determined. The pressure can be assumed to be hydrostatic (as it is an open fracture system) and the depth of the overlying water column is known (2500 meters ≈ 250 bars). The pressure can be calculated and converted to a depth within the oceanic crust at which the reaction occurred. Several assumptions are inherent in this approach:

1. The solutions reached equilibrium with quartz and are not in equilibrium with a different phase.

2. The solutions have not cooled, except adiabatically since achieving equilibrium.

3. The solutions have not precipitated quartz (due to cooling or a decrease in pressure) since they reached equilibrium.

There are essentially no checks, except for the consistency of the data on the above assumptions.

Most of the work done on quartz solubility has been done in pure water, not salt solutions. The 21° N solutions which contain ~0.6 M NaCl are relatively dilute solutions when compared to the salinities observed or inferred for most hydrothermal solutions. Fournier et al. (1982) recently performed a series of experiments to see how the salt content of a solution affects quartz solubility. Their experiments were done at 350° C, pressures of 180-500 bars and 0, 2, 3 and 4 M NaCl solutions. Their data do not cover the range of SiO_2 concentrations observed at 21° N and the temperature is too high for the Guaymas system. The major conclusion of their work is that at the studied pressure and temperature conditions NaCl increases the solubility of quartz. The experimental data of Kennedy (1950), although in distilled water, covers the entire range of pressure and temperature conditions and SiO_2 concentrations observed at 21°N and Guaymas. The data of Kennedy (1950) are therefore used to find the pressures at 21° N and Guaymas (Table 2-12), as the use of a single data set will assure that the conclusions are internally consistent. The pressures obtained from this data set should be treated as maximum values as the presence of NaCl in the solutions will increase the solubility of quartz (i.e. have the same effect as a higher pressure).

The four vent areas at 21° N display a variation in SiO_2 content. The highest value (19.5 mmoles/kg) is observed at NGS which is the most northeasterly vent and the values decrease to the southwest. The OBS vent

Table 2-12: Temperature, Silica and the Depth of Reaction

	T °C	SiO_2 m[1]	P bars	Depth[3] kms
21° NORTH				
NGS (+)	273(350)	19.5	>1000(600)	>7.5(3.5)
OBS (△)	350	17.6	450	2.0
SW (◇)	355	17.3	400	1.5
HG (□)	351	15.6	300	0.5
GUAYMAS				
Area: 1 (◇)	291	12.9		
2 (△)	291	12.5		
3 (+)	285(310)	13.5	>1000(300)	>7.5(0.5)
4 (□)	315	13.8	300	0.5
5 (•)	287	12.4		
6 (X)	264	10.8		
7 (◇)	300	12.8	300	0.5
8 (△)	273			
9 (□)	100	9.3		
10 (X)				
GSC[2]	<20	21.9	>600	>3.5
SEAWATER	2	0.16(21°) 0.18(GY)	250 200+50	

[1]Units: m = millimoles/kg

[2]All GSC data is /liter.

[3]Depth is below the seawater-basalt or sediment-basalt interface.

contains 17.6 mmoles/kg which is slightly greater than the SW area at 17.3 mmoles/kg which is significantly greater than the HG vent at 15.6 mmoles/kg. SiO_2 is one of the few species which shows a geographically consistent trend, decreasing from the northeast to the southwest. Ballard and Francheteau (1982) have presented a model in which they propose that the zone of most recent activity is the topographic high along a given section of ridge crest. HG is closest to this high point and NGS is the furthest away. If a magma chamber is present in this area the SiO_2 content of the solutions may indicate a gradual deepening of the isotherms or depth to the top of the magmas chamber as more of its top surface has been cooled due to longer times of hydrothermal circulation.

The temperature of the hydrothermal solutions was measured with a thermocouple on Alvin at the time they were collected. Measuring the temperature is not trivial as it is often difficult to insert the probe into the chimney orifices long enough to achieve a stable reading. The highest stable reading recorded is taken as the true temperature. The vents at 21° N were all visited on several different dives over a twelve day period and the same temperatures were recorded on different days, placing additional confidence in the values.

Figure 2-25 is a plot of the data of Kennedy (1950) with the different vent areas plotted from their measured temperature and SiO_2 contents. From the plot the following pressures can be determined: HG = 300 bars, SW = 400 bars, OBS = 450 bars and NGS >1000 bars. Once the pressure from the overlying water column is removed (250 bars) the following pressures/depths of reaction can be calculated: HG = 50 bars or ~0.5 kms below the seafloor and into the ocean crust, SW = 150 bars or 1.5 kms, OBS = 200 bars or 2.0 kms and NGS >750 bars or >7.5 kms. On a physical basis it appears unlikely

Figure 2-25: Solubility of quartz as a function of temperature and pressure. Data are those of Kennedy (1950) in distilled water. Pressures are in bars. The 21° N areas are plotted on the figure as follows:

N = NGS
O = OBS
S = SW
H = HG.

The Guaymas areas are also shown and are designated by their area numbers.

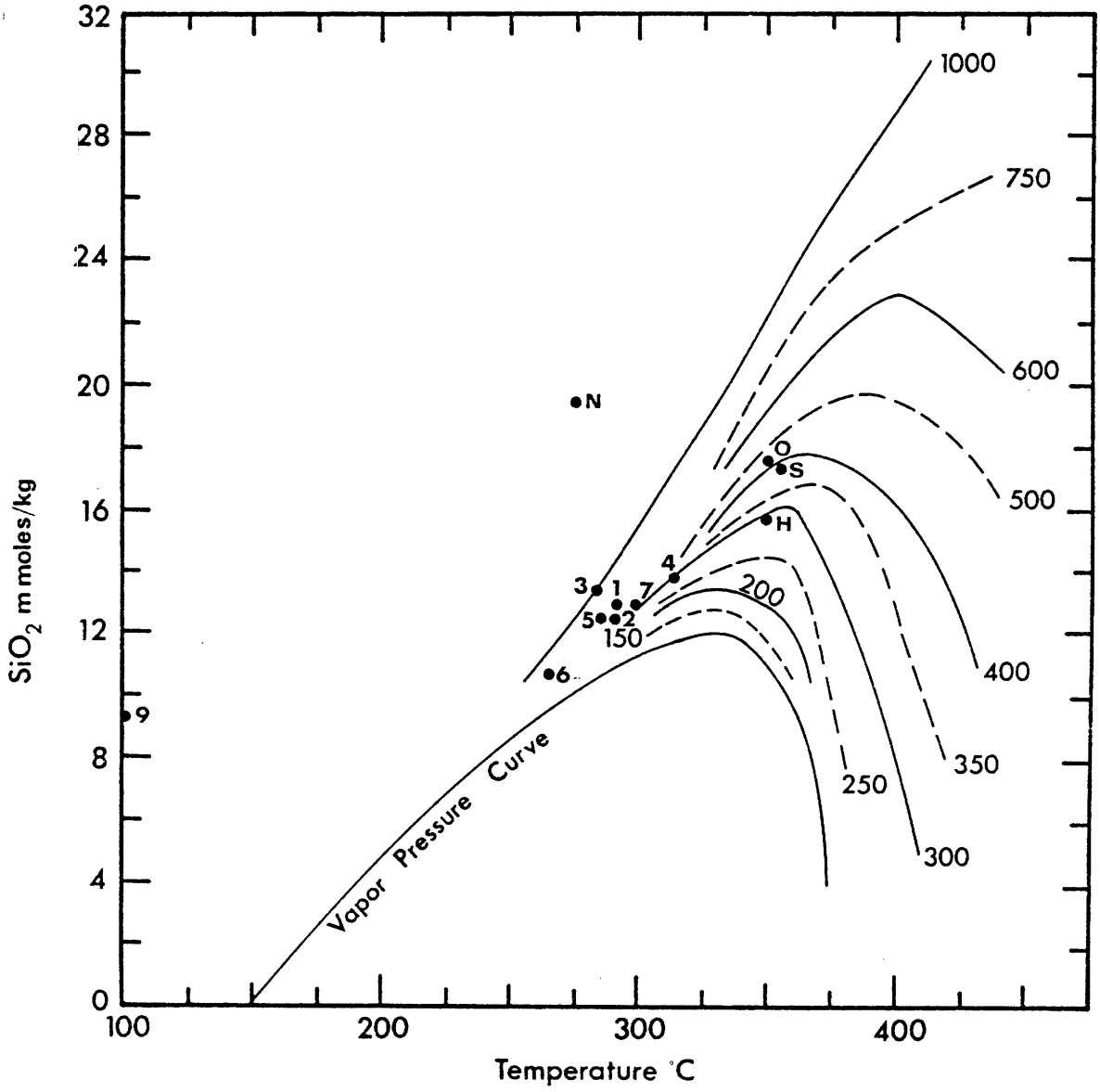
32
28
24
20
16
12
8
4
0
100
200
300
400
Temperature °C
SiO2 m moles/kg
1000
750
600
500
400
350
300
250
200
150
Vapor Pressure Curve
N
O
S
H
1
2
3
4
5
6
7
9

that NGS which is only 400 meters from OBS has a depth of reaction >5.5 kms deeper. A more reasonable explanation is that NGS reacted at a higher temperature but has conductively cooled since leaving the zone of reaction (an explanation which is consistent with the pyrite saturation). If it is assumed that NGS was 350° C, as are the other vents, its inferred pressure becomes ~600 bars or 3.5 kms into the basalt, a geologically more reasonable value based on what is observed at the other vents.

Using the measured temperature and calculated pressure a temperature at depth can be back calculated assuming adiabatic expansion over the depth interval, and if necessary a new pressure based on the new temperature can be calculated until the values converge. For this calculation it is assumed that no conductive cooling occurs, as has already been shown to be false for NGS, and enthalpy is conserved. In practice, as the net pressure difference is small, so is the temperature difference and within all the uncertainities the pressures calculated on the "first pass" do not change in subsequent calculations. HG, with a measured temperature of 351° C would have a temperature of 350-355° C (these temperatures are given as 5° ranges due to the uncertainities), SW measured at 355° C would increase to 360-365° C and OBS measured at 350° C would increase to 355-360° C. Thus unless conductive cooling is invoked for all the vent areas, the temperatures at depth are less than 10° C higher than the measured temperatures. If conductive cooling is occurring the points on figure 2-25 would all move to the right. Because of the form of the isobars in the figure, this would require very little increase in the depth of reaction for temperatures of 350-400° C. (Based on the physical properties of water it is unlikely that they are much hotter than 400° C at depth (Green, 1980)). If HG is actually in the temperature range 350-363° C at depth it

will have a lower pressure for the same silica content and hence a shallower depth of reaction into the oceanic crust. Based on the 350° C temperature, reaction at HG occurs 500 meters into the oceanic crust. This reaction must occur below the seafloor (2500 m = 250 bars), therefore the pressure determined by this method must be greater than 250 bars. The temperatures at depth cannot be much higher based on the pressure constraint. As noted earlier the pressures determined by this method are maximum values because of the increased solubility of SiO_2 in salt soluitons. A summary of the calculated pressures and depths of reaction are given in Table 2-12.

The data from the 1979 cruise implied that the endmember silica concentration was 21.5 mmoles/kg. Sampling was poor on that cruise (Appendix 1) and the endmember concentration is based on essentially one sample (Mg = 7 mmoles/kg, 86% hydrothermal water). The 1979 value is higher than the 1981 value for this area but this difference is attributed to sampling problems.

Supporting evidence for these silica depths of reaction comes from geophysical evidence. An array of ocean bottom seismographs were deployed at the 21° N site in 1980 (Riedesel et al., 1982) including one within 300 meters of a black smoker. Most of the recorded events occur within 1.75-2.75 kms below the seafloor. The authors suggest that this may be the depth of hydrothermal circulation. The seismographs were closest to the OBS vent (hence its name) which gives a depth of reaction of 2.0 kms based on SiO_2; in excellent agreement with the geophysical data.

The depth of hydrothermal circulation inferred at 21° N varies between vent areas from 0.5-3.5 kms. These are maximum depths of reaction because the effect of salt on quartz solubility was not considered. The data for

three of the vent areas does not require them to be any hotter at depth as suggested by Bischoff (1981) but one vent (NGS) appears to be undergoing conductive cooling. If NGS is also assumed to be ~350° C at the time of reaction its depth is consistent with that obtained for the other vents. The depth of hydrothermal circulation inferred from the earthquake data (Riedesel et al., 1982) is in agreement with that calculated by SiO_2 geobarometry. The depth of circulation at 21° N appears to be shallower than that inferred for the GSC (Edmond et al., 1979a) which was highly uncertain.

2.5 21° N Model

No rigorous model can be proposed to explain the differences in solution chemistry between the vent fields at 21° N. Mechanisms which can control individual elements have been previously discussed in this chapter. The main difficulty in modelling the 21° N system is that the conditions and reactions occuring at depth in the system are unknown and can only be inferred from the solution chemistry. The chemistry at the four vent areas differs; what is occurring at depth must also differ. NGS has lower exit temperatures therefore some of its chemical differences can be attributed to this. The other areas all have 350° C "smokers"; therefore, exit temperature cannot be used to explain their differences. Several parameters imply that HG may be a "younger" vent reacting with "fresher" basalt. This still leaves the SW and OBS vents with chemical differences between them that cannot be explained. As discussed in section 2.2 equilibrium is not achieved between the water and the rock in these systems and this accounts for the observed differences. Several general models will be examined for their influence on solution chemistry. None of these models alone can account for the observed differences in solution but

presumably some combination of these models is correct.

1. Aging Trend. If it is assumed that the hydrothermal activity is moving to the southwest then NGS is the oldest vent and HG is the youngest. The older vent should be flowing through more leached rocks and therefore should have lower alkali concentrations. The channel walls would also be armored from previous reactions, again resulting in a more dilute concentration for many of the elements. Certain phases, such as the pyroxenes appear to be more resistant to alteration, hence elements in these phases (such as Ca) might have relatively higher concentrations in an older vent. An immediate problem for this model is that NGS has the highest K content of any vent area. As alteration increases so should the observed water/rock ratio. As the water/rock ratio increases the mineral assemblage within the greenschist facies should change. Mottl (1983) has presented the following reaction sequence:

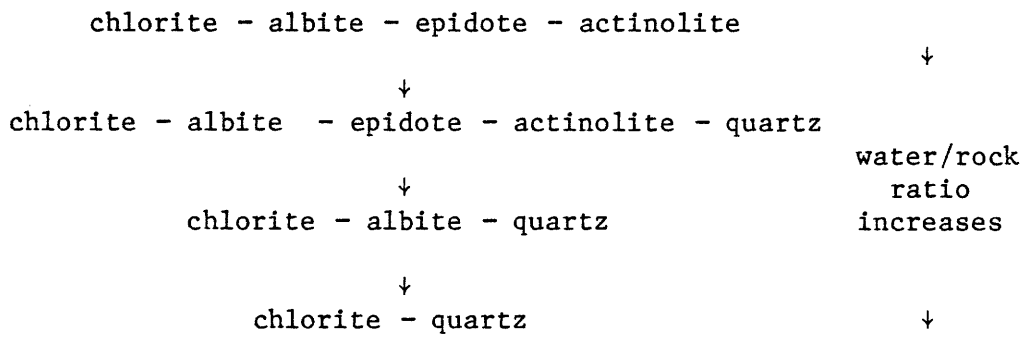

Hence albite and epidote should be converted to chlorite as the "aging" increases with a resultant release of Na and Ca to solution. Although higher Na and Ca are seen at NGS the isotopic and chemical data give no evidence of an increase in water/rock ratio compared to OBS and SW.

2. Pathlength. If the silica concentrations can be assumed to be due to equilibrium with quartz, it can be used in conjunction with the measured temperature to calculate a pressure (depth) of reaction. The silica

implies an increasing depth of reaction from HG to NGS. An increasing depth of reaction may also imply an increase in the pathlength of the cell. Williams (1974) in a study of cellular convection in the laboratory and in the field (GSC) found the ratio of the two dimensions (horizontal:vertical) of the flow cell to be approximately 1.6. This would imply that water which has a deeper depth of reaction (vertical distance) also has a longer recharge distance (horizontal distance). Green (1980), in a further study at the GSC, found this ratio to be 40 ± 10 but did not believe that he or Williams had sufficient data to truly define this parameter. (Williams data when combined with silica geobarometry on the solutions implies a recharge zone 0.8-5.6 kms from the vents. Green's data implies a distance of 15-175 kms.) While the relationship between the increase in horizontal length to vertical depth in these cells remains an open question, it is obvious that a greater depth of reaction requires a longer path length. A longer pathlength may have implications for the chemistry of the solutions. First, the solutions come in contact with more rock (giving a smaller effective water/rock ratio). Second, if flow rates do not vary between vent areas this means the water will spend more time in contact with the rock. More time in contact with the rock presumably means more time for leaching to occur from the rock to the solution and more of a chance that equilibrium is reached (or more closely approached). More leaching would imply increases in the concentration of some dissolved species while equilibrium could imply either increases (from undersaturation) or decreases (from supersaturation). A secondary effect of longer pathlength may be longer time spent in the upflow zone. Longer time may permit conductive cooling to occur and this may result in a temperature drop in the solution. Attendant with a temperature drop may be the precipitation

of species which are now supersaturated in the solutions. This cooling and loss of pyrite appears to be occurring in the NGS vent, which based on Increased pathlength may be as important on the inflow (or downflow) limb of the hydrothermal circulation as on the upflow. If the downflow limb is long this may mean that the solutions cross the isotherms slowly, inferring that they spend more time at intermediate temperatures. This may be especially important for the sulfur chemistry of the springs and, as a result, for their metal chemistry as well. Seawater becomes saturated with respect to anhydrite ($CaSO_4$) merely by heating to >130° C at the pressure conditions of the ridge crest (Haymon and Kastner, 1981). The experiments have shown that Ca can be leached out of the rocks at this temperature (Seyfried and Bischoff,1979). The experiments have also shown that it takes a finite amount of time to precipitate this anhydrite (Seyfried and Bischoff, 1979) i.e. it is not instantaneous. If the solution spends a great deal of time at 100-200° C it will probably lose most of its SO_4 as anhydrite. If the pathlength is shorter and the solution traverses the isotherms rapidly there is a greater potential for the SO_4 to reach the >300° C zone where it can be reduced relatively rapidly to sulfide (Shanks et al., 1981). The pathlength in the downflow zone may therefore be as important as that for the upflow zone.

3. Residence Time. It cannot be presumed a priori that the flow rates are the same in all the vent areas or even how they vary. Hence, the residence time that the water spends in the fissures is not necessarily directly proportional to the pathlength. An increased residence time does not infer that the solution will come in contact with more rock as will occur with an increase in pathlength. An increased residence time does imply that more time is available for the solution to react with the rock, hence leaching may increase and equilibrium may be more closely approached.

It may also mean that the solution has time to conductively cool after it has reacted, leading to precipitation. Many of the effects of increased pathlength (d) and residence time (τ) are the same and they are difficult to separate. If flow rates (v) are the same in all vent areas these two parameters are directly related:

$$v = d/\tau$$

and need not be separated. As mentioned for the pathlength the residence time in the downflow zone may be as critical for the final solution chemistry as that for the upflow zone. Lister (1982 and references therein) has modelled hydrothermal circulation extensively and although his models permit calculation of a residence time for the upflow zone he does not believe that they are representative of real conditions.

4. Temperature. Experimental work (section 2.9) has shown that temperature is an important parameter in leaching species from basalt into solution. Higher temperatures result in increased leaching efficiency. Variations in the temperature of the hot springs at depth would be another mechanism to explain differences in their observed chemistries. At 21° N vents with temperatures of approximately 273° C at the seafloor contain no copper, while those with temperatures of 350° C do. The 273° C vents are however, inferred to be ~350° C at depth and to have conductively cooled (section 2.4). The measured temperatures at 21° N range from 270° C to 355° C. Adiabatic expansion, over the depth calculated from the silica data, would add less than 10° C to these temperatures. Bischoff (1980) has suggested that the hot springs are closer to 400° C at depth. This would require conductive cooling as well as cooling due to adiabatic expansion. As three of the vent areas have exit temperatures of 350-355° C this would require them to cool to the same temperature although they are spread over

almost 8 kms. This suggests that the 21° N solutions are all of similar temperature and are not much hotter at depth. The maximum temperatures recorded at 13° N are less than 350° C (Michard et al., 1983) and the inferred temperature for GSC was 344° C (Edmond et al., 1979a). The highest temperature recorded from continental hydrothermal systems is ~370° C at Cerro Prieto and the Salton Sea (Barnes, 1979).

From the preceding discussion it can be seen that several factors such as age, pathlength, residence time and temperature, and the changes which they imply in other parameters, are important in fixing the solution chemistry. These factors may imply different chemical reactions and controls on the system but at present cannot be uniquely separated from the observed net changes in solution chemisty.

2.6 Chimney Chemistry

The mineralogy and chemistry of the chimneys, associated smoke and basal mounds at 21° N has been examined by several groups. Hekinian et al. (1980) described samples collected on the Cyamex expedition in 1978 on which only extinct chimneys were found. Haymon and Kastner (1979, 1981) examined samples from active and extinct chimneys collected during the RISE project in early 1979. Styrt et al. (1981) and Goldfarb (1982) examined a suite of samples collected on the November 1979 cruise on which preliminary water samples were taken. Oudin (1981, 1983) worked on samples collected on RISE and the November 1979 expedition. The mineral assemblages found by Hekinian et al. (1980) are different from those of the other workers because they are from extinct chimneys and the sulfates dissolved prior to sampling. Haymon and Kastner (1979, 1981) also noted differences between active and inactive chimneys. The samples examined by Oudin (1981, 1983),

Styrt et al. (1981) and Goldfarb (1982) are especially valuable because they can be correlated with water samples which were collected from some of the chimneys. Hekinian et al. (1980) and Oudin (1981, 1983) examined chimney samples for more trace metals than the other workers.

All of the workers note the large abundance of zinc sulfides (either as wurtzite or sphalerite) in the chimneys. It is always present in much greater abundance than the copper sulfides (principally chalcopyrite). This agrees with the solution composition in which Zn:Cu is always $\geq$3:1. Iron sulfides are also a major component. This is consistant with the large amount of iron found in the solutions. In all of the solutions dissolved sulfide predominates over dissolved Fe + Cu + Zn, etc. therefore the deposition of the metals is not limited by the sulfur content.

The solutions contain no sulfate. Abundant anhydrite and minor barite found in the active chimneys are formed when seawater sulfate mixes with the hydrothermal solutions which contain elevated levels of Ca and Ba. This has been substantiated by the sulfur isotopic value of the sulfates (Styrt et al., 1981). Oudin (1981, 1983) also reports the presence of $PbSO_4$.

Elemental sulfur is found associated primarily with worm tubes in the chimneys and is probably a secondary or biological product, as there appears to be no elemental sulfur in the hydrothermal solutions (Table 2-9).

Oxides and hydroxides are found as alteration products on the exteriors of the chimneys. Amorphous silica is often found inside the chimney.

The different workers analyzed for different suites of trace metals. All of them found some lead as galena. Hekinian et al. (1980) also report

the presence of silver, cadmium and cobalt with lesser selenium, gold and platinum. They found essentially no nickel. Nickel was not found in the hydrothermal solutions but all of the other elements (except gold and platinum which were not analyzed) were also found in the hydrothermal solutions. Oudin (1981, 1983) reported the presence of the arsenic minerals tennantite [$(CuAg)_{10}(Fe,Zn,Cu)_2As_4S_{13}$] and jordanite [$Pb_{14}As_6S_{23}$] and As was also found in the solutions. Goldfarb (1982) also analyzed for Cr but did not detect any in the solids.

The coexistence of sulfates and sulfides in the chimneys suggests they are disequilibrium assemblages which is not unexpected based on the rapidity of the mixing process. This is verified as well by the sulfur isotopes in the sulfides. If equilibrium is established the sulfide isotopic fractionation between various pairs of sulfide minerals can be used as geothermometers. Kerridge et al. (1983) has found that almost all the temperatures determined in this manner are incompatible with the observed temperatures inferring that the sulfide mineral assemblages are not at equilibrium.

Many of the chimneys are banded suggesting that the conditions of mineral deposition have changed with time. Styrt et al. (1981) suggest that the difference between "zinc-rich" and "copper-rich" chimneys is that the temperature of the hydrothermal solutions is less than or greater than 300° C respectively. Although this is a thermodynamically reasonable hypothesis, the temperature data from the 1979 cruise on which these samples were collected is not good enough to support this hypothesis. On the 1981 cruise the hydrothermal solutions at two chimneys with exit temperatures of 270-273° C (one at SW and the other at NGS) were found to contain no measurable copper, while still containing large amounts of zinc.

Thus the mineralogical or chemical content of the chimneys may well reflect changes occurring in the vent chemistry. This approach needs to be explored further. In general the chemical agreement found between the hydrothermal solutions and the chimneys they are forming is very good although the mineral phases forming are not necessarily in equilibrium with each other or the solutions.

2.7 Comparison to Ore Deposits

A major class of ore deposits are the volcanic-associated massive sulfide deposits, a subclass of which are the ophiolite-hosted deposits. Ophiolites are presumed to be sections of ancient oceanic lithosphere which have been emplaced on the continents. The massive sulfide deposits they contain are most likely formed by hydrothermal activity similar to that observed at 21° N today. In fact these deposits were cited as evidence for hydrothermal activity on the seafloor before it was actually observed. A comparison can be made between these ancient deposits and the 21° N solutions and deposits to better constrain whether the same processes are occurring in both cases.

Recent comprehensive reviews of ophiolite deposits are given by Coleman (1977) and Franklin et al. (1981) and the comparison given below is based on these two works.

The physical setting of massive sulfide deposits and the hot springs and their deposits at 21° N are similar. Massive sulfide deposits occur primarily on top of or within the pillow terrain; the chimneys at 21° N also occur on pillows, which may yet be covered (and preserved) by subsequent lava flows. The deposits are usually located near faults as are the 21° N hot springs. The ore bodies tend to be small yet several may

occur in a stratigraphic level. All the deposits found to date at 21° N are too small to be considered ore deposits (based on their surface expression) and the chimneys with associated deposits are often separated by several kilometers. SW site, with its several active chimneys meters apart and collapse pit which could provide a trap for some of the sulfides may be an early stage of an ore deposit in formation. Malahoff (1982) found an ore deposit sized massive sulfide body on the GSC to the east of the vents. Above the ore body itself is often found a sedimentary deposit known as the umbers which are iron and manganese sediments, and the ochres which are the product of iron sulfide oxidation. These deposits may also contain some diatoms and chert which may be a late late stage product of the hydrothermal circulation. The deposits often contain blocky pieces of ore. At the OBS site there is a large mound of weathered sulfide with blocks of fallen chimney on top. Below the massive ore body there is often a basal siliceous ore. Although this has not been observed at 21° N it may well be present as the solutions are extremely silica rich. Below the ore itself is often found a stringer zone which may extend for hundreds of meters below the deposit. Although we cannot see below the surface of the 21° N system, it is likely the circulation penetrates up to several kilometers into the oceanic crust (section 2.4) and may well be depositing sulfides at depth. DSDP Hole 504B (Anderson et al., 1982) penetrated for the first time what appears to be a hydrothermal feeder zone in the oceanic crust. In pillow basalts (911-929 m below the seafloor or 636.5-654.5 m into the basalt) they found a stockwork with abundant veins of chlorite, laumontite (a Ca-zeolite), quartz, minor talc, and the sulfides sphalerite, chalcopyrite and pyrite.

The chemistry of ophiolite deposits is relatively constant with iron

(as pyrite) predominating, followed by copper (as chalcopyrite), then zinc (as sphalerite) and sometimes with lead (as galena). Although much emphasis has been placed on the high Cu content of these deposits Franklin et al. (1981) point out that several actually have Zn>Cu or the two elements present in subequal amounts. In the 21° N solutions Fe>Zn>Cu>Pb. Au, Ag, As and Sn may also be found in these deposits (Coleman, 1977) and Ag and As were found in the 21° N solutions (Au and Sn were not measured). Franklin et al. (1981) note that the ore bodies contain high Co and low Ni, again in agreement with the solutions. Franklin et al. (1981) also note that the deposits are often underlain by Cu-rich vein and disseminated sulfides and that the deposits are often zoned with a decrease upward and/or outward in Cu/(Cu+Zn+Pb) ratio. This is in agreement with what is occurring at the NGS site. In 1979 this vent was 350° C while in 1981 it was only 273° C. Preliminary data suggested that it contained Cu (~15 μmoles/kg) in 1979, but it contained <0.02 μmoles/kg in 1981. Presumably Cu is depositing at depth (section 2.2) as a result of pyrite deposition due to conductive cooling. As a vent system cooled or aged, a resultant temperature drop could account for the observed decreasing Cu trend.

2.8 Comparison of Solution Chemistry to Observed Basalt Alteration

The 21° N hydrothermal solutions are seawater which has been modified through reaction with basalt at elevated temperatures. Concomitantly the chemistry of the basalt must change. Small differences in rock chemistry are more difficult to see than in the solution. Basalt alteration occurs at both high and low temperatures and at these different temperatures reactions may occur in opposite directions. An example of this is the alkalis which are leached from the rock during high temperature alteration

but are added to the rock at low temperature (Hart, 1969). It is difficult to separate these two effects as samples collected will usually have an unkown combination of the two processes. In an attempt to examine only the high temperature effects and to avoid the overprint of low temperature reactions, Humphris and Thompson (1978a,b) used rocks that were dredged from the ridge crest on the assumption that they have spent minimal time under the low temperature conditions. All comparisons will be made to this study as it is one of the most complete, with both major and trace element analyses and petrographic examination of the rocks.

Honnorez (1981) has argued that dredged rocks do not truly reflect the alteration of the oceanic crust because they have been exposed to large amounts of seawater for extended periods of time. Basalt drilled on several DSDP legs show different alteration assemblages from those seen in dredged rocks, but the degree of alteration also varies widely between DSDP sites. Drilled basalt samples are relatively rare and the studies do not include as many species as were determined in the Humphris and Thompson work (1977 a,b); thus the best comparison is still made to the latter work.

In general the direction of reaction (loss or gain) Humphris and Thompson observed in the rocks agrees well with the changes in solution chemistry.

Silica - Humphris and Thompson note a loss of silica during alteration to a maximum of 11 weight percent (1.7 moles/kg) which is more than adequate to account for the maximum solution gain of 0.02 moles/kg.

Calcium - They observe a linear decrease with water gain up to a maximum of 10 weight percent (2.4 moles/kg), again more than the observed solution increase.

Magnesium - It increases in the rocks by up to a factor of 2, or approximately 8 weight percent (3.3 moles/kg), which is much greater than the solution loss.

Iron - A loss is observed from the rocks but it is difficult to quantify due to localized pyrite precipitation. A gain occurs in solution chemistry.

Sodium - The rocks show no consistent trend. The solutions show both gains and losses but this is complicated by hydration reactions.

Potassium - The rocks show no consistent trend. Potassium shows a large gain in the solutions but goes into basalt during low temperature alteration.

Trace Elements

Boron - This is probably leached from the rocks but the value is close to their detection limit. There is an increase in the 21° N solutions (Spivack and Edmond, unpublished data).

Lithium - They found it to be mobilized in the rocks with a net loss from the interior of the pillows and an increase on their surface. It is greatly enriched in the 21° N solutions, but is known to go into rocks during low temperature alteration.

Strontium - It is mobilized in the rocks, but shows both losses and gains. The hydrothermal solutions show both small losses and gains.

Barium - Although it is mobilized in the rocks with the interiors showing some enrichment they suggest it is not very mobile. This disagrees with the solution data which suggest a large proportion of it is removed from the rock.

Nickel - They found no major effect on this element and it does not appear to be enriched in the hydrothermal solutions.

Cobalt - They found no major effect on this element although it is enriched in the hydrothermal solutions, but has a low extraction efficiency from the rock.

Copper - It was found to be leached from the rocks to a maximum of 1.6 mmoles/kg which is much greater than the elevated levels observed in the solutions (maximum 0.04 mmoles/kg).

Manganese - They found it to be mobilized with a maximum loss from the rock of 4.6 mmoles/kg which is greater than four times the observed amount in the solutions.

The results of Humphris and Thompson agree very well in the direction of change with the hydrothermal solutions themselves. The magnitudes of change are, as would be expected, different. These differences are however in the correct direction i.e. the value purportedly leached from the rocks is greater than the enrichment appearing in the solution. Therefore in no case does it appear that the system is "rock limited". Work by Hart et al. (1974) on altered basalts included data for S and Cl which are not often reported. Their rocks have undergone extensive low temperature alteration, making it impossible to separate the high temperature effects. They report loss of S (20 mmoles/kg) and gain of Cl (8 mmoles/kg) which are consistent with the hydrothermal solution data.

2.9 Comparison to Experimental Work

As seawater-basalt reactions at elevated temperatures were inferred to occur at oceanic spreading centers before they were actually discovered several investigators reacted these components in the laboratory (Bischoff and Dickson, 1975; Hajash, 1975; Seyfried and Bischoff, 1977; Seyfried and Mottl, 1977; Mottl and Holland, 1978; Mottl, Holland and Corr, 1979;

Seyfried and Dibble, 1980). The aim of these studies was to see what affect these reactions could have on seawater chemistry; if they could turn seawater into the metal-rich solution needed to produce the massive sulfide deposits seen in ophiolites and which could supply the metals seen in metalliferous sediments; and to see if they could produce the mineral alteration assemblages observed in submarine rocks. These experiments were done at the temperature and pressure conditions presumed to be typical of the in situ oceanic systems. An important variable in both the experimental and actual systems is the water/rock mass ratio as this is a strong determinant in fixing the final solution composition as well as the alteration assemblage observed in the solid phase. An obvious difficulty with the experimental work is that they are closed systems being used to replicate open systems, with many attendant limitations. The experiments were run at a variety of temperatures (70-500° C), pressures (1-1000 bars) and water/rock ratios (1 to 125). Natural seawater as well as various synthetic seawaters and brines were used as the reactant solution. Basalt of varying crystallinity as well as other types of oceanic rock were used as the starting substrate.

The experiments can be divided into two general groups, dependent on the experimental method employed. The experiments done by Bischoff, Dickson, Seyfried and co-workers were done in the "Dickson Apparatus". This system allows water to be withdrawn from the apparatus during the course of the experiment. The entire system could also be rocked, speeding reaction. The disadvantage of this system is that a higher water/rock ratio, often $\geq$ 10 was used as solution is withdrawn during the course of the experiment. The high water/rock ratio allows more samples to be taken over the time course of the experiment as there is a limit to how much the

reaction cell can deform as solution is withdrawn. This is a much higher ratio than has been observed to date in the oceanic systems. The experiments done by Hajash, and Mottl and co-workers were done in a different kind of apparatus. It is a batch process, i.e. no solution can be analyzed until the experiment is terminated. The problem arises because there is no way to separate the solution from the solids during the quench. Various back reactions have been shown to occur during this process (Hajash and Archer, 1980) and they alter both the solution composition and the observed mineral assemblage. Water/rock ratios as low as one (very close to the observed ocean values) were used in these experiments. Thus when comparing 21° N solutions to the experimental work they must be either compared to solutions created at much higher water/rock ratios or to solutions which have back reacted to an unknown extent with the solid phase. The pressures used in the experiments (~500 bars in many cases) are close enough to the pressures in actual systems (still not exactly known) and appear to have a relatively small affect in comparison to the other variables.

Several limitations exist on which elements can provide useful data. All the experiments done at temperatures >260° C necessitated the use of Au (or Pt) sample cells. Cu and Pb were found to form an amalgam with the Au and therefore no meaningful solution data can be obtained for these elements. When seawater is heated above ~130° C it precipitates anhydrite ($CaSO_4$). This may slow the reduction of sulfate to sulfide. It causes the most serious problem in the quenched samples because it redissolves at low temperatures. The precipitation and dissolution of anhydrite can affect the Ca, Sr and S composition of the solutions and may affect the redox state as well.

In order to be able to compare the experiments at higher water/rock ratios the extraction efficiency of the species in solution was calculated for both the experiments and the 21° N solutions. This approach can only be used for water/rock ratios <50. At water/rock ratios >50 the system becomes solution dominated and the reaction progress is quite different, (there is always an excess of Mg which maintains the solution at a lower pH). The formation of anhydrite, its metastable persistence throughout the experiment and its redissolution in the quench prevent meaningful comparisons of the Ca, Sr, Ba , SO_4 and reduced sulfur data. In some of the experiments there are possible diffusion/leakage problems therefore Cl is assumed to be conservative (Bischoff and Dickson, 1975) while there is an active Cl sink in at least 3 out of the 4 areas at 21° N. The sodium is calculated on the basis of charge balance and often its changes are not significant within the sum of the analytical errors. The species which can best be compared between the experiments and the hot springs themselves are in many cases reduced to pH, K, Fe and Mn. A problem arises in one of the experiments (Bischoff and Dickson, 1975) because a low K basalt was not used, therefore the K values cannot be compared. After all the above limitations are considered the experiments which produced the solutions most similar to those at 21° N are those of Mottl et al. (1978, 1979) at 400° C, 700 bars, water/rock ratio = 1 using a crystalline basalt with glass present (Table 2-13). The experiments were therefore able to predict the solution composition reasonably well.

The experiments can provide insights into two aspects of the solutions which we cannot deduce from the real system. The experiments in the Dickson apparatus allow the progress of the reactions to be monitored. They help to define the exchange process as well as the relative kinetics

Table 2-13: Comparison of 21° N to Experiments

Element		21° N	Experiments 2B	2C
Li	μ[1]	891→1322	-	-
Na	m	432→510	470	514
K	m	23.2→25.8	29.6	29.3
Rb	μ	27→33	-	-
			-	-
Be	n	10→37	-	-
Mg	m	0	0.4	0.3
Ca	m	11.7→20.8	52.0	38.1
Sr	μ	65→97	72	102
Ba	μ	8→16	740	657
pH		3.3→3.8	3.9	3.6
Alk_t	meq	-0.19→-0.50	-	-
Cl	m	489→579	-	-
SiO_2	m	15.6→19.5	27.7	27.9
Al	μ	4.0→5.2	<9.6	<9.6
NH_3	m	<0.01	-	-
SO_4	m	0	5.66	5.53
H_2S	m	6.57→8.37	6.72	7.74
Mn	μ	699→1002	670	1000
Fe	μ	750→2429	2100	2000
Co	n	22→227	<1400	<1400
Cu	μ	0→44	<0.8	<0.8
Zn	μ	40→106	-	-
Ag	n	<1→38	-	-
Cd	n	17→180	-	-
Pb	n	183→359	<720	<720

[1]Units: n = nanomoles/kg
μ = micromoles/kg
m = millimoles/kg
meq = milliequivalents/kg.

[2]Experimental data is from Mottl and Holland (1978) and Mottl et al. (1979). Both experiments were done at 400° C, 700 bars, water/rock mass ratio = 1, and lasted 272 days. Run 2B was done with a glassy basalt and run 2C was done with a mix of glassy and crystalline basalt.

of the reaction. The kinetic information derived from the experiments can help in defining the time scales of reactions occurring in the vents. The second set of information we can obtain is on the solid alteration assemblage. The 21° N system at depth has not been directly observed. Based on the solution chemistry and studies of altered deep sea rocks from dredging and DSDP drill cores the basalt-seawater reactions which must be occurring are inferred. There are large differences between the assemblages found in the dredged rocks and those in the drill cores (Honnorez, 1981). The experiments provide detailed information on which mineral assemblages form and how they can vary with water/rock ratio.

In general, the experimental solutions are in good agreement with the 21° N solutions but in particulars there are significant differences. These mostly can be attributed to limitations in experimental design. Another limitation is that certain elements of interest which may help in elucidating processes were not measured in the experiments (e.g. Li, Rb, As, Se); certain elements of interest cannot be determined due to reaction with the gold capsule (Cu, Ag, Pb); and certain elements have never reached the same levels as are found in the 21° N solutions for unknown reasons (e.g. Zn).

2.10 Comparison to Metalliferous Sediments

Iron and manganese rich metalliferous sediments were first recovered on the Challenger expedition in the 1870's but not until the 1960's (Bostrom and Peterson, 1966) was the correlation of these sediments with the crest of the East Pacific Rise established. Much work has now been done on these sediments (Bostrom and Peterson, 1966; 1969; Bostrom et al., 1969; Horowitz, 1970; Piper, 1973; Heath and Dymond, 1977; Dymond, 1981) which

are highly enriched in many of the transition metals. Volcanic and/or hydrothermal exhalations on the ridge crest were postulated as a possible source of these depositions, although a source from hydrogenous precipitation from seawater could not be eliminated. Their strong areal association with the ridge crest favored the former of these explanations. An isotopic study by Bender et al. (1971) established that the U and Sr in these sediments had a seawater source, while the Pb had a volcanogenic source. Based on the high accumulation rates for Mn in these sediments they determined that it must also have a volcanogenic input. Bostrom and Peterson (1966), Bostrom and Fisher (1969), Fisher and Bostrom (1969) and Horowitz (1970) reported enrichments of the elements Fe, Mn, Ni, Co, Cu, Tl, Mo, Ti, As, B, Zn, V, Cd, Pb, Hg, Ag and U in the sediments. The source of most of these elements cannot be determined isotopically. The composition of the 21° N hydrothermal solutions can be used to determine if an element may have a hydrothermal source. This does not eliminate the possibility of an element being present in the hydrothermal solutions but precipitating near the vents with the later addition of this element from seawater to the Fe and Mn oxides and hydroxides (which must have a hydrothermal source). If an element is not present in the hydrothermal solutions it must be attributed to a hydrogenous source. Of the elements listed above Fe, Mn, Ni, Cu, Zn, Co, Cd, Ag, Pb, As and B were determined in the hydrothermal solutions. Field et al. (1981) presents data for these elements in metalliferous sediments from the crest of the East Pacific Rise. Table 2-14 presents this data as the ratio of these species to the Fe content of the sediment, as well as the ratios of these elements to Fe in the four vent areas at 21° N. In the case of Ni and Co the ratios are lower in the hydrothermal solutions than in the metalliferous sediments,

Table 2-14: Ratios of Elements to Iron in Metalliferous Sediments and the 21° N Hydrothermal Solutions

Ratio[1]	Sediment[2]	NGS	OBS	SW	HG
Fe/Fe	1	1	1	1	1
Mn/Fe	0.34	1.2	0.6	0.9	0.4
Ni/Fe	0.063	0	0	0	0
Zn/Fe	0.0023	0.05	0.06	0.1	0.04
Cu/Fe	0.0064	0	0.02	0.01	0.02
Co/Fe	0.0013	3×10^{-5}	1×10^{-4}	9×10^{-5}	9×10^{-5}
Ag/Fe	1.4×10^{-5}	$<1\times10^{-6}$	2×10^{-5}	4×10^{-5}	2×10^{-5}
Pb/Fe[3]	3×10^{-4}	2×10^{-4}	2×10^{-4}	3×10^{-4}	1×10^{-4}

[1]Ratios are molar ratios.

[2]Sediment data is as listed in Field et al. (1981).

[3]Sediment data for lead is from Bender et al. (1971).

implying two possible mechanisms. In the first case additional iron is added to these sediments after they leave the vents. In the second case, additional amounts of the element of interest are scavenged onto the Fe-Mn precipitates after they leave the vents. Nickel has an insignificant hydrothermal source and therefore must be completely hydrogenous. The Pb/Fe ratio is very similar in the sediments and in the solutions. For Mn, Zn, Cu and Ag the ratio in the hydrothermal solutions is greater than or equal to the ratio in the sediments. A hydrothermal source may be the major input of these elements to these sediments. A proportion of these elements may be lost to seawater or additional iron may be gained. Many of the elemental ratios in the metalliferous sediments are close to those in the hydrothermal solutions at 21° N. Besides being due to losses or gain occurring in the water column, the sedimentary variations may reflect differing hydrothermal inputs.

2.11 Summary - Chapter 2

The solution chemistry at 21° N varies between the four vent areas. These variations cannot be explained by a simple model incorporating "age", pathlength, residence time and temperature. The system has a low water/rock ratio (~1) and hydration reactions appear to be active. The hydrothermal circulation results in a net loss of sulfur. Only reduced sulfur is present in the exit solutions and this sulfur is a mix of reduced seawater sulfate and basaltic sulfur. The SiO_2 contents of the solutions imply depths of reaction ranging from 0.5 kms into the basalt at HG to 3.5 kms at NGS. The NGS vent solutions appear to be cooling conductively before they reach the seafloor. The vent chemistry except for silica (and pyrite at NGS) does not appear to be solubility controlled.

The chemistry of the solutions is in good agreement with that of the

chimneys, ophiolite deposits, the alteration observed in seafloor basalts and where comparable the experimental work on seawater-basalt reactions. The solution chemistry also suggests that Ni in metalliferous sediments is from a hydrogenous source while most of the other metal enrichments could be explained by a hydrothermal source.

CHAPTER 3

Guaymas Basin - Results and Discussion

This chapter is a presentation and discussion of the chemistry of the Guaymas Basin hydrothermal solutions. A model will be presented to explain the solution composition. Results of thermodynamical modelling of the solutions will also be presented. The observed chemistry will be compared to that of related phenomenon such as ore deposits and the pore water chemistry found in DSDP Holes 477 and 477A which were drilled in the Guaymas Basin.

3.1 Sample Setting

The East Pacific Rise continues northward into the Gulf of California where it is covered by sediment and forms a series of basins. The Guaymas Basin appears to be the most hydrothermally active at the present time based on ^{3}He in the basin waters (Lupton, 1979) and heat flow (Lawver and Williams, 1979). The Guaymas Basin is separated into a northern and southern trough by a transform fault (Figure 3-1). All of the vents sampled occur in the southern trough of the basin. Bad weather precluded diving on the northern trough as planned. Lonsdale et al. (1980) had collected hydrothermal deposits there on a previous Seacliff dive and Williams et al. (1979) had also measured elevated heat flow in the northern trough - although not as high as they observed in the southern trough. Ten vents were sampled over approximately 8 km (Figure 3-2), lying between 27°00' and 27°03' N latitude and 111°22' and 111°25' W longitude. All but one of the sampled hydrothermal areas lies in the deepest part of the basin; the vents sampled on dive 1175 lie on the inward facing faults on

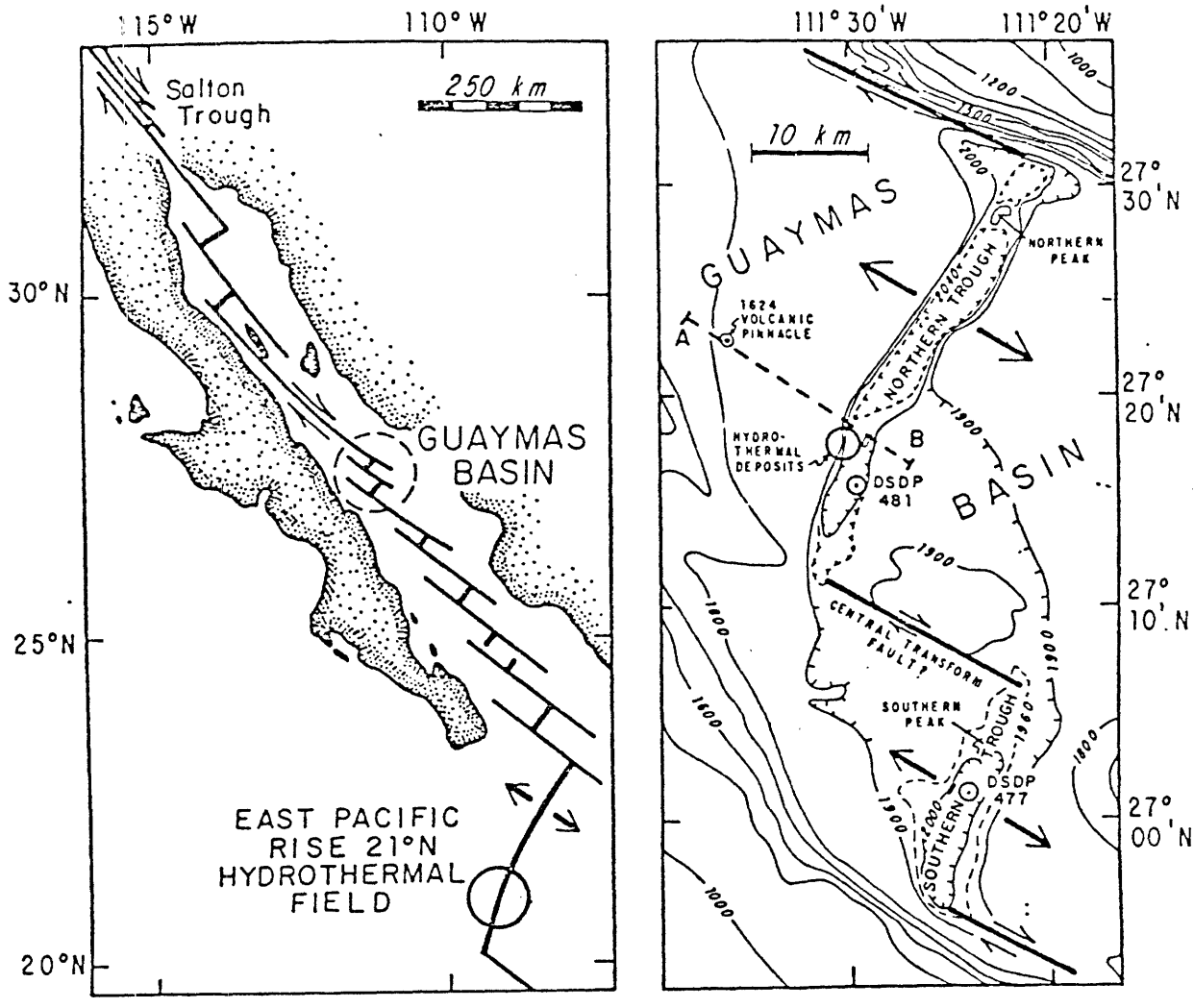

Figure 3-1: Location map for Guaymas from Lonsdale et al. (1980).

Figure 3-2: Dive and vent locations at Guaymas. From Simoneit and Kawka (1983). DSDP sites 477 and 477A are also noted. ⟩ denotes fault traces and ⊘ denotes hills. Dive 1177 visited the same hydrothermal sites as dive 1171 but is not labelled due to lack of space on the figure. No water samples were taken on dives 1170, 1171 or 1174.

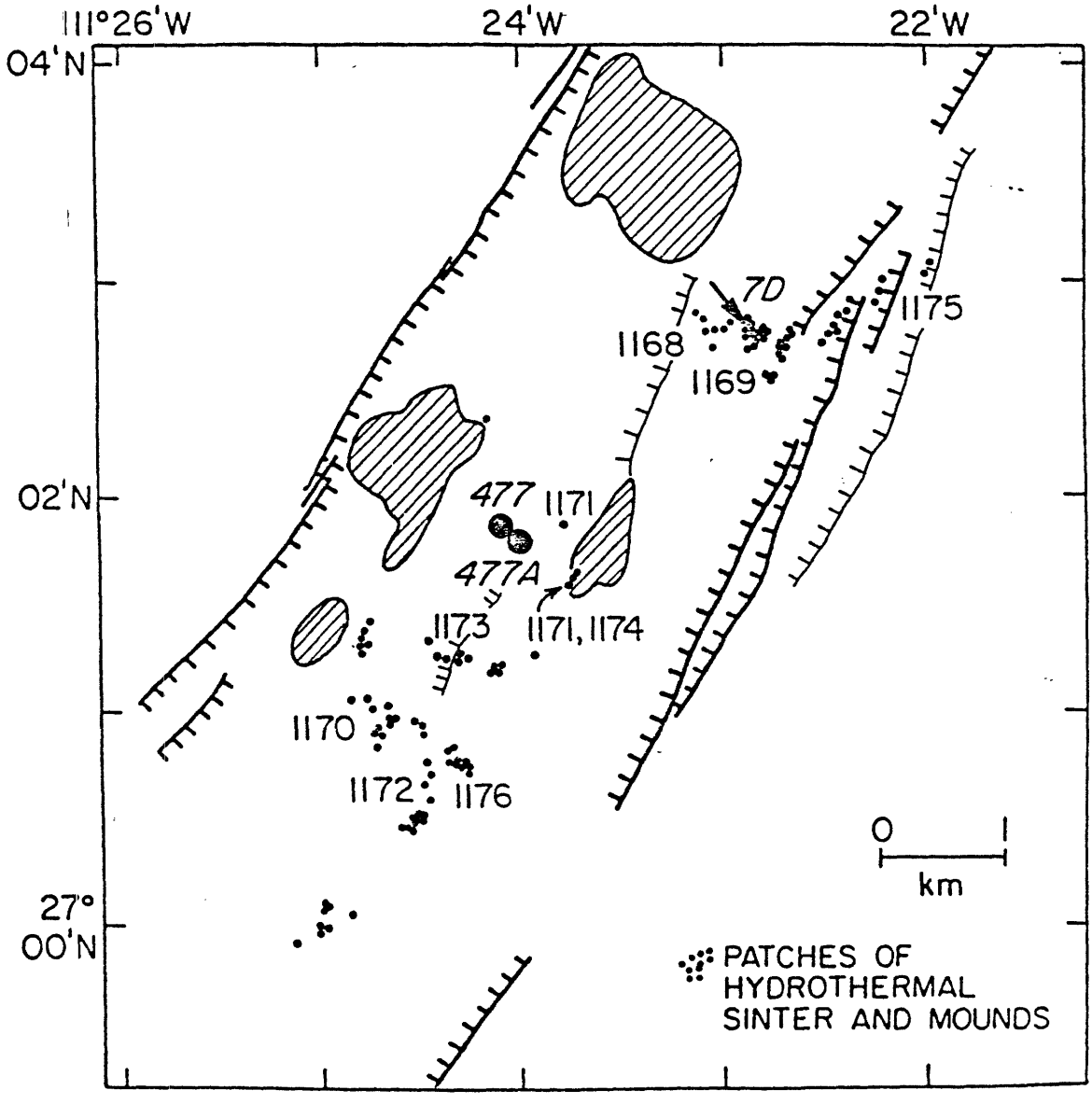
111°26'W
24'W
22'W
04'N
02'N
27°
00'N
7D
1168
1169
1175
477
1171
477A
1173
1171, 1174
1170
1172
1176
0
1
km
PATCHES OF
HYDROTHERMAL
SINTER AND MOUNDS

the eastern edge of the basin.

The unique aspect of the Guaymas hydrothermal system is that the solutions must pass through approximately 0.5 km (Lawver et al., 1975) of sediment before they exit on the seafloor. Since a wedge of sediment fills the basin, the solutions from the dive 1175 site, lying off on the flank probably pass through less sediment than the other areas. Most of the solutions exit from large constructional features on the seafloor but some exit from holes in the sediment. As seen on figure 3-2, dives 1171 and 1177 are extremely close to DSDP holes 477 and 477A.

The sedimentation at Guaymas is extremely rapid (>1 m/1000y) (van Andel, 1964; Calvert, 1966) due mainly to the high productivity of the overlying waters. Kastner (1982) gives the sediment composition as follows:

30-50 % diatoms, with some radiolarians and silicoflagellates
30-45 % detrital clay minerals
10-15 % calcareous nannofossils with some foraminifers
4-15 % feldspars
3-10 % quartz
1-2 % heavy minerals.

The sediments also contain 2-4 % organic carbon (van Andel, 1964).

3.2 Solution Chemistry

As at 21° N the solution chemisty is due to the reaction of seawater with basalt at elevated temperatures. These reactions may or may not have reached equilibrium (see section 2.2). The solution chemistry at Guaymas is complicated by additional reactions occurring between the basalt-derived hydrothermal solutions and the sediments, which may not have reached equilibrium. The solutions can be described simplistically as:

$$x\ \text{seawater} + y\ \text{basalt} \rightarrow [\text{hydrothermal solution}]_i + [\text{alteration products}]_i \rightarrow \ldots$$

$$\rightarrow [\text{hydrothermal solution}]_n + [\text{alteration products}]_n$$

$$a\ [\text{hydrothermal solution}]_n + b\ \text{sediments} \rightarrow [\text{hydrothermal solution}]_m + [\text{altered sediment}]_m \rightarrow \ldots$$

$$\rightarrow [\text{hydrothermal solution}]_o + [\text{altered sediment}]_o.$$

The hydrothermal solutions at Guaymas are therefore the results of two sets of reactions.

The possibility exists that the solutions at Guaymas could be due to reactions occurring only in the sediment, with the heat being added conductively from basaltic sills intruded at greater depth in the sediment column:

$$a\ \text{seawater} + b\ \text{sediment} \rightarrow [\text{hydrothermal solution}]_i + [\text{altered sediment}]_i \rightarrow \ldots$$

$$\rightarrow [\text{hydrothermal solution}]_f + [\text{altered sediment}]_f.$$

Kastner (1982) found that some of the hydrothermal systems seen in the pore waters and altered sediments from DSDP Leg 64 Sites 477 and 477A which were drilled in the Guaymas Basin are from sill driven systems and do not represent reaction with the "basement" basalt. The chemistry of the hydrothermal solutions reported here appear to be from reaction with the basement based on: (1.) the pressure (depth) of reaction inferred from the silica content of the solutions, (2.) the high reduced sulfur content of the solutions, (3.) the apparent complete absence of Mg and SO_4 from solution, (4.) the high ^3He content of the solutions (Lupton, unpublished data), (5.) the high temperatures of the solutions.

Kastner (1982) has found the water/rock ratio in this system to be 2-3:1 based on the oxygen isotopes in coexisting mineral phases and pore

solutions. A water/rock ratio based principally on the alkali content of the solutions cannot be calculated as was done for 21° N due to the addition of these elements from the sediment column (discussed below). The oxygen isotopic data which could provide information on the water/rock ratio are not yet available for these solutions.

A model is developed in which the solution chemistry at Guaymas is treated as a 21° N solution chemistry which is altered by further reaction in the sediment column. Various overprinting reactions are postulated for the observed chemistries. A distinct advantage to the Guaymas system is that we have direct information on what is occurring at depth. DSDP Holes 477 and 477A are located within meters of several of the vents (Figure 3-2) and drilled approximately half way through the sediment column. The proposed alteration reactions with their predicted mineral products can therefore be tested against the observed mineral assemblage.

A limitation to this model is that the solution chemistry as it exits from the basalt is assumed to be the same as that observed at 21° N. The maximum temperatures observed at the two sites (355° C at 21° N and 315° C at Guaymas) are similar and therefore what is leached from the basalts should not be different due to temperature effects. The metals Fe, Mn, Cu, Zn etc. can be leached from the rock at temperatures of 300° C and it is unlikely that their extraction efficiencies vary very much for a 40° C temperature difference in the 300-400° C range. If the solutions react with the sediment during the downward limb of the convection cell this may affect the reactions which occur in the basalt. For example, if much of the Mg is lost in reaction in the sediment cover it may lower the acidity of the solutions reacting with the basalt, resulting in a smaller degree of reaction than is observed at 21° N. Alternatively, the overlying sediment

cover may make it more difficult for the solutions to exit from the basalt, increasing their residence time in the rock and thereby increasing the extent of reaction. This may explain the ^{3}He data. The observed ^{3}He/heat ratio at 21° N and GSC is the same (Jenkins et al., 1978; Welhan and Craig, 1983). This may be merely fortuitous or may be due to the mechanisms responsible for extracting He from the rock. The ratio at Guaymas is lower than that observed at 21° N (Lupton, personal communication). A possible explanation for this is that the solutions extract He and heat from the rock at Guaymas in the same ratio as at 21° N and GSC but then "sit" in the rock because they cannot escape. The solutions may continue to heat conductively due to this but have no source from which to gain additional He. A mechanism such as this could alter the ^{3}He/heat ratio. If sedimentary derived hydrothermal solutions (with no ^{3}He) are mixed with the basaltic ones, they could dilute the ^{3}He signal from the basalt and lower this ratio. The 21° N solutions are very similar to those at GSC, except for the sulfide or sulfate forming elements. Preliminary results from 13° N show these solutions to have a slightly different chemistry (Michard et al., 1982). We cannot sample the Guaymas solutions after their reaction with basalt but prior to that with the sediment and the DSDP holes did not reach basement. As the 21° N results are the only ones currently available for "simple" high temperature solutions (versus GSC where subsurface mixing with cold seawater and precipitation occurs) we assume that the Guaymas solutions have the 21° N solution chemistry prior to their reaction with the sediments. As ranges exist in the vent compositions at both these sites, the differences between them is taken as a range. Although evidence exists that there may be differences in water/rock ratios between these two areas (Kastner, 1982), this will not be taken into account in the following

model due to the other large uncertainities inherent in these calculations.

MAJOR ELEMENTS

The calculated endmember concentrations for Guaymas and 21° N are given in Tables 2-4, 2-5, 2-6, 2-8, 2-10 and 2-11. As at 21° N magnesium is assumed to be zero in the undiluted hydrothermal solutions. To obtain the net change occurring due to reactions in the sediment column the 21° N values are subtracted from the Guaymas values.

$$\Delta \equiv [\text{Guaymas}] - [21° \text{ N}]$$

These Δ concentrations are presented in Table 3-1. A positive number (+) implies a gain and a negative number (-) indicates a net loss of the element as the solution passes through the sediment column.

THE ALKALIS

Lithium, sodium, potassium and rubidium were determined in the Guaymas solutions.

Lithium: The lithium values at Guaymas range from 630 μmoles/kg to 1076 μmoles/kg (Figure 3-3, Table 2-4). The samples with the highest lithium values are those from dive 1176 in the southernmost field (Area 7).

The range in observed Li concentrations is much greater at Guaymas than at 21° N. The resulting $\Delta = -692 \rightarrow +182$ μmoles/kg (Table 3-1) which suggests that Li may be lost, gained or remain unchanged due to sedimentary reactions. Li has a sink in the low temperature alteration of basalt and also may have a sink in marine sediments as they appear to be enriched in this element. Alternatively the Li source may be the dissolution of diatoms (Gieskes et al., 1982) although based on unpublished data M. Delaney (personal communication) believes this is unlikely. At these high

Table 3-1: Δ Values for Guaymas Solutions

Element		21° N	Guaymas	Δ
Li	μ[1]	891→1322	630→1076	-692 → +185
Na	m	432→510	478→513	-35 → +81
K	m	23.2→25.8	32.5→48.5	6.7 → 26
Rb	μ	27→33	57→86	24 → 59
Be	n	10→37	12→91	-25 → +81
Mg	m	0	0	0
Ca	m	11.7→20.8	26.6→41.5	5.8 → 29.8
Sr	μ	65→97	160→253	63 → 188
Ba	μ	8→16	15→54	0 → 46
pH		3.3→3.8	5.9	2.1 → 2.6
Alk_t	meq	-0.19→-0.50	2.8→10.6	3 → 11.1
Cl	m	489→579	581→637	2 → 148
SiO_2	m	15.6→19.5	9.3→13.8	-1.8 → -10.2
Al	μ	4.0→5.2	0.9→7.9	-4.3 → 3.9
NH_4	m	<0.01	10.3→15.6	10.3 → 15.6
SO_4	m	0	0	0
H_2S	m	6.57→8.37	3.80→5.98	-0.59 → -4.57
Mn	μ	699→1002	132→236	-463 → -874
Fe	μ	750→2429	17→180	-570 → -2412
Co	n	22→227	<5	→
Cu	μ	0→44	<0.001	≤-44
Zn	μ	40→106	0.1→40	-106 → 0
Ag	n	<1→38	0→230	-38 → +230
Cd	n	17→180	0→46	-180 → +29
Pb	n	183→359	0→652	-359 → +469
As	n	<30→452	283→1074	-169 → >1044
Se	n	<1→72	15→103	-57 → >102

[1]Units: n = nanomoles/kg
μ = micromoles/kg
m = millimoles/kg
meq = milliequivalents/kg.

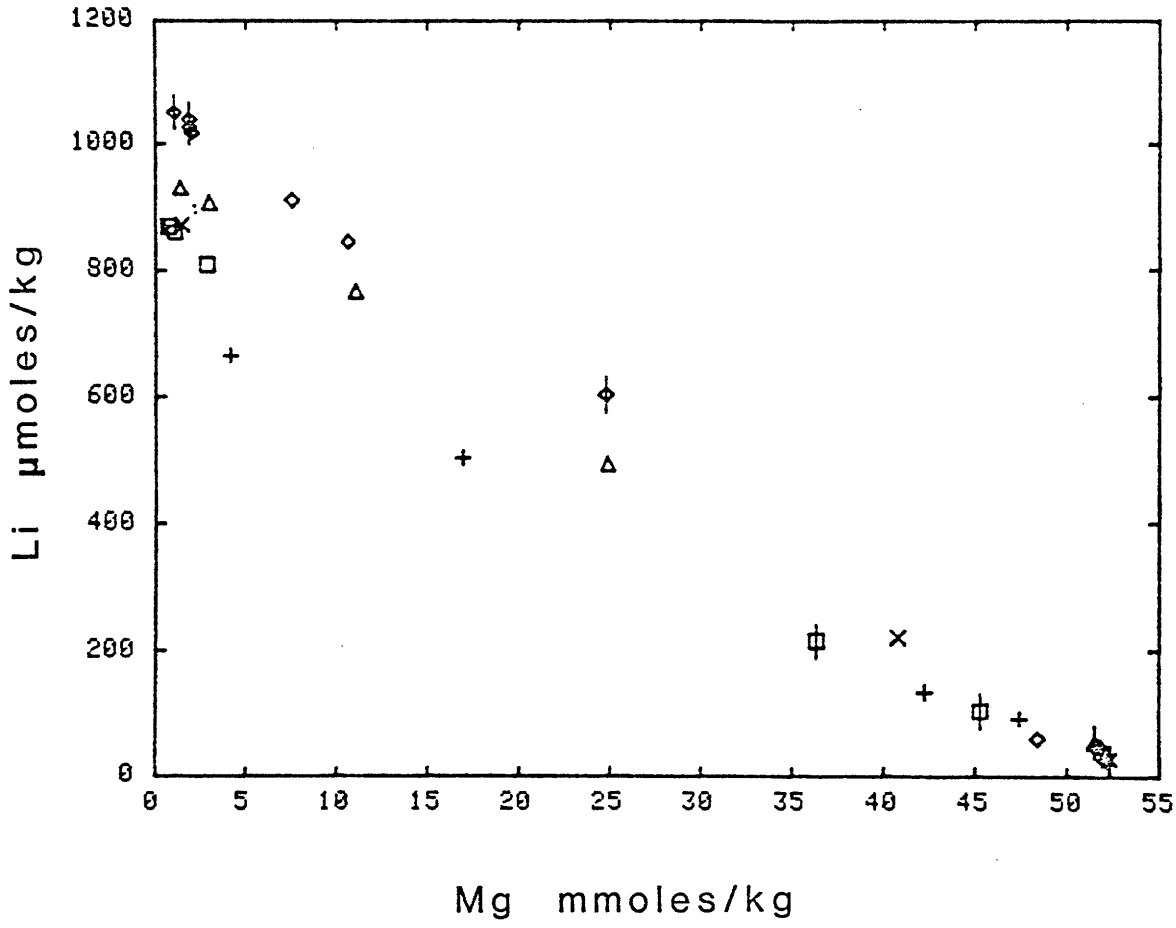

Figure 3-3: Lithium versus magnesium at Guaymas. The plot symbols distinguish the areas sampled and are as follows for this and all subsequent Guaymas data plots:

◇ = Area 1: Dive 1172, bottles 1, 2, 7, 10
Dive 1176, bottles 3, 5, 7, 14
△ = Area 2: Dive 1173, bottles 3, 5, 6, 14
+ = Area 3: Dive 1175, bottles 5, 9, 15, 16
□ = Area 4: Dive 1177, bottles 5, 6, 11, 13
• = Area 5: Dive 1173, bottles 11, 13
× = Area 6: Dive 1173, bottles 12, 16
◇ = Area 7: Dive 1176, bottles 6, 10, 11, 13
△ = Area 8: Dive 1169, bottles 12, 16
□ = Area 9: Dive 1177, bottles 9, 15
✳ = Area 10: Dive 1168, bottles 11, 13.

temperatures the Li may be leached from the clays and into solution, and the high NH_4^+ in the solutions may be exchanging for it. Thus potential sources and sinks exist that can explain the observed Li concentration although their relative importance cannot be assessed.

Sodium: Unlike 21° N sodium increases in all the vent fields at Guaymas (Table 2-4). Again, the analytical precision is not sufficient to distinguish between vent fields (Figure 3-4a) but when sodium is calculated from the difference in charge balance among the other major species a more detailed picture emerges (Figure 3-4b). The endmember sodium ranges from 475 mmoles/kg to 513 mmoles/kg, an increase of 3-11% above the ambient value of 463 mmoles/kg. The samples from dive 1175 (Area 3) have the highest sodium concentration.

Sodium shows a loss and gain (Δ = -35 → +81 mmoles/kg) with respect to the 21° N data. This is because the data for 21° N show both an increase and a decrease. The Na (and Cl) story is complicated by hydration reactions which are assumed to occur in both areas. The Na and Cl data should not be treated by the Δ method with respect to 21° N but should be analyzed with respect to each other at Guaymas. Na at Guaymas shows only a net increase with respect to the seawater composition. A discussion of whether only hydration is active will be deferred until after the Cl data are presented.

Potassium: The potassium concentrations at Guaymas are the highest yet observed in submarine hot springs; this is most likely due to the hot waters leaching additional potassium out of the sediments. The values range from 32.5 mmoles/kg in the 100° C samples from dive 1177 (Area 9) to 49.2 mmoles/kg in the dive 1176 samples (Area 3) (Figure 3-5, Table 2-4).

As potassium is always present at higher concentration levels in the

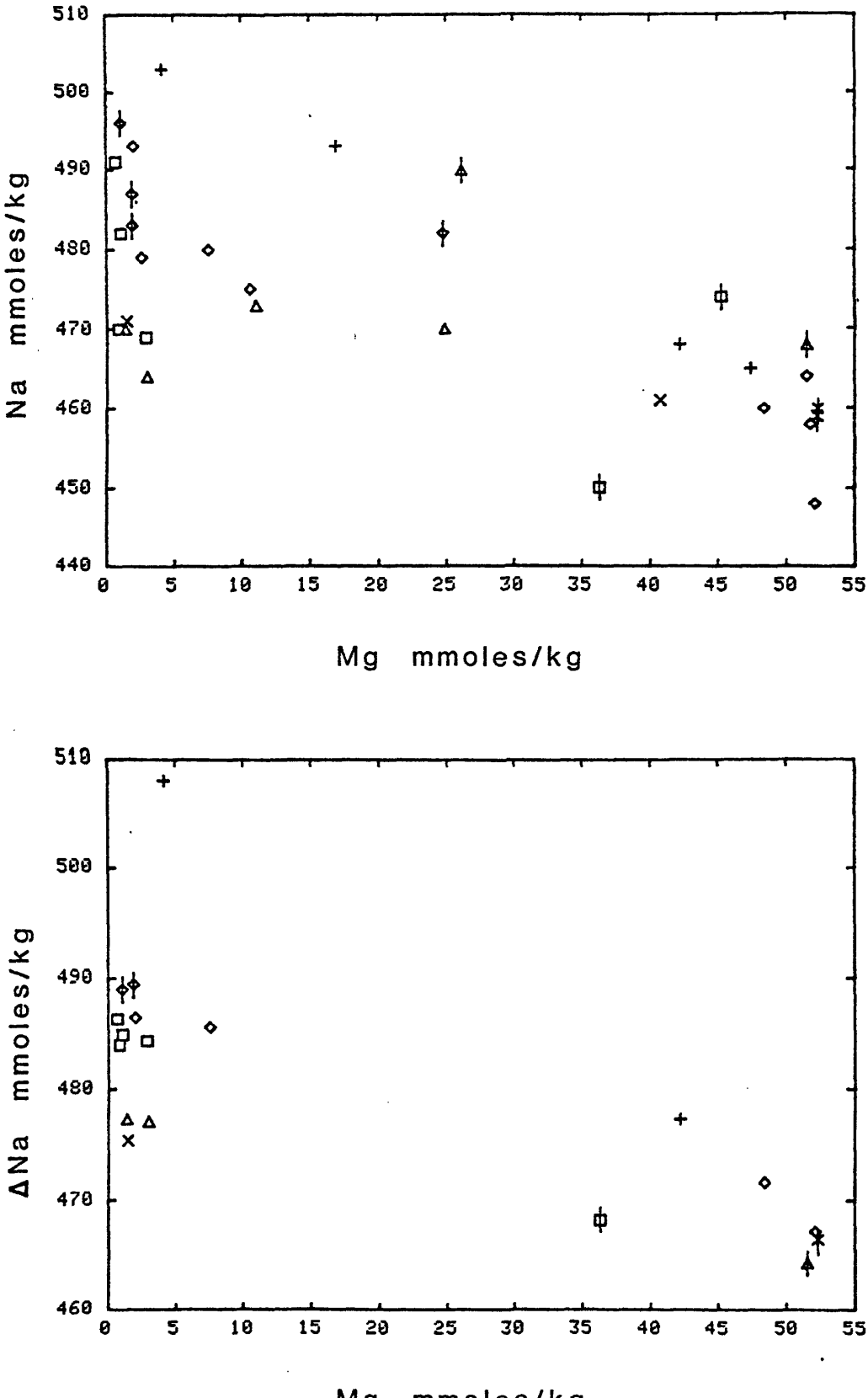

Figure 3-4: Sodium versus magnesium at Guaymas.
a. measured sodium.
b. sodium calculated from the charge balance.

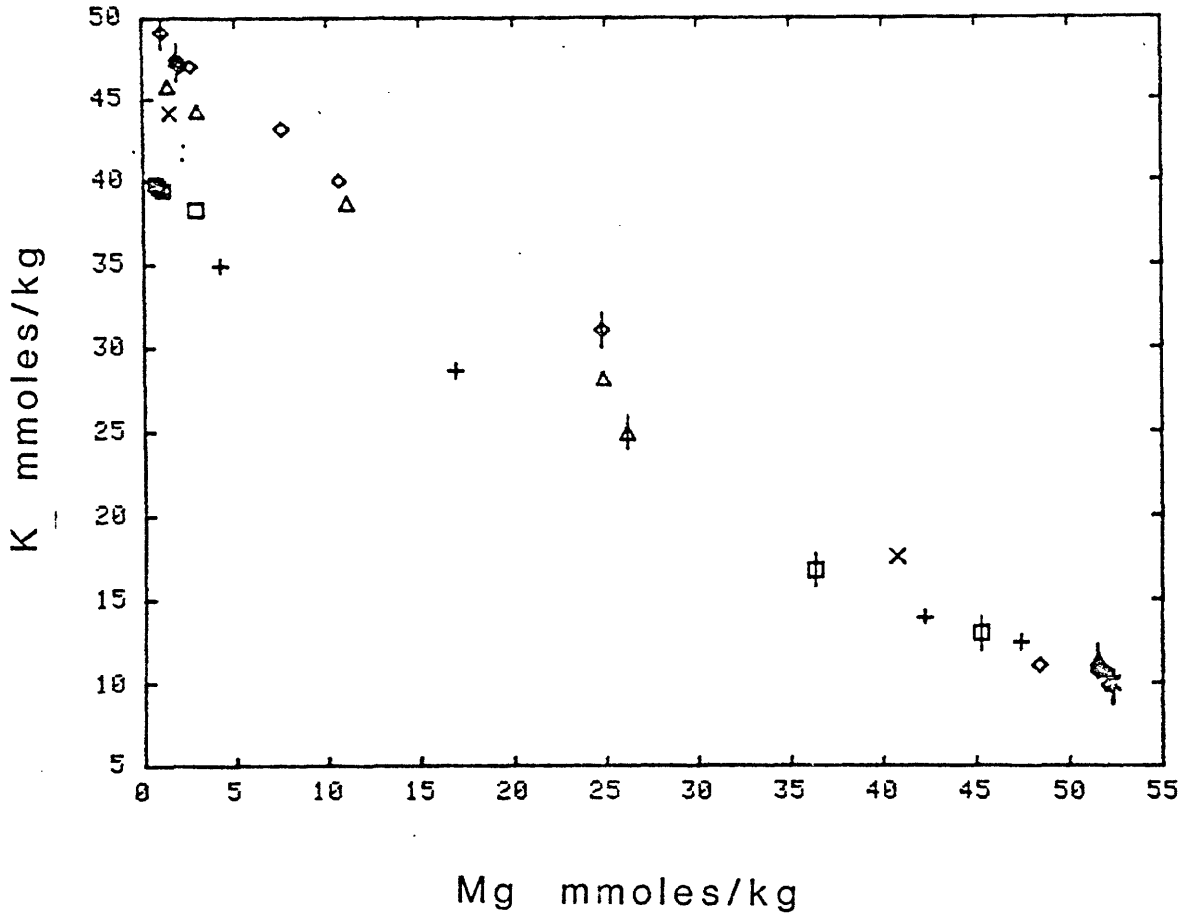

Figure 3-5: Potassium versus magnesium at Guaymas.

Guaymas solutions than the 21° N solutions it has a positive Δ (+6.7 → +26.0 mmoles/kg) (Table 3-1). Hence K appears to be added from the sediment cover. Its source is presumably detrital clays and it may be released by a NH_4^+ for K^+ exchange. In her work on the solid material from the DSDP cores at Sites 477 and 477A Kastner (1982) found hydrothermal K-feldspar which indicates more K may be mobilized than we see in the solutions and that a sink may also be active.

Rubidium: As for potassium the rubidium concentrations observed at Guaymas are higher than at either 21° N or GSC (Table 2-4). The values range from a low of 57 μmoles/kg in the samples from dive 1175 and the 100° C samples from dive 1177 (Areas 3 and 9) to 86 μmoles/kg in the dive 1176 samples (Area 7) (Figure 3-6, Table 2-4). As rubidium is always higher in the Guaymas solutions than those at 21° N the Δ = +24 → +59 μmoles/kg (Table 3-1). This addition is presumably due to reactions occurring with the clay fraction of the sediment such as an NH_4^+ exchange for rubidium as was also suggested for K.

The Li/K ratio observed in the Guaymas solutions is further evidence for the K being sediment derived rather than basalt derived. The Li/K ratio in the Guaymas solutions (0.02) is distinctly different from that in the basalts (0.05) or the 21° N solutions (0.04-0.06) and is closer to the value seen for marine sediments (~0.01) (Heier and Adams, 1964). All of the Guaymas solutions are similar in this respect as is shown in Figure 2-6.

THE ALKALINE EARTHS

The elements beryllium, magnesium, calcium, strontium and barium were determined and as at 21° N they show a wide diversity of behavior.

Beryllium: The range in beryllium at Guaymas includes that found at

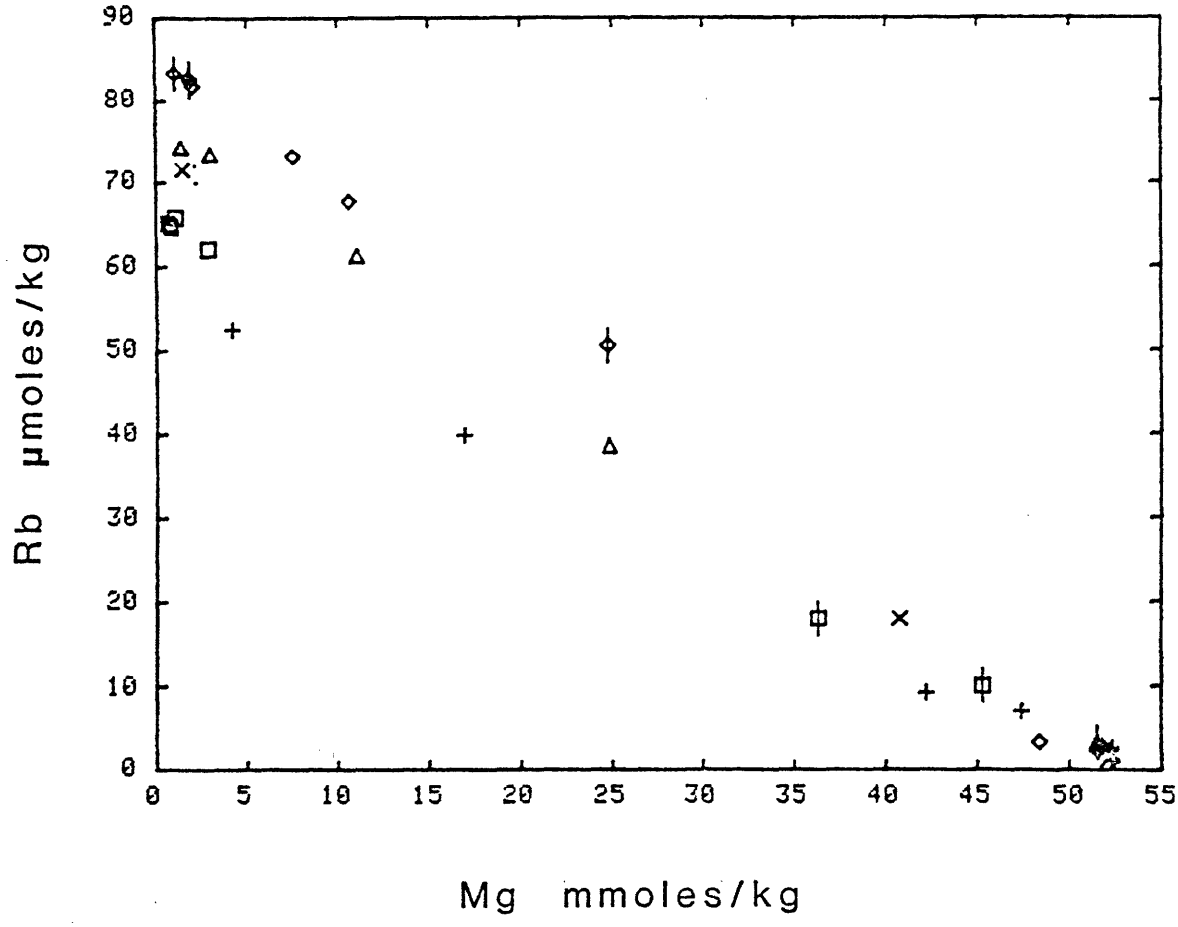

Figure 3-6: Rubidium versus magnesium at Guaymas.

21° N and extends to much higher values; up to 91 μmoles/kg (Figure 3-7, Table 2-5). The highest values are from the lowest temperature (100° C) vent on dive 1177 (Area 9). Be shows both a net increase and decrease after the sedimentary reactions (Δ = -25 → +81 mmoles/kg). As mentioned above the largest increase occurs in Area 9 where the water has apparently conductively cooled (based on silica - section 3.4) due to a long residence time in the sediments. This long contact time with the sediments is responsible for the large increase in solution. Too little is known about the geochemical cycle of Be to identify sources and sinks.

Magnesium: Magnesium decreases in all fields and as mentioned in Chapter 2 it is assumed to be zero in the hydrothermal solutions. This is the basis on which the endmember compositions for all the elements are calculated. Mg concentrations as low as 0.60 mmoles/kg were measured in some of the Guaymas solutions, therefore this assumption is assumed to be valid for all the vent areas. The poor sampling at some of the vents precludes this hypothesis from being proven at the present time. The Mg/SO_4 ratio is close to the seawater value and the amount of these two ions present is assumed to be a sampling artifact. The extremely low measured magnesium implies that the solutions have not mixed with unreacted seawater in the sediment column. (As mentioned earlier the solutions must have a source in the basalt, not just in the sediment.) As no Mg is seen in the hydrothermal solutions, if any fraction of these solutions is sediment derived, there must be an active Mg sink in the sediments. This would be chlorite which has been observed in the sediments (Kastner, 1982).

Calcium: Calcium increases in all the vent areas at Guaymas from 26.6 mmoles/kg to 41.5 mmoles/kg (Figure 3-8, Table 2-5). The highest concentration is found in the samples from dive 1175 (Area 3) while the

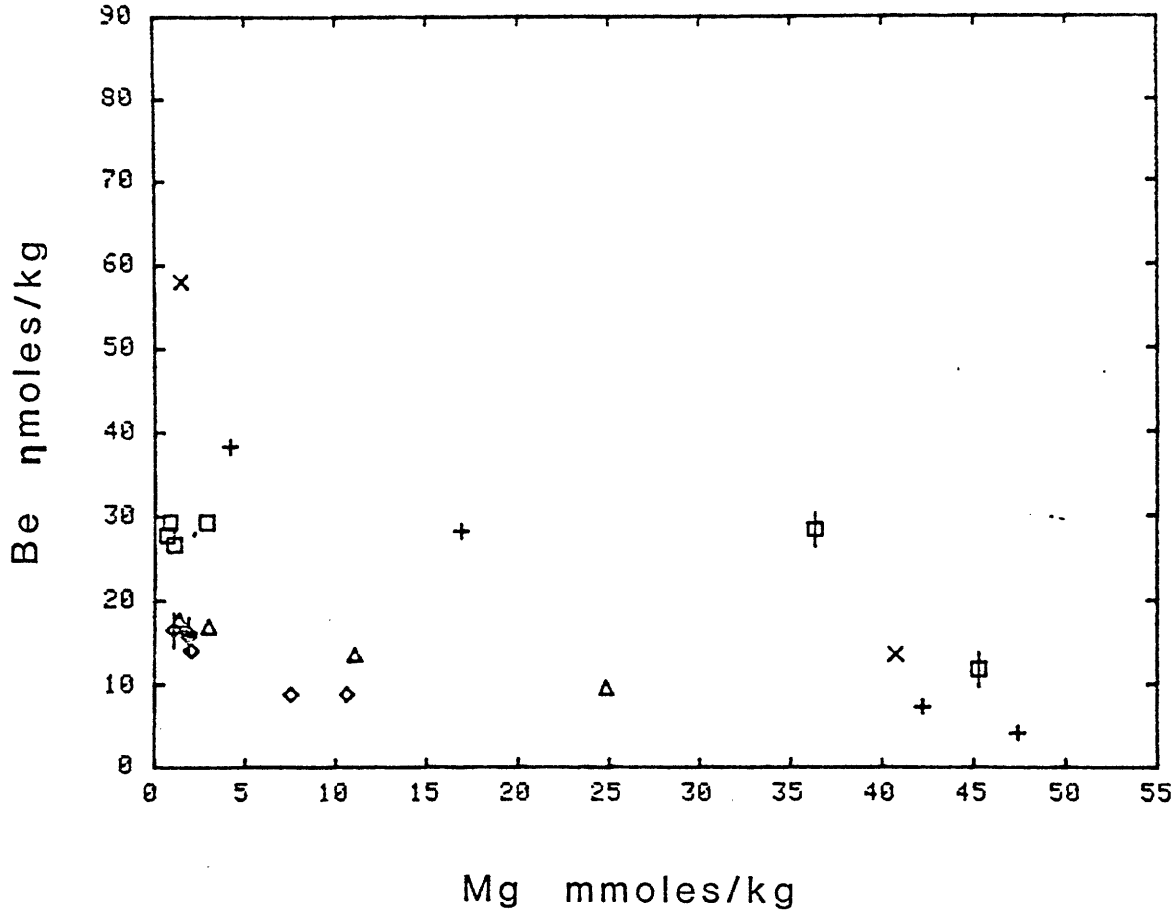

Figure 3-7: Beryllium versus magnesium at Guaymas.

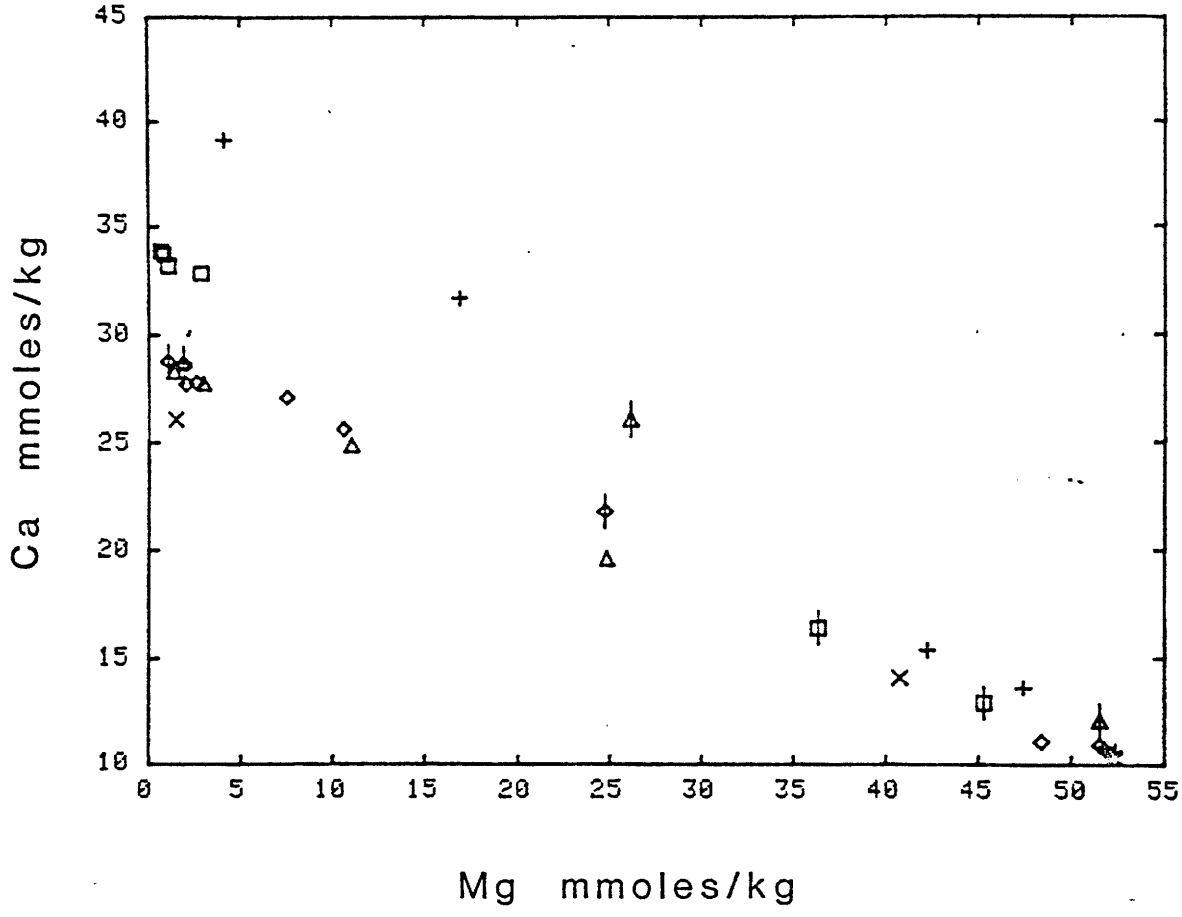

Figure 3-8: Calcium versus magnesium at Guaymas.

lowest is from some of the dive 1173 samples (Area 6). Calcium is greatly enriched in the Guaymas solutions compared to those at 21° N (Δ = +6 → +30.5 mmoles/kg). The net input from the sediments may be smaller than this Δ implies as the Ca values in the 21° N solutions are lower than those observed in the GSC (Edmond et al., 1979a) and 13° N solutions (Michard et al., 1982). Calcium has two potential sources in the sediment: from dissolution of $CaCO_3$ tests and conversion of anorthite (Ca-plagioclase) to albite. If Ca is from the dissolution of $CaCO_3$ there should be an attendant increase in the alkalinity. As there are other sources for the alkalinity (see discussion for that species) and Ca sinks may be active in the sediment column it is not possible to make a stoichiometric balance for these species. The sediment is up to 15% $CaCO_3$ (Kastner, 1982) therefore a source is available. Epidote, anhydrite, gypsum and sphene are all possible sinks for calcium from the solutions which have been identified in the Guaymas drill cores.

Solubility calculations (Bowers, Von Damm and Edmond, 1983) have shown that the calcium concentrations in the Guaymas solutions may be solubility controlled. Areas 1, 2, 3, 5 and 7 are saturated with respect to calcite and aragonite ($CaCO_3$), wollastonite ($CaSiO_3$), andradite ($Ca_3Fe_2Si_3O_{12}$), and hedenbergite ($CaFe(SiO_3)_2$). Areas 4 and 7 are saturated with respect to all of the above phases except for hedenbergite and Area 6 with all except wollastonite. Areas 3 and 6 are also supersaturated with respect to Ca-nontronite ($Ca_{.165}Fe_2(Al_{.33}Si_{3.67}O_{10})(OH)_2$). The solutions in Area 9 are not saturated with respect to the above minerals (except the $CaCO_3$ ones) but are saturated with respect to other calcium silicates. Most of these phases have not been identified in the drill cores. This may be due to several reasons: (1.) due to kinetic reasons they may not actually form,

(2.) they may have formed deeper in the section than was drilled, (3.) they may have formed in such small quantities that the cannot be identified. The solubility programs do not treat solid solutions. The saturation of several Ca-silicate minerals suggests that calcium is solubility controlled, however due to the presence of solid solutions in nature, phases not considered here may be the ones actually forming.

Strontium: Strontium increases by a factor of 2-3 over the ambient seawater value in all the Guaymas solutions. The strontium concentration ranges from 160 μmoles/kg in the 100° C samples of dive 1177 (Area 9) to 253 μmoles/kg in the dive 1175 samples (Area 3) (Figure 3-9, Table 2-5).

Strontium, like Ca, displays only an increase in the Guaymas solutions with respect to the 21° N solutions (Δ = +63 → +188 μmoles/kg). Strontium may have two sources in the sediment: $CaCO_3$ tests or clays. Two lines of evidence support the hypothesis that some of the Sr comes from the clay. Gieskes et al. (1982) found a depletion in the Sr content of the solids with depth. Sr is the first element examined which has an isotopic signature which is distinct in the basalt from the sediments. Basalt is 0.703 while the hydrothermal solutions are ~0.705 (T. Trull, unpublished data), indicating that either the solutions have not completely exchanged with the basalt or a more radiogenic source of Sr is added to the solutions from the sediments. Sr has essentially the same sinks as Ca and may be incorporated into the epidote, etc. found in the sediments.

Barium: Barium increases in all the vent fields. The barium in the samples is controlled by barite solubility which is approximately 4.4 μmoles/kg in distilled water at 300° C and 500 bars (Blount, 1977). Some seawater and hence some sulfate is entrained during sampling and in fact the constructional chimneys are probably leaky as well. The highest barium

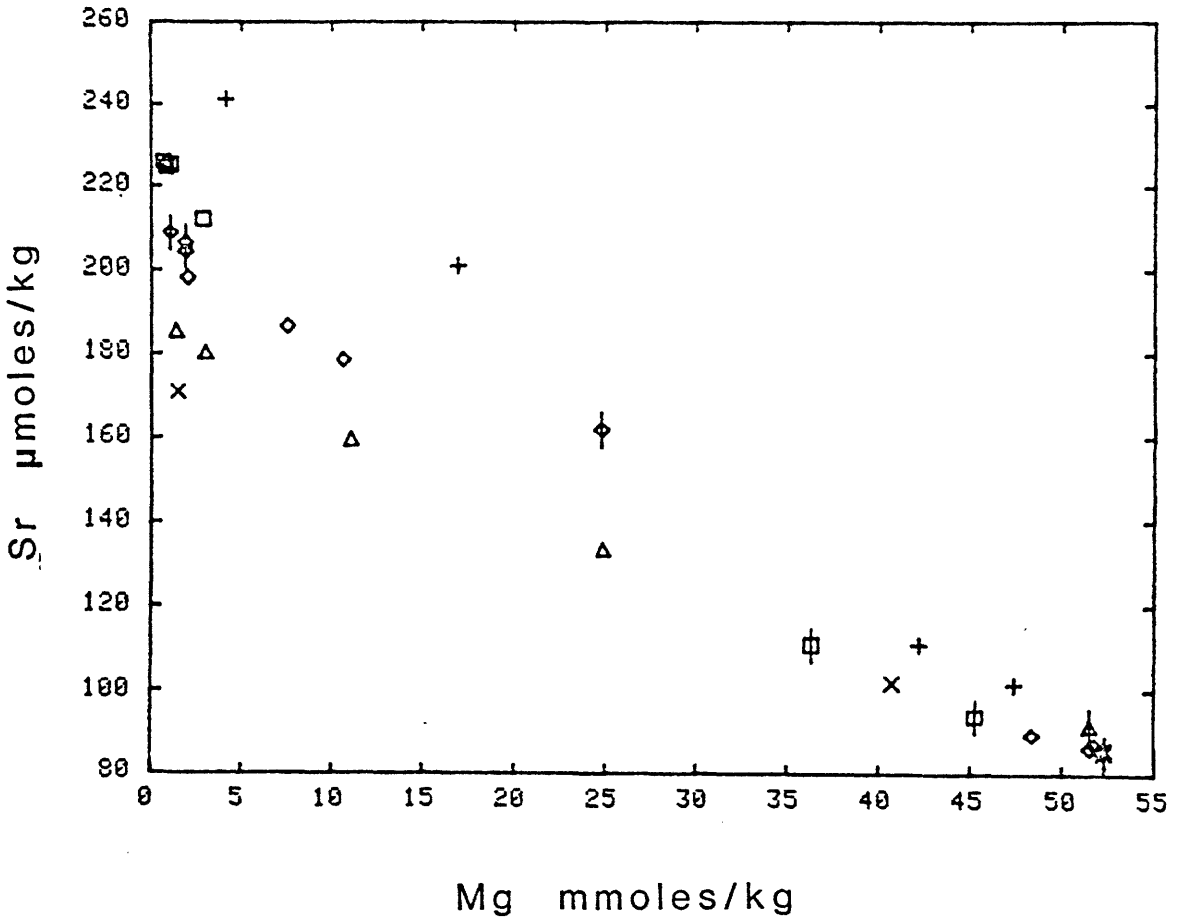

Figure 3-9: Strontium versus magnesium at Guaymas.

values measured in the Guaymas solutions are approximately 42 μmoles/kg. This can be considered a lower limit on the barium concentration in the solutions (Figure 3-10, Table 2-5). Additional barium was found in particles filtered from the solutions, raising the maximum measured barium to 54 μmoles/kg.

Barium may or may not have a source in the sediments at Guaymas (Δ = 0 → +46 μmoles/kg) (Table 3-1). The solutions at Guaymas appear to be more Ba-rich than those at 21° N but the precipitation of Ba in the samplers and in the chimneys is again a problem for making the balance.

ALUMINUM

Aluminum: Aluminum increases in all the vent fields, from a minimum of approximately 1 μmole/kg in the vents visited on dives 1172, 1173 and 1176 (Areas 1, 2 and 7) to a maximum of 7.9 μmoles/kg in the 100° C vent on dive 1177 (Area 9) (Figure 3-11, Table 2-6). The high aluminum values in the high magnesium samples are due to entrainment of sedimentary clay particles which released aluminum to the solutions when the samples were acidified.

Aluminium may increase, decrease or remain unchanged as a result of reactions occurring in the sediment cover (Δ = -4.3 → +3.9 μmoles/kg) (Table 3-1). The low concentration of aluminum in the Guaymas solutions may be due to its incorporation into alteration products.

SILICA

Silica: Silica varies in the Guaymas vent fields from 9.30 mmoles/kg in the 100° C vent on dive 1177 (Area 9) to a maximum of 13.8 mmoles/kg in the 315° C vent on that dive (Area 4) (Figure 3-12, Table 2-6). Silica at Guaymas is less than that observed at 21° N (Δ = -1.8 → -10.2 mmoles/kg).

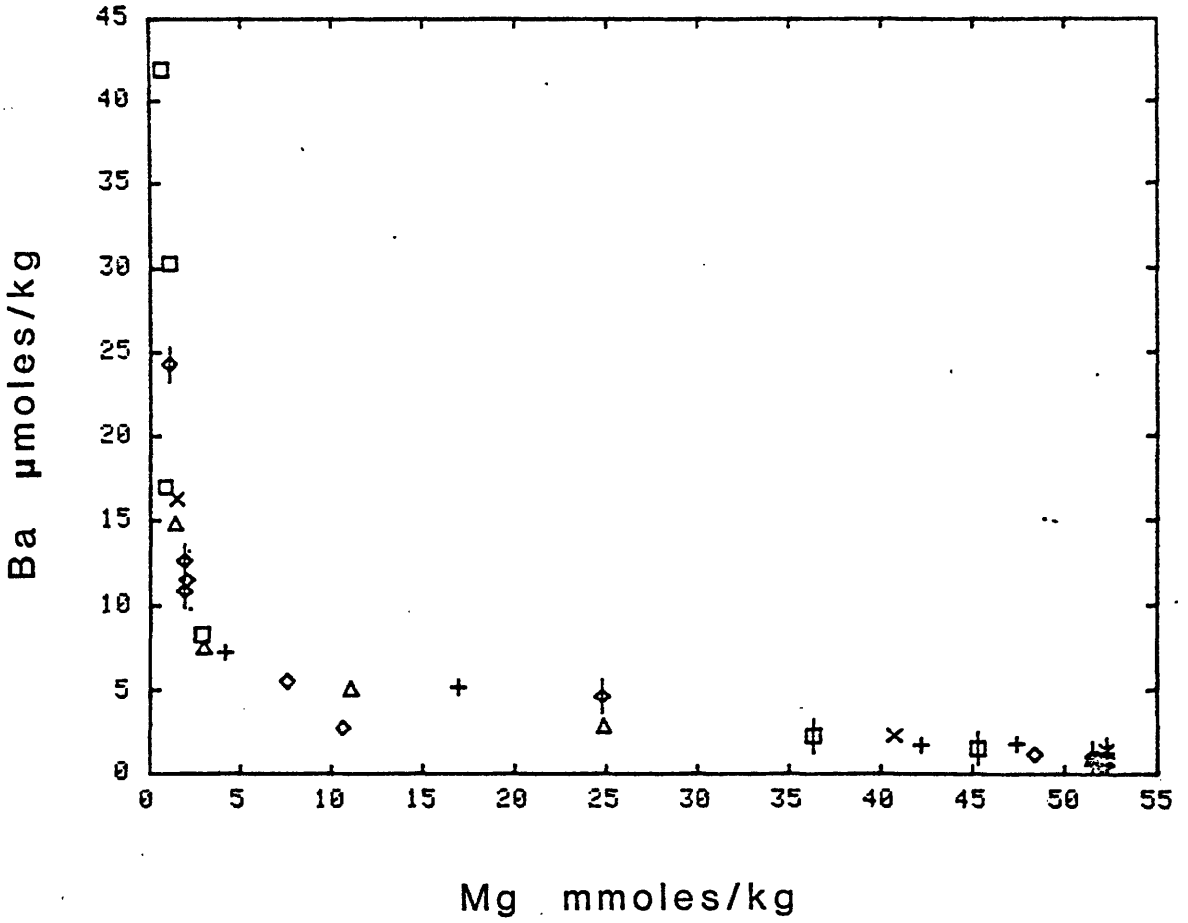

Figure 3-10: Barium versus magnesium at Guaymas.

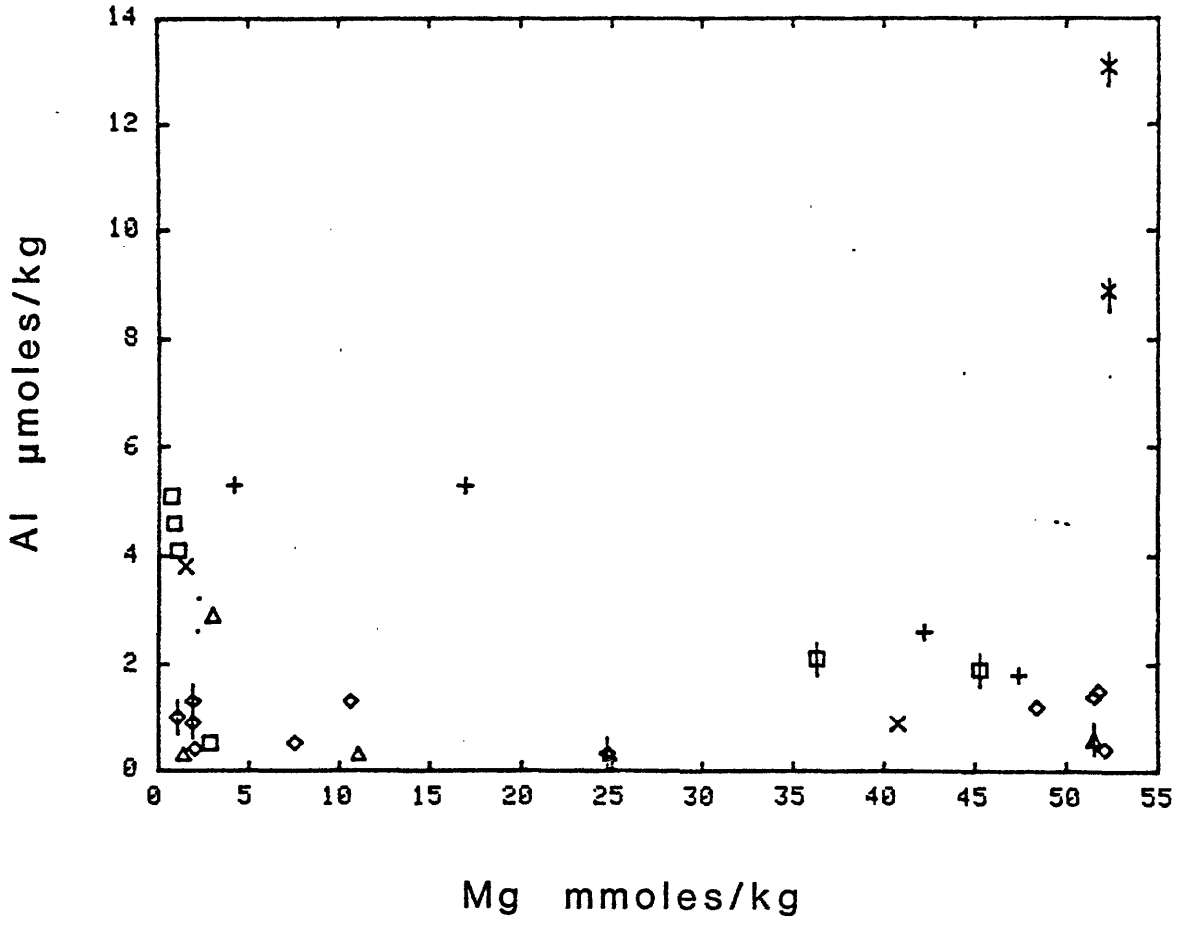

Figure 3-11: Aluminum versus magnesium at Guaymas.

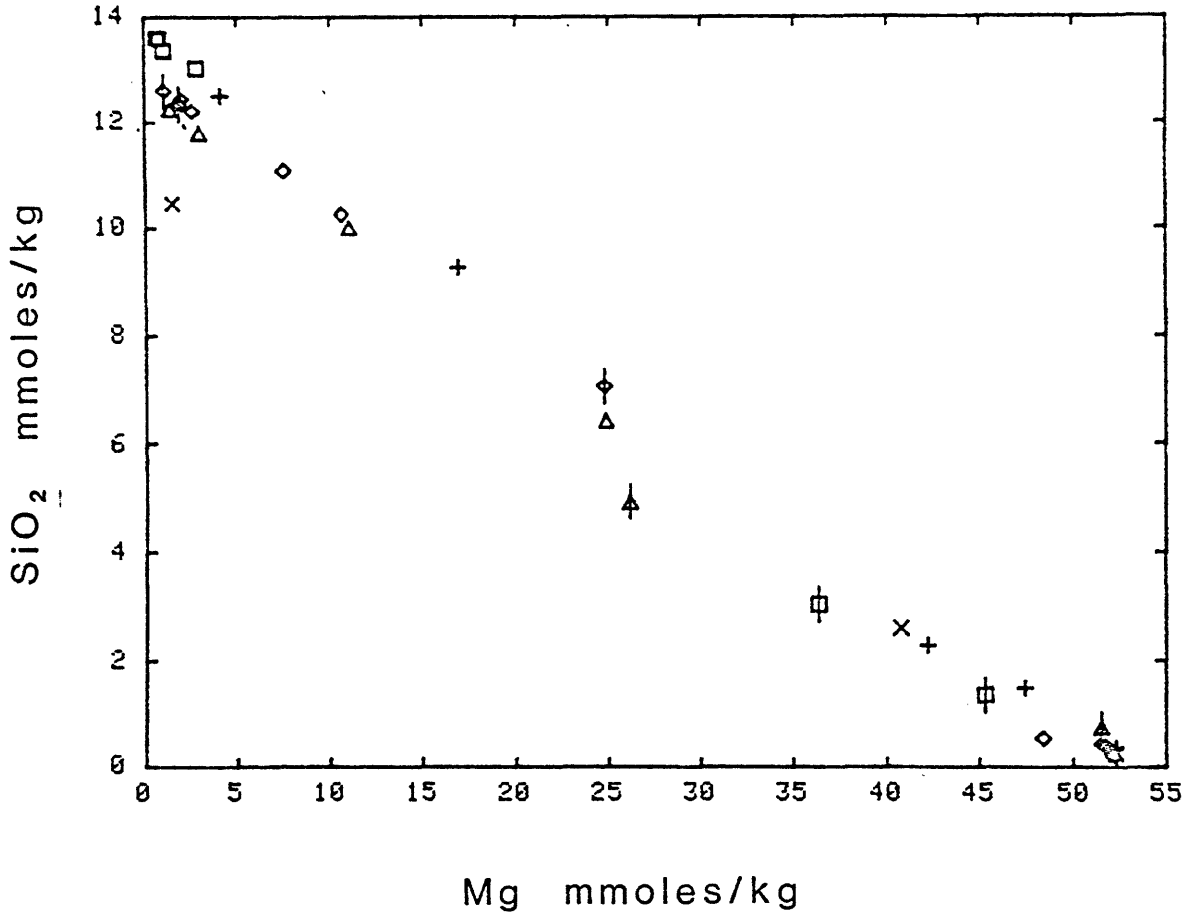

Figure 3-12: Silica versus magnesium at Guaymas.

The SiO_2 content is assumed to be controlled by quartz solubility and the solubility calculations (Bowers, Von Damm and Edmond, 1983) support this hypothesis. The lower concentrations at Guaymas than at 21° N are due to a lower pressure and/or temperature of reaction. Silica is the subject of section 3.4.

pH

pH: The pH values are from shipboard measurements at approximately 25° C and 1 atmosphere (Figure 3-13, Table 2-6). Within the precision of the measurement the pH at Guaymas is constant in all the vent fields and is significantly higher than was observed at 21° N (Δ = +2.1 → + 2.6) (Table 3-1). The high pH is a result of buffering by the carbonate (and ammonium) as evidenced by the high alkalinity. Under the in situ conditions the pH is ~6.5 and the solutions are alkaline, due to the change in the dissociation constant of water at high pressure and temperature.

CARBON

The solutions at Guaymas are extremely carbon rich as evidenced by the presence of yellow "oil" globules in samples from dive 1172 (Area 1) and the strong "diesel" smell of many of the water and rock samples. The composition of this organic matter is being determined by B. Simoneit (Simoneit, 1982).

Alkalinity: Alkalinity increases in all the vent areas at Guaymas (Figure 3-14, Table 2-6) in contrast to the decrease observed at 21° N (Δ = 3.0 → 11.1 meqs/kg) (Table 3-1). The increase is due to the dissolution of $CaCO_3$ and thermal degradation and oxidation of organic matter occurring in the sediment column:

$$\text{Alkalinity} \equiv [HCO_3^-] + 2[CO_3^{2-}] + [OH^-] - [H^+]$$

$$CaCO_3 = Ca^{2+} + CO_3^{2-}$$

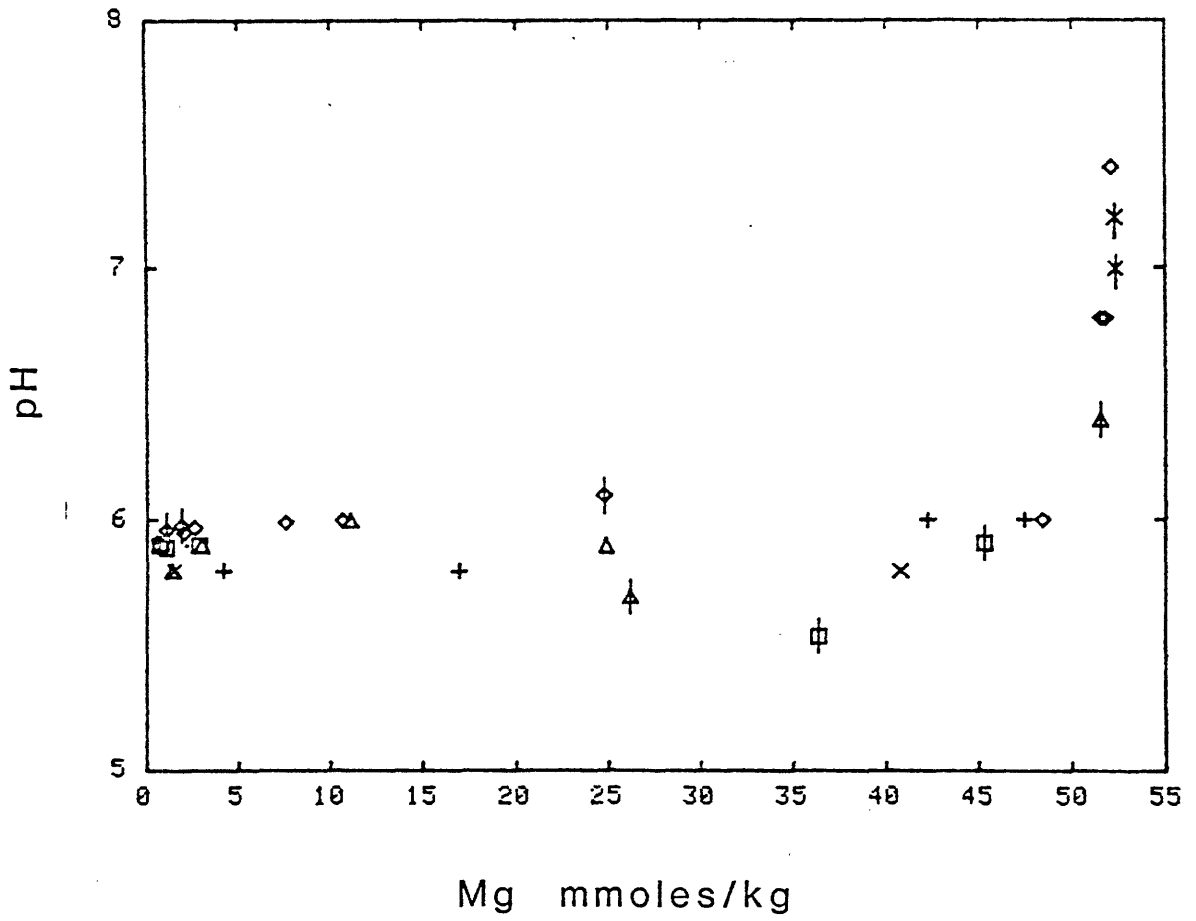

Figure 3-13: pH versus magnesium at Guaymas.

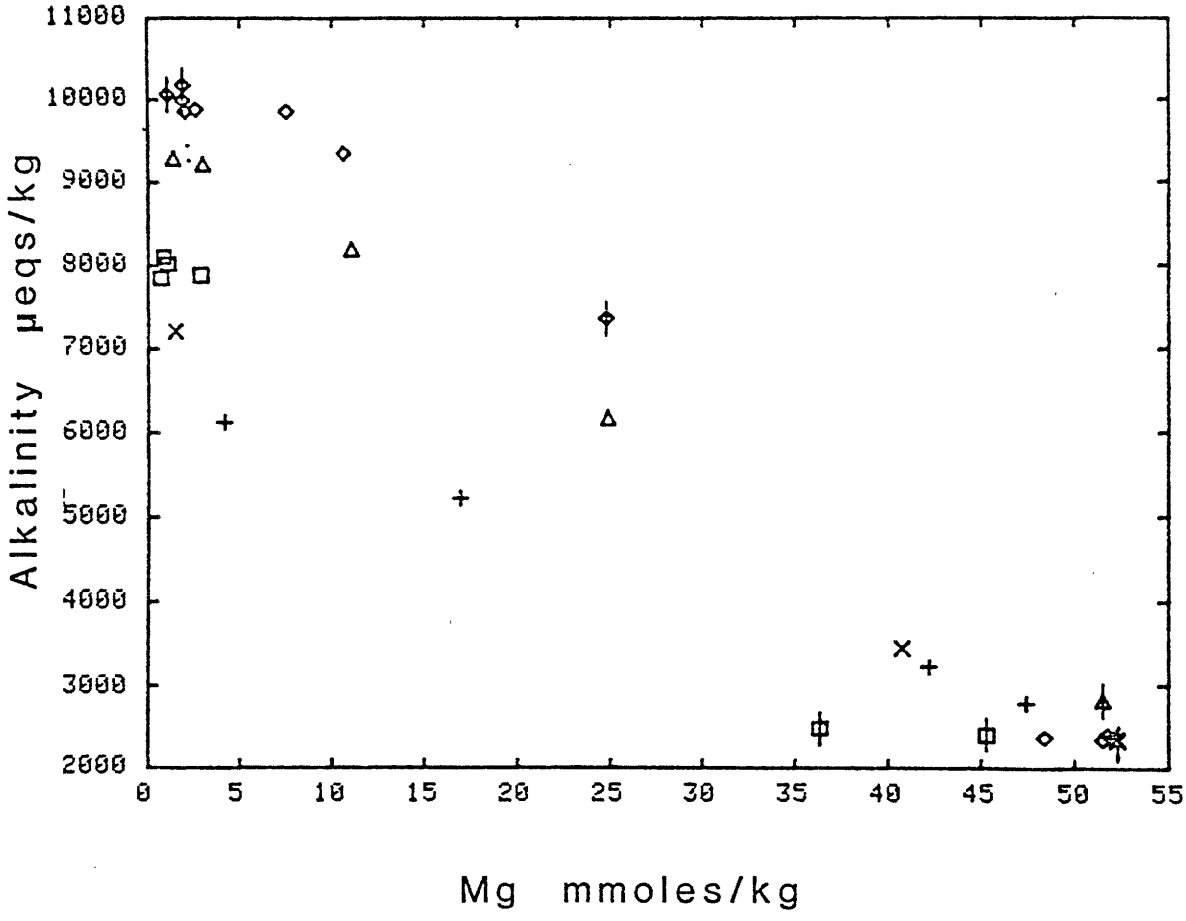

Figure 3-14: Alkalinity versus magnesium at Guaymas.

$$CO_3^{2-} + H^+ = HCO_3^-$$

$$HCO_3^- + H^+ = H_2CO_3$$

$$NH_3 + H^+ = NH_4^+$$

$$[C_{106}H_{263}O_{110}N_{16}P_1] + 107O_2 + 14H^+ = 106\ CO_2 + 16NH_4^+ + HPO_4^{2-} + 108H_2O$$

(Stumm and Morgan, 1981)

$$CO_2 + H_2O = H_2CO_3$$

$$H_2CO_3 = H^+ + HCO_3^-$$

The highest alkalinity (10.6 meq/kg) is found in the vents visited on dives 1172 and 1176 (Area 1). This high alkalinity buffers the pH to the relatively high values discussed above.

AMMONIUM

Ammonium: There is a large increase in the ammonium content of the solutions at Guaymas, to a maximum of 15.6 mmoles/kg in the solutions from dives 1172 and 1176 (Area 1) (Figure 3-15, Table 2-6). While ammonium is present in high concentrations at Guaymas only a trace was present in the 21° N solutions (Δ = +10.3 → +15.6 mmoles/kg) (Table 3-1) . It is a major species in the Guaymas solutions. NH_4^+ is produced either by the incomplete oxidation:

$$[C_{106}H_{263}O_{110}N_{16}P_1] + 107O_2 + 14H^+ = 106\ CO_2 + 16NH_4^+ + HPO_4^{2-} + 108H_2O$$

(Stumm and Morgan, 1981);

or the thermolytic degradation of organic matter:

$[C_{106}H_{263}O_{110}N_{16}P_1] + nH^+ = 16NH_4^+ + HPO_4^{2-}$ + shorter chain hydrocarbons.

Cooper and Raabe (1982) have found aureoles of NH_4^+ around a basalt dike which was intruded into a shale, suggesting that heating of organic rich sediment is a viable method of NH_4^+ production. The NH_4^+ may be responsible for the large increase in alkalinity through the consumption of protons. The ionic radius of NH_4^+ (1.43 A°) is similar to that of K (1.33 A°) and Rb

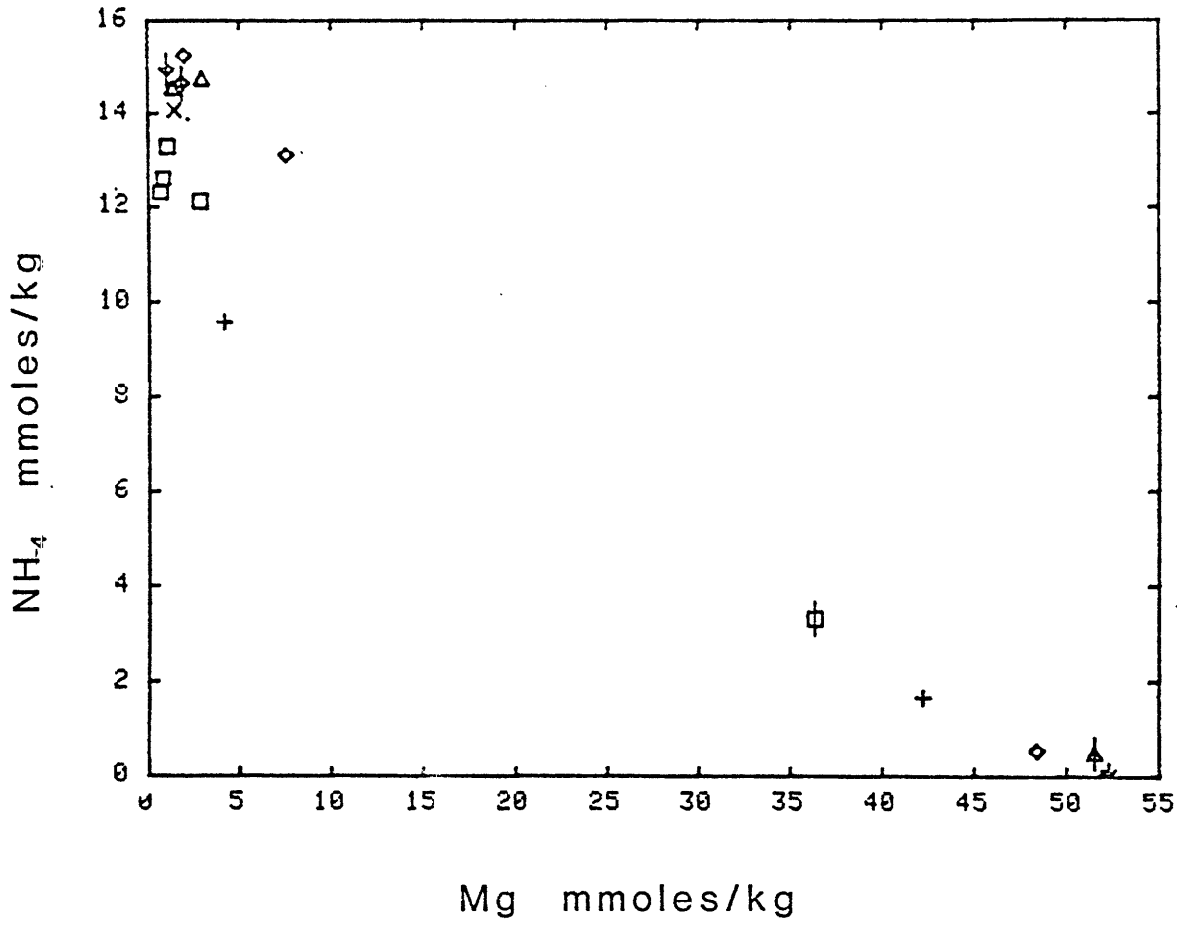

Figure 3-15: Ammonium versus magnesium at Guaymas.

(1.47 A°) and it can probably replace both of these alkalis in clays, resulting in the very high concentrations of these two elements in solution. Sterne et al. (1982), Cooper and Abedin (1981) and Cooper and Evans (1983) have found that NH_4^+ replaces K^+ in shales. The NH_4^+-illites described by Sterne et al. (1982) are found in a black shale, surrounding a metal deposit similar to the type believed to be forming at Guaymas.

THE HALOGENS

Chloride: Chloride, like sodium, increases in all the vent areas at Guaymas from the ambient value of 540 mmoles/kg (Figure 3-16, Table 2-6). The values range from 582 mmoles/kg to 637 mmoles/kg, or 8-18% above the seawater value. This is presumably due to hydration. No areas at Guaymas show a Cl sink relative to seawater values. It cannot be stated with certainty that no Cl sink is active. If a Cl sink is active (as was observed at 21° N) then the amount of water loss due to hydration would be higher. The differences in Cl may be due to differing amounts of hydration in the various vents or the same amount of hydration at all the vents but varying amounts going into a Cl sink (as at 21° N). Until the water isotopic data are available the relative importance of these two possibilities cannot be determined.

SODIUM versus CHLORIDE

As at 21° N, Na and Cl are the charged species present in the greatest abundance and additional information can be gained by examining their relationship to each other (Figure 3-17). Table 3-2 presents the net changes observed in Na and Cl and the amount of change of Na with respect to Cl. These two species do not behave conservatively and in every case the gain in Na is not sufficient to balance the gain in Cl. As the gain in

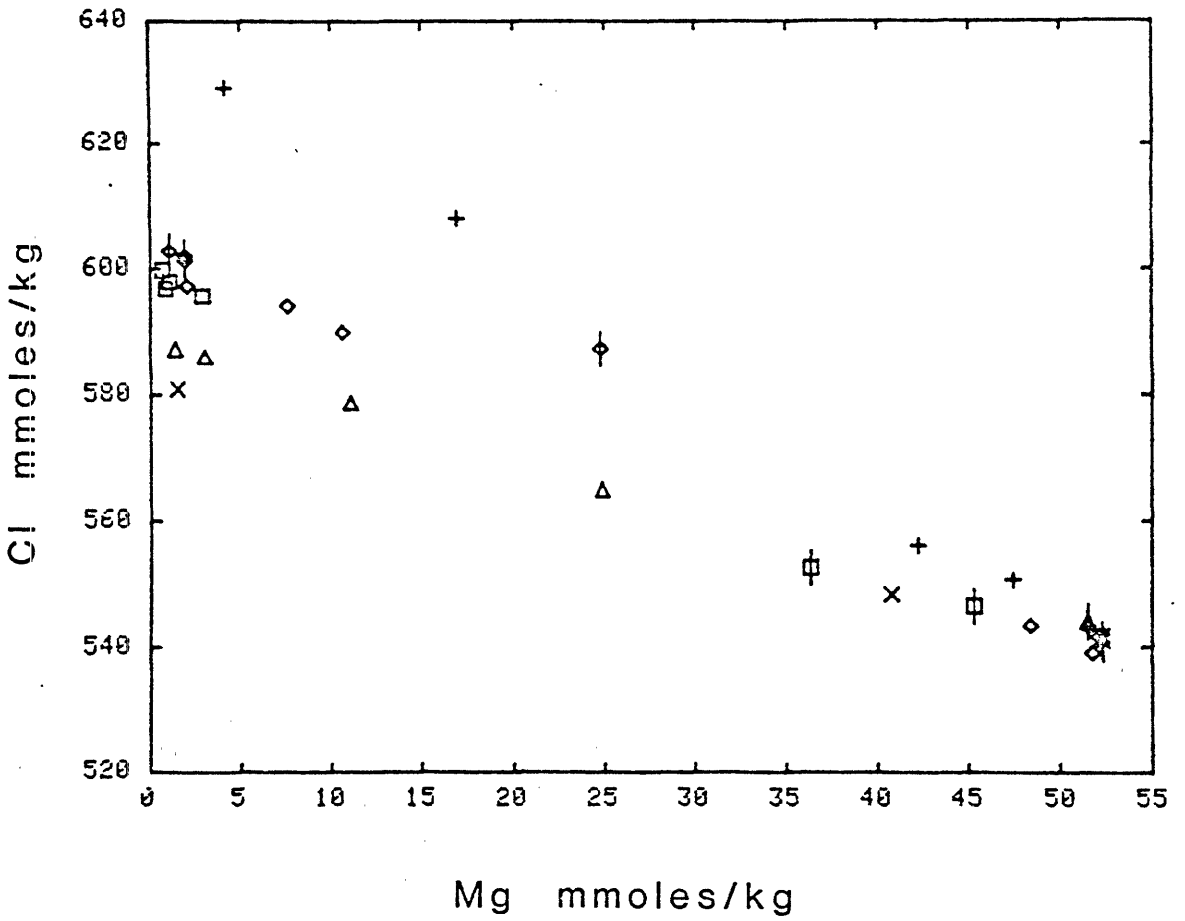

Figure 3-16: Chloride versus magnesium at Guaymas.

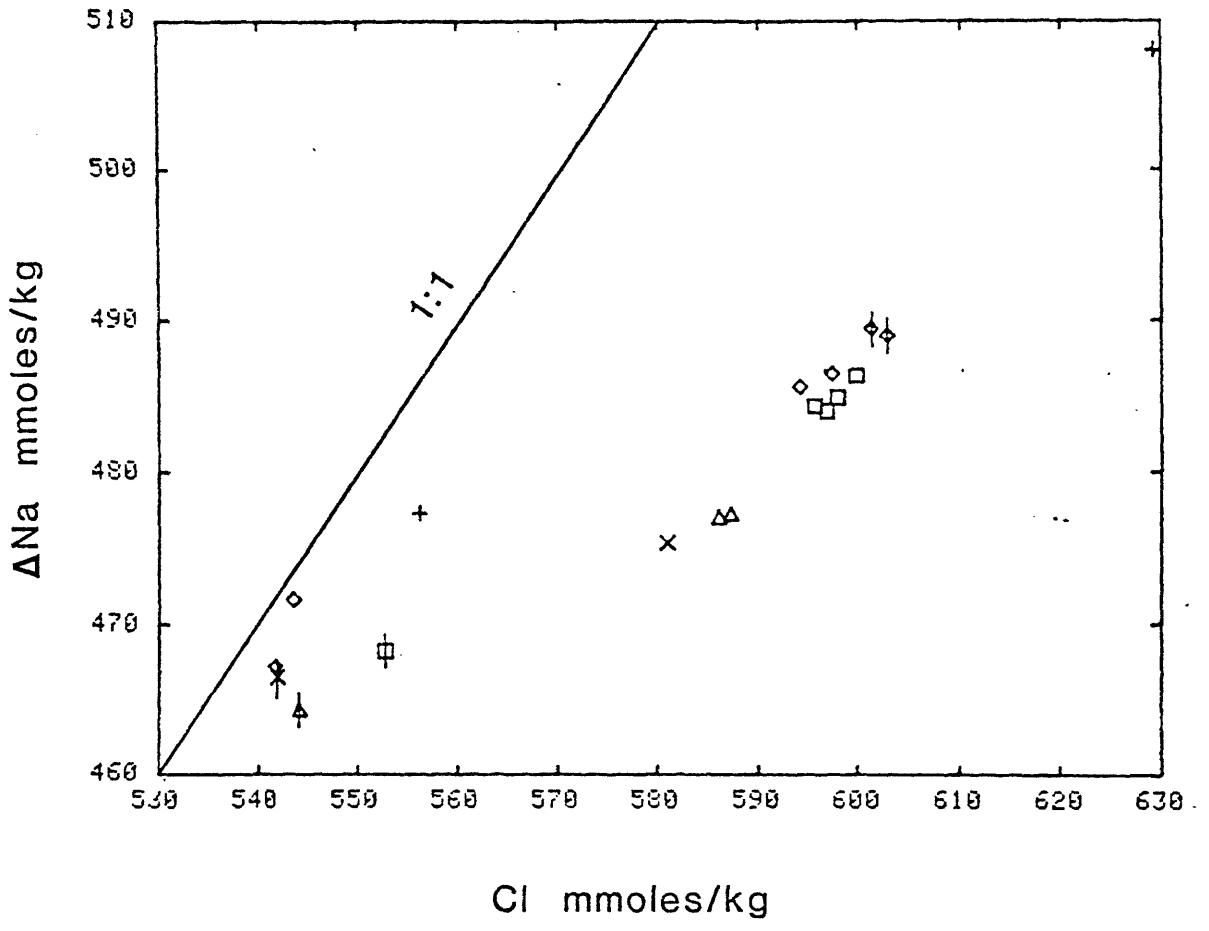

Figure 3-17: Charge balance sodium versus chloride at Guaymas. Note 1:1 line.

Table 3-2: Sodium versus Chloride - Guaymas

	Na	ΔNa	Cl	ΔCl	ΔNa/ΔCl
AREA:					
1	489	26	601	61	0.43
2	478	15	589	49	0.31
3	513	50	637	97	0.52
4	485	22	599	59	0.37
5	488	25	599	59	0.42
6	475	12	582	42	0.29
7	490	27	606	66	0.41
8	-	-	-	-	-
9	480	17	581	41	0.41
10	-	-	-	-	-
SEAWATER	463		540		

All units are millimoles/kg.

Cl is presumably due to hydration this implies a net loss of Na. The probable sink is albite which is found throughout the DSDP cores.

SULFUR

Sulfate: Sulfate decreases to a measured value of 0.35 mmoles/kg in Area 4 at Guaymas and, within the analytical uncertainty, appears to go to zero with magnesium in the endmember (Figure 3-18, Table 2-8).

Hydrogen sulfide: Hydrogen sulfide increases in all the vent areas to a maximum of 6.0 mmoles/kg in the vent sampled on dive 1176 (Figure 3-19, Table 2-8). The lowest value observed was 3.8 mmoles/kg on dive 1173. The hydrogen sulfide at Guaymas is lower than at 21° N and (Δ = -0.59 → -4.57 mmoles/kg) (Table 3-1) also represents a net loss of sulfur as seawater passes through the hydrothermal system.

Total Sulfur: As at 21° N, samples were taken in ampoules with bromine present and total sulfate determined. In four of the six areas the sum of the sulfate and hydrogen sulfide is 4-29% greater than the sulfate measured in the ampoule (Table 2-9) and this suggests that any organo-sulfur or intermediate sulfur species are quantitatively unimportant. In samples from the two vent areas visited on dive 1173 the ampoule sulfate is 23-24% greater than the other total. There were some difficulties in analyzing hydrogen sulfide from that dive shipboard and as a result those values may be low, causing the sulfur sum to be lower than that from the ampoule. A second possibility is that some other sulfur species are quantitatively important in these vent waters. At present there is no way to distinguish between these two possibilities. A more detailed discussion of sulfur is presented in section 3.3.

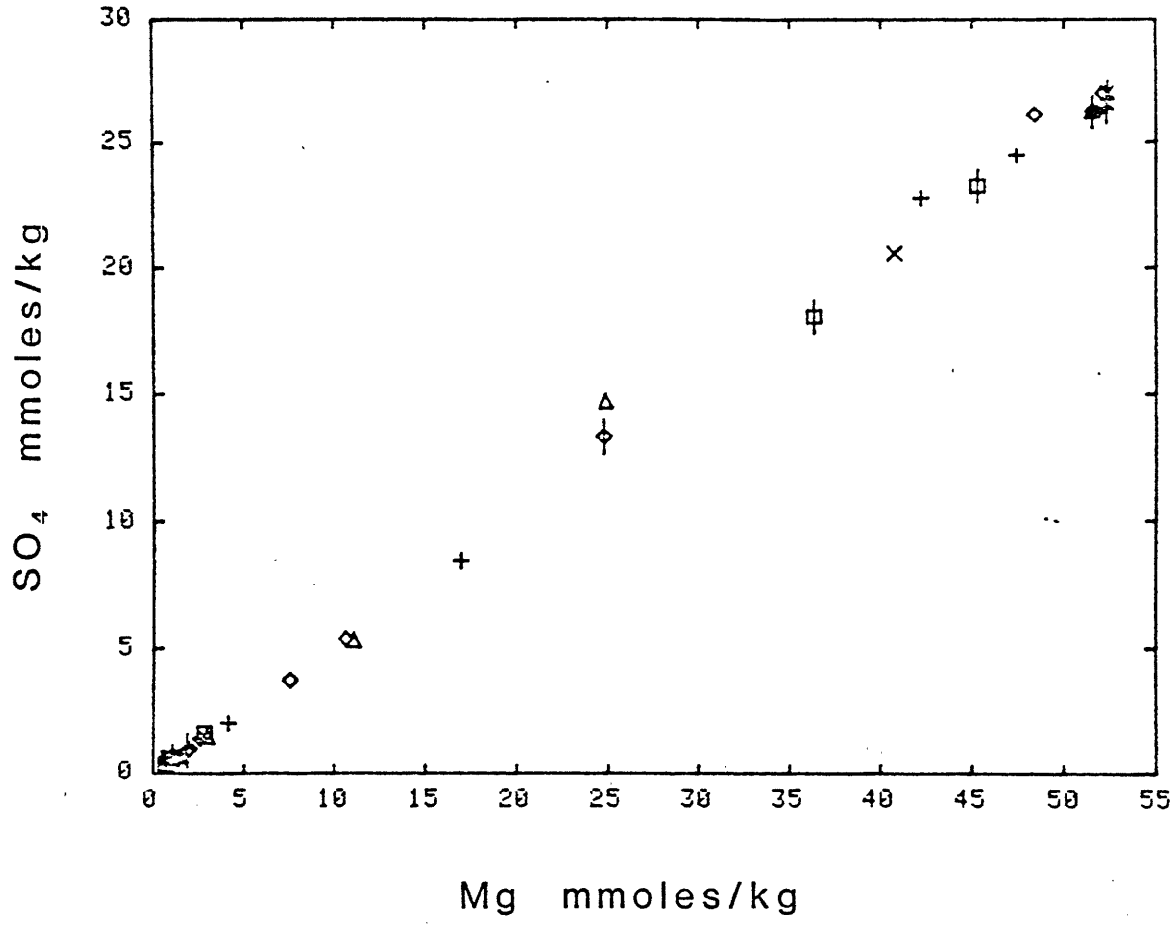

Figure 3-18: Sulfate versus magnesium at Guaymas.

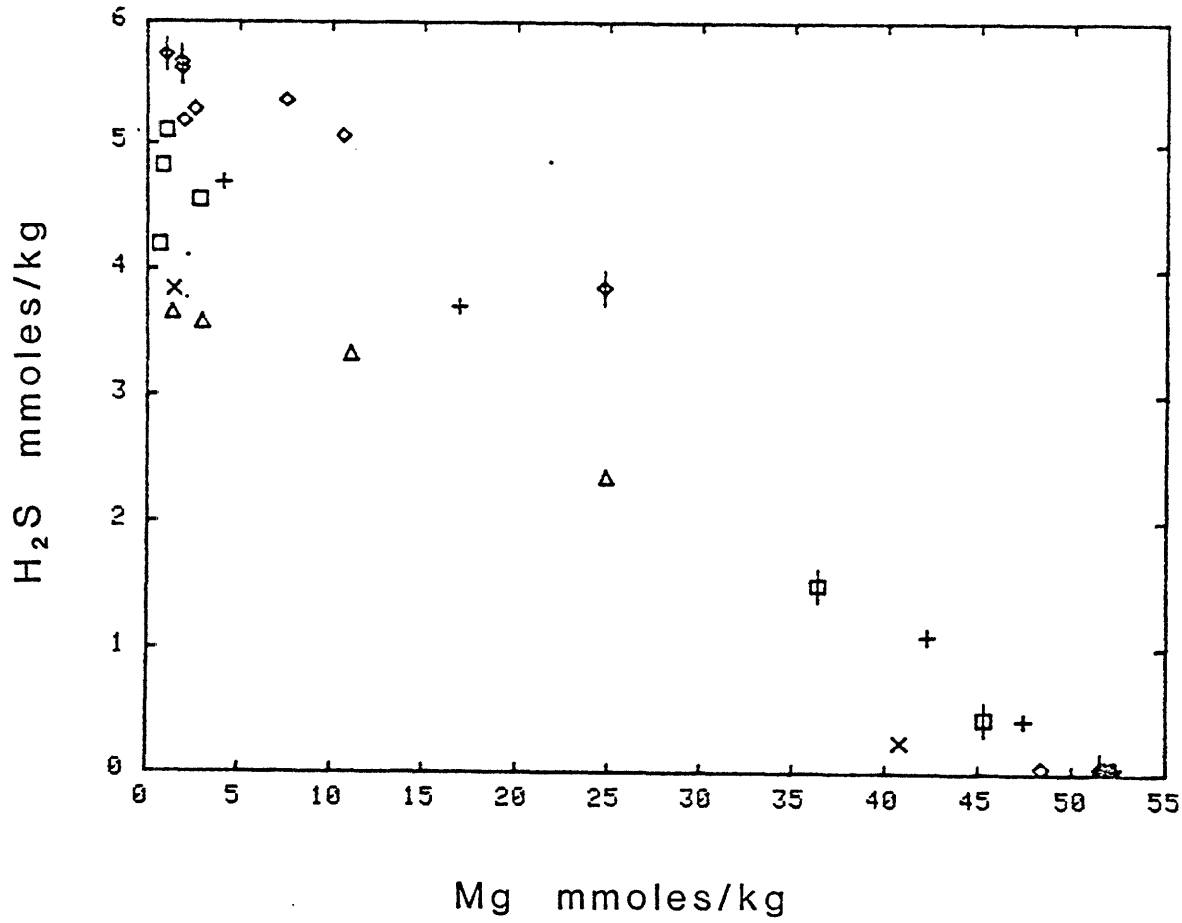

Figure 3-19: Hydrogen sulfide versus magnesium at Guaymas.

TRACE METALS

As at 21° N the metals Mn, Fe, Co, Ni, Cu, Zn, Ag, Cd, Pb and Hg which from insoluble sulfides and As and Se which can substitute for sulfur were determined in the Guaymas solutions. Cobalt and nickel were below the detection limit (5 nmoles/kg and 140 nmoles/kg respectively) in all of the solutions. Hg, as was also the case at 21° N, was found to be contaminated in these samples, prohibiting a determination of the endmember.

At 21° N only those samples with Mg <5 mmoles/kg were used to determine the endmember concentrations of these elements. Precipitation of sulfides or entrainment of particles during sampling which occurs in the more mixed samples can cause either deficiencies or enrichments of these elements. Unfortunately there are too few samples at Guaymas to use only those samples with Mg <5 mmoles/kg and still determine an endmember for many of the vent areas. The Guaymas endmembers therefore have a greater uncertainty than those at 21° N as they are more likely to be affected by precipitation reactions or by entrainment of sediment, chimney or smoke particles. The endmembers for Guaymas are determined by fitting a line to all of the data points for a given vent area, forcing the line through the seawater value and extrapolating to Mg = 0 mmoles/kg. The extrapolation for Area 3 is based primarily on one sample. This area appears to have considerably higher concentrations for several of the metals. The possibility that this sample has been contaminated cannot be eliminated with the present data set. The fact that no other sample appears to be contaminated suggests that the results for Area 3 are correct, but the possibility of contamination cannot be ignored.

The major difference which occurs between the 21° N solutions and the Guaymas solutions are the much lower trace metal concentrations found in

the Guaymas solutions. This is presumably due to the high alkalinity and high pH of the Guaymas solutions which results in reduced metal solubilities. The metals are postulated to be leached into solution through reaction with the basalt but are then deposited as the pH and alkalinity of the solutions rise during their ascent through the sediment column. Other possible explanations must also be examined. The first of these is that the solutions are not derived from the basalt but only from the sediments and thus never acquire the metals. Arguments have already been presented as to why these solutions must have reacted with the basalt. Additional evidence comes from the Pb isotopes (Chen et al., 1983) which show that the solutions are more radiogenic than MORB but not as radiogenic as would be expected from a purely sedimentary source. Pb is a mix of both basaltic and sedimentary components. A second argument is that these solutions were not hot enough to leach metals at the 21° N levels from the rocks. The temperature difference between these two areas is not very great (315° versus 350° C). The experiments have shown that metals can be leached at 260° C (Seyfried and Bischoff, 1977) and based on the isotopic evidence Pb is leached from the rock. It is unlikely that due to temperature effects the solutions never contained these metals. Based on the low extraction efficiencies from the basalt seen for the metals in the 21° N solutions it is also unlikely that the rocks were too altered to supply the metals. The preferred explanation for the low metal concentrations is that they are lost in the sediment column. A discussion on an element by element basis follows.

Manganese: The Guaymas solutions contain about five times less manganese than those at 21° N. The range of 128-236 μmoles/kg observed at Guaymas (Figure 3-20, Table 2-10) is still over a factor of 100 above the

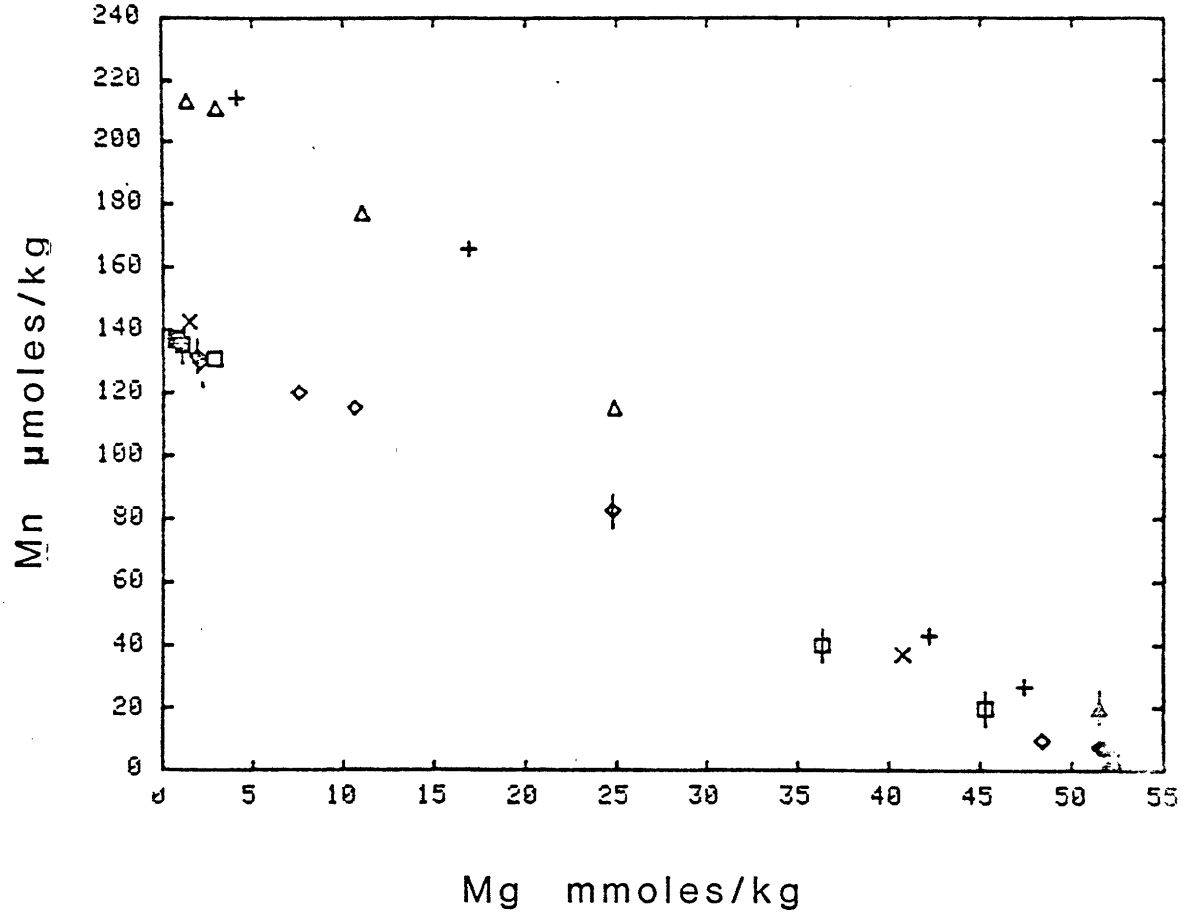

Figure 3-20: Manganese versus magnesium at Guaymas.

seawater levels. Equilibrium calculations show that all the vent areas except for 9 at Guaymas are saturated with respect to alabandite (MnS) (Bowers, Von Damm and Edmond, 1983). The concentration of manganese therefore appears to be solubility controlled.

Iron: The Guaymas solutions contain about an order of magnitude less iron than 21° N, ranging from 17-180 μmoles/kg (Figure 3-21, Table 2-10). This is still much higher than the seawater value of ~0.5 nmoles/kg. The solutions are saturated with respect to pyrite in Areas 1, 3, 5, 6 and 9 and are saturated with respect to pyrrhotite in Areas 3, 6 and 9 (Bowers, Von Damm and Edmond, 1983). Iron is also a constituent of several of the calcium silicates (andradite, hedenbergite and Ca-nontronite) which are saturated in many of the vent areas. Areas 3 and 6 are also saturated or supersaturated with respect to the iron silicates minnesotaite ($Fe_3Si_4O_{10}(OH)_2$), ferrosilite ($FeSiO_3$), fayalite (Fe_2SiO_4), greenalite ($Fe_3Si_2O_5(OH)_4$ - Area 6 only) and the iron oxides magnetite and hematite. The iron concentrations in most of the Guaymas vents therefore appear to be solubility controlled.

Iron/Manganese: At Guaymas these values are all less than unity, i.e. the concentration of manganese is always greater than the concentration of iron (Figure 3-22, Table 2-10). As mentioned above both of these metals appear to be solubility controlled.

Copper: Vent Area 3 at Guaymas contained 1.1 μmoles/kg copper and the only other samples which contained some copper, about 0.1 μmoles/kg were from Area 4 (Table 2-10). The particles filtered from the solutions in Area 4 contained additional copper and the total value for this area may be as high as 6 μmole/kg (Table A1-1). Only Area 9 is saturated with respect to a copper phase.

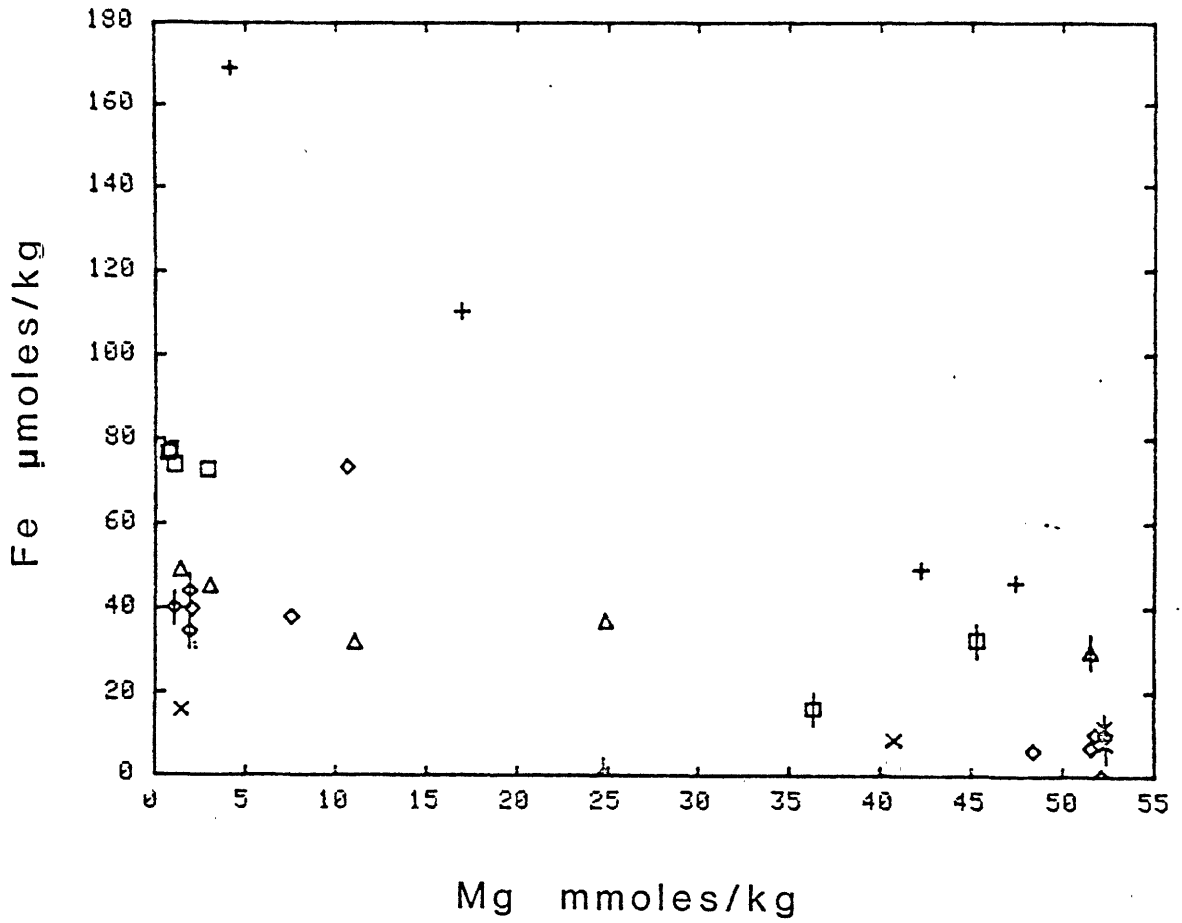

Figure 3-21: Iron versus magnesium at Guaymas.

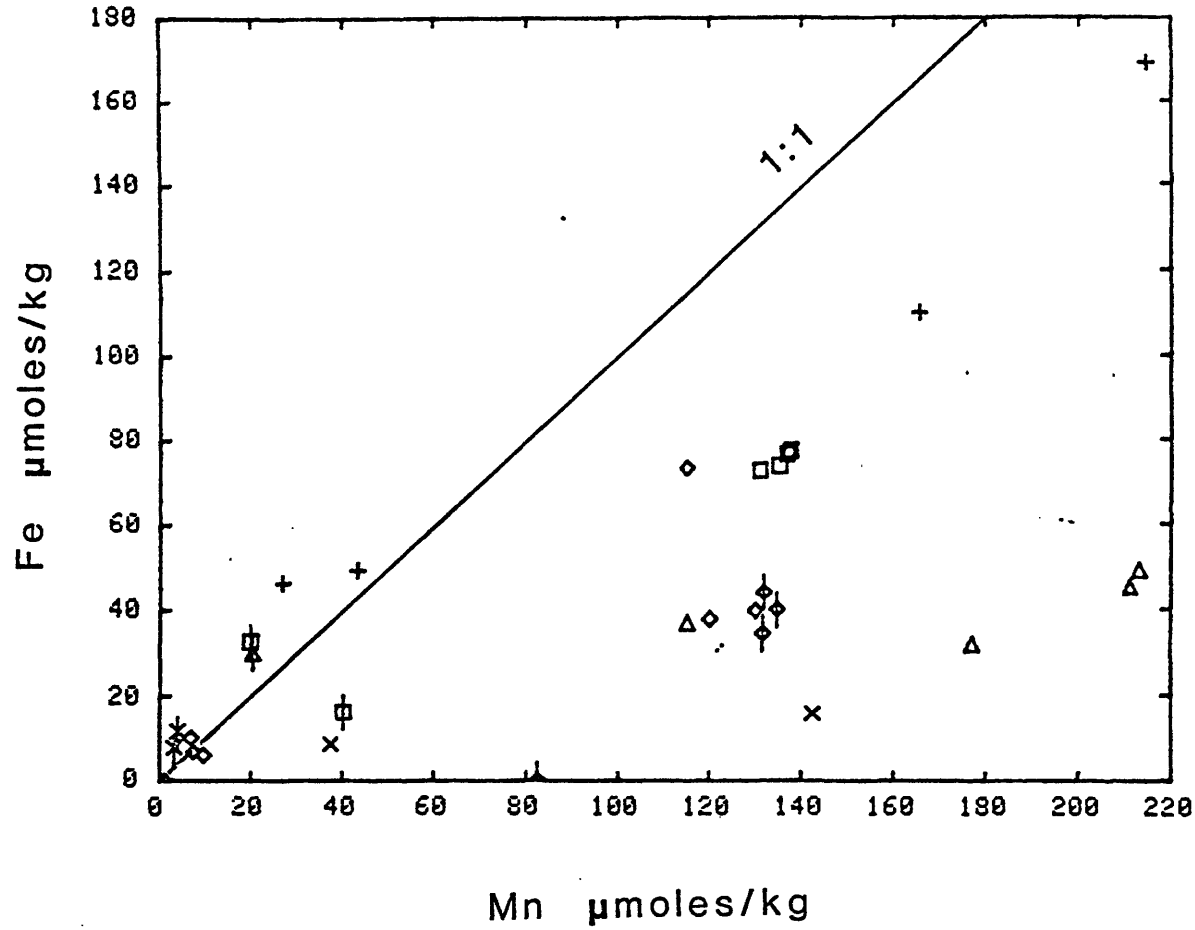

Figure 3-22: Iron versus manganese at Guaymas. Note 1:1 line.

Zinc: At Guaymas the zinc concentration ranges from 0.2 (Area 6) to 40 μmoles/kg (Area 3) (Figure 3-23, Table 2-10). Areas 1, 3, 4, 5 and 9 are saturated with respect to sphalerite and the other three areas, although undersaturated, are not far from saturation (Bowers, Von Damm and Edmond, 1983). Zinc in these solutions therefore appears to be solubility controlled in almost every case.

Silver: Only a few samples at Guaymas contained detectable amounts of silver giving the following endmember concentrations: Area 1 has 230 nmoles/kg, Area 3 has 24 nmoles/kg and Area 4 has 2 nmoles/kg (Table 2-10).

Cadmium: Again only a few samples at Guaymas contained greater than the detection limit of 10 nmoles/kg giving an endmember concentration of 46 nmoles/kg for Area 3 and 27 nmoles/kg for Area 4 (Table 2-10).

Lead: The lead values for Guaymas are about the same level (230-304 nmoles/kg) although Area 3 is considerably higher at 652 nmoles/kg (if the sample is not contaminated) (Table 2-10). The isotopic data do not lie within the MORB field (Chen et al., 1983), but imply that some lead has been added from the sediments. Areas 1, 2 and 3 are saturated with respect to galena (PbS) and Area 4 is close to saturation (Bowers, Von Damm and Edmond, 1983). These are the only areas at Guaymas in which lead was detected. Lead in solution is therefore also controlled by mineral solubility at Guaymas.

Arsenic: The Guaymas vents contain higher concentrations of arsenic than were found at 21° N; ranging from 283-1074 nmoles/kg (Table 2-11). These elevated levels suggest that additional arsenic is added to the solutions from the sediments (Δ = -169 → >1044 mmoles/kg) (Table 3-1).

Selenium: As for 21° N no selenium was found in the water samples from 21° N. Se was found in the particle fraction in the 6 areas measured

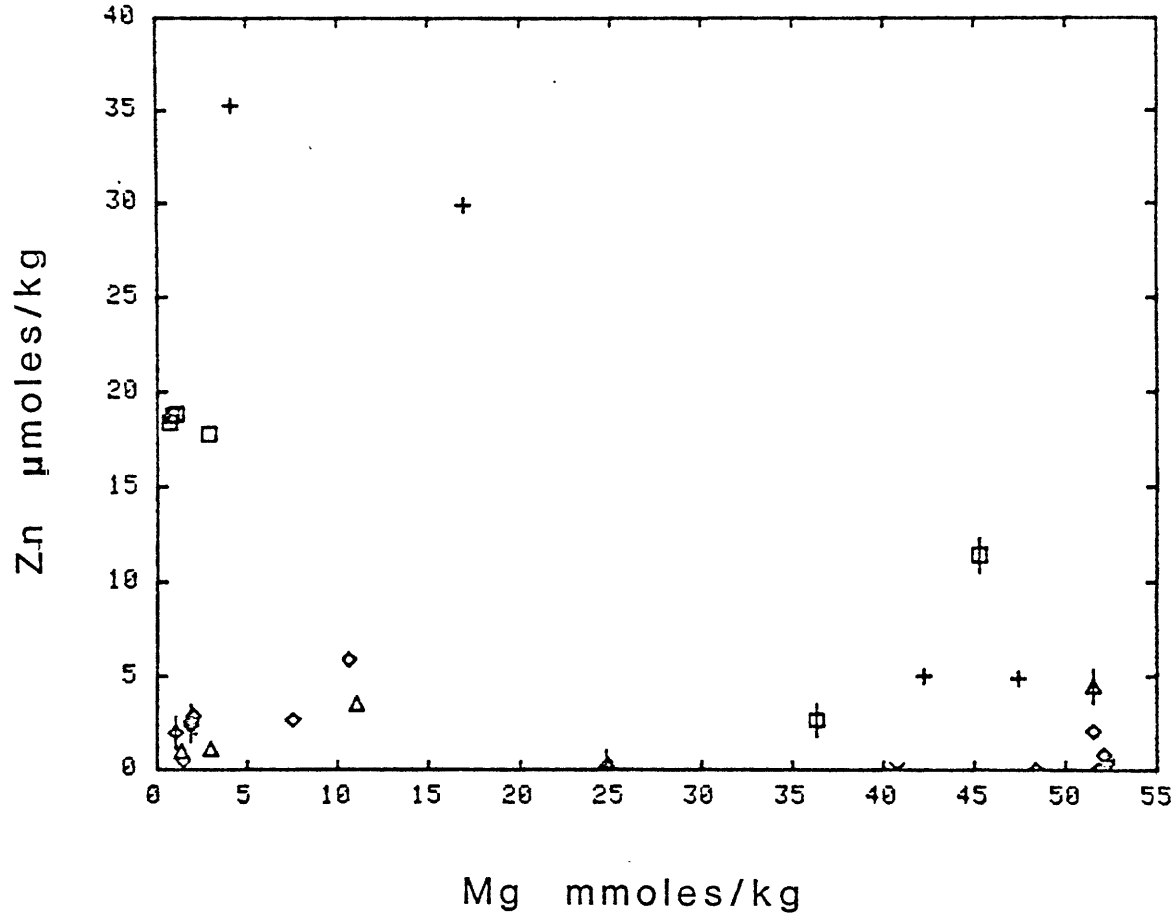

Figure 3-23: Zinc versus magnesium at Guaymas.

at Guaymas (Table 2-11). Selenium was also measured in the ampoule subsamples. The measured values ranged from 15 (Area 3) to 103 nmoles/kg (Area 4), suggesting that the levels are comparable to those found at 21° N (Δ = -57 → >102 nmoles/kg) (Table 3-1).

3.3 Sulfur System

Many of the same arguments as were presented for the 21° N system are valid for Guaymas and will not be presented here again. Sulfur isotopic data are not yet available for the Guaymas solutions and chimneys, hence there are fewer constraints on the sulfur system. Bischoff et al. (1981) found lower H_2S values in reactions with seawater and graywacke than are observed in the Guaymas solutions, suggesting that some, if not all of the sulfur comes from the basalt or basaltic reduction of seawater SO_4 with Fe^{2+}. Most, if not all, of the sulfur in the Guaymas solutions is present as H_2S (Table 2-5) and the H_2S values are significantly lower than those at 21° N (Table 2-4). The difference in H_2S between the two areas is balanced by the loss of Fe, suggesting that an Fe (or other metal) sulfide phase may be precipitating at depth.

The As concentrations are higher at Guaymas than at 21° N suggesting either an additional basaltic source (which might imply a higher basaltic sulfur input or a sedimentary input. Bischoff et al. (1981) found very high levels of As (8 umoles/kg) to be derived from the graywacke. Arsenic is enriched in marine sediments compared to basalt (Wedepohl, 1969). Se is both higher and lower in the Guaymas solutions than those at 21° N. Little data exists but it suggests that Se is enriched in marine sediments compared to basalts and that its concentration correlates with that of organic C (Wedepohl, 1969). The Guaymas sediments contain 2-4% organic matter. As organic matter always contains some sulfur, it could also have

a source in the sediments. SO_4 in the seawater pore water could also be biologically reduced to sulfide and then added to the hydrothermal solutions. Isotopic data could help to define this source as sulfur produced by biological reduction is lighter than even the basaltic sulfur.

The source of the sulfur in the Guaymas solutions cannot at present be identified. The amount present is not incompatible with a purely basaltic source or a mixed source from basalt, seawater and sedimentary organic matter.

3.4 Silica Concentration and the Depth of Reaction

A full description of quartz geobarometry and the limitations inherent in the calculations was given in section 2.4. More uncertainty exists in the calculations for the Guaymas Basin as the temperature data are not as good. Due to bad weather with loss of Alvin dives and the reconnaissance nature of the cruise most vents were visited only once. Therefore the temperatures were not verified over several days and may be treated as minimum values as stable readings were not always obtained. As the samples contained more entrained seawater than those used to calculate the endmember concentrations at 21° N, greater extrapolations to the endmember are sometimes involved. For several of the vents, the sampling was so poor that no endmember can be reliably estimated. A potential problem arises from the presence of diatoms in the sediments. If the solutions are in equilibrium with these, which are amorphous silica, the SiO_2 content of the solution will be higher than if it were in equilibrium with quartz. However Kastner (1982) has found all the SiO_2 present in the hydrothermally altered sediment to be present as quartz, therefore the assumption of equilibrium with respect to this phase is probably justified.

At Guaymas the depth of the overlying water column is ~2000 meters

(200 bars) and the sediments overlying the basalt basement are probably ~500 meters thick (50 bars). To calculate a depth of reaction into basalt, ~250 bars should be subtracted from the calculated pressures. If a negative value results, it implies that the source of the hydrothermal solution is with in the sediment cover and is probably due to a sill driven system (Kastner, 1982).

As at 21° N a variey of SiO_2 concentrations are observed for the vents at Guaymas (Table 2-12). A larger temperature range is observed for the Guaymas vents. Based on their measured temperature and SiO_2 contents the Guaymas vents are plotted onto the data of Kennedy (1950) in figure 2-25. Unfortunately most of the points fall in the area where the isobars converge, making it difficult to assign pressures to most of the areas. Area 4, the 315° C vent sampled on dive 1177 falls on the 300 bar line. This infers that the depth of reaction is 0.5 kms into the basalt. This depth agrees with that found for the HG vent at 21° N, and this helps to support the validity of this calculation. If the measured temperature of this vent is too low (or if it is hotter at depth) the pressure must decrease, if the same SiO_2 content is to be maintained. The pressure cannot be decreased below 250 bars or the solution would have its source in the sediment cover. The high ^3He content of the solution (Lupton, personal communication) argues against a purely sedimentary source. The 315° C measured temperature must therefore be within ~10° C of the temperature at depth. Area 7 with a measured temperature of 300° C also falls on the 300 bar isobar suggesting a similar depth of reaction and a correct measured temperature. For areas 1, 2, 5 and 6 no pressure (depth) can be calculated. Area 3 falls on the 1000 bar isobar inferring a depth of reaction >7.5 kms into the basalt. This great depth appears unlikely based

on the shallow depth calculated for areas 4 and 7 which are at most 4 kms away. Also none of the 21° N areas appear to circulate this deep. Although this area is out of the most central depression and overlies a fault scarp it seems unlikely that its hydrologic regime is so different. This suggests that either the measure temperature (285° C) is too low or that, as at NGS, the solution has conductively cooled. An exit temperature of 310° C would bring this area onto the 300 bar line. Area 9 had a measured temperature of only 100° C and, based on its position on the figure has probably cooled and possibly precipitated quartz during its passage through the sediment column. (At this temperature it should be in equilibrium with amorphous silica, not quartz.) Other chemical parameters for this area also suggest a longer residence time in the sediment or basalt.

The same problems as were noted for the use of the quartz geobarometer at 21° N apply at Guaymas. The quality of the temperature data at Guaymas is worse, adding another uncertainty to these calculations. No geophysical data which could help in confirming the depth of hydrothermal circulation are available for Guaymas. The agreement between the depth of reaction for one of the 21° N areas and two of the Guaymas areas increases the confidence placed in these calculations and suggests that hydrothermal circulation may at times occur at very shallow depths (~0.5 kms) in the oceanic crust.

3.5 Guaymas Model

As stated earlier (section 3.2) Guaymas is modelled as a 21° N system (seawater + basalt) with additional reactions occurring in the sediment cover. Kastner (1982) demonstrated the existence of two types of hydrothermal systems at Guaymas: the first with the solutions derived from

the underlying basalt and the second with the solutions derived from sill-driven hydrothermal systems in the sediments. Although an input from a sill-driven system to the Guaymas hydrothermal solutions cannot be completely ruled out the data (high silica, high ^{3}He, high sulfur and high iron, manganese and zinc concentrations) suggest the source of most of the solutions is from a deeper system and that the proposed model is a valid one.

3.6 Comparison to DSDP Leg 64

Prior to the discovery of actual discharging hot springs on the floor of the southern trough of Guaymas Basin, DSDP had drilled (Leg 64, Sites 477 and 477A) and found evidence of hydrothermal systems. Evidence from the solids and pore waters suggested that two types of hydrothermal systems exist at Guaymas: one driven by sills intruding into the sediments and a second driven by a shallow magma chamber below the sediment cover (Kastner, 1982). The solids which were influenced by the deep hydrothermal system were altered to a greenschist facies assemblage (Kastner, 1982). The pore waters displayed a chemistry which was unique and appeared similar to that found at GSC and 21° N (Gieskes et al., 1982). In both of these sites sills were encountered but they appeared to be "old" as they showed no temperature anomaly and most of the chemical anomalies which they had induced in the pore waters had previously decayed away by diffusion. The sills also appeared to act as a cap with hydrothermally altered pore waters and sediments below them and unaltered pore waters and sediments above (beyond a ~20 meter sill cooked margin). As the DSDP cores penetrated approximately half of the sediment column, we must infer what is occurring deeper in the section.

The maximum concentrations observed in the pore water solutions and in

Table 3-3: Comparison of Guaymas Hydrothermal Solutions and Pore Waters

Element		Hydrothermal	Pore Waters[2]
Li	μ[1]	630→1076	927
Na	m	478→513	-
K	m	32.5→48.5	92
Rb	μ	57→86	61
Be	n	12→91	-
Mg	m	0	0
Ca	m	26.6→41.5	53.3
Sr	μ	160→253	312
Ba	μ	15→54	-
$^{87}Sr/^{86}Sr$		0.705[3]	0.7049
pH		5.9	6.00
Alk_t	meq	2.8→10.6	9.58→(60.1)[4]
Cl	m	581→637	629
SiO_2	m	9.3→13.8	4.87
Al	μ	0.9→7.9	-
NH_3	m	10.3→15.6	12.2
SO_4	m	0	0?
H_2S	m	3.80→5.98	-
Mn	μ	132→236	277
Fe	μ	17→180	-
Co	n	<5	-
Cu	μ	<0.001	-
Zn	μ	0.1→40	-
Ag	n	0→230	-
Cd	n	0→46	-
Pb	n	0→652	-

[1]Units: n = nanomoles/kg
μ = micromoles/kg
m = millimoles/kg
meq = milliequivalents/kg.

[2]Data from Gieskes et al. (1982) and is the maximum (or mimimum) value observed in Sites 477 and 477A. Mg is assumed to be 0 below 155 m.

[3]T. Trull (1983) unpublished data.

[4]The high value is from the top, unaltered section of the core.

the hydrothermal solutions are given in Table 3-3. The values are in good agreement with the hydrothermal solutions generally having a slightly higher concentration. The greatest discrepancy occurs in the case of silica, which is not unexpected. The hydrothermal solutions are presumably in equilibrium with quartz at their elevated temperatures and pressures while the pore waters are considerably cooler, resulting in supersaturation and precipitation of quartz. This is supported by the presence of quartz throughout the sediment cores. If the pore water profiles themselves are examined (Gieskes et al., 1982) it is apparent that many of the pore water values continue to increase with depth and probably reach their maximum values deeper in the sediment column. The pore waters therefore appear to be hydrothermal waters which have infiltrated the sediment column and cooled, while maintaining most of their chemical signature.

The chemistry of the solids is also important to consider as the hydrothermal solutions are inferred to react with the sediments before they exit on the seafloor. Gieskes et al. (1982) found essentially quantitative removal of K from the solid phase at depth, which agrees with the high K observed in the solutions and was assumed to be partially derived from the sediments. Kastner (1982) found the assemblage quartz-albite-chlorite-epidote with pyrite and some pyrrhotite in the bottom 83 meters of site 477. This agrees with the loss of Si, Na, Mg, Fe and S from solution. The presence of chlorite may indicate that the hydrothermal solutions contain some Mg due to incomplete reaction with the basalt or that they may be in contact with unaltered seawater present in the sediment column. The Fe-sulfides appear to contain some Zn (Kastner, 1982) and some Mn (Kelts, 1982). Unfortunately Cu, which shows a large deficit in the solutions with respect to 21° N (Table 2-10) was not analyzed in the sulfide phases but

may have already been deposited deeper in the section as at 173 m below the seafloor the pH of the pore water solutions is >6 (Gieskes et al., 1982). Analysis of the bulk solids shows an increase of Cu in the 230 and 239 m intervals in site 477A, which were the deepest samples measured (Niemitz, 1982). The presence of some MnS in the Fe-sulfides agrees with the thermodynamic calculations which show MnS to be saturated in the hydrothermal solutions. The sulfur isotopic data suggest that both bacterial and hydrothermal reduction of seawater sulfate and basaltic sulfur may be the source of sulfur (Shanks and Niemitz, 1982) in the sulfides, while anhydrite is formed from seawater sulfate. The coexistence of pyrite and pyrrhotite indicates temperatures of approximately 300° C for the deeper part of this site in good agreement with the observed solution temperature of 315° C.

The pore water and solid chemistry from DSDP sites 477 and 477A is in excellent agreement with the chemistry of the sampled hydrothermal solutions and inferred sedimentary reactions. The hydrothermal solutions sampled appear to be from a deep not sill driven system.

3.7 Comparison to Chimney Chemistry

The chimneys at Guaymas are different in their mineralogy from those at 21° N. Pyrrhotite is the most common sulfide with lesser ZnS and rare chalcopyrite (S.D. Scott, personal communication). Some galena is also found in the chimneys. This agrees with the solution chemisty at Guaymas where Fe > Zn > Pb with Cu often being absent from the solutions or present at very low concentrations. Scott (personal communication) also estimates the ratio of (sulfate + carbonate)/sulfide to be 10-100 at Guaymas versus 1-10 at 21° N. This is also in agreement with the solution chemistry as Ca, Sr and Ba (all sulfate formers) are much more concentrated in the

Guaymas solutions, as are the carbonate species while the sulfide formers Fe, Zn, Cu and sulfide itself are lower in concentration. The differences in mineralogy are therefore in excellent agreement with the differences in solution chemistries observed for the two areas.

In 1977 Lonsdale et al. (1980) found a hydrothermal deposit in the northern trough of the Guaymas Basin. The deposit they found was composed primarily of talc and pyrrhotite. The sulfide phase contained Cu, Zn and Co but only Cu was present at levels significantly greater than the surrounding sediment. The $\delta^{18}O$ value of the talc indicated a temperature of formation of 280° C and the presence of anhydrite also suggested a high temperature of formation. The deposit was also coated with Fe and Mn oxides. The presence of talc and iron sulfides and the inferred temperature of formation is in good agreement with the observed temperature, reduced nature and high SiO_2 and Fe contents of the solutions observed in the southern trough.

3.8 Comparison to Ore Deposits

The environment in which the Guaymas hydrothermal system occurs is more suggestive of the terrain in which Besshi-type deposits are found, rather than ophiolite-type deposits. Franklin et al. (1981) give a concise description of Besshi-type deposits on which much of the following discussion is based. These deposits are named for their type locality in Japan and are sediment-hosted deposits. Within the sediments (or shales or schists to which they have been metamorphosed) are always found basaltic bodies (often metamorphosed to greenschist facies). These deposits also appear to be found near a tectonic boundary such as a continent-ocean crust transition as is observed in the Gulf of California. The schists that the

Besshi deposits are found in are black which is indicative of a high organic matter content, consistent with the sediments found at Guaymas. Some of the ore bodies are found in carbonaceous rocks, again consistent with the Guaymas sediments.

The ores found in these deposits typically contain chalcopyrite and pyrite with lesser sphalerite, as well as Pb and Co. The ore bodies may be massive or banded and are in general very thin (several meters) while they may be hundreds of meters wide and long. The massive ore contains pyrite, chalcopyrite, sphalerite and bornite with minor magnetite, and quartz and calcite as the gangue minerals. The banded ore contains pyrite, with minor chalcopyrite and sphalerite in a gangue of quartz, carbonate, albite, chlorite and minor epidote, amphiboles and tourmaline (Franklin et al., (1981).

The composition and habit of the Besshi ores and gangue minerals are consistent with what one would expect to find forming subsurface at Guaymas. DSDP Holes 477 and 477A penetrated only half the sediment column and although they did find some sulfides they did not drill into an "ore deposit" which may occur deeper in the section. Based on the model presented in section 3.2 the Guaymas solutions have lost much of the Fe, all of the Cu, some of the Zn, all of the Co and possibly some of the Ag, Cd and Pb they contain at depth in the system. These elements are presumably deposited as sulfides, as sulfur also shows a net loss. These predictions are in good agreement with the observed metal content of the deposits. Presumably this deposition at depth occurs for two reasons. First, the solubility of these metals is temperature dependent and a drop in temperature, caused by conductive cooling in a low flow system, may cause their deposition. A second cause of deposition could be due to a

change in pH. Crerar and Barnes (1976) have shown how large changes in solubility are due to temperature decreases and pH increases. The Guaymas solutions have a pH which is approximately two units higher than the 21° N solutions and this may be the controlling factor on metal solubilities. The Guaymas solutions gain alkalinity and hence increase their pH due to reactions, many of which involve organic matter, which can occur in the sediment column (section 3.2). The large amount of hydrocarbons found in these solutions (Simoneit and Lonsdale, 1982) suggests that the supply of organic matter is not limiting the progress of these reactions in the Guaymas case. The very thin ore bodies of the Besshi-type deposits suggests that they have encountered some kind of a front. Presumably a drop in temperature would be a more gradual process, suggesting it is a chemical front which they have encountered. The rise in alkalinity accompanied by a rise in pH due to organic matter degradation and carbonate dissolution is therefore suggested as the primary mechanism of deposition for these deposits.

Although the literature references to it are scant, there is other evidence that the chemical reactions are important. Another product of the above reactions is NH_4^+, which is present at millimolar levels in the hydrothermal solutions (Table 2-3). Sterne et al. (1982) recently noted the large amounts of NH^{4+}-illite found in the black shales surrounding the ore bearing strata in Lik and Competition Creek stratiform Zn-Pb-Ag base metal deposits in the Delong Mountains, northern Alaska. They could propose no explanation for this observation. The deposits in northern Alaska such as they and Nokleberg and Winkler (1982) have described are presumed to have formed on the seafloor. If they formed in a method analagous to the deposits we believe to be forming today at Guaymas the

explanation for the high NH_4^+-illite is obvious. These Alaskan deposits may have also formed due to the degradation of organic matter as they occur with black shales and dark cherts. The type ore deposit is also consistent with the Guaymas deposits. The Guaymas solutions appear to lose some of their Zn, they are saturated with galena (some of the Pb is sediment derived, based on the isotopes) and contain variable amounts of Ag.

It therefore appears likely that a Besshi or sediment-hosted type stratiform deposit is forming at depth at Guaymas. The cause of deposition is most likely increased alkalinity and pH due to organic matter degradation (possibly due to heating) and $CaCO_3$ dissolution. Guaymas is an extremely productive area of the ocean which results in the high sedimentation rates with high organic matter and $CaCO_3$ content. In general a hydrothermal system covered by sediment without these components may not result in a deposit. The overlying water column chemistry and physics (upwelling leading to high nutrients and high productivity) may therefore play a controlling role in this type of deposit formation on the seafloor.

3.9 Comparison to Experimental Work

Very few of the experiments are comparable to the Guaymas system as most were done with basalt or andesite, not sediments, as the solid and seawater. The most directly applicable is that of Bischoff et al. (1981) in which graywacke was reacted with seawater at temperatures of 200° and 350° C, pressures of 500 bars and a water/rock ratio of 10:1. Graywackes are sedimentary rocks and as a first approximation may be considered as analogues to the sedimented Guaymas system. Two shortcomings exist with this approach: 1) the sediments at Guaymas are extremely organic rich which may have a profound effect on the net solution chemistry and 2) the Guaymas solutions undergo prior reaction with the basalt. This second point, which

is a disadvantage for reproducing the solution chemistry is actually an advantage when trying to separate the basalt from sediment reactions.

Bischoff et al. (1981) observed a net gain of Ca, K and Fe and a net loss of SO_4, Cl, Na and Mg in their seawater solutions. The changes of Fe and Cl are very small and may not be significant. Anhydrite, albite and smectite-chlorite were found to be the alteration products. Anhydrite is an artifact in these experiments as was discussed in section 2.9. The species which are gained or lost, respectively, in the experiments show the same direction of change in the inferred sedimentary reactions at Guaymas. The alteration products are those found in the DSDP cores. The H_2S is much lower in the experiment, presumably due to the lack of either basaltic sulfur or the basaltic reduction of seawater sulfate in the solutions. Fe, Mn, Cu, Zn and Pb are present at levels comparable to those in the Guaymas solutions. The solubility of these elements is pH dependent and the experimental solutions are more acid than the Guaymas solutions (4.8 versus 5.9) and this may be important in maintaining the slightly higher metal levels. Ba, As, Ca and K have a source in the graywacke and a sedimentary source was inferred for them at Guaymas. Cd is leached from the graywacke into seawater and is present at levels higher than those found in the Guaymas solutions. The Cd concentration of the Guaymas solutions again may be controlled by the solubility of a sulfide phase. The experiment also demonstrates that Mg can be consumed in sedimentary reactions alone.

While this experiment is not a complete analog for the Guaymas system the chemical changes seen in the solutions and solids are consistent with those inferred for the sedimentary reactions at Guaymas. Where differences do exist they can be explained in terms of the missing basalt and organic matter components.

3.10 Comparison to Metalliferous Sediments

Metalliferous sediments were discussed with respect to the 21° N hydrothermal system in section 2.10. At that time it was noted that the Fe/Mn ratio in these sediments is 3:1 which is indicative of a high temperature source (based on the much lower ratios observed at the GSC). This ratio coupled with the large amounts present indicates hydrothermal activity as the primary source of iron and manganese in these sediments. The Fe/Mn ratio at Guaymas is always <1. This suggests that Guaymas-type heavily sedimented hydrothermal systems are not quantitatively important for the formation of metalliferous sediments. The lower content of the other metals (Cu, Zn, etc.) in these solutions lends further support to this hypothesis.

3.11 Summary - Chapter 3

The Guaymas solutions are a result of reactions occurring between seawater and basalt with an overprint of sedimentary reactions. A model has been presented which attempts to separate these two sets of reactions. The major difference between the Guaymas and 21° N solutions is the high pH, alkalinity and ammonium present in the Guaymas solutions. This may be responsible for the much lower concentrations of the sulfide-forming elements in the solutions. As at 21° N a net loss of sulfur occurs in the solutions and the source of the reduced sulfur in the exit solutions cannot be determined unambiguously. Quartz geobarometry can only be applied to a few areas but these areas indicate a 0.5 kms depth of reaction into the basalt (below the sediment) in good agreement with the HG area at 21° N.

The agreement of the solution chemistry with the pore water chemistry in DSDP Sites 477 and 477A is amazingly good. The chimneys are different compositionally from those at 21° N and these differences are in good

agreement with the changes in solution chemistry. The Guaymas system appears to be analagous to a Besshi-type ore deposit in formation. An experiment done with graywacke at 350° C is the most comparable to the Guaymas system and the resulting solution chemistry shows some of the same enrichments. Sediment covered hydrothermal systems are probably not quantitatively important for the formation of metalliferous sediments.

CHAPTER 4

Conclusions

This chapter consists of three sections. The first section summarizes the results of the studies of the 21° N and Guaymas Basin solution chemistries and includes a comparison of these two systems. The second section is a discussion of hydrothermal fluxes to the ocean and is an attempt to evaluate the importance of this source term. The final section contains suggestions for further work.

4.1 Comparison of 21° N and Guaymas

The 21° N and Guaymas Basin hydrothermal systems both occur on the East Pacific Rise, at areas with similar spreading rates of approximately 6 cm/yr. Both solutions originate from the reaction of seawater with basalt at elevated temperatures and pressures. The major difference between the 21° N and Guaymas hydrothermal systems is that the Guaymas solutions pass through and react with ~500 meters of sediment before reaching the seafloor. The 21° N solutions exit from constructional features, "chimneys", which they have formed through cooling and mixing with seawater on top of the pillow basalts. They do not react with sediments. The Guaymas solutions have also formed constructional features, on top of the sediment, which have a different mineralogy than those at 21° N due to differences in solution chemistry. The maximum measured temperature of the solutions at 21° N was 355° C and at Guaymas was 315° C. The pressures for the two systems are also similar as the hot springs at 21° N occur under 2500 meters of water and those at Guaymas occur under 2000 meters of water but the zone of reaction with the basalt is at least 500 meters greater, beneath the sediment cover.

The chemistry of the hot springs at 21° N is not determined by equilibrium solubility controls except for quartz. The amount of a given species in solution must therefore be due to either the limited amount of it present in the seawater-basalt system or kinetic factors. The low calculated extraction efficiency for many of the elements suggests that kinetic factors are more important. The NGS vent is saturated with respect to pyrite at its measured 273° C exit temperature. Based on the silica content of the solutions (section 2.4) this vent is assumed to have cooled conductively from ~350° C. At 350° C this vent is not saturated with pyrite, suggesting that this saturation is a result of cooling and not an original control on the solution chemistry.

The Guaymas solutions have a different chemistry than those at 21° N due to reactions which occur in the sediment cover. Table 3-1 is a comparison of their chemistries. In the absence of direct information on the composition of the Guaymas hydrothermal solutions as they leave the basalt and before they react with the sediment it is assumed that they have the same composition as the 21° N solutions. Table 3-1 also gives the net difference (Δ) between the two sets of solutions. Note the large gain of K, Rb, Ca, Sr, NH_4, pH and alkalinity in the Guaymas solutions with respect to 21° N and the loss of most of the "trace" metals which form insoluble sulfides such as Mn, Fe, Co, Cu and Zn. Although there is some variation between vent fields most of the Guaymas solutions are saturated with respect to alabandite (MnS), sphalerite (ZnS), galena (PbS) and pyrite (FeS_2) or pyrrhotite (FeS). The decreased solubility of these phases (and resulting lower solution concentrations) are due to the higher pH of these solutions. The high pH is a result of the dissolution of $CaCO_3$ and decomposition of organic matter; both of which cause increases in

alkalinity and pH. The Guaymas solutions are also saturated with respect to $CaCO_3$ and several calcium and iron silicates. If the Guaymas Basin was not under a highly productive area of the ocean which results in the sediments being 2-4% organic matter and 10-15% $CaCO_3$, the solution chemistry would be more similar to that observed at 21° N.

In summary the 21° N solution composition must be either rock-limited or kinetically controlled while the Guaymas solutions are solubility controlled by $CaCO_3$, calcium and iron silicates, and the metal sulfides. The metal sulfides which are saturated are those found in sediment-hosted deposits (especially lead and zinc). The Guaymas solutions may be thought of as "spent" solutions. Although epidote is abundant throughout the DSDP cores the solutions are not saturated with respect to this phase. This is due to the low aluminum in the solutions, which is probably due to the precipitation of epidote and other aluminum containing phases at depth. Both the 21° N and Guaymas solutions are saturated with respect to quartz; a necessary condition for the application of quartz geobarometry.

4.2 Hydrothermal Fluxes

The reaction of seawater with basalt at elevated temperatures in the oceanic crust has been shown to greatly modify the chemistry of seawater. The resulting hydrothermal solutions are injected back into the oceanic water column and may play an important role in determining the chemistry of seawater. This requires the evaluation of the net hydrothermal input; a calculation fraught with difficulties. Seawater composition is also strongly dependent on the riverine input. Unfortunately great uncertainties also exist for the net river input of many elements.

After the analysis of the first oceanic ridge crest hydrothermal solutions from the GSC Edmond et al. (1979a,b) calculated a net

hydrothermal input based on the ratio of ^3He to heat observed in the waters. They assumed that the oceanic ^3He flux came from axial hydrothermal solutions with the same ratio to heat as was observed at GSC.

The fluxes in Table 4-1 were calculated using the same assumptions as Edmond et al. (1979a,b). Several authors have suggested that these values are too high. Hart and Staudigel (1982) have pointed out that the annual potassium flux, based on these calculations, is larger than the amount of potassium present in newly intruded basalts. The conductive heat flow anomaly extends tens of kilometers away from the ridge axis and the above calculation assumes that all the heat is lost via axial hot springs. Based on thermal modelling Sleep and Wolery (1978) and Sleep et al. (1983) believe that these axial springs remove heat from only a few kilometers off axis and account for perhaps 10% of the conductive heat flow anomaly. The above calculation also assumes that all of the oceanic ^3He input is at the ridge axis while some may also be input at convergent margins or oceanic islands which are the result of mantle plumes (Craig and Lupton, 1981; Kurz, 1982). While several authors have suggested that these values may be too high, none have suggested that they are too low. The values in Table 4-1 may be viewed as the maximum hydrothermal input; this can still provide a useful comparison to the river flux and between systems.

The major differences which occur between the 21° N and Guaymas systems are the much lower inputs of Mn, Fe, Co, Cu and somewhat lower inputs of Zn and Cd from the Guaymas system. For these elements the Guaymas system is similar to the GSC system where these elements are lost subsurface as sulfides. The input of Sr and NH_4 from Guaymas is at least an order of magnitude larger than that from 21° N (or GSC in the case of Sr). Guaymas also has a larger input of K and Rb than the other areas.

Table 4-1: Comparison of Hydrothermal and River Fluxes

	21° N[1]	Guaymas	GSC[2]	River[3]
Li	$1.2 \rightarrow 1.9 \times 10^{11}$	$8.6 \rightarrow 15 \times 10^{10}$	$9.5 \rightarrow 16 \times 10^{10}$	1.4×10^{10}
Na	$-8.6 \rightarrow 1.9 \times 10^{12}$	-	+,-	6.9×10^{12}
K	$1.9 \rightarrow 2.3 \times 10^{12}$	$3.2 \rightarrow 5.5 \times 10^{12}$	1.3×10^{12}	1.9×10^{12}
Rb	$3.7 \rightarrow 4.6 \times 10^{9}$	$8.0 \rightarrow 12 \times 10^{9}$	$1.7 \rightarrow 2.8 \times 10^{9}$	5×10^{6}
Be	$1.4 \rightarrow 5.3 \times 10^{6}$	$1.7 \rightarrow 13 \times 10^{6}$	$1.6 \rightarrow 5.3 \times 10^{6}$	3.3×10^{7}
Mg	-7.5×10^{12}	-7.5×10^{12}	-7.7×10^{12}	5.3×10^{12}
Ca	$2.4 \rightarrow 15 \times 10^{11}$	$2.4 \rightarrow 4.5 \times 10^{12}$	$2.1 \rightarrow 4.3 \times 10^{12}$	1.2×10^{13}
Sr	$-3.1 \rightarrow +1.4 \times 10^{9}$	$1.0 \rightarrow 2.4 \times 10^{10}$	0	2.2×10^{10}
Ba	$1.1 \rightarrow 2.3 \times 10^{9}$	$2.1 \rightarrow 7.7 \times 10^{9}$	$2.5 \rightarrow 6.1 \times 10^{9}$	1.0×10^{10}
F	-1.0×10^{10}	n.a.[4]		
Cl	$0 \rightarrow -1.2 \times 10^{13}$	0	$-31 \rightarrow +7.8 \times 10^{12}$	6.9×10^{12}
SiO_2	$2.2 \rightarrow 2.8 \times 10^{12}$	$1.3 \rightarrow 2.0 \times 10^{12}$	3.1×10^{12}	6.4×10^{12}
Al	$5.7 \rightarrow 7.4 \times 10^{8}$	$1.3 \rightarrow 11 \times 10^{8}$	n.a.	6.0×10^{10}
NH_4	0	$1.5 \rightarrow 2.2 \times 10^{12}$	n.a.	
SO_4	-4.0×10^{12}	-4.0×10^{12}	-3.8×10^{12}	3.7×10^{12}
H_2S	$9.4 \rightarrow 12 \times 10^{11}$	$5.4 \rightarrow 8.5 \times 10^{11}$	+	
ΣS	$-2.8 \rightarrow -3.1 \times 10^{12}$	$-3.2 \rightarrow -3.5 \times 10^{12}$	-	
Mn	$1.0 \rightarrow 1.4 \times 10^{11}$	$1.9 \rightarrow 3.4 \times 10^{10}$	$5.1 \rightarrow 16 \times 10^{10}$	4.9×10^{9}
Fe	$1.1 \rightarrow 3.5 \times 10^{11}$	$2.4 \rightarrow 26 \times 10^{9}$	+	2.3×10^{10}
Co	$3.1 \rightarrow 32 \times 10^{9}$	0	n.a.	1.1×10^{8}
Cu	$0 \rightarrow 6.3 \times 10^{9}$	0	-	5.0×10^{9}
Zn	$5.7 \rightarrow 15 \times 10^{9}$	$.01 \rightarrow 5.7 \times 10^{9}$	n.a.	1.4×10^{10}
Ag	$0 \rightarrow 5.4 \times 10^{6}$	$0 \rightarrow 3.3 \times 10^{7}$	n.a.	8.8×10^{7}
Cd	$2.3 \rightarrow 26 \times 10^{6}$	$0 \rightarrow 6.6 \times 10^{6}$	-	
Pb	$2.6 \rightarrow 5.1 \times 10^{7}$	$0 \rightarrow 8.9 \times 10^{7}$	n.a.	1.5×10^{8}
As	$0 \rightarrow 6.5 \times 10^{7}$	$0 \rightarrow 1.5 \times 10^{8}$	n.a.	7.2×10^{8}
Se	$0 \rightarrow 1.0 \times 10^{7}$	$0 \rightarrow 1.5 \times 10^{7}$	n.a.	7.9×10^{7}

[1]All numbers are in moles/yr.

[2]GSC data is from Edmond et al. (1979a,b).

[3]River concentrations and fluxes are from either Edmond et al. (1979a,b) or Broecker and Peng (1982).

[4]n.a. = not analyzed

Except for the species noted above the fluxes calculated for the three areas are very similar. The major difference occurs for those elements which form insoluble sulfides as these can have either a large input term (as at 21° N), a removal term (as at GSC) or be somewhere inbetween (as at Guaymas). Whether a hydrothermal system is leaky, tight or sediment covered (Figure 1-2) will have a major influence on the amounts of these species added to the oceanic water column.

The fluxes calculated for the sulfide formers are difficult to evaluate on another basis as well. These fluxes are calculated from the dissolved solution concentrations. Some of the metal load of the solutions may have already been lost to form the chimneys. An unknown proportion of the dissolved load is incorporated into (or onto) a solid phase (the "black smoke")and an unknown proportion of the solid phase is redissolved in the oxic environment of the water column and seafloor. The flux calculations for these elements therefore have additional inherent uncertainties.

Table 4-1 also contains data for the river flux of these elements. These numbers are also poorly defined because many rivers have not been measured, and those which have may only have been sampled once, making no allowance for the variation in concentration which accompanies variation in flow. The values for the transition metals are especially uncertain as they have been measured in very few rivers and have very complicated estuarine chemistries, which often result in their removal from solution. The quoted values for their fluxes may be too high by several orders of magnitude (Shiller, personal communication). The most important point is that the hydrothermal input is the major source of lithium and rubidium to the ocean. This remains the case even if the hydrothermal input is only 10% of what is assumed here. For many of the other elements the ridge

crest source may be comparable to or significantly less than the river flux, depending on the assumptions made regarding the hydrothermal fluxes.

4.3 Further Work

The hot springs at 21° N were the first undiluted high temperature submarine hot springs to be sampled. Their chemistry agrees very well with that inferred from the diluted GSC hot springs. Workers in France have recently observed and sampled hot springs at 13° N on the East Pacific Rise. Preliminary reports of their chemistry (Michard et al., 1982) show them to be somewhat different than those at 21° N. A detailed comparison between these two systems may help to explain differences between systems as well as differences between vents. The study of additional axial vents will define their range in composition which is important for flux considerations.

The Guaymas system, with its sediment cover provides a somewhat different input to the ocean. Further work on this system will help in elucidating the formation of sediment hosted ore deposits.

Although all of the above solutions meet the criteria of "ore forming" solutions they have chlorinities very similar to seawater. Based on studies of fluid inclusions from ore deposits, many "ore forming" solutions have much higher chlorinities. The recent report of warm water (<15° C above ambient) flowing downhill on Larson's seamounts (Lonsdale et al., 1982) suggests that these high chlorinity solutions may also be present on the seafloor. Seamounts may, in some cases, be the location of another type of hydrothermal activity on the seafloor and may be forming another class of mineral deposits, known broadly as "caldera-hosted". Future work will hopefully elucidate the processes occurring at seamounts and establish if this type of activity is widespread over the seafloor.

All of the hot springs sampled to date are on moderate spreading rate ridges (6-9 cm/yr). As a large proportion of the oceanic ridge crest system is slow spreading, and some is much faster spreading, it is important to establish if the same type of hydrothermal activity exists on these other sections of the ridge system.

REFERENCES

Anderson, R.N., J. Honnorez, K. Becker, A.C. Adamson, J.C. Alt, R. Emmermann, P.D. Kempton, H. Kinoskita, C. Laverne, M.J. Mottl, R.L. Newmark, DSDP Hole 504B, The first reference section over 1 km through layer 2 of the oceanic crust, Nature 300 (1982) 589-594.

Ballard, R.D. and J. Francheteau, The relationship between active sulfide deposition and the axial processes of the mid-ocean ridge, Marine Technology Society Journal 16 (1982) 8-22.

Ballard, R.D., J. Francheteau, T. Juteau, C. Rangin, W. Normark, East Pacific Rise at 21°N: the volcanic, tectonic, and hydrothermal processes of the central axis, Earth Planet. Sci. Lett. 55 (1981) 1-10.

Barnes, H.L. (editor), Geochemistry of Hydrothermal Ore Deposits, 2nd ed., John Wiley and Sons, New York (1979) 798pp.

Barnes, H.L. and G.K. Czamanske, Solubilities and transport of ore minerals, in Geochemistry of Hydrothermal Ore Deposits, 1st ed., ed. by H.L. Barnes, Holt Rinehart and Winston, New York, (1967) 334-381.

Bender, M., W. Broecker, V. Gornitz, U. Middel, R. Kay, S. Sun, P. Biscaye, Geochemistry of three cores from the East Pacific Rise, Earth Planet. Sci. Lett. 12 (1971) 425-433.

Bischoff, J.L., Geothermal system at 21°N, East Pacific Rise: physical limits on geothermal fluid and role of adiabatic expansion, Science 207 (1980) 1465-1469.

Bischoff, J.L. and F.W. Dickson, Sea water basalt interaction at 200°C and 500 bars: implications for origin of seafloor heavy metal deposits and regulation of sea water chemistry, Earth Planet. Sci. Lett. 25 (1975) 385-397.

Bischoff, J.L., A.S. Radtke, R.J. Rosenbauer, Hydrothermal alteration of graywacke by brine and seawater: roles of alteration and chloride complexing on metal solubilization at 200°C and 350°C, Econ. Geol. 76 (1981) 659-676.

Blount, C.W., Barite solubilities and thermodynamic quantities up to 300°C and 1400 bars, American Mineralogist 62 (1977) 942-957.

Bonatti, E., Metallogenesis at oceanic spreading centers, in Annual Review of Earth and Planetary Sciences, ed. by F.A. Donath 3 (1975) 401-432.

Bostrom, K. and M.N.A. Peterson, Precipitates from hydrothermal exhalations on the East Pacific Rise, Econ. Geol. 61 (1966) 1258-1265.

Bostrom, K. and M.N.A. Peterson, The origin of aluminum-poor ferromanganoan sediments in areas of high heat flow on the East Pacific Rise, Mar. Geol. 7 (1969) 427-447.

Bostrom, K., M.N.A. Peterson, O. Joensuu and D.E. Fisher, Aluminum-poor ferromanganoan sediments on active oceanic ridges, Journal of Geophysical Res. 74 (1969) 3261-3270.

Bowers, T.S., K.L. Von Damm and J.M. Edmond, The chemical evolution of ridge crest hot springs (1983) manuscript in preparation.

Brewer, P.G. and D.W. Spencer, Colorimetric determination of manganese in anoxic waters, Limnol. Ocean. 16 (1971) 107-110.

Broecker, W.S. and T.H. Peng, Tracers in the Sea, Lamont-Doherty Geological Observatory, Columbia University, Palisades, NY (1982) 690p.

Calvert, S.E., Accumulation of diatomaceous silica in the sediments of the Gulf of California, Geol. Soc. Am. Bull. 77 (1966) 569-596.

Chen, J., G. Wasserburg, K.L. Von Damm, J.M. Edmond, Lead, uranium and thorium in hot springs on the EPR at 21° N and Guaymas Basin, Gulf of California (1983) manuscript in preparation.

Cline, Joel D., Spectrophotometric determination of hydrogen sulfide in natural waters, Limnol. Ocean. 14 (1969) 454-458.

Coleman, R.G., Ophiolites - ancient oceanic lithosphere?, Springer-Verlag, New York, (1977) 229 pp.

Cooper, J.E. and K.Z. Abedin, The relationship between fixed ammonium-nitrogen and potassium in clays from a deep well on the Texas Gulf Coast, Texas Journal of Science 33 (1981) 103-111.

Cooper, J.E. and W.S. Evans, Ammonium - Nitrogen in Green River formation oil shale, Science 219 (1983) 492-493.

Cooper, J.E. and B.A. Raabe, The effect of thermal gradient on the distribution of nitrogen in shale, Texas Journal of Science 34 (1982) 175-182.

Corliss, J., The origin of metal-bearing submarine hydrothermal solution, Journal of Geophysical Res. 76 (1971) 8128-8138.

Corliss, J.B., J. Dymond, L.I. Gordon, J.M. Edmond, R.P. von Herzen, R.D. Ballard, K. Green, D. Williams, A. Bainbridge, K. Crane, Tj. H. van Andel, Submarine Thermal springs on the Galapagos Rift, Science 203 (1979) 1073-1083.

Craig, H. and J. Lupton, Helium-3 and mantle volatiles in the ocean and the oceanic crust in The Sea, vol. 7, ed. by C. Emiliani, John Wiley and Sons, New York (1981) 391-428.

Crerar, D.A. and H.L. Barnes, Ore solution chemistry V. Solubilities of chalcopyrite and chalcocite assemblages in hydrothermal solutions at 200° to 350°C, Econ. Geol. 71 (1976) 772-794.

Curray, J.R., D.G. Moore et. al., Init. Repts. DSDP, 64: Washington (U.S. Govt. Printing Office) 1982.

CYAMEX SCIENTIFIC TEAM: J. Francheteau, H.D. Needham, P. Choukroune, T. Juteau, M. Seguret, R.D. Ballard, P.J. Fox, W.R. Normark, A. Carranza, D. Cordoba, J. Guerrero, C. Rangin, First manned submersible dives on the East Pacific Rise at 21°N (Project Rita): General Results, Mar. Geophysical Researches 4 (1981) 345-379.

Deer, W.A., R.A. Howie, and J. Zussman, Rock-forming Minerals, Vol. 2 Chain Silicates, Longmans, Green and Co. Ltd., London (1963) 379pp.

Delaney, J.R., D.W. Mogk and M.J. Mottl, Quartz-cemented, sulfide-bearing greenstone breccias from the mid-Atlantic ridge-samples of a high-temperature hydrothermal upflow zone, Science (1983) in press.

Dymond, J., Geochemistry of Nazca plate surface sediments: An evaluation of hydrothermal, biogenic, detrital and hydrogenous sources, in GSA Memoir 154, Nazca Plate: Crustal Formation and Andean Convergence, ed. by L.D. Kulm, J. Dymond, E. Dasch, D. Hussong (1981) 824 pp.

Edmond, J.M., C. Measures, R.E. McDuff, L. Chan, R. Collier, B. Grant, L.I. Gordon and J. Corliss, Ridge crest hydrothermal activity and the balances of the major and minor elements in the ocean: the Galapagos data, Earth Planet. Sci. Lett. 46 (1979a) 1-18.

Edmond, J.M., C. Measures, B. Mangum, B. Grant, F.R. Sclater, R. Collier, A. Hudson, L.I. Gordon and J. Corliss, On the formation of metal-rich deposits at ridge crests, Earth Planet. Sci. Lett. 46 (1979b) 19-30.

Elder, J., Physical processes in geothermal areas in Terrestrial Heat Flow, ed. by W.H.K. Lee, AGU Geophysical Monography 8 (1965) 211-239.

Field, C.W., D.G. Wetherell and E.J. Dasch, Economic appraisal of nazca plate metalliferous sediments, in GSA Memoir 154, Nazca Plate: Crustal Formation and Andean Convergence, ed. by L.D. Kulm, J. Dymond, E. Dasch, D. Hussong (1981) 315-320.

Fournier, R.O., R.J. Rosenbauer, J.L. Bischoff, The solubility of quartz in aqueous sodium chloride solution at 350°C and 180 to 500 bars, Geochim. Cosmochim. Acta 46 (1982) 1975-1978.

Franklin, J.M., J.W. Lydon, and D.R. Sangster, Volcanic-associated massive sulfide deposits, Econ. Geol., 75th Anniversary Vol. (1981) 485-627.

Green, K.E., Geothermal processeses at the Galapagos Spreading Center, M.I.T.-W.H.O.I. unpublished Ph.D. thesis (1980) 226pp.

Goldfarb, M.S., Hydrothermal sulfide deposits on the East Pacific Rise, 21°N, M.I.T. unpublished Ph.D. dissertation (1982) 336 pp.

Hajash, A., Hydrothermal processes along mid-ocean ridges: an experimental investigation, Contrib. Min. Petrol 53 (1975) 205-226.

Hajash, A. and P. Archer, Experimental seawater/basalt interactions: effects of cooling, Contrib. Mineral. Petrol. 75 (1980) 1-13.

Hart, S.R., K, Rb, Cs contents and K/Rb, K/Cs ratios of fresh and altered submarine basalts, Earth Planet. Sci. Lett. 6 (1969) 295-303.

Hart, S.R. and H. Staudigel, The control of alkalies and uranium in seawater by ocean crust alteration., Earth Planet. Sci. Lett. 58 (1982) 202-212.

Hart, S.R., A.J. Erlank and E.J.D. Kable, Sea floor basalt alteration: some chemical and Sr isotopic effects, Contr. Mineral. and Petrol. 44 (1977) 219-230.

Haymon, R.R., Growth history of hydrothermal black smoker chimneys, Nature 301 (1983) 695-698.

Haymon, R.M. and M. Kastner, Descriptive catalog of RISE sulfide samples from the East Pacific Rise, 21°N, Univ. of California, SIO Reference 19-28 (1979).

Haymon, R.M. and M. Kastner, Hot spring deposits on the East Pacific Rise at 21°N: preliminary description of mineralogy and genesis, Earth Planet. Sci. Lett. 53 (1981) 363-381.

Heath, G.R. and J. Dymond, Genesis and transformation of metalliferous sediments from the East Pacific Rise, Bauer Deep, and Central Basin, northwest Nazca plate, Geol. Soc. Am. Bull. 88 (1977) 723-733.

Heier, K.S. and J.A.S. Adams, The geochemistry of the alkali metals, Phys. Chem. Earth 5 (1964) 253-381.

Hekinian, R., M. Fevrier, J.L. Bischoff, P. Picot and W.C. Shanks, Sulfide deposits from the East Pacific Rise near 21°N, Science 207 (1980) 1433-1444.

Honnorez, Jose´, The aging of the oceanic crust at low temperature, in The Sea, vol. 7 ed. by C. Emiliani, John Wiley and Sons, New York (1981) 525-588.

Horowitz, A., The distribution of Pb, Ag, Sn, Tl and Zn in sediments on active oceanic ridges, Mar. Geol. 9 (1970) 241-259.

Hudson, Andrew G., The chemistry of iron and manganese in submarine hydrothermal systems, M.I.T. unpublished M.S. thesis (1980) 80pp.

Humphris, S.E., The hydrothermal alteration of oceanic basalts by seawater, M.I.T.-W.H.O.I. unpublished Ph.D. thesis (1977) 248pp.

Humphris, S.E. and G. Thompson, Hydrothermal alteration of oceanic basalts by seawater, Geochim. Cosmochim. Acta 42 (1978a) 107-125.

Humphris, S.E. and G. Thompson, Trace element mobility during hydrothermal alteration of oceanic basalts, Geochim. Cosmochim. Acta 42 (1978b) 127-136.

Jenkins, W., J. Edmond and J. Corliss, Excess ^{3}He and ^{4}He in Galapagos submarine hydrothermal waters, Nature 272 (1978) 156-158.

Juteau, T., J.P. Eissen, J. Francheteau, D. Needham, P. Choukroune, C. Rangin, M. Seguret, R.D. Ballard, P.J. Fox, W.R. Normark, A. Carranza, D. Cordoba, J. Guerrero (CYAMEX Scientific Team) Homogeneous basalts from the East Pacific Rise at 21°N: steady state magma reservoirs at moderately fast spreading centers, Oceanol. Acta 3 (1980) 487-503.

Kastner, M., Evidence for two distinct hydrothermal systems in the Guaymas Basin. In Curray, J.R., Moore, D.G. et. al., Init. Repts. DSDP 64 Pt. 2: Washington (U.S. Gov't Printing Office), 1143-1157.

Kay, R.W. and N. Hubbard, Trace elements in ocean ridge basalts, Earth Planet. Sci. Lett. 38 (1978) 95-116.

Kelts, K.R., (1982) Petrology of hydrothermally metamorphosed sediments at Deep Sea Drilling Site 477, southern Guaymas Basin rift, Gulf of California. In Curray, J.R., Moore, D.G., et. al., Init. Repts. DSDP 64, Pt. 2: Washington (U.S. Govt. Printing Office) 1123-1136.

Kennedy, G.C., A portion of the system silica-water, Econ. Geol. 45 (1950) 629-653.

Kerridge, J., R.M. Haymon and M. Kastner, Sulfur isotope systematics at the 21° N site, East Pacific Rise (1983) submitted EPSL.

Klinkhammer, G., M. Bender and R. Weiss, Hydrothermal Mn in the Galapagos Rift, Nature 269 (1977) 319-320.

Kurz, M.D., Helium isotope geochemistry of oceanic volcanic rocks: implications for mantle heterogeneity and degassing, M.I.T.-W.H.O.I. unpublished Ph.D. thesis (1982) 290pp.

Larson, R.L., Near-bottom geologic studies of the East Pacific Rise crest, Geol. Soc. Am. Bull. 82 (1971) 823-841.

Lawver, L.A., D.L. Williams and R.P. Von Herzen, A major geothermal anomaly in the Gulf of California, Nature 257 (1975) 23-28.

Lawver, L.A. and D.L. Williams, Heat flow in the central Gulf of California, Journal Geophysical Res. 84 (1979) 3465-3478.

Lebel, J. and A. Poisson, Potentiometric determination of Ca and Mg in seawater, Mar. Chem. 4 (1976) 321-332.

Liberti, A. and M. Mascini, Anion Determination with ion selective electrodes using Gran's plot: application to fluoride, Analytical Chemistry 41 (1969) 676-678.

Lister, C.R.B., "Active" and "passive" hydrothermal systems in the oceanic crust: predicted physical conditions, in The Dynamic Environment of the Ocean Floor, ed. by K.A. Fanning and F.T. Manheim, Lexington Books, Lexington, Mass. (1982) 441-470.

Lonsdale, P., R. Batiza and T. Simkin, Metallogenesis at seamounts on the East Pacific Rise, Marine Technology Society Journal 16 (1982) 54-61.

Lonsdale, P.F., J.L. Bischoff, V.M. Burns, M. Kastner and R.E. Sweeney, A high-temperature hydrothermal deposit on the seabed at a Gulf of California Spreading Center, Earth Planet. Sci. Lett. 49 (1980) 8-20.

Lupton, J.E., Helium-3 in the Guaymas Basin: evidence for injection of mantle volatiles in the Gulf of California, Journal Geophysical Research 84 (1979) 7446-7452.

Lupton, J. and H. Craig, A major helium-3 source at 15°S on the East Pacific Rise, Science 214 (1981) 13-18.

McDuff, R.E. and J.M. Edmond, On the fate of sulfate during hydrothermal circulation at mid-ocean ridges, Earth Planet. Sci. Lett. 57 (1982) 117-132.

Makrides, A.C., M.J. Turner, W.W. Harvey, J. Slaughter, S.B. Brunner, P.O.D. Offenhartz, G.F. Pearson, Study of silica scaling from geothermal brines, Final Report for 15 Nov. 74 - 30 Apr. 74 EIC Corp., prepared for U.S. Dept. of Energy cob-2607-5, January 1978, 72pp.

Malahoff, A., A comparison of the massive submarine polymetallic sulfides of the Galapagos Rift with some continental deposits, Marine Technology Society Journal 16 (1982) 39-45.

Measures, C.I. and J.D. Burton, Gas chromatographic method for the determination of selenite and total selenium in seawater, Analytica Chimica Acta 120 (1980) 177-186.

Measures, C.I. and J.M. Edmond, Beryllium in the water column of the central North Pacific, Nature 297 (1982) 51-53.

Measures, C.I. and J.M. Edmond, The geochemical cycle of beryllium-9: a reconnaissance, Earth Planet. Sci. Lett. (1983) in press.

Michard, G., A. Michard, F. Albarede, J.F. Minster and J.L. Charlou, The chemistry and $^{87}Sr/^{86}Sr$ ratios of the hydrothermal vent waters at 13°N (East Pacific Rise) EOS 63 (1982) 1014.

Michard, A., F. Albarede, G. Michard, J.F. Minster and J.L. Charlou, REE and U in high temperature solutions from the EPR 13°N hydrothermal vent field, Nature 303 (1983) 795-797.

Moore, J.G., W.R. Normark, G.R. Hess and C.E. Meyer, Petrology of basalt from the East Pacific Rise near 21° north latitude, J. Res. U.S. Geol. Survey 5 (1977) 753-759.

Mottl, M., Metabasalts, axial hot springs, and the structure of hydrothermal systems at mid-ocean ridges, Geol. Soc. Am. Bull. 94 (1983) 161-180.

Mottl, M. and H. Holland, Chemical exchange during hydrothermal alteration of basalt by seawater - I. Experimental results for major and minor components of seawater, Geochim. Cosmochim. Acta 42 (1978) 1103-1115.

Mottl, M., H. Holland, and R. Corr, Chemical exchange during hydrothermal alteration of basalt by seawater - II. Experimental results for Fe, Mn and sulfur species, Geochim. Cosmochim. Acta 43 (1979) 869-884.

Niemitz, J., Geochemistry of sediments, Leg 64, Gulf of California. In Curray, J.R., Moore, D.G. et. al., Init. Repts. DSDP 64 Pt. 2: Washington (U.S. Gov't Printing Office), 695-716.

Nokleberg, W.J. and G.R. Winkler, Stratiform zinc-lead deposits in the Drenchwater Creek area, Howard Pass quadrangle, northwestern Brooks Range, Alaska, USGS Professional Paper 1209 (U.S. Gov't Printing Office) 1982, 22pp.

Normark, W.R., J.E. Lupton, J.W. Murray, R.A. Koski, D.A. Clague, J.L. Morton, J.R. Delaney, H.P. Johnson, Polymetallic sulfide deposits and water-column tracers of active hydrothermal vents on the southern Juan de Fuca ridge, Marine Technology Society Journal 16 (1982) 46-53.

Ohmoto, H. and R.O. Rye, Hydrogen and oxygen isotopic compositions of fluid inclusions in the Kuroko deposits, Japan, Econ. Geol. 69 (1974) 947-953.

Oudin, E., Etudes mineralogique et geochimique des depots sulfures sous-marins actuels de la ride est - pacifique (21°N) Documents du BRGM #25 (1981) 241 pp.

Oudin, E., Hydrothermal sulfide deposits of the East Pacific Rise (21°N) part I: descriptive mineralogy, Marine Mining 4 (1983) 39-72.

Piper, D.Z., Origin of metalliferous sediments from the East Pacific Rise, Earth Planet. Sci. Lett. 19 (1973) 75-82.

Quinby-Hunt, M.S. and K.K. Turekian, Distribution of elements in sea water, EOS 16 (1983) 130-131.

Riedesel, M., J.A. Orcutt, K.C. Macdonald, J.S. McClain, Microearthquakes in the black smoker hydrothermal field, East Pacific Rise at 21°N, Journal of Geophysical Research 87 (1982) 10613-10623.

Riley, J.P. and G. Skirrow (editors) Chemical Oceanography, vol. 1, Academic Press, New York (1965) 712 pp.

RISE Project Group, East Pacific Rise: Hot springs and geophysical experiments, Science 207 (1980) 1421-1433.

Seyfried, W. and J. Bischoff, Hydrothermal transport of heavy metals by seawater: the role of seawater/basalt ratio, Earth Planet. Sci. Lett. 34 (1977) 71-77.

Seyfried, W. and W. Dibble, Seawater-peridotite interaction at 300°C and 500 bars: implications for the origin of oceanic serpentinites, Geochim. Cosmochim. Acta 44 (1980) 309-321.

Seyfried, W. and M. Mottl, Origin of submarine metal-rich hydrothermal solutions: experimental basalt-seawater interaction in a seawater dominated system at 300°C 500 bars in Proceedings of the Second International Symposium on Water-Rock Interaction, ed. by Paquet and Tardy, Strasbourg, France (1977) IV 173-IV 180.

Seyfried, W. and M. Mottl, Hydrothermal alteration of basalt by seawater under seawater-dominated conditions, Geochim. Cosmochim. Acta 46 (1982) 985-1002.

Shanks, W.C. III, J.L. Bischoff and R.J. Rosenbauer, Seawater sulfate reduction and sulfur isotope fractionation in basaltic systems: interaction of seawater with fayalite and magnetite at 200-350°C, Geochim. Cosmochim. Acta 45 (1981) 1977-1995.

Shanks, W.C. and J. Niemitz, 1982, Sulfur isotope studies of hydrothermal anhydrite and pyrite, Deep Sea Drilling Project Leg 64, Guaymas Basin, Gulf of California. In Curray, J.R. Moore, D.G., et.al., Init. Repts. DSDP 64, Pt. 2: Washington (U.S. Gov't Printing Office), 1137-1142.

Simoneit, B.R.T., Hydrothermal petroleum sampled by DSRV Alvin in Gulf of California, EOS 63 (1982) 1015.

Simoneit, B.R.T. and O.E. Kawka, Hydrothermal petroleum from diatomites in the Gulf of California, in Marine Petroleum Source Rock Conference, the Royal Society, London (1983) in press.

Simoneit, B.R.T. and P.F. Lonsdale, Hydrothermal petroleum in mineralized mounds at the seabed of Guaymas Basin, Nature 295 (1982) 198-202.

Sleep, N.H., J.L. Morton, L.E. Burns and T.J. Wolery, Geophysical constraints on the volume of hydrothermal flow at ridge axes, in NATO-ARI volume Hydrothermal Processes at Seafloor Spreading Centers, ed. by P.A. Rona, Plenum Press (1983) in press.

Sleep, N.H. and T.J. Wolery, Egress of hot water from midocean ridge hydrothermal systems: some thermal constraints, J. Geophys. Res. 83 (1978) 5913-5922.

Solorzano, L., Determination of ammonia in natural waters by the phenolhypochlorite method, Limnol. Ocean. 14 (1969) 799-801.

Stein, V.B., E. Canelli and A.H. Richards, Determination of arsenic in potable, fresh and estuarine water by flameless atomic absorption, Atomic Spectroscopy, 1 (1980) 133-137.

Stookey, L.L., Ferrozine: A new spectrophotometric reagent for iron, Analytical Chemistry 42 (1970) 779-781.

Strickland, J.D.H. and T.R. Parsons, A Practical Handbook of Seawater Analysis, Fisheries Research Board of Canada, Bulletin 167, Ottawa (1968) 311pp.

Styrt, M.M., A.J. Brackmann, H.D. Holland, B.C. Clark, V. Pisutha-Arnond, C.S. Eldridge and H. Ohmoto, The mineralogy and the isotopic composition of sulfur in hydrothermal sulfide/sulfate deposits on the East Pacific Rise, 21°N latitude, Earth Planet. Sci. Lett. 53 (1981) 382-390.

Uchida, H., Y. Shimoishi and K. Toei, Gas chromatographic determination of selenium (-II,0), -(IV), and -(VI) in natural waters, Environ. Sci. Technol. 14 (1980) 541-544.

van Andel, Tj.H., Recent marine sediments of Gulf of California, in Marine Geology of the Gulf of California, ed. by Tj.H. van Andel and G.G. Shorr, Am. Assoc. Pet. Geol. Mem. 3 (1964) 216-310.

Warner, T.B., Electrode determination of fluoride in ill-characterized natural waters, Water Research 5 (1971) 459-465.

Wedepohl, K.H., Handbook of Geochemistry, Springer-Verlag, New York, 1969.

Weiss, R.F., Hydrothermal manganese in the deep sea: scavenging residence time and $Mn/^3He$ relationahips, Earth Planet. Sci. Lett. 37 (1977) 257-262.

Welhan, J.A. and H. Craig, Methane, hydrogen and helium in hydrothermal fluids at 21°N on the East Pacific Rise in NATO-ARI volume, Hydrothermal Processes at Seafloor Spreading Centers, ed. by P.A. Rona, Plenum Press (1983) in press.

Williams, D.L., Heat loss and hydrothermal circulation due to sea-floor spreading, M.I.T.-W.H.O.I. unpublished Ph.D. thesis (1974) 139 pp.

Williams, D.L., K. Becker, L.A. Lawver and R.P. Von Herzen, Heat flow at the spreading centers of the Guaymas Basin, Gulf of California, Journal of Geophysical Research 84 (1979) 6757-6769.

Wolery, T. and N. Sleep, Hydrothermal circulation and geochemical flux at mid-ocean ridges, Journal of Geophysical Research 84 (1976) 249-275.

APPENDIX 1 - Sample Collection and Treatment

Sample Collection

The samples discussed in this thesis were collected primarily on two cruises: Pluto IV in November 1981 on the R/V Melville with the DSR/V Alvin / R/V Lulu to 21° N and Pluto VI in December 1981-January 1982 on the R/V E.B. Scripps with the DSR/V Alvin / R/V Lulu to Guaymas Basin. Occasional reference is made to samples collected in November 1979 on the R/V Gilliss with the DSR/V Alvin / R/V Lulu to 21° N.

The 1979 cruise utilized samplers developed by J. Archuleta for the Los Alamos Hot Dry Rock project. These were stainless steel bottles of approximately 750 ml capacity which had been gold plated on the inside. They were evacuated prior to deployment and had to be rigidly mounted on the basket of the submersible. Therefore the entire submersible had to be manuevered to position their small (1/4") inlet valves into the hot water, making sampling extremely difficult. In a series of five dives fourteen samples were collected all of which were mixtures of ambient seawater and hydrothermal solution with only two of the samples containing greater than 50% hydrothermal solution.

Based on the sampling experience gained in the 1979 dives new samplers were developed for the 1981 dives at 21° N and were used again at Guaymas. The samplers were designed by Barrie Walden of the Alvin Group at Woods Hole. The sampler is basically of a syringe type. The piston is held forward in the bottle by a spring and held in place by a pin. There is an actuator on the hydraulic arm which when activated from inside the submarine presses on the inlet valve assembly, releasing the pin and allowing a second spring to pull the piston back, allowing the sampler to

fill. The inlet valve assembly is designed so that it and the snorkel may be flushed with hydrothermal solution before the valve to the sampling chamber is opened. There are vent holes on the top of the inlet valve assembly and hydrothermal fluid could be seen venting from these, assuring that the snorkel and valve were indeed flushed. Venting was allowed to continue for 1-2 minutes before the actuator was activated, opening the bottle. The bottles themselves took approximately one minute to fill and were closed once the piston stem and outside spring were observed to have stopped moving. The samplers consist of two titanium bottles each of 755 ml volume joined by a T-handle so they can be picked up and placed in the vents by Alvin's hydraulic arm. This made sampling considerably easier as the whole submarine did not have to be navigated so close to the vent; only the arm with the attached sampler needed to be manuevered into the vent. Once sampling was completed the sampler was returned to the basket on the front of Alvin and the arm was free to perform other tasks. A long titanium "snorkel" was placed on the inlet valves to the bottles so that the sample could be taken from within the vent orifice before it mixed with ambient seawater. Figure A1-1 is a picture of the sampler.

The tandem sampler was designed to avoid the problems encountered in the 1979 samples. On that cruise water from individual samplers was divided between investigators from M.I.T., S.I.O. and O.S.U. The samples also contained particles which had a large proportion of the iron and copper in them. When it came time to reconstruct the solution composition the particles caused severe budgetary problems as it was not known whether to calculate them on the total volume of the sampler or just from the volume remaining after the S.I.O. and O.S.U. splits were removed. Some of the particles seemed to be completely extraneous and looked like pieces of

a

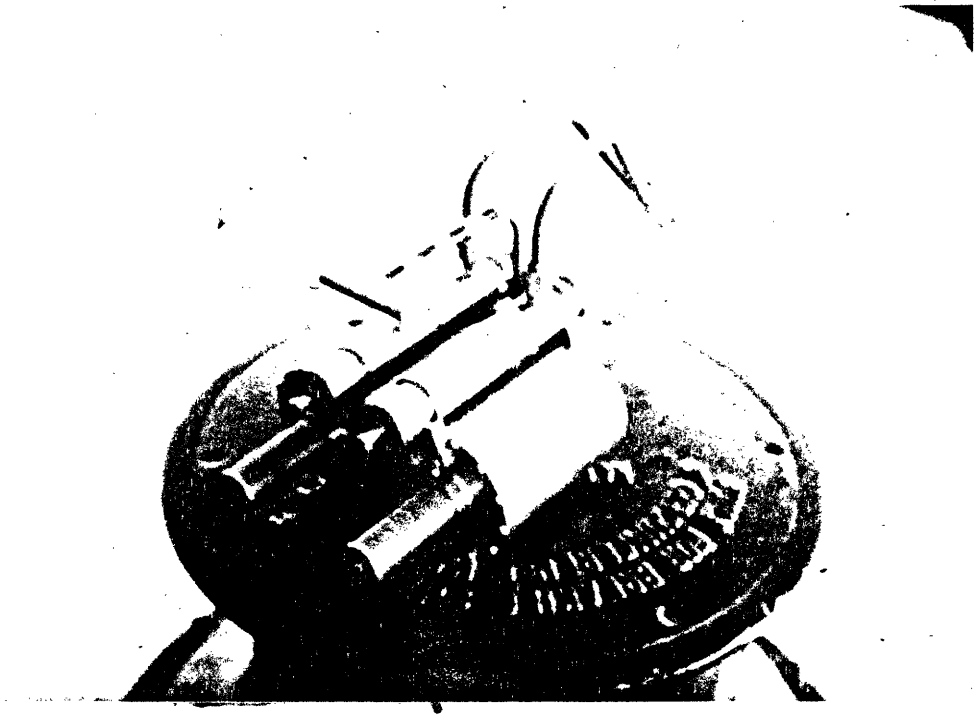

b

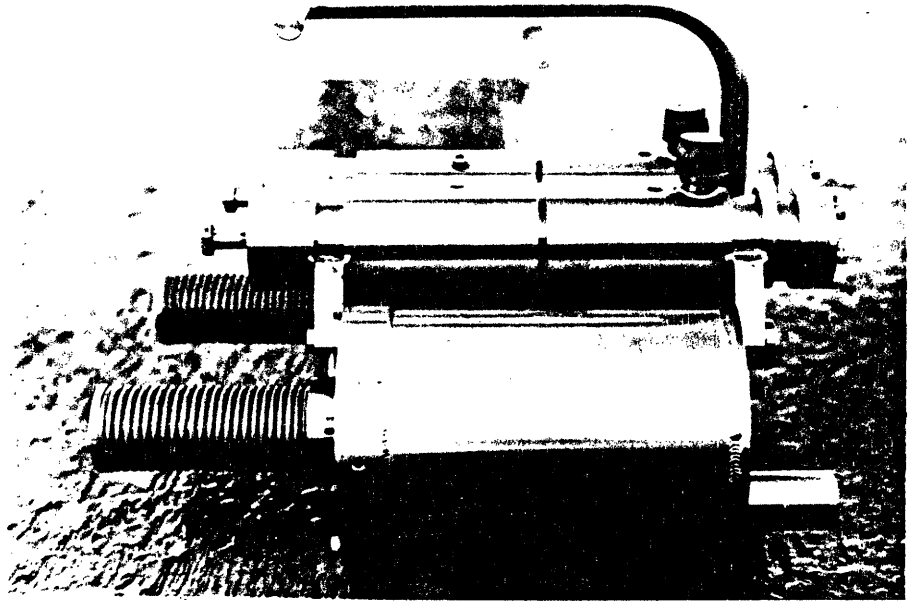

Figure A1-1: The titanium water sampler. The barrel is 6 inches long.
a. with snorkel.
b. side view.

chimney which had been cored during sampling. The tandem design used in 1981 allowed one sampler to go to the M.I.T. group and one sampler to go to the S.I.O. group.

The snorkel consisted of two 1/2" titanium tubes -one leading to each bottle - hose clamped together so that they could be placed into the vent as a unit; the hope being that they would take identical samples. In practice there was still some difficulty in getting the snorkel into the chimney orifice, which is on the scale of centimeters in diameter. The snorkels sometimes cored the chimney resulting in pieces of chimney, up to several millimeters, being found inside the sample bottles and inlet valves when they were disassembled for cleaning. In general, when the snorkel could be well placed into the chimney both samples contain very little seawater and, compositionally, are very close to each other. When the snorkel was not well placed, one sample often contains a much larger proportion of seawater than the other resulting in different compositions.

The bottles were not evacuated and have a 3.8 ml (0.05%) dead volume. This dead volume had to be filled with water to prevent air from being included in the sample and to prevent the breakout force between the front of the piston and inner front plate of the bottle from becoming too great. Surface seawater was used to fill this dead volume for a variety of reasons and also was readily available in large amounts. Due to the dead volume every hydrothermal sample contains at least 3.8 mls of seawater. It should be noted that if the piston was not correctly seated, due to its large surface area, an increase of 1 mm in its distance from the front plate would increase the dead volume by 7.9 mls.

The materials for the sampler construction were of major concern since they must be able to withstand 350° C temperatures and the corrosiveness of

pH=3.5 solutions, as well as be rugged enough to withstand the trip in the submarine basket. Since a primary interest was to measure the metals iron, copper and zinc the material also needed to be relatively clean; stainless steel was not acceptable. The material used was titanium, which to-date has not caused any measurable contamination. Another difficult problem was what material to use for the seals. A seal was needed on the piston to prevent solution from leaking behind it but this material also needed to deform enough to slide and withstand high temperatures. A teflon omniring was employed here and in one location on the inlet valve (where there is another metal-metal seal as well). We thought, and later found to be true, that because the sampler was immersed in 2° C ambient seawater it would cool rapidly and the seals would not be heated to a full 350° C. The teflon seals, rated to below 300° C, showed no heat damage even after repeated use. A red silicon o-ring (rated to below 200° C) inside the front plate also showed no visible heat damage.

A problem was encountered with the samplers when the Guaymas solutions were sampled. These solutions contain a large amount of gas which apparently exsolved from the solutions as the pressure decreased during the ascent of the submarine. This pressure increase in the bottle apparently forced the inlet valve open causing solution and gas to leak from the samplers. When the samplers were opened on ship, they did not contain the full volume of water (one sampler contained only approximately 80 mls out of a possible 755). This loss of water and gas should not be a problem for the species reported here (except possibly H_2S), as the water in the samplers should be well mixed. It is however a serious problem for determining the gas concentrations.

Sample Treatment

Due to the length of a dive and the time involved in the recovery of the submersible, the transfer of samplers and personnel to the escort ship and the time actually needed to process the samplers, our samples may have sat for a maximum of twelve hours in the sampling bottles. Our actual "sample draw" was relatively quick, requiring only fifteen minutes per sampler. The gas extraction of the S.I.O. samplers was somewhat slower and our subsamples from these may have sat in the samplers for up to 18 hours.

The sample itself was divided into several aliquots shipboard at the time of the draw. A major consideration was to keep the shipboard draw small - <10% of the total volume to go into splits and the remainder to go into a one liter bottle. This was to avoid the budgetary problems encountered in the 1979 samples. If less than 10% were drawn then any particles which might form in these fractions should also be less than or equal to 10% of the total. Since many of the elements which might be in the precipitates are analyzed by GFAAS, with an analytical precision of around 10%, the loss of these particles would be on the order of the measurement precision and would not be important in the budgetary calculations.

The shipboard draw proceeded as follows:

1. 100-200 mls of the sample were drawn into the one liter bottle to flush out the tygon tubing and valves used to draw the sample. This was to purge any oxygen out of the line as it can affect the measurements done on the next few aliquots.
2. 3 mls were drawn into a cutoff N_2 purged testtube which was capped with no headspace (to prevent H_2S oxidation) for the pH

measurement.

3. 30 mls were drawn into a N_2 purged 25 ml erlenmeyer flask which was capped with no headspace for the alkalinity determination.
4. 6 mls were drawn into a N_2 purged weighing vial and capped with a ground glass stopper (again with no headspace) for the H_2S determination.
5. 10 mls were drawn into a N_2 purged ampoule which contained bromine for a total sulfur measurement.
6. 15-20 mls were drawn into a 20 ml glass scintillation vial and acidified with 100 µl 6 N HCl for nutrient analyses.
7. The remainder of the sample was then drawn into the one liter bottle.

At the end of the draw it was noted whether a gas phase seemed to be present. At 21° N in most cases it was estimated to be just a few milliliters. It was confirmed that the gas phase (if any) was quantitatively small by adding together the volumes of the different aliquots and comparing to the sampler volume. As mentioned above, at Guaymas a gas phase often comprised a significant proportion of the sample.

The pH, alkalinity and H_2S were measured shipboard as soon as possible. Extra water remaining from the pH or alkalinity measurements was used for the silica analysis. The nutrient vials were stirred under an N_2 atmosphere to expel H_2S which interferes with the nutrient analyses, and then capped.

The one liter bottles were acidified immediately with double distilled 6 N HCl. The samples which contained very little admixed seawater (<5%) were colorless to slightly yellow. Samples which contained more seawater

were grey in color due to the presence of extremely fine precipitate. When these samples were acidified, the precipitate redissolved and the solutions became colorless to very light grey in color. The solutions were acidified at the rate of 1 ml of acid to 250 mls of sample, resulting in a final pH ≅ 1.6.

Upon their return to the lab the bulk samples were filtered to remove any particles which had not dissolved. All of the analyses were then done on the filtered samples. The particles from this filtration were then digested in 8 N HNO_3 and bromine.

Particles

Particles present a major problem in these hydrothermal solutions. The particles may be either a precipitate from the solutions in the samplers or may be from the chimney or "sediment" which was "cored" by the snorkel during sampling. I believe the second is the source of most of the particles found in the samplers for several reasons. First, often the particles are several millimeters in diameter, the largest of which would fit through the inlet valve. (The presence of a Pompeii worm in one of the samples is evidence that material of this size can pass through the inlet valve.) Particles of this large size seem unlikely to have precipitated inside the sampler. In several samplers large particles were also found inside the inlet valve assembly when the samplers were disassembled for cleaning. Secondly, many of the very good samples (>95% hydrothermal solution) were colorless and contained no visible particles. The samplers which contain more entrained seawater, implying that they were difficult to deploy and may well have cored into the chimney, contain more particles.

A potential problem comes from the immediate acidification of the one

liter bottle. In addition to preventing precipitation and causing redissolution of (presumably) fresh precipitates (as evidenced by the color change from dark to light grey or colorless), it may have caused the dissolution of entrained particles that do not belong in the solution. The best argument against this comes from the solution chemistry. Entrainment of particles would be a random process, and if these particles were quantitatively important this should be reflected by a large scatter in the solution composition for these elements. The very mixed samples do not fall along a mixing line (often scattering high), indicating that entrainment of particles may be important. For those samples with Mg <5 mmoles/kg the agreement between samples within vent areas is quite good, indicating that "foreign" particle dissolution is not a significant problem. That any remaining resistant particles are quantitatively unimportant was verified by measuring the digestions of the particles filtered from solution (Table A1-1). The amount of, for example iron, found in these particles was insignificant compared to that in the solution.

A second group of particles is those which were found in the bottom of the sampler once it was disassembled for cleaning. These particles were found in some, but not all of the samplers. They tended to be large, several millimeters in size and are believed to be the result of coring as discussed earlier. This group of particles was not analyzed.

Table A1-1: Particle Digestion Analyses

Sample	Area	Element	Wt Part Soln(g)	Conc Part Soln(μM)	Normalized Part Conc (μM/kg)	Soln Comp (μM/kg)	Σ Part + Soln (μM/kg)
CDW Blank		Fe	42.34	0.06	0.004	0	0
		Cu		0	0	0	0
		Zn		0.05	0.003	0	0
21° NORTH							
1153-7	Amb	Fe	56.61	3.8	0.3	0	0.3
		Cu		0	0	0	0
		Zn		1.0	0.07	0.4	0.5
1149-7	SW	Fe	60.11	43	3.4	736	739
		Cu		11	0.9	7.7	8.6
		Zn		29	2.3	74	76
1150-11	SW	Fe	49.38	71	4.6	760	765
		Cu		26	1.7	11	13
		Zn		114	7.5	99	106
1155-1	NGS	Fe	48.26	25	1.6	854	856
		Cu		12	0.8	0	0.8
		Zn		58	3.7	40	44
1155-18	NGS	Fe	48.97	29	1.9	856	858
		Cu		13	0.9	0	0.9
		Zn		87	5.6	39	45
1158-11	OBS	Fe	44.38	115	6.7	1679	1686
		Cu		68	4.0	44	48
		Zn		125	7.3	112	119
1158-16	OBS	Fe	50.41	119	8.0	1697	1705
		Cu		79	5.2	43	48
		Zn		112	7.4	114	121
1160-6	HG	Fe	51.53	116	8.0	2452	2460
		Cu		67	4.6	36	40
		Zn		186	13	99	112
1160-16	HG	Fe	55.19	154	11	2397	2408
		Cu		79	5.7	46	52
		Zn		100	7.3	107	114
GUAYMAS							
1173-6	2	Fe	52.80	56	7.2	50	57
		Cu		12	1.5	0	1.5
		Zn		1.2	0.15	1.0	1.1
1175-16	3	Fe	50.54	262	27	173	200
		Cu		21	2.2	1.1	3.3
		Zn		50	5.1	36	41
1177-6	4	Fe	48.35	41	10	79	89
		Cu		25	6.1	0.1	6.2
		Zn		5.2	1.3	19	20
1177-13	4	Fe	47.26	29	9.0	79	88
		Cu				0.2	
		Zn		0.5	0.16	19	19

APPENDIX 2 - Analytical Methods

The measured species are listed in Table A2-1 along with the method used for the determination. This appendix is organized according to the method used: potentiometry, colorimetry, ion chromatography, gas chromatography, flame atomic absorption spectrophotometry or graphite furnace atomic absorption spectrophotometry. Shipboard analyses are specifically noted.

Potentiometric

The species H^+ (as pH), chloride, and fluoride and calcium-magnesium (in the 1979 samples) were determined by a variety of potentiometric and titration methods.

pH: pH was determined using a Corning Model 130 pH Meter with an Altex (Beckman) Futura™ glass combination pH electrode. All pH measurements were done shipboard at room temperature. The electrode was calibrated with pH=4, 7 and 10 buffers before, and usually after, the pH in the samples was measured. (All measurements were taken in millivolts.) The pH measurements were made immediately. It was one of the first aliquots taken during the draw and was often measured while the draw continued. As the samples contain millimolar levels of H_2S, the oxidation of which will lower the pH, it was important to keep air out of the sample. It was drawn into a nitrogen purged cut off testtube (volume ≅ 3 mls) containing a small magnetic stir bar and capped by displacing some of the solution (i.e. no headspace). A Nalgene hollow plastic stopper with the bottom cut out was slipped over the electrode and provided a tight seal when the electrode was placed in the solution. The electrode occupied a

Table A2-1: Analytical Determinations and Methods

Element	Method
H^+ (pH)	Potentiometric
Li	Flame atomic absorption spectrophotometry
Na	Flame atomic absorption spectrophotometry
K	Flame atomic absorption spectrophotometry
Rb	Flame atomic absorption spectrophotometry
Be	Gas chromatography
Mg	Flame atomic absorption spectrophotometry & Potentiometric
Ca	Flame atomic absorption spectrophotometry & Potentiometric
Sr	Flame atomic absorption spectrophotometry
Ba	Graphite furnace atomic absorption spectrophotometry
Mn	Colorimetric
Fe	Colorimetric
Co	Graphite furnace atomic absorption spectrophotometry
Ni	Graphite furnace atomic absorption spectrophotometry
Cu	Flame & graphite furnace atomic absorption spectrophotometry
Ag	Graphite furnace atomic absorption spectrophotometry
Zn	Flame atomic absorption spectrophotometry
Cd	Graphite furnace atomic absorption spectrophotometry
Pb	Graphite furnace atomic absorption spectrophotometry
Al	Graphite furnace atomic absorption spectrophotometry
$Alkalinity_t$	Potentiometric
Si	Colorimetric
NH_3	Colorimetric
NO_2	Colorimetric
PO_4	Colorimetric
$S:SO_4$	Ion Chromatography
H_2S	Colorimetric
Σ S	Ion Chromatography
As	Graphite furnace atomic absorption spectrophotometry
Se	Gas chromatography
F	Potentiometric - specific ion electrode
Cl	Potentiometric

large volume of the tube, thus solution was displaced and no headspace was present. The solution was stirred until a stable reading was achieved (at most a few minutes). On a few samples where air was entrained a rapid drop in the pH was observed.

Alkalinity: Alkalinity was determined shipboard using the same electrode and pH meter as above. A Gilmont 2.5 ml total volume microburette with a metal body and a glass plunger was used to add the acid. The measurement was done on a 20 ml aliquot (dispensed from a glass pipet) under a nitrogen atmosphere to prevent H_2S oxidation which would lower the alkalinity. For the Guaymas samples the acid was nominally 1 N HCl while for 21° N the concentration was nominally 0.1 N. A Gran plot method was used to determine the endpoint. All alkalinities measured are total alkalinities. The error on the 21° N alkalinities is, except in a very few cases better than $\pm$10 ueq/liter. For very low alkalinities this results in a precision of $\pm$5% while for the higher alkalinities the error is a few tenths of a percent. The precision for the Guaymas samples is better than $\pm$0.4 %.

Chloride: Chloride was determined using a potentiometric method based on the silver nitrate titration and is the method used by Gieskes (personal communication). Essentially the method makes use of a bucking potential created by a 1.5 V battery and a potentiometer. A silver wire is implanted in a microburette containing the $AgNO_3$ solution. Another silver wire is placed in the beaker containing the sample solution and silver ions therefore creating a $Ag_{(s)}|Ag^+[(titrant)\text{-}Cl^-(soln)]||Ag^+(titrant)|Ag_{(s)}$ cell and the potentiometer is used to match the potential in the cell. A series of additions of $AgNO_3$ is made and the endpoint is the largest jump in potential which occurs for a given addition size. APSO seawater is

used to standardize the $AgNO_3$ titrant. 0.5 ml of sample are needed per determination and the precision is ±0.05%.

Fluoride: Fluoride was determined only on the samples collected in 1979. The pH meter mentioned above was used in conjunction with an Orion specific ion electrode and single reference electrode. The method of Warner (1971) was used, but was modified so that the Gran plot method could be used (Liberti and Mascini, 1969). Analytical precision is ±5%.

Calcium-Magnesium: In the 1979 samples calcium and magnesium were determined by titration with EDTA and EGTA (Lebel and Poisson, 1976). The sum of Mg+Ca+Sr present is measured by the EDTA titration, using a potentiometric endpoint. Calcium alone is determined by the EGTA titration using GHA (Gloxal-bis (2-hydroxyanil)) as the indicator for a colorimetric endpoint. Analytical precision is ±0.2%.

Colorimetric

Manganese, iron, silica, hydrogen sulfide, ammonium, phosphate and nitrite were determined colorimetrically. A Perkin Elmer Model 55 Spectrophotometer was used in conjunction with either a 1 cm flow cell and "sipper system" or a 4 cm (~3 ml volume) cell (both cells are quartz). The Guaymas H_2S analyses were analyzed on a Gilford spectrophotometer with a 1 cm flow cell and sipper system.

Manganese: Manganese was determined by the formaldoxime method (Brewer and Spencer, 1971) which is specific for Mn^{2+}, the form in which it should be present in these samples. The level of iron interference found by Hudson (1980) in similar solutions would be <1% of the manganese signal at the dilutions at which these samples were analyzed. No correction was made for an iron interference at this level. Those samples with Mn >100

µmoles/kg were measured in a 1 cm cell with an analytical precision ≅0.5 % and a detection limit of ~20 µmoles/kg. Samples with Mn <100 µmoles/kg were measured in a 4 cm cell with an analytical precision ≅2% and a detection limit ≅1 µmole/kg.

Iron: Iron was determined by the ferrozine method (Stookey, 1970) which is specific for Fe^{2+}. The method was used with the modification of Hudson (1980) where the hydroxylamine hydrochloride reduction of Fe(III) to Fe(II) is done by heating in a 60° C oven rather than boiling. The method was further modified by heating the samples for at least one hour and often longer (no difference was noted with increased time) in capped vials. Since everything was done volumetrically with Eppendorf or Finn pipets and a repipet and the vials capped, the final volumes did not have to be adjusted for variable loss during heating. Samples with Fe >50 µmoles/kg were measured in a 1 cm cell with an analytical precision of <1% and a detection limit of ~20 µmoles/kg. Samples with Fe <50 µmoles/kg were measured in a 4 cm cell with an analytical precision ≅2 % and a detection limit of 3 µmoles/kg.

Silica: Silica was measured by the silicomolybdate method (Strickland and Parsons, 1968). At 21° N all of the samples were diluted to <66 µmoles/kg (to keep the absorbance below 0.75 absorbance units). The samples were also acidified with distilled 6 N HCl to pH~1.6 to slow the polymerization of silica as this method will measure only the monomeric and dimeric forms. At 21° N the measurements were made shipboard. At Guaymas lack of time precluded measuring SiO_2 shipboard. From the 1979 and 1981 21° N cruises we found that polymerization of silica to longer than the dimeric form was very slow in our alkalinity aliquots, which we had titrated shipboard and then brought home stored in plastic. The alkalinity

samples are acidified to pH~3, which is the pH at which polymerization is the slowest (Makrides et al., 1978). The Guaymas alkalinities were measured for silica very shortly after the cruise. Analytical precision is around ±1%.

Hydrogen Sulfide: Hydrogen sulfide was determined by the method of Cline (1969), modified so that it could be used at millimolar levels. The standards were prepared from $Na_2S \cdot 9H_2O$ dissolved in Corning distilled water which had been boiled and bubbled with N_2. They were usually kept in glass volumetrics or bottles that were close to full (small headspace) filled with nitrogen and sealed with greased glass stoppers. Under these conditions the standards were stable for at least one week and they were standardized almost daily iodometrically. A more concentrated reagent (maintaining the same diamine:ferric ratio) was prepared to extend the workable range up to 10 mmoles/kg. This is a colorimetric method which can be diluted after the color develops. The samples were diluted with nitrogen bubbled surface seawater to bring the absorbances into the linear range. Some of the samples were analyzed in duplicate but most were done in triplicate. The agreement between replicates is in most cases better than ±5%. A 1 cm cell was used resulting in a detection limit of 3 µmoles/kg. All of these analyses were done shipboard.

Ammonium: Ammonium was analyzed by the method of Solozano (1979), as modified by Gieskes (personal communication). The best reproducibility and lowest blank was achieved by adding all three reagents to each sample in quick succession, before proceeding to the next sample. The presence of H_2S prevents color development. This problem was avoided by acidifying and stirring the samples under a N_2 atmosphere before analysis. An additional problem arises from the elevated levels of calcium present in the

hydrothermal solutions, which due to the high pH of the reaction causes the precipitation of $Ca(OH)_2$. To avoid this problem all samples were diluted by at least a factor of two, bringing the calcium level down to the seawater level in all cases. For the reaction to proceed a pH=9.8 is needed and for the 21° N samples this required neutralization with sodium hydroxide. The 21° N samples were run shipboard. The Guaymas samples were run in the lab 1 year after collection. During that time they were stored acidified in glass, tightly capped vials. They contained high levels of ammonia requiring a large dilution factor (~200 times), obviating the need for neutralization. The Guaymas samples have a precision of better than ±3%. A signal was barely discernible in the 21° N samples. The blank, seawater, which had been treated exactly as the samples (acidified, stirred and stored) gave the same absorbance as the reagent blank. The detection limit was ~3 μmoles/kg.

Phosphate: Phosphate was analyzed shipboard on only a few of the 21° N samples according to the method of Strickland and Parsons (1968). It was not analyzed on the Guaymas samples.

Nitrite: Nitrite was analyzed shipboard on only a few of the 21° N samples according to the method of Strickland and Parsons (1968). It was not analyzed on the Guaymas samples.

Ion Chromatography

Sulfate (and total sulfur as sulfate) was the only species measured by ion chromatography. A Wescan Model 262 ion analyzer with 269-001 anion column and a 100 μl sample injection loop was used for the analysis. The eluant solution was 4 mM potassium phthlate adjusted to pH=4.5 with KOH. The analyses were done on 100 fold dilutions in the case of the sulfates and 250 times dilutions in the case of total sulfur as sulfate. The larger

dilution was used to keep the amount of bromine passing through the machine to a minimum because these solutions came from the bromine containing ampoules. For the sulfates the peak height was measured by hand while for the total sulfur an Hewlett-Packard Model 3390A integrator was used. IAPSO seawater was also analyzed and the samples were normalized to this, based on the salinity of an ambient sample. Analytical precision is better than ±1%.

Gas Chromatography

Beryllium and selenium were measured by gas chromatographic methods.

Beryllium: Beryllium was analyzed by the method of Measures and Edmond (1982,1983). This method is based on the electron capture detection of the volatile trifluoroacetylacetonate complex of beryllium. Analytical precision is approximately ±5%.

Selenium: Selenium was determined by the electron capture detection of the 5-nitropiazselenol complex (Measures and Burton, 1980). Less than 0.2 nmoles/kg of Se were present in the solutions. It was however present in the particles filtered from the acidified samples, presumably as Se°. As this method is specific for Se^{4+}, the Se was oxidized to this form by using a Br_2/Br^- redox couple (Uchida et al., 1980). Excess Br_2 was then reduced with hydroxylamine hydrochloride before proceeding with the analysis. The detection limit is 1 nmole/kg and the precision ±10%. Se was also determined in the ampoules treated with Br_2 which were used for total S.

Flame Atomic Absorption Spectrophotometry

The elements lithium, sodium, potassium, rubidium, magnesium, calcium, strontium, copper and zinc were analyzed by flame atomic absorption

spectrophotometry using a Perkin Elmer Model 403 spectrophotometer. All of the above were run using an air-acetylene flame - oxidizing or reducing depending on the recommendation in the Perkin Elmer handbook on analytical conditions.

Lithium: The samples were diluted ten times with Corning distilled water. To match the matrix, the standards were prepared in 50 mM NaCl. The precision is ±1% and the detection limit was 1 μmole/kg absolute or 10 μmoles/kg as the samples were diluted.

Sodium: The samples were diluted ~20000 times with corning distilled water to bring them into the linear range for sodium by flame a.a.s. This dilution was done in two steps; first a hundredfold dilution (which was used as a starting solution for many of the flame analyses) and then a two hundredfold dilution. Potassium (in the form of KCl) was added as an ionization suppressant to both the samples and standards, achieving a final concentration of 25 mM in these solutions. IAPSO seawater was analyzed with the samples to provide a check on the absolute concentration of sodium in both samples and standards. The analytical precision is ±2%.

Potassium: The samples were diluted 600 times to bring them into the linear range for flame a.a.s. analysis. This was a 100 times followed by a 6 times dilution. The samples and standards were made 20 mM in sodium (as NaCl) to prevent variable ionization effects. IAPSO seawater was again analyzed with the samples. The analytical precision is slightly better than ±1%.

Rubidium: The samples were diluted 6.7 times to prevent salt from becoming a problem in the nebulizer and burner while still assuring a good rubidium signal. The standards were prepared with NaCl to match the sodium concentrations in the sample to prevent ionization effects. As these

dilutions were also used for strontium a lanthanum solution was added to the samples as well. The lanthanum helps prevent interference effects from silicon, aluminum, phosphate and sulfate in the determination of the alkaline earths. The final concentration of lanthanum in the samples and standards was ~72 mM. An electrodeless discharge lamp was used and the analytical precision is ~3%.

Magnesium: The magnesium analyses were done on 4000 times dilutions of the original sample. Lanthanum was added to the samples in the same proportions as noted above. Due to the low levels of magnesium present in some of the samples and the high dilution factor, all of the samples with Mg <2.5 mmoles/kg were rerun at a 400 times dilution to increase the absorbances. No significant differences were found between the two runs. IAPSO was analyzed in both cases. Analytical precision is better than ±1%.

Calcium: Calcium was analyzed on a 300 times dilution of the sample. Lanthanum, as above, was added to the solutions. IAPSO seawater was analyzed along with the samples. Analytical precision is better than ±1%.

Strontium: Strontium was analyzed on the 6.7 times dilution used above for rubidium. Lanthanum had been added to these solutions. Analytical precision is ±1%.

Copper: Copper was determined on the same dilution used for rubidium and strontium and, as a result, the solutions also contained lanthanum. The standards were prepared to match the lanthanum, salt and acid composition of the samples. The detection limit was 2 μmoles/kg and the precision was ±2%. The NGS and Guaymas samples were below the detection limits for flame a.a.s. and were analyzed by graphite furnace a.a.s. (as were the particle solutions).

Zinc: Zinc was determined on the ten times dilutions used for the

lithium determinations. The standards were prepared to match the 50 mM NaCl content of the samples. Analytical precision is 5% and the detection limit is 0.05 μmoles/kg.

Graphite Furnace Atomic Absorption Spectrophotometry

The elements silver, aluminum, arsenic, barium, cadmium, cobalt, copper, nickel and lead were analyzed by graphite furnace atomic absorption spectrophotometry. (Most of the copper analyses were done by flame a.a.s., only those with Cu <1 μM were analyzed using the graphite furnace.) Barium and copper in the solutions were analyzed on a Perkin Elmer Model 5000 Spectrophotometer with an HGA 400 furnace and AS-1 autosampler. All of the other elements as well as barium and copper in the particle digests were analyzed on a Perkin Elmer Zeeman Model 5000 Spectrophotometer with an HGA 500 furnace and AS-40 autosampler. Hollow cathode lamps were used as the light source for silver, aluminum, barium, cobalt, copper and nickel. Electrodeless discharge lamps were used for arsenic, cadmium and lead. Two injections were done from each cup and the results averaged. The spectrophotometers were run in concentration mode usually with a ten times expansion factor. The wavelength was peaked manually. Injection sizes ranging from 10 to 30 μl were used on the AS-40 and either 10 or 20 μl injections were used on the AS-1.

The Zeeman-5000 was equipped with a Perkin Elmer Model 3600 data station which was used during methods development to graphically watch the peaks during atomization. This simplified optimization of parameters such as char and atomization temperatures and times. No coprecipitation or separation methods were used therefore seasalt was present in all samples. Optimization of conditions and detection limit therefore became a trade-off

between how much the sample could be diluted and still give a signal and how much seasalt the machine could handle. Several elements were attempted directly, others were diluted a minimum of four times. The preferred dilution was at least ten times, if a signal could be resolved.

Two matrix modifiers were used to aid in reducing the salt interference. Ascorbic acid, prepared fresh almost daily, was added to the samples to have a final concentration of 1% by weight as the sample was injected into the graphite tube. Ascorbic acid was not found to have a significant blank for any of the analyzed elements except cadmium. It was not used in the cadmium determinations. Ascorbic acid aids atomization by changing the wetting properties of the sample, causing it to spread out more inside the graphite tube. It therefore aids in keeping the size of any salt crystals which form small, resulting in a more even char and atomization. NH_4NO_3 was the second modifier used and has a chemical effect. The amount added to the solution was enough to insure that an excess of ammonia with respect to chloride was present as the sample was injected into the tube. The ammonia combines with the chloride resulting in loss of this salt during the char step, leaving an excess of nitrate behind. Nitrate salts are stable to higher temperatures than are chlorides, and the purpose is to have the element of interest form the nitrate salt and which will not be lost during the char but will remain stable until a higher atomization temperature is reached. This would allow separation of the element of interest from the salt matrix if the char can be raised to 1400° C. Neither the ascorbic acid nor the ammonium nitrate works ideally but the use of one or both of these modifiers will often significantly improve the results. All of the samples were diluted with a dilute HNO_3 matrix, to increase the amount of available nitrate. The

concentration of the dilueant was either 0.05% or 0.2% HNO_3 (w/w).

On the Perkin Elmer 5000 a deuterium arc lamp was used to provide background correction in the ultraviolet region and a tungsten halide lamp was used in the visible region (for barium). On the Zeeman-5000, the Zeeman effect, created by a strong magnetic field during atomization was used for background correction. For both instruments argon was used as the purge gas.

For all analyses (unless otherwise noted) a Perkin Elmer pre-pyrolized tube (PE 290-1821), which is a style only recently introduced was used. These tubes were found to have greater stability and longer life than either "home" pyrolized tubes or the older style of Perkin Elmer pre-pyrolized tubes.

The hydrothermal samples are rather unique compositionally and it was difficult to match the matrix of the standards to that of the samples. Other species besides those usually present in seawater were important was shown by preparing standard additions in surface seawater and in the samples. In the case of many elements, the slopes did not agree. The data station provided further proof of differences in speciation between the matrices. Observation of absorbance changes during atomization of the peak of interest often had a different characteristic shape or came off at a slightly different time with the same machine parameters. Since the matrices could not be matched, the method of standard additions was used for many of the samples. Two additions (10 µl and 20 µl) were made on each sample resulting in a three point curve. As the sample size was >1000 µl the size of the addition was within the precision of the measurement. The aim (not always achieved) was to have a 45° slope from the additions which would give the greatest resolution in calculating the composition of the

unknown. Since standard additions had to be used for most of the GFAAS analyses, the precision is worse ($\geq \pm 10\%$) than for the other analyses. All of the standard addition analyses were run at least in duplicate.

Silver: Silver was analyzed on a 12 times dilution with the addition of ascorbic acid. The method of standard additions was used. Silver was charred at 800° C and atomized at 2750° C with a 0 second ramp time (maximum power heating = MPH) using a 25 µl injection. For the Guaymas samples and some of the lower concentration 21° N samples the dilution factor was reduced to 4.4 or 6.5 times. The dilutant was 0.05% HNO_3. Samples were run until the results of the standard additions agreed within $\pm 10\%$.

Aluminum: Aluminum was analyzed on either an 11, 22 or 46 times dilution depending on the sample concentration. Standard additions were not used because adding surface seawater to the standards was sufficient to match the matrices, based on standard additions to both. A monitor was run every fourth sample and a full standard curve at the beginning and end of every tray of 30 samples so that the run could be drift corrected. The conditions were a 1500° C char and 2700° C MPH atomization and a 25 µl injection. Ascorbic acid was added to all samples which were diluted with 0.05% HNO_3. Duplicates within a run agreed to $\pm 3\%$ while duplicates between runs agreed within $\pm 10\%$.

Arsenic: Arsenic was analyzed by the method of standard additions with the addition of ascorbic acid. Nickel was also added to the solutions as recommended by Stein et al. (1980). The addition of nickel stabilizes the arsenic and allowed the char temperature to be raised to 1400° C, removing the seasalt. Arsenic was atomized at 2700° C MPH with a 30 µl injection size. The samples were made 450 µM in nickel as opposed to the

8.5 mM levels recommended by Stein et al. (1980). Increasing the nickel over the levels used gave no noticeable improvement in the results. 0.05% HNO_3 was used as the dilueant. Replicates were rerun until at least three agreed within ±10%.

Barium: Barium in the solutions was analyzed on the Perkin Elmer Model 5000 Spectrophotometer. Ascorbic acid was used with a 10 µl injection size. Standard additions were not needed. The char was at 1500° C and the atomization was at 2800° C MPH. Analytical precision is 10%. Barium in the particle digest solutions was analyzed on the Zeeman-5000 with no matrix modification due to the very low seasalt present in the particle fraction and the high dilutions (500 times) used. Analytical precision was ±10%.

Cadmium: Cadmium was analyzed by the method of standard additions with NH_4NO_3 added as a matrix modifier. It was run at either a 21 or 41 times dilution with 0.2% HNO_3 as the dilutant. The program included a char at 600° C and atomization at 2500° C MPH. The analytical precision is ±5%.

Cobalt: Cobalt was analyzed by the method of standard additions with both NH_4NO_3 and ascorbic acid added as matrix modifiers. A 25 µl injection was used with a char of 1400° C and atomization at 2700° C MPH. 0.2% HNO_3 was used as the dilueant and the dilution factor was either 4.5 or 12 times. The samples were rerun until replicates agreed within ±10%.

Copper: Only those samples with copper <1 µmole/kg were analyzed with the 5000. Copper in the particle digests were analyzed on the Zeeman-5000. The other samples were analyzed by flame a.a.s. For the solutions a 40 fold dilution factor was used and ascorbic acid was added to the solutions. The analytical precision was ±5%. For the particle digests copper was diluted 1000 times and no matrix modifiers were used. Analytical precision

is ±10%.

Nickel: Nickel was analyzed on the Zeeman-5000 using the 3600 data station to observe the peaks. Both ascorbic acid and NH_4NO_3 were used as matrix modifiers. A char of 1100° C and atomization of 2700° C MPH with an injection size of 20 µl were used. Several dilutions were used and the samples were finally injected directly. No signal above the background was observed.

Lead: Lead was analyzed on a 20 µl injection with an 800° C char and 2600° C MPH atomization, using the method of standard additions. Ascorbic acid and NH_4NO_3 were used as matrix modifiers. 0.2% HNO_3 was used as the dilutant and the dilution factors were 12, 23 and 45 times. The reproducibility between samples was not good and each sample was rerun until the agreement between replicates was at least ±20%.

Selenium: An attempt was made to measure selenium on the Zeeman-5000 with an EDL light source but no signal was observed. The selenium concentration in the samples is <1 µmole/kg.

Appendix 3

Appendix 3 is a complete listing of the analytical data. Table A3-1 contains the results of the major element analyses and table A3-2 contains the results of the trace element analyses.

The following abbreviations are used in the tables:

Dive = dives 1148-1160 were at 21° N in 1981 and dives 1168-1177 were at Guaymas in 1982.
dives 978-982 were at 21° N in 1979.

Btl = the number of the sampling bottle (1-16).

Pr = the number of the pair of samplers (1-6).

Area = the vent area sampled:
21° N: 1 = SW
2 = OBS
3 = NGS
4 = HG
Guaymas: the numbers (1-10) are the same as the vent areas (1-10).

T = temperature in ° Celcius

m = millimoles/kg.

μ = micromoles/kg.

μeq = microequivalents/kg.

n = nanomoles/kg.

TABLE A3-1

Dive	Stl	Pr	Area	T °C	Mg m	SiO_2 m	Li μ	Na meas m	Na calc m	K m	Rb μ	Be n	Ca m	Sr μ	Ba μ	pH	Alk_t μeq	Cl m	SO_4 m	H_2S m	NH_4 m	NO_2 μ	PO_4 μ
1149	1	0	1		2.13	16.65	865	437	438	22.8	27		15.6	82	6.0	3.73	-218	496	1.2	7.38	0.0	0.1	1.04
1149	2	0	1		1.92	16.40		426		22.5			17.4			3.86	-210						
1149	3	1	1	353		1.46											2051			0.43			
1149	4	1	1	353	51.04	0.77	61	459	464	10.6	1		10.6	86		6.85	2241	537	27.9	0.38	0.0	0.1	3.07
1149	6	5	1		3.74	16.21	843	433	438	22.8	25		15.4	81	4.0	3.76	-185	497	2.0	5.14	0.0	0.2	1.00
1149	7	2	1	346	4.76	15.87	828	443	439	22.4	25		17.5	92	3.7	3.73	-218	499	4.7	7.46	0.0	0.2	1.66
1149	8	2	1	346	7.05	15.29		435		21.6			17.1				-184			4.05			
1149	9	3	1	346	4.09	16.06	836	439	440	22.4	26		16.2	85	4.2	3.81	-90	499	2.9	6.53	0.0	0.0	1.33
1149	11	4	1	355	2.01	16.65	870	437	439	22.7	27		15.9	83	7.8	3.80	-179	498	1.1	6.72	0.0	0.2	1.00
1149	12	4	1	355	2.29	16.70		435		22.5			16.0				-186			6.58			
1149	13	5	1		5.67	15.77		426		22.1			15.4				-159			5.33			
1150	1	0	1	350	2.07	16.60	873	438	438	22.8	27		15.8	82	6.4	3.72	-232	497	1.1	7.93	0.0		1.35
1150	2	0	1	350	4.33	15.83		439		22.3			15.9							7.05			
1150	3	4	1	350	2.68	16.45		436		22.6			15.9							7.78			
1150	4	1	1	350	43.35	3.28	183	462	464	12.3	6		11.6	84		5.99	1837	534	24.7	2.09	0.0		2.58
1150	6	5	1	350	3.74	16.40	853	443	439	22.4	26		15.8	82	3.2	3.84	-166	499	2.2	7.33	0.0		2.11
1150	7	2	1	350	44.73	3.12	172	462	463	12.0	6		12.7	90		6.03	1792	533	26.5	1.40	0.0		2.57
1150	9	3	1	350	13.00	10.47	698	442	448	19.8	21		20.2	108		4.67	-245	507	14.5	5.88	0.0		1.94
1150	10	2	1	350																			
1150	11	4	1	350	1.03	17.09	885	436	437	22.7	27	9.4	16.0	82	9.1	3.65	-282	496	0.6	7.72	0.0		1.87
1150	13	5	1	350	6.55	14.95		433		21.5			15.7							7.33			
1150	15	3	1	350	24.93	7.50		457		17.8			17.5				707						
1150	17	1	1	350	46.65	2.29		462		12.0			12.6							0.66			
1151	4	1	3	273	8.68	16.01	864	500	503	22.4	26	31.1	18.8	92		4.30	22	573	4.6	5.42			
1151	5	2	3	273	20.02	12.27		498		20.4			17.3				423			4.18			
1151	6	3	3	273	2.90	18.69	974	507	506	24.7	29		19.9	94	3.2	3.82	-150	577	1.2	6.92			
1151	14	2	3	273	17.21	12.51	690	491	495	20.2	21		17.2	89		4.79	277	566	9.7	4.61			
1151	15	3	3	273	3.12	18.28		513		25.4			20.1				-136			5.75			
1151	17	1	3	273	8.73	16.40		506		23.9			19.2				-20			6.38			
1152	1	0	2	351	8.05	15.00	754	433	436	20.8	25		14.4	78		3.70	-303	497	4.3	5.90			
1152	2	0	2	351	7.70	14.80		435		21.5			14.5				-195			6.15			
1152	3	2	2	351	5.11	15.68		435		22.1			14.9				-237			7.23			
1152	5	3	2	351	42.55	3.14		463		12.8			12.9				1368			1.09			
1152	7	5	2	351	2.08	16.89	853	433	433	21.8	26	14.7	15.4	81	3.4	3.45	-405	491	1.4	6.45			
1152	9	3	2	351	45.94	2.38	135	462	465	11.3	3		12.8	80		6.08	1763	534	28.2	0.62			
1152	10	1	2	351	2.27	16.79		434		22.9			15.5				-326			6.38			
1152	11	1	2	351	1.44	17.23	861	433	432	22.5	28	14.7	15.5	83	4.8	3.47	-405	491	1.3	7.29			
1152	12	4	2	351																			
1152	13	5	2	351	3.10	16.40		435		23.0			15.2				-267			6.61			
1152	16	2	2	351	6.75	15.24	771	435	439	21.0			14.4	78		3.61	-238	496	3.6	6.38			
1152	18	4	2	351	9.85	14.12	724	436	437	20.6	21	12.5	15.1	83		4.36	15	499	6.1	6.23			
1153	5	3	1	352	6.13	15.48		442		22.4			16.3				-72			7.57			
1153	6	0	1	270	12.36	12.14	625	416	416	18.2	20	14.4	13.3	72	2.4	4.82	376	471	7.4	5.06			
1153	7	5	1	2	52.83	0.16	28	460		9.8	1		10.3	84	0.9			540	29.3				
1153	9	3	1	352	3.60	16.35	848	433	438	22.0	26		16.1	82		3.86	-145	497	2.2	7.68			
1153	10	1	1	274																			
1153	11	1	1	274	16.49	10.02	636	442	448	18.5	20		13.7	78		4.81	339	510	8.7	5.49			
1153	12	4	1	270	21.04	10.60	496	424		16.6	16		12.7	75	2.5			483	11.5				
1153	13	2	1	352	16.71	12.07		449		19.8			13.9				78			5.99			
1153	14	2	1	352	9.85	13.68	742	435	442	20.5	22	7.5	14.7	78		3.78	-185	504	5.2	6.62			
1153	15	0	1	270	5.23	15.63		412		20.6		11.4	14.0				15			6.45			
1153	17	5	1	2																			
1153	18	4	1	270	20.91	9.52	500	424	427	16.3	16	11.4	12.6	74		5.08	652	487	11.3	4.25			
1154	2	2	2	15																			
1154	3	5	3	273	20.98	9.50		499		20.4			17.0				227			3.82			
1154	4	4	3	273	16.04	11.39	734	496	497	20.7	22	25.2	17.4	90		4.56	150	569	8.6	4.31			
1154	5	4	3	273	17.24	11.09		507		21.4			17.7				224			4.20			
1154	6	5	3	273	28.75	8.35	482	477	487	16.6	14	16.7	14.9	88		5.24	732	559	16.0	2.56			
1154	12	1	3	273	22.21	7.35		499		19.8			16.8				370			3.80			
1154	14	2	2	15	51.67	0.39	29	459	473	9.7	2		10.6	85		7.30	2294	540	31.4				
1154	16	1	3	273	23.08	9.65	592	472	490	18.1			16.1	88		4.98	440	562	12.6	3.66			

Dive	Bcl	Pr	Area	T °C	Mg m	SiO_2 m	Li μ	Na meas m	Na calc m	K m	Rb μ	Be n	Ca m	Sr μ	Ba μ	pH	Alk_c μeq	Cl m	SO_4 m	H_2S m	NH_4 m	NO_2 μ	PO_4 μ
1155	1	0	3	273	2.10	18.69	999	497	508	24.3	30	36.4	20.2	96	13.5	3.88	-130	578	0.8	6.06			
1155	3	2	3	273	4.43	17.87		501		24.5			19.6				-44			5.94			
1155	10	1	3	273	3.40	18.21		505		25.4			20.1				-101			5.83			
1155	14	2	3	273	2.27	18.69	993	504	508	24.2	30		20.0	97	10.5	3.78	-163	578	0.9	6.40			
1155	15	0	3	273	2.78	18.54		519		25.7			20.5				-134			6.04			
1155	18	1	3	273	2.13	18.74	996	491	507	24.1	31	33.6	20.1	97	10.5	3.77	-164	577	0.8	6.51			1.01
1156	3	1	2																				
1156	6	2	2		44.55	2.91	162	457	463	11.8	5		11.4	85		5.90	1646	533	25.3	0.64			
1156	9	3	2		46.06	2.62	151	456	462	11.3	6		12.3	90		6.00	1728	534	26.1	1.67			
1156	11	4	2		25.16	8.43	479	444	452	16.3	15	7.6	13.3	82		4.94	385	518	14.3	3.40			
1156	12	2	2															514					
1156	13	3	2		15.71	12.46		441		19.3			14.2				-110						
1156	16	1	2		40.37	4.21	229	453	460	12.7	7	2.9	11.7	83		5.64	1279	528	23.5	0.77			
1156	17	4	2		6.34	15.43		436		22.3			15.2				-205			6.23			
1157	2	0	1	150	32.85	6.80		462		15.7		4.1	12.9				1189			2.98			
1157	4	5	1	150	39.31	4.44	244	452	461	12.8	9	2.3	11.8	84	1.9	5.79	1560	529	22.2	1.57			
1157	5	5	1	150	42.74	3.27	185	456	468	11.7	5	1.5	11.4	91	2.2	6.02	1751	537	24.0				
1157	6	3	1	275	40.92	4.36	235	453	464	12.8	7		11.7	92		5.79	1629	533	22.8	1.56			
1157	7	0	1	150	18.16	9.05	619	449	447	18.7	19	6.8	14.5	83	1.8	4.74	280	512	9.9	5.54			1.23
1157	9	2	1	52	42.11	4.35	229	455	462	12.9	7		12.2	85		5.92	1814	535	22.6	1.58			3.33
1157	10	4	1	52	9.21	12.90		455		22.3		17.0	16.1				613			5.81			
1157	13	2	1	52	31.53	4.71		460		15.5			13.1				1220	537		2.65			
1157	14	1	1	182	44.56	3.16	174	459	464	11.8	6		11.3	83		6.03	1917	524	24.3	1.21			
1157	15	3	1	275	37.06	5.21		463		14.5			11.7				1474			1.93			
1157	17	1	1	182	47.76	1.98	115	457	465	11.1	4		10.9	83		6.34	2073		26.0				
1157	18	4	1	146	22.79	5.51	540	451	458	17.5	16	12.8	14.2	82	1.8	5.22	806		12.3	4.15			
1158	2	5	2		1.95	17.09		435		22.9			15.3				-343			7.70			
1158	3	1	2		1.33	17.18		437		23.5			15.4				-391			7.38			
1158	6	2	2		2.31	16.94	854	426	435	22.4			15.2	80	5.8	3.51	-352	490	1.2	7.78			
1158	10	0	2		2.11	16.89		437		23.1			15.3				-353			7.15			
1158	11	0	2		1.39	17.23	879	426	432	22.5	28		15.3	81	5.9	3.49	-340	491	0.8	7.38			0.32
1158	13	2	2		2.59	16.89		435		22.8			15.2				-341			5.94			
1158	14	5	2		3.91	16.35	835	430	432	21.9	27		14.8	79	4.6	3.52	-338	492	2.1	6.38			0.49
1158	16	1	2		1.14	17.28	869	427	431	22.5	29		15.2	80	7.2	3.46	-390	490	0.6	7.78			
1159	1	3	1		32.63	4.03	371	450	457	15.1	12		11.7	79	2.0	5.42	1091	525	17.1	2.94			2.56
1159	3	1	1		47.02	1.91	124	458	469	11.2	5		10.8	84			1974	541	25.8				
1159	4	4	1		44.43	3.12	179	448	469	12.2	6		11.1	82		5.96	1867	541	24.0	1.28			
1159	5	5	1																				
1159	7	0	1		52.98	0.29	34	450		9.8	1		10.4	85		7.37		541	29.1	0.00			3.05
1159	9	5	1		52.81	0.20	29	455		9.8	2		10.3	86		7.58		541	29.0	0.00			
1159	10	0	1																				
1159	12	3	1		44.00	2.74		461		11.8			10.9										
1159	15	2	1		42.08	3.19	178	451	467	12.1	6		11.3	83			1801	534	24.1				
1159	16	1	1		32.83	6.13	361	456	457	14.9	13		11.9	80	2.0	5.42	1119	525	17.3	2.82			
1159	17	4	1		47.47	1.83	110	458	465	11.0	3		10.7	84			2041	537	25.9				
1159	18	2	1		37.65	5.18	283	452	460	13.5	9	3.1	11.8	83		5.63	1500	528	20.8	2.20			
1160	1	3	4	241	2.25	15.04	1262	438	443	22.6	32	12.8	11.6	66	5.5	3.46	-386	498	1.4	7.59			1.02
1160	2	2	4	350	1.96	15.14		458		23.7			11.6				-392			8.65			
1160	3	1	4	350	4.35	14.56		452		23.2			11.7				-386			7.12			
1160	5	5	4	224	2.94			453		23.7			11.7							7.21			
1160	6	5	4	224	0.95	15.43	1305	432	441	23.1	33	11.7	11.6	65	10.4	3.38	-458	496	0.6	8.61			0.50
1160	7	0	4	224	2.69	14.90	1258	432	443	22.8	32	11.7	11.6	65	5.6	3.48	-391	498	1.6	7.86			1.11
1160	10	0	4	224	2.63	14.85		451		23.6			11.8				-353			7.40			
1160	11	2	4	350	2.00	15.19	1284	436	446	22.7	32	12.8	11.6	66	4.6	3.43	-391	500	1.1	8.59			0.65
1160	12	3	4	241	2.60	14.90		450		23.8			11.7				-385			8.89			
1160	13	4	4	241	28.66		608	450		15.6	15		10.8	75				523	16.4	3.16			
1160	14	4	4	241	36.72	4.57	385	451	464	13.4	9	4.3	10.7	77		5.29	955	529	21.6	2.06			2.30
1160	16	1	4	350	1.84	14.56	1281	439	442	23.4	30	12.1	11.6	65	7.4	3.42	-417	497	1.0	8.35			0.64

Dive	Btl	Pr	Area	T °C	Mg m	SiO_2 m	Li μ	Na meas m	Na calc m	K m	Rb μ	Be n	Ca m	Sr μ	Ba μ	pH	Alk_t μeq	Cl m	SO_4 m	H_2S m	NH_4 m	NO_2 μ	PO_4 μ
1168	11	2	10	36	52.28	0.22	28	459	466	10.0	2		10.2	85	1.3	7.20	2322	542	26.6	0.00	0.0		
1168	13	2	10	36	52.32	0.24	28	460		10.0	2		10.4	86	0.9	7.00	2353	541	27.0	0.00			
1169	12	1	8	273	51.52	0.73	55	468	464	11.4	3		12.1	92	0.9	6.40	2825	544	26.3	0.04	0.5		
1169	16	1	8	273	26.18	4.94		490		25.0			26.1			5.70							
1172	1	4	1	194	52.10	0.20	25	448	467	9.9			10.4	86	0.5	7.40	2364	542	27.0	0.04	0.0		
1172	2	4	1	194	51.54	0.43	48	464		10.7	2		10.9	86	1.0	6.80	2341	543	26.3	0.04			
1172	7	5	1	194	48.40	0.53	60	460	472	11.1	3		11.0	89	1.1	6.00	2365	544	26.2	0.04	0.5		
1172	10	5	1	194	51.77	0.38	47	458		10.8	3		10.7	87	0.9	6.80	2404	539	26.3	0.04	.		
1173	3	3	2	291	24.85	6.43	495	470		28.2	39	9.7	19.6	134	2.9	5.90	6181	565	14.7	2.47			
1173	5	0	2	291	2.97	11.80	907	464	477	44.3	73	17.0	27.8	180	7.6	5.90	9226	586	1.5	3.92	14.8		
1173	6	3	2	291	1.36	12.24	931	470	477	45.9	74	17.7	28.3	186	14.9	5.80	9291	587	0.6	4.00	14.6		
1173	11	2	5	287	2.15	11.91	890	486	487	42.2	70	28.1	30.1	206	9.8	5.90	9264	597	1.1	4.52	13.9		
1173	12	1	6	264	40.75	2.60	221	461		17.6	18	13.6	14.1	102	2.3	5.80	3452	548	20.6	0.24			
1173	13	2	5	287	2.13	11.95	902	483		41.3	72	27.9	30.0	205	13.2	5.90	9454	597	1.1	4.12			
1173	14	0	2	291	11.00	10.02	768	473		38.7	61	13.6	24.9	160	5.1	6.00	8198	579	5.3	3.62			
1173	16	1	6	264	1.44	10.47	872	471	475	44.2	72	58.0	26.1	171	16.3	5.80	7212	581	0.7	3.84	14.1		
1175	5	5	3	285	16.90	9.27	505	493		28.6	40	28.2	31.7	201	5.2	5.80	5223	608	8.5	3.70			
1175	9	0	3	285	42.26	2.28	135	468	477	14.0	9	7.3	15.4	111	1.7	6.00	3220	556	22.8	1.09	1.7		
1175	15	0	3	285	47.45	1.49	92	465		12.4	7	4.1	13.6	101	1.8	6.00	2784	551	24.5	0.43			
1175	16	5	3	285	4.11	12.50	666	503	508	34.9	52	38.4	39.1	241	7.3	5.80	6124	629	2.0	4.21	9.6		
1176	3	3	1	291	10.58	10.27	846	475		40.1	68	8.8	25.6	179	2.7	6.00	9346	590	5.4	5.07			
1176	5	0	1	291	2.55	12.22		479		47.1			27.8			5.97	9893		1.4	5.29			
1176	6	1	7	300	1.86	12.36	1028	483	489	47.2	83	16.1	28.7	205	10.9	5.98	10186	601	0.9	5.68	14.7		
1176	7	0	1	291	1.99	12.43	1019	493	486	47.1	82	14.1	27.7	198	11.5	5.95	9863	597	0.9	5.19	15.2		
1176	10	2	7	300	1.00	12.60	1053	496	489	49.2	83	16.6	28.8	209	24.3	5.96	10071	603	0.4	5.74	15.0		
1176	11	2	7	300	24.75	7.06	604	482		31.1	51		21.8	162	4.6	6.10	7358	587	13.3	3.85			
1176	13	1	7	300	1.88	12.33	1041	487		47.5	82	15.7	28.6	207	12.6	5.98	10006	602	0.9	5.62			
1176	14	3	1	291	7.48	11.09	911	480	486	43.2	73	8.8	27.1	187	5.5	5.99	9860	594	3.7	5.37	13.1		
1177	5	5	4	312	2.82	13.03	809	469	484	38.3	62	29.3	32.9	212	8.3	5.90	7889	596	1.6	4.56	12.1		
1177	6	5	4	312	0.80	13.60	869	470	484	39.6	65	29.3	33.7	225	17.0	5.91	8104	597	0.6	4.83	12.6		
1177	9	1	9	100	36.36	3.04	215	450	468	16.8	18	28.4	16.4	111	2.3	5.54	2472	553	18.1	1.50	3.7		
1177	11	3	4	315	1.05	13.37	861	482	485	39.4	66	26.7	33.2	225	30.3	5.89	8024	598	0.5	5.11	13.3		
1177	13	3	4	315	0.64	13.62	868	491	486	39.8	65	27.9	33.9	226	42.0	5.90	7847	600	0.3	4.19	12.3		
1177	15	1	9	100	45.34	1.35	104	474		13.0	10	11.9	12.9	94	1.5	5.91	2399	547	23.3	0.44			

Dive	Btl	Pr	Area	T °C	Mg m	H_2S m	Mn μ	Fe μ	Co n	Cu μ	Zn μ	Ag n	Cd n	Pb n	As n	Se part n	Se amp n	Al μ
978	Bag		3	4.5	52.44	0	5	-			-				-			
978	5/6		3	220	24.24	0.65	-	1349			62				308			
978	7/8		3	120	46.67	-	227	293			-				-			
979	1/2		2	120	52.47	0.33	40	-			26				<30			
979	3/4		2	170	29.83	1.43	319	364			27				43			
979	11/12		2	100	52.84	0.06	13	49			24				<30			
980	5/6		1	30	48.59	0.34	65	331			11				82			
980	7/8		1	84	45.90	0.93	66	168			289				<30			
980	9/10		1	112	34.52	1.50	157	-			-				<30			
981	1/2		1	-	53.03	0.11	22	101			15				<30			
981	3/4		1	-	44.31	1.18	102	160			31				<30			
981	11/12		1	-	50.35	0.12	33	109			34				59			
982	5/6		3	225	32.75	0	53	-			-				-			
982	7/8		3	290	7.02	5.71	892	1292			105				347			

TABLE A3-2

Dive	Btl	Pr	Area	T °C	Mg m	H_2S m	Mn μ	Fe μ	Co n	Cu μ	Zn μ	Ag n	Cd n	Pb n	As n	Se part n	Se amp n	Al μ
1149	1	0	1		2.13	7.38	737	722	58	11.0	95	30	173	185	249			4.1
1149	2	0	1		1.92				44				132					
1149	3	1	1	353		0.43												
1149	4	1	1	353	51.04	0.38	23	20		0.0	5							
1149	6	5	1		3.74	5.14	703	684	44	8.3	73	21	132	150	172			4.3
1149	7	2	1	346	4.76	7.46	688	646	78	8.2	45	19	76	113	79	36.0		12.6
1149	8	2	1	346	7.05	4.05												
1149	9	3	1	346	4.09	6.53	702	692	54	7.1	82	15	121	175	173			4.3
1149	11	4	1	355	2.01	6.72	735	720	57	7.6	73	18	112	185	160			4.5
1149	12	4	1	355	2.29	6.58												
1149	13	5	1		5.67	5.33												
1150	1	0	1	350	2.07	7.93	741	735	79	11.5	113	42	180	340	288			4.9
1150	2	0	1	350	4.33	7.05												
1150	3	4	1	350	2.68	7.78												
1150	4	1	1	350	43.35	2.09	116	108		0.0	27							
1150	6	5	1	350	3.74	7.33	697	711	76	8.3	87	20	142	156	215			11.0
1150	7	2	1	350	44.73	1.40	108	92		4.0	22							
1150	9	3	1	350	13.00	5.88	535	514		5.9	48							
1150	10	2	1	350														
1150	11	4	1	350	1.03	7.72	723	742	74	10.7	97	27	155	152	278	60.0	70	4.7
1150	13	5	1	350	6.55	7.33												
1150	15	3	1	350	24.93													
1150	17	1	1	350	46.65	0.66												
1151	4	1	3	273	8.68	5.42	840	707		0.0	39							
1151	5	2	3	273	20.02	4.18												
1151	6	3	3	273	2.90	6.92	971	823	28	0.0	39	0	19	142	<30			3.6
1151	14	2	3	273	17.21	4.61	663	488		0.0	38							
1151	15	3	3	273	3.12	5.75												
1151	17	1	3	273	8.73	6.38												
1152	1	0	2	351	8.05	5.90	824	1349		42.5	95							
1152	2	0	2	351	7.70	6.15		1531										
1152	3	2	2	351	5.11	7.23												
1152	5	3	2	351	42.55	1.09												
1152	7	5	2	351	2.08	6.45	913	1539	189	38.8	88	28	128	174	231			5.0
1152	9	3	2	351	45.94	0.62	108	113		11.6	13							
1152	10	1	2	351	2.27	6.38												
1152	11	1	2	351	1.44	7.29	941	1618	210	41.7	102	37	168	286	231			4.8
1152	12	4	2	351														
1152	13	5	2	351	3.10	6.61												
1152	16	2	2	351	6.75	6.38	854	1418		39.1	81							
1152	18	4	2	351	9.85	6.23	800	1371		34.8	93							
1153	5	3	1	352	6.13	7.57												
1153	6	0	1	270	12.36	5.06	375	199		0.0	26		0					
1153	7	5	1	2	52.83		0			0.0	0		0					
1153	9	3	1	352	3.60	7.68	651	706		9.8	91							
1153	10	1	1	274														
1153	11	1	1	274	16.49	5.49	435	254		0.0	21							
1153	12	4	1	270	21.04		292	125		0.0	33							
1153	13	2	1	352	16.71	5.99												
1153	14	2	1	352	9.85	6.62	545	509		8.3	74							
1153	15	0	1	270	5.23	6.45												
1153	17	5	1	2														
1153	18	4	1	270	20.91	4.25	293	125		0.0	31							
1154	2	2	2	15														
1154	3	5	3	273	20.98	3.82												
1154	4	4	3	273	16.04	4.31	681	549		0.0	30							
1154	5	4	3	273	17.24	4.20												
1154	6	5	3	273	28.75	2.56	440	376		0.0	27							
1154	12	1	3	273	22.21	3.80												
1154	14	2	2	15	51.67		5	28		0.0	4							
1154	16	1	3	273	23.08	3.66	553	442		0.0	1							

Dive	Btl	Pr	Area	T °C	Mg m	H_2S m	Mn µ	Fe µ	Co n	Cu µ	Zn µ	Ag n	Cd n	Pb n	As n	Se part n	Se amp n	Al µ
1155	1	0	3	273	2.10	6.06	966	835	20	0.0	39	0	16	189	<30	0.3		4.0
1155	3	2	3	273	4.43	5.94												
1155	10	1	3	273	3.40	5.83												
1155	14	2	3	273	2.27	6.40	967	835	20	0.0	37	0	14	182	<30			3.7
1155	15	0	3	273	2.78	6.04												
1155	18	1	3	273	2.13	6.51	959	837	17	0.0	39	0	17	183	<30	0.4	1	3.9
1156	3	1	2															
1156	6	2	2		44.55	0.64	131	146		9.7	17							
1156	9	3	2		46.06	1.67	133	148		32.3	18							
1156	11	4	2		25.16	3.40	496	868		60.0	75							
1156	12	2	2															
1156	13	3	2		15.71													
1156	16	1	2		40.37	0.77	218	274		22.4	29							
1156	17	4	2		6.34	6.23												
1157	2	0	1	150	32.85	2.98												
1157	4	5	1	150	39.31	1.57	143	36		0.0	4		0					
1157	5	5	1	150	42.74		103	23		0.0	4		0					
1157	6	3	1	275	40.92	1.56	141	52		0.0	5							
1157	7	0	1	150	18.16	5.43	408	251		0.0	24		0					
1157	9	2	1	52	42.11	1.58	140	46		0.0	12							
1157	10	4	1	52	9.21	5.81												
1157	13	2	1	52	31.53	2.65												
1157	14	1	1	182	44.56	1.21	100	37		0.0	2							
1157	15	3	1	275	37.06	1.93												
1157	17	1	1	182	47.76		65	26		0.0	2							
1157	18	4	1	146	22.79	4.15	357	168		0.0	12		0					
1158	2	5	2		1.95	7.70												
1158	3	1	2		1.33	7.38												
1158	6	2	2		2.31	7.78	933	1647	230	40.8	108	40	153	328	237	62.0		5.0
1158	10	0	2		2.11	7.15												
1158	11	0	2		1.39	7.38	937	1641	204	43.2	110	42	166	323	240	64.0	72	5.2
1158	13	2	2		2.59	5.94												
1158	14	5	2		3.91	6.38	884	1547		37.4	96		104					
1158	16	1	2		1.14	7.78	929	1659	196	42.4	112	38	172	376	257			5.2
1159	1	3	1		32.63	2.94	240	103		0.0	13		0					
1159	3	1	1		47.02		71	34		0.0	5							
1159	4	4	1		44.43	1.28	108	61		0.0	9							
1159	5	5	1															
1159	7	0	1		52.98	0.00	0	0		0.0	0							
1159	9	5	1		52.81	0.00	0	0		0.0	1							
1159	10	0	1															
1159	12	3	1		44.00													
1159	15	2	1		42.08		110	78		0.0	22							
1159	16	1	1		32.83	2.82	245	145		0.0	17		0					
1159	17	4	1		47.47		63	32		0.0	12							
1159	18	2	1		37.65	2.20	188	124		0.0	22							
1160	1	3	4	241	2.25	7.59	835	2318	198	44.2	95	40	161	399	380			4.2
1160	2	2	4	350	1.96	8.65												
1160	3	1	4	350	4.35	7.12												
1160	5	5	4	224	2.94	7.21												
1160	6	5	4	224	0.95	8.61	878	2397	210	35.1	97	28	160	320	430	52.0	60	4.4
1160	7	0	4	224	2.69	7.86	840	2289	238	37.6	102	34	189	357	450			4.1
1160	10	0	4	224	2.63	7.40												
1160	11	2	4	350	2.00	8.59	829	2347	222	48.9	102	31	173	316	467			4.5
1160	12	3	4	241	2.60	8.89												
1160	13	4	4	241	28.66	3.16	432	1152		41.8	86							
1160	14	4	4	241	36.72	2.06	264	644		21.2	54							
1160	16	1	4	350	1.84	8.35	832	2343	222	45.0	105	44	183	335	452	68.0		4.5

Dive	Btl	Pr	Area	T °C	Mg m	H_2S m	Mn µ	Fe µ	Co n	Cu µ	Zn µ	Ag n	Cd n	Pb n	As n	Se part n	Se amp n	Al µ
1168	11	2	10	36	52.28	0.00	4	12			0							13.1
1168	13	2	10	36	52.32	0.00	3	8			0							8.9
1169	12	1	8	273	51.52	0.04	20	30			5			91				0.6
1169	16	1	8	273	26.18													
1172	1	4	1	194	52.10	0.04	1	0			1	5		38				0.4
1172	2	4	1	194	51.54	0.04	7	7			2	3						1.4
1172	7	5	1	194	48.40	0.04	10	6			0							1.2
1172	10	5	1	194	51.77	0.04	7	10			0							1.5
1173	3	3	2	291	24.85	2.47	115	37			0	19		450	1238			0.3
1173	5	0	2	291	2.97	3.92	211	45			1			166	868			2.9
1173	6	3	2	291	1.36	4.00	213	49			1			257	356	61.0	87	0.3
1173	11	2	5	287	2.15	4.52	122	31			2				845			3.2
1173	12	1	6	264	40.75	0.24	37	9			0				269			0.9
1173	13	2	5	287	2.13	4.12	123	32			2				147			2.6
1173	14	0	2	291	11.00	3.62	177	32			4				255			0.3
1173	16	1	6	264	1.44	3.84	143	16			0	3			629		49	3.8
1175	5	5	3	285	16.90	3.70	166	110			30		24	262	320			5.3
1175	9	0	3	285	42.26	1.09	43	49			5	7		271	240			2.6
1175	15	0	3	285	47.45	0.43	27	46			5							1.8
1175	16	5	3	285	4.11	4.21	215	169		1.1	35	22	48	703	1294	38.0	15	5.3
1176	3	3	1	291	10.58	5.07	115	73			6			266	405			1.3
1176	5	0	1	291	2.55	5.29												
1176	6	1	7	300	1.86	5.68	132	35			3				184			0.9
1176	7	0	1	291	1.99	5.19	130	40			3				193		82	0.4
1176	10	2	7	300	1.00	5.74	135	40			2				703		92	1.0
1176	11	2	7	300	24.75	3.85	83	0			0							0.3
1176	13	1	7	300	1.88	5.62	132	44			2				1185			1.3
1176	14	3	1	291	7.48	5.37	120	38			3			177	174			0.5
1177	5	5	4	312	2.82	4.56	131	73			18		21	124	137			0.5
1177	6	5	4	312	0.80	4.83	138	78		0.1	19	2	33	362	1972	72.0		4.6
1177	9	1	9	100	36.36	1.50	40	16			3				178			2.1
1177	11	3	4	315	1.05	5.11	135	74		0.2	19		26	224	1137		103	4.1
1177	13	3	4	315	0.64	4.19	137	77		0.2	18	1	27	184	912	88.0		5.1
1177	15	1	9	100	45.34	0.44	20	32			11	3	37	448	146			1.9

Dive	Btl	Pr	Area	T °C	Mg m	SiO_2 m	Li μ	Na meas m	Na calc m	K m	Rb μ	Be n	Ca m	Sr μ	Ba μ	pH	Alk_t μeq	Cl m	SO_4 m	H_2S m	F μ
978	Bag		3	4.5	52.44	0.31	32	472	-	10.2	2		10.4		-	7.21	2370	541	-	0	64
978	5/6		3	220	24.24	10.58	554	484	483	18.7	15		15.8	89	11.1	5.12	190	554	14.0	0.65	24
978	7/8		3	120	46.67	4.25	195	459	471	12.7	6		22.4		-	6.04	1680	543	38.8	-	55
979	1/2		2	120	52.47	0.15	29	474	460	10.2	2		10.2		0.6	6.96	2350	537	28.0	0.33	66
979	3/4		2	170	29.83	9.29	404	455	447	16.1	11		12.5	87	15.5	4.91	160	514	16.7	1.43	40
979	11/12		2	100	52.84	0.15	26	467	462	9.8	2		10.3	86	0.5	7.53	2450	541	27.4	0.06	65
980	5/6		1	30	48.59	1.95	106	479	460	11.5	4		11.0	87	4.1	6.46	2270	537	25.7	0.34	60
980	7/8		1	84	45.90	3.18	143	474	453	12.1	5		11.1		6.4	6.27	1950	528	24.7	0.93	62
980	9/10		1	112	34.52	5.09	349	441	-	14.7	-		12.0		-	5.56	-	518	17.6	1.50	51
981	1/2		1	-	53.03	0.17	28	475	464	10.1	2		10.2		0.6	7.22	2410	543	28.0	0.11	65
981	3/4		1	-	44.31	3.87	187	482	456	12.8	-		11.8	88	17.5	5.81	1640	533	23.6	1.18	52
981	11/12		1	-	50.35	1.19	68	462	460	10.8	3		10.9		3.5	6.61	2030	538	26.8	0.12	63
982	5/6		3	225	32.75	0.67	88	460	-	10.7	-		10.1		-	-	-	546	-	-	48
982	7/8		3	290	7.02	18.74	873	497	487	23.4	23		19.9	89	84.4	4.24	30	560	2.5	5.71	17

BIOGRAPHICAL NOTE

The author was born on February 7, 1955 in Astoria, New York where she lived until entering college. She was graduated from the Stuyvesant High School in June 1973 and entered Yale University that fall. At Yale she had her first introduction to the earth sciences and graduated in May 1977 with a B.S. degree in Geology and Geophysics with a concentration in geochemistry. She spent the following year as a research assistant in geochemistry at Yale. In July 1978 the author entered the M.I.T.-W.H.O.I. Joint Program in Oceanography as a candidate for the degree of Doctor of Philosophy. Besides this thesis the author has been involved with research in natural radionuclides, especially the uranium series, in both fresh and marine waters and lake sediments, as well as the chemistry of evaporative lakes.

Publications:

Von Damm, K.L., L.K. Benninger & K.K. Turekian, The Lead-210 chronology of a core from Mirror Lake, New Hampshire, Limnol. & Ocean. 24, 434-439, 1979.

Krishnaswami, S., L.K. Benninger, R.C. Aller & K.L. Von Damm, Atmospherically-derived radionuclides as tracers of sediment mixing and accumulation in nearshore marine and lake sediments: evidence from Be-7, Pb-210 and Pu-239,240, Earth & Planet. Sci. Lett. 47, 307-318, 1980.

Nozaki, Y., K.K. Turekian & K.L. Von Damm, Pb-210 in GEOSECS water profiles from the North Pacific, Earth & Planet. Sci. Lett. 49, 393-400, 1980.

Edmond, J.M., K.L. Von Damm, R.E. McDuff & C.I. Measures, Chemistry of hot springs on the East Pacific Rise and their effluent dispersal, Nature 297, 187-191, 1982.

Von Damm, K.L., B. Grant & J.M. Edmond, Preliminary report on the chemistry of hydrothermal solutions at 21° north, East Pacific Rise, in NATO ARI volume "Hydrothermal Processes at Seafloor Spreading Centers," P.A.Rona ed., Plenum Press, in press, 1983.

Von Damm, K.L. & J.M. Edmond, Reverse weathering in the closed basin lakes of the Ethiopian Rift and in Lake Turkana (Kenya), Amer. J. of Sci., submitted 1983.

Edmond, J.M. & K.L. Von Damm, Hot springs on the ocean floor, Scientific American 248, 78-93, 1983.